SYNTHESIS AND IN VITRO EVALUATION OF FUSED HETEROCYCLES AND TRIAZINE ANALOGUES

Thesis submitted in fulfillment of the

requirement of the degree of

Doctor of Philosophy

by

Prinka

(Regd. No. 901109004)

Under the supervision of

Dr. Kamaldeep Paul

(Associate Professor)

School of Chemistry and Biochemistry

Thapar University

Patiala – 147004

Punjab, India

December – 2015

Certificate

This is to certify that thesis entitled "**Synthesis and *In Vitro* Evaluation of Fused Heterocycles and Triazine Analogues**" being submitted by Prinka in the fulfillment of the requirement for the award of the Degree of Doctor of Philosophy to the School of Chemistry and Biochemistry, Thapar University, Patiala, is a authentic record of candidate's own work carried out by her under my supervision and guidance. The matter presented in this thesis has not been submitted in part or full for the award of any degree in any other University or Institute.

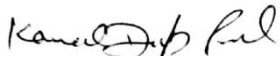

(Supervisor)

Dr. Kamaldeep Paul

Associate Professor

School of Chemistry and Biochemistry

Thapar University, Patiala - 147 004

Punjab (India)

(Head)

Dr. Bonamali Pal

Professor & Head

School of Chemistry and Biochemistry

Thapar University, Patiala - 147 004

Punjab (India)

Candidate's Declaration

I, hereby declare that the work presented in the thesis entitled "**Synthesis and *In Vitro* Evaluation of Fused Heterocycles and Triazine Analogues**" in partial fulfillment of the requirement for the award of the Degree of Doctor of Philosophy, School of Chemistry and Biochemistry, Thapar University, Patiala, is an authentic record of my own work carried out under the supervision of Dr. Kamaldeep Paul, Associate Professor, School of Chemistry and Biochemistry, Thapar University, Patiala, India. The matter embodied in this thesis has not been submitted in part or full to any other university or institute for the award of any degree in India or Abroad.

Prinka

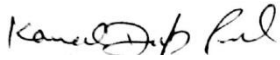

(Supervisor)

Dr. Kamaldeep Paul

Associate Professor

School of Chemistry and Biochemistry

Thapar University, Patiala - 147 004

Punjab (India)

Dedicated to
My Beloved
Mother

Acknowledgements

I wholeheartedly thank my mighty God for giving me the vision, power, spirit and endurance to complete this interesting research.

Completion of this doctoral dissertation was possible with the support of several people. I would like to express my sincere gratitude to all of them.

First and foremost, I would like to express my sincere gratitude to my adored research supervisor, **Dr. Kamaldeep Paul**, Associate Professor, School of Chemistry and Biochemistry, for introducing me to this exciting field of Science and for his valuable guidance, continuous support, motivation, patience, scholarly inputs and consistent encouragement I received throughout the Ph.D. work. I have learnt extensively from his, including how to regard an old question from a new perspective and how to approach a problem by systematic thinking. He has always made himself available to clarify my doubts despite his busy schedules and I consider it as a great opportunity to do my doctoral programme under his guidance and to learn from his research expertise. His mentorship was paramount in providing a well rounded experience consistent my long-term career goals. His persistent courage and confidence will always inspire me, and I hope to continue to work with his noble thoughts.

I am profoundly obliged to **Dr. Bonamali Pal**, Professor and Head, School of Chemistry and Biochemistry, Thapar University, Patiala for their good wishes and motivation.

I am also very grateful to **Dr. Vijay Luxami, Dr. Vinay Kumar Jain** and my doctoral committee members **Dr. Manmohan Chibber**, **Dr. Satyendra Pandey** and **Dr. Siddharth Sharma** for their fruitful discussion and encouragement, constructive criticism and inspirations. My sincere thanks also go to Mr. **Chander Thakur** for their support and help.

Special thanks to my close friends **Dr. Jaspreet Kaur**, **Anirudh Sharma**, **Shweta Sareen**, **Dr. Indrajeet, Dr. Bhupender Pal**, **Rupinder Kaur** and **Dr. Vishal Mutreja** for always standing by my side and sharing a great relationship as compassionate friends. I will forever cherish the warmth shown by them, whose smiling face always made me refreshing and also for

unforgettable memories during my research work. I gained a lot from them, through their personal and scholarly interactions.

I am thankful to my labmates **Alka Goyal, Richa Goel, Dr. Alka Sharma, Richa Rani, Dr. Meenakshi Verma, Gulsan Sharma, Anila, Roopchand Prajapati** and **Akul Sen Gupta** who all have extended their support during my research work.

Most of the results described in this thesis would not have been possible without the help of laboratories at the institutes like, **SAI** labs, Thapar University, Patiala, **SAIF**, Punjab University, Chandigarh, **IISER**, Mohali Research Institute and **NCI**, USA is gratefully acknowledged for investigating antitumor activities.

I gratefully acknowledge, **Department of Science and Technology** for **INSPIRE SCHEME** for providing me financial support during my Ph.D. research work.

I am especially thankful to my father Mr. **Hem Raj Singla**, mother Mrs. **Sunita Singla,** uncle Mr. **Prem Deep Singla,** aunt Mrs. **Raksha Singla** and younger brother **Tarun Singla** and other family members who have always showered unconditional love on me, encouraged and supported me in every aspect. My mother has been my best friend all my life and I love her dearly and thank her for all her advice and support.

Despite all this co-operation rendered generously by one and all, I am solely responsible for any and all the errors and short comings of this dissertation.

Prinka

ABBREVIATIONS

AIDS	Acquired immunodeficiency syndrome
ATP	Adenosine triphosphate
AR	Analytical reagents
BSA	Bovine serum albumin
ct	Calf thymus
CNS	Central nervous system
CDK	Cyclin dependent kinase
Flt-3	Cytokine receptor
COX-2	Cyclooxygenase-2
DNA	Deoxyribonucleic acid
DHFR	Dihydrofolate reductase
D4	Dopamine receptors
DMPM	Diffuse malignant peritoneal mesothelioma
DYRKIA	Dual specificity tyrosine-phosphorylation-regulated kinase 1A
EGFR	Epidermal growth factor receptor
EtBr	Ethidium bromide
FRET	Forster resonance energy transfer
GSK-3	Glycogen synthase kinase 3
GI %	Percentage growth inhibition

Hsp90	Heat shock protein 90
HT1AR affinity	Higher-Affinity Agonists of 5-HT1AR
H4R	Histamine H4 receptors
HDAC1	Histone Deacetylase 1
hCA I	Histone cytosolic isoform
hERG activity	Human Ether-a-go-go-related gene
H-bonding	Hydrogen bonding
HEPES	(4-(2-Hydroxyethyl)-1-piperazineethanesulfonic acid)
HMPMM	Hydroxymethylpentamethylmelamine
5-HT1A	5-Hydroxytryptamine
5-HT7R	5-Hydroxytryptamine (Serotonin) Receptor 7
IC_{50}	Inhibition concentration
IL2	Interleukin 2
IKK	The I kappa B kinase
JAK3	Janus kinase 3
LC_{50}	Median lethal concentrations
LDR	Ligand–DNA ratio
LE	Ligand efficiency
mTOR	Mammalian target of rapamycin
MGMID	Mean-graph midpoint
MTX	Methotrexate

MT1	Melatonin receptor agonists
MSK-1	Mitogen- and stress-activated protein kinase-1
NCI	National Cancer Institute
NK2 antagonist	Antagonists of neurokinin-1
NADPH	Nicotinamide adenine dinucleotide phosphate
NIH3T3	Normal human fibroblasts
nt	Not treated
NMR	Nuclear magnetic resonance
NOE	Nuclear Overhauser effect
PM3	Parameterized model number 3
Phe	Phenylalanine
PI3 kinase-A	Phosphatidylinositol-4,5-biphosphate-3-kinase
PARP-1	Poly ADP ribose polymerase
PLK	Polo kinase
PDB	Protein data bank
AKA/ AKB	Protein kinase C Inhibitors
RNA	Ribonucleic acid
RSK-1	Ribosomal s6 kinase
5-HT	Serotonin receptors
SAR	Structure activity relationship
SRB	Sulforhodamine B

TBK-1	TANK-Binding kinase-1
TLC	Thin-layer chromatography
TGI	Total growth inhibitory
TPSA	Total polar surface area
TCA	Tricyclic antidepressant
TNBC	Triple Negative Breast Cancer
TNFα	Tumor necrosis factor
Tyr	Tyrosine
Trp	Tryptophan
TCS	Two-component signal transduction
UV	Ultraviolet
U.S.	United states
Val851	Valine
VEGFR-2	Vascular specific growth factors
VchCA	Vibrio enzyme
ZSTK474	(Difluoromethyl)-1-[4,6-di-(4-morpholinyl)-1,3,5-triazin-2-yl]-1*H*-benzimidazole
CH_3COOH	Acetic acid
$B(OH)_2$	Boronic acid
CO_2	Carbondioxide
$CHCl_3$	Chloroform

Cs_2CO_3	Cesium carbonate
$CDCl_3$	Deuterated chloroform
D_2O	Deutrated water
DIPEA	N,N-Diisopropylethylamine
DMF	Dimethylformamide
DMSO	Dimethylsulfoxide
C_2H_5OH	Ethanol
DMSO-d_6	Hexadeuterodimethyl sulfoxide
HMTA	Hexanmethylenetetramine
HCl	Hydrochloric acid
NH_2NH_2	Hydrazine
I^-	Iodide
IPA	Isopropranol
HNO_3	Nitric acid
$POCl_3$	Phosphorusoxychloride
K_2CO_3	potassium carbonate
KI	potassium iodide
Na^+	Sodium
$NaHCO_3$	Sodium bicarbonate
NaCl	Sodium chloride
Na_2CO_3	Sodium carbonate

NaOH	Sodium hydroxide
NaH	Sodium hydride
$SnCl_4.2H_2O$	Stannous chloride
H_2SO_4	Sulphuric acid
THF	Tetrahydrofuran
$Pd(PPh_3)_4$	Tetrakis(triphenylphosphine)palladium
TFA	Trifluoroacetic acid
NH_2CONH_2	Urea

Table of Contents

INTRODUCTION

Despite many therapeutic successes, cancer is a major worldwide public health problem and the leading cause of human mortality exceeded only by cardiovascular diseases. In 2015, there are estimated 16,58,370 new cancer cases diagnosed worldwide and about 5,89,430 cancer deaths are reported in the United State. This supplemental data set provides the estimated numbers of new cancer cases and deaths in 2015 by state for 21 cancer sites and by age group for the major sites (lung, breast, colorectum, and prostate).[1] More recently, components of the mitotic machinery have been targeted in an attempt to develop novel anticancer agents[2] that are used to control the growth of cancerous cells. Development of new anticancer drugs and more effective treatment strategies for cancers are of utmost importance as traditionally prescribed chemotherapeutic agents have problems with toxicity and drug resistance. In recent years, great advances in elucidating molecular structures have allowed precise determination of the interaction between proteins and therapeutic agents. Identifying the exact nature of interaction for a drug is the key to control its specificity and reducing side effects.[3] Detailed structural information are employed to design molecules that bind to specific targets, and many of these efforts are aimed at enzymes. Enzyme inhibitors have been used as therapeutic agents by interacting with targets through the weak linkage of hydrogen bonding and van der Waals contact that result in side effects due to the shorter residency time of the drug at the target, allowing more nonspecific interactions with non-target molecules. Nitrogen-containing heterocycles are present in a wide variety of bioactive natural products and biological molecules that acts as good drug candidates. Specifically, triazine, pyrrolopyridine, quinazolinone, pyrazolopyrimidine and benzimidazole, and their derivatives, which belong to nitrogen-containing heterocyclic compounds, caused universal concerns due to their widely and distinct pharmaceutical activities.

Triazine moiety has been matured into indispensable heterocyclic scaffold that make it one of the extensively studied heterocycle with wide range of biological activities[4] like anticancer,[5] antimalarial,[6] antiprotozoal,[7] antiviral,[8] antimicrobial,[9] antitubercular, antiulcer, anti-inflammatory etc. Some of triazine derivatives available in the market are shown in Figure 1. These diverse properties of triazine derivatives have prompted us to synthesize new molecules in order to study their different biological activities.

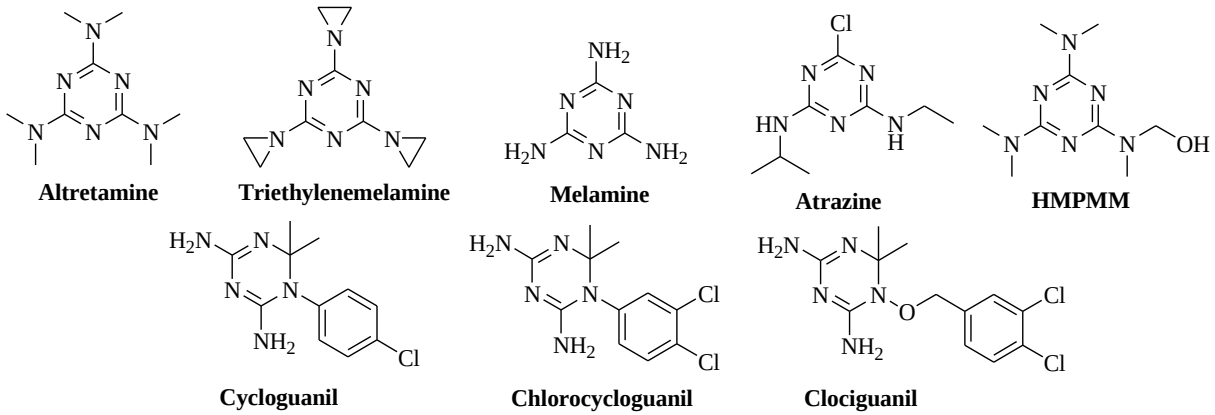

Figure 1. Biologically active moieties containing the 1,3,5-triazine core unit.

Fused heterocyclic compounds containing sulphur, nitrogen or oxygen atom(s) in the core structure shows number of pharmacologically and biologically activity by themselves or are essential components of very important naturally occurring substances (*i.e.*, nucleic acids, proteins). Fused rings such as pyrazolopyrimidine[10] (**1**), pyrrolopyridine[11] (**2**), quinazolinone[12] (**3**), purine[13] (**4**), azapurine[14] (**5**), thiazolopyrimidine[15] (**6**), pyrimidopyrimidine, pyrazolopyridine etc. (Figure 2) have high impact in the field of pharmaceutical sciences like antimalarial, anticancer, analgesic, antiinflammatory, antiviral, antimicrobial, antileishmanial and inhibitors of CDK2, EGFR, DHFR and PI3 kinase-A. With their wide range of pharmacological applications, these fused heterocycles have attracted the attention of numerous researchers over many years.

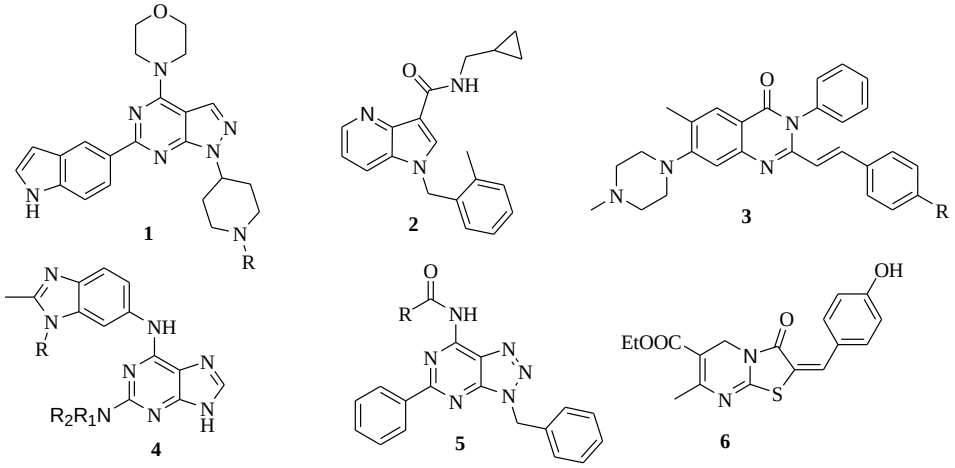

Figure 2. Biologically active compounds containing fused heterocyclic unit.

Moreover, number of important compounds containing benzimidazole nucleus are also used in different therapeutic areas such as proton pump inhibitors (omeprazole), antihypertensives[16]

(candesartan), antihistaminics (astemizole), antihelmintics[17] (albendazole), as well as several other kinds of still investigational therapeutic agents, including antitumors[18] and antivirals.[19] Benzimidazole is usually attributed to their selective binding to parasite β-tubulin and DNA minor groove, serotonin receptors (5-HT), histamine (H4) receptors, dopamine (D4) receptors,[20] and act as inhibitors of TCS **(7)**, PARP-1 **(8)**,[21] NK2 antagonist **(9)**[22] that inhibit a large array of DNA and RNA processing enzymes, such as Topoisomerase 1 **(10)**,[23] DNA and RNA polymerase **(11)**[24] and DNA intercalating agent (**12**)[25] (Figure 3).

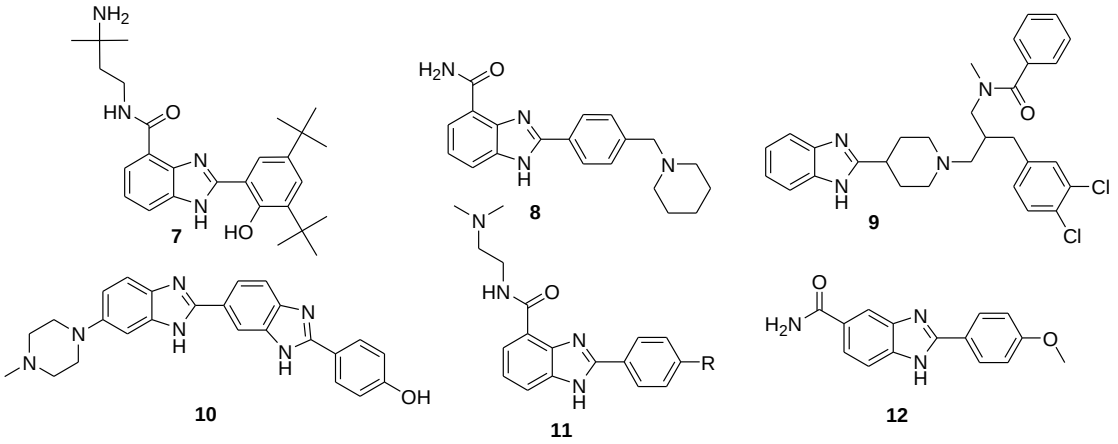

Figure 3. Biologically active compounds containing benzimidazole moiety.

The strategy of using substituted heterocyclic moieties, benzimidazole linked to triazine derivatives or other fused heterocycles are particularly attractive as it is expected to provide a scope of preparing more interactions with the target site and thus, further affect the activity. In the quest for biologically potent agents, we have designed and synthesized a new series of triazine and fused heterocyclic molecules and evaluated *in vitro* as human cancer cell lines and dihydrofolate reductase kinase inhibitors as anticancer agents. These compounds were further studied for their interaction with DNA and bovine serum albumin. The role of different structural fragments in affecting the properties of the drug has also been studied on the basis of structure-activity relationship (SAR). The present work in this dissertation has been divided into following parts:

Chapter 1: Review of Literature

Chapter 2: Triazine-benzimidazole analogues

Chapter 3: Fused heterocyclic moieties linked benzimidazoles

CHAPTER-1
REVIEW OF LITERATURE

Design, synthesis and evaluation of molecules with some human therapeutic values remain one of the main objectives of organic and medicinal chemistry. Synthesis of triazine and fused heterocyclic motieties has attracted increasing interest because of their utility for various biological receptors with high degree of binding affinity. In the pharmaceutical industry, over 75% of the top two hundred branded drugs have heterocyclic fragments in their structures. Nitrogen containing heterocyclic motif is 'Master Key,' as acting at different targets to elicit varied pharmacological properties by inhibiting the action of an inducible membrane protein.

1.1. BIOLOGICAL ACTIVITY OF TRIAZINE BASED MOLECULES

Owing to immense synthetic importance and varied bioactivities exhibited by triazine derivatives, efforts have been made from time to time to generate libraries of these compounds due to its specific structure and electronic properties that offer access to useful molecules.

Smith *et. al.*[26] has been designed and synthesized a highly selective series of inhibitors of the class I phosphatidylinositol 3-kinases (PI3Ks) that starts from the dual PI3K/mTOR inhibitor **1**. A structure-based approach was used to improve potency and selectivity, resulting in the identification of compound **2** by the replacement of benzimidazole with pyridyl moiety and introduction of methylsulphonylpiperazine group at 5-position of pyridine ring,[27] as a potent inhibitor of the class I PI3Ks with excellent selectivity over mechanistic target of rapamycin (mTOR). Replacement of phenyl with pyridyl ring at 2-position of pyridyl moiety of triazine ring **3** showed potent, selective, and efficacious activities in both the biochemical and cellular assays. To pursue a hybrid strategy for second generation potent pan class I PI3K/mTOR inhibitors was exemplified by generic structure **5** that address the shortcomings of compound **3** that improved solubility over compound **4.**[28] The chloropyridyl sulfonamide affinity pocket moiety of **4** has been replaced with 2-methoxypyridyl group of **3** to give a pan class I PI3K inhibitor **5** with a moderate (>10-fold) selectivity over the mammalian target of rapamycin.[29]

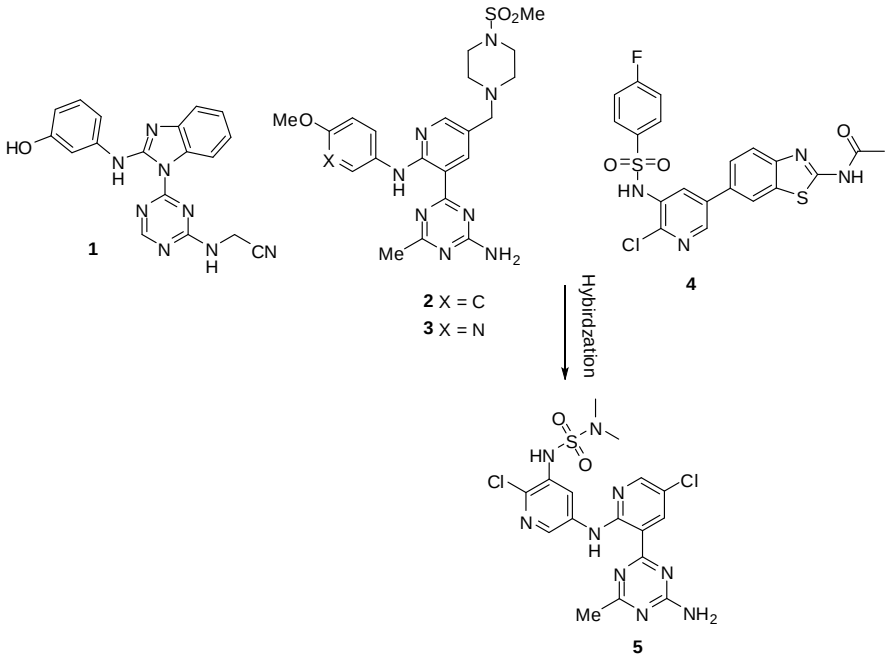

2-(Difluoromethyl)-1-[4,6-di-(4-morpholinyl)-1,3,5-triazin-2-yl]-1*H*-benzimidazole[30] (ZSTK474), **6a** is a potent ATP competitive pan class I PI3K inhibitor. Replacement of both morpholines in (**6a**) with 2,6-bridged morpholines (**6b)** led to 19-fold increase in mTOR selectivity due to the deeper binding pocket in mTOR relative to PI3K. Substitution at 4 and 6 positions of the benzimidazole ring with 6-amino-4-methoxy analogue **7a** displayed greater than 1000-fold potency enhancement over the corresponding 6-aza-4-methoxy analogue **7b**.[31]

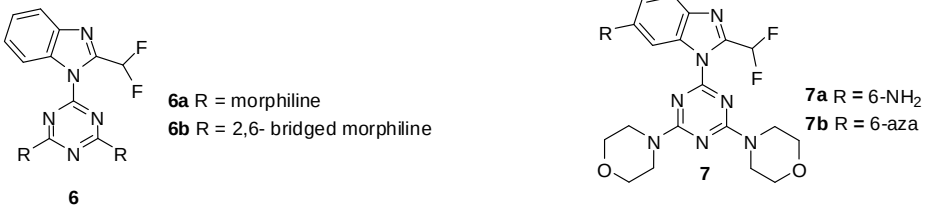

Peterson *et. al.*[32] aimed at developing ATP-competitive mTOR inhibitors by transposing benzimidazole nitrogen (**8**) to provide imidazopyridine (**9**) that maintained the broader planarity between the triazine hinge-binder and the imidazopyridine ring which was essential for good potency. A series of tetrahydro-β-carbolines and *s*-triazine hybrids were evaluated for their cytotoxicity against human cancer cell lines and normal human fibroblasts (NIH3T3) that led to discovery of racemic compounds (**10a-c)** which has shown selectivity in cytotoxicity towards oral cancer cell line; while their enantio pure **10d**, trans forms are less active and non-selective.[33]

Compound **10d** showed 2.5 times more selectivity towards MCF7 cells over normal fibroblast NIH3T3 cells.

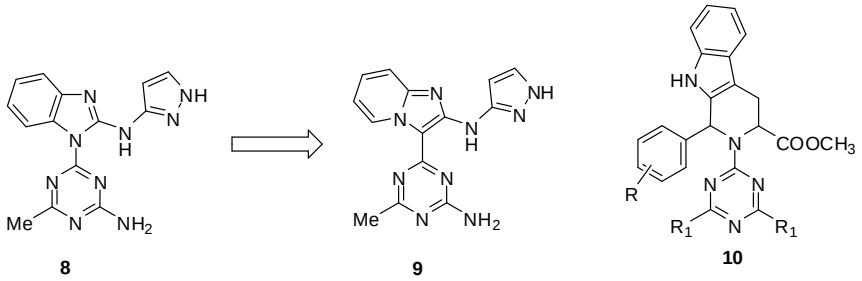

8 **9** **10**

10a DL, Trans; R = 4-methyl; R_1 = N-methylpiperazine
10b DL, Trans; R = 4-methyl; R_1 = propylamine
10c DL, Trans; R = 4-methoxy; R_1 = propylamine
10d L, Trans; R = 4-methoxy; R_1 = N-methylpiperazine

Venkatesan and co-workers[34,35] have been reported a series of morpholino triazine derivatives bearing 3-oxa-8-azabicyclo[3.2.1]octane as potent dual PI3K/mTOR inhibitors. Morpholine in **11** was kept, as it formed a pivotal hinge region hydrogen bond interaction with Val851 and also urea appendage involved in vital hydrogen bond interactions with PI3Ka in the solvent exposed region. Replacement of one of the bis-morpholines in lead compound **11** (PKI-587) resulted in compound **12**, as an orally efficacious dual PI3-kinase/mTOR inhibitor.

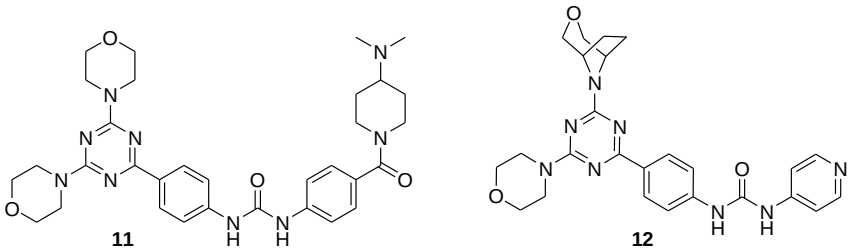

11 **12**

Saczewski *et. al.*[36] has been synthesized novel 2-amino-4-(3,5,5-trimethyl-2-pyrazolino)-1,3,5-triazine derivatives that caused considerable growth inhibition on distinct tumor cell lines. Compound **14** with 5-nitrothienyl substituent is proved to be superior to 6-bromomethyl derivative (**13**) but elimination of the nitro group (**15**) yielded compound with no anticancer activity. A new series of aromatic benzenesulfonamides incorporating with compact moieties at the triazine (**16)**, such as amino, hydrazino, ethylamino, dimethylamino or amino acyl groups, showed more activity but incorporation of bulky groups viz., n-propyl, n-butyl, diethylaminoethyl, piperazinylethyl, pyridoxal amine or phenoxy have been shown less effectiveness towards physiologically relevant carbonic anhydrase isozymes.

Raeppel *et. al.*[37] has been diversified new therapeutic agents (s-triazin-2-ylamino)methyl]-*N*-(2-aminophenyl)benzamides (**17**) brought about to an increase in potency against HDAC1 with concomitant increase in anti-proliferative activity.

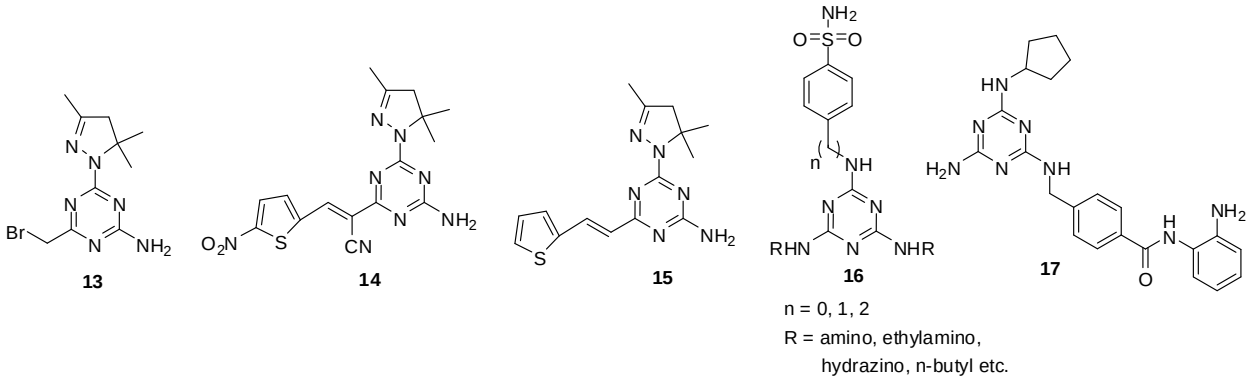

Sączewski *et. al.*[38] has been evaluated triazine derivatives of iminoacetonitriles bearing (4-phenylpiperazin-1-yl) substituent (**18a)** at 6-position of triazine ring, exhibited remarkable activity and selectivity for melanoma MALME-3M cell line. Substitution of the phenyl ring with either 4-nitro (**18b**) or 3-chloro (**18c**) resulted in reduction in activity. Symmetrical trisubstituted triazine hydrazones **19a** and **19b** bearing fluoro and chloro substituents respectively exhibited broad spectrum of antitumor activity against the human liver carcinoma cell line HepG2 with % inhibition of 4.32 and 6.41, while in case of human cervix carcinoma cell line HeLa, compounds **19c** and **19d** bearing nitro and methoxy substituents showed % inhibition of 8.36 and 9.37 respectively.[39]

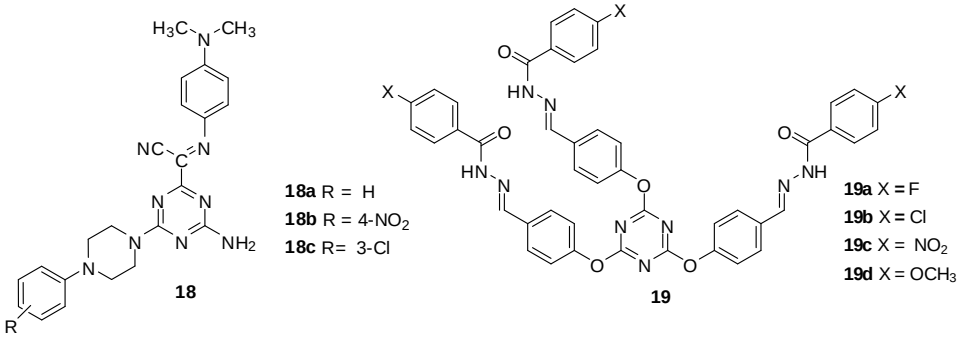

Supuran *et. al.*[40] has revealed that the slow cytosolic isoform hCA I was moderately inhibited by triazinyl-substituted benzenesulfonamide compounds **20**-**22**, while difluoro- and methylamino derivatives of sulfanilamide (**20a** and **22**) indicated the best hCA I inhibitors than its longer congener difluoro derivative of **21a**, 2.3-fold less effective. The secreted isoform hCA VI was poorly inhibited by **20** and better inhibited by compounds **20**, **21(a-c)** and **22**. Compounds possessing a longer spacer between the triazine and benzenesulfonamide rings (n = 2), such as

20c and **21(a-c)** were more effective inhibitors compared to the sulfanilamide derivatives (n = 0). Best hCA XIV inhibitor of this series was difluorotriazine derivative of 4-aminoethylbenzenesulfonamide **21a**.

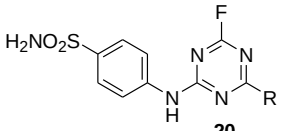

20

20a R = F
20b R = $NHCH_2CH_2OH$
20c R = $NHCH_3$

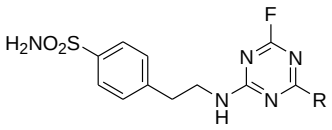

21

21a R = F
21b R = $NHCH_2COOMe$
21c R = $NHCH_2COOH$

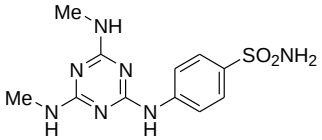

22

Seo and co-workers[41] have been attempted to discover and screen the antiproliferative activities of triazine (**23a-c**, **24a-c** and **25a-b**) against gefitinib-resistant H1975 cells. Compound **23a** was the most effectively inhibited cell proliferation among other triazine compounds and most compounds **23(a**,**c**), **24(a-c**) and **25a**,**b** blocked cell proliferation in a dose-dependent manner with modest efficacies in cell proliferative assay. The expression level of Her2 was substantially decreased upon the treatment of cells with **25b** at a concentration of 50 μM, while the incubation with 100 μM of compound **25b** almost completely depleted Her2 protein and significantly degraded Met and Akt. Thus, by introducing benzyloxy, phenylamino and phenoxy groups at the hydrophobic moiety of 2,6-dimethylbenzyloxy group at 6-position of 2-amino-4-chloro-1,3,5-triazine led to significant improvement in the potency. 2-Amino-4-chloro-1,3,5-triazine moiety of **25b** bound to the hydrophilic pocket of Hsp90 through hydrogen bonding while 2,6- dimethylphenyl moiety of **25b** reached the hydrophobic region of Hsp90 for van der Waals interactions with antiproliferative activity against H1975.

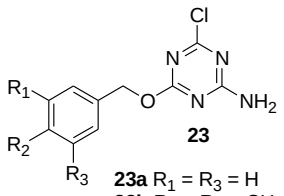

23

23a $R_1 = R_3 = H$ $R_2 = OMe$
23b $R_1 = R_2 = CH_2OCH_2$ $R_3 = H$
23c $R_1 = R_2 = R_3 = OMe$

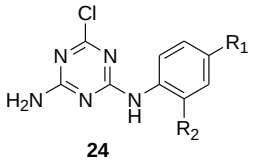

24

24a $R_1 = R_2 = H$
24b $R_1 = OH$ $R_2 = H$
24c $R_1 = H$ $R_2 = Cl$

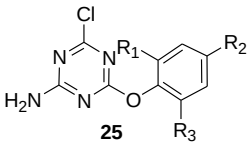

25

25a $R_1 = R_3 = H$ $R_2 = OMe$
25b $R_1 = R_3 = Me$ $R_2 = H$

Suda *et. al.*[42] described 2-amino-1,3,5-triazines bearing a tricyclic moiety as heat shock protein 90 (Hsp90) inhibitors having strong anti-proliferative activity against human cancer cell lines (HCT116). The transformation of methyl group on the sulfur atom to other substituent's improved the affinity while retaining the tricyclic moiety. Introducing hydrogen bond acceptors like acetylamino (**26a**) and mesylamino (**26b**) increased affinity to Hsp90 by 4- to 8-fold in comparison with that of compound **27a**. Introduction of the acetylamino group **27b** to compound

26a decreased affinity by 10-fold while methyl group (**27c**) slightly improved affinity and chiral methyl group (**27d)** showed almost the same activity as racemate (**27c**). These data suggested hydrophobic substituents are favorable on a methylene carbon, but introducing the geminal dimethyl group (**27e**) as a hydrophobic substituent caused a significant decrease in affinity. Among these, **27f** showed strong *in vitro* cell growth inhibition against human cancer cell lines HCT116.

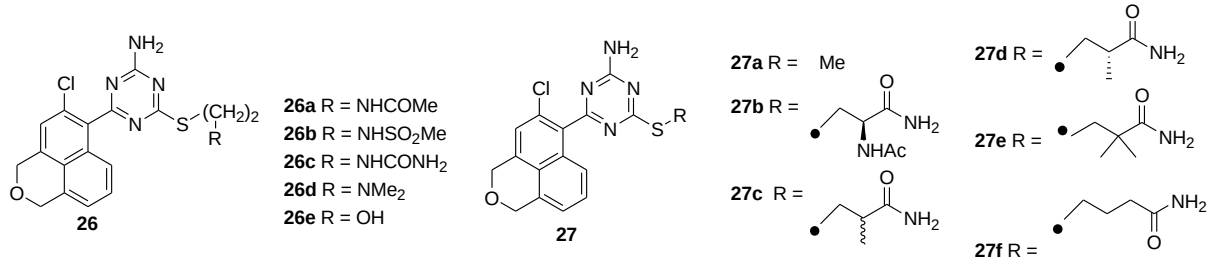

Kononowicz *et. al.*[43] synthesized and evaluated a series of novel triazine derivatives with different aryl substituent's at 6-position for histamine H4 receptor (H4R) affinity in S*f*9 cells. Substitution of chlorine in the *para* position (**29a)** of phenyl ring was the most potent due to highest affinity with hH4R. By changing substituent position from *para* to *meta* (**29b**) and to *ortho* (**29c**), affinity has drastically reduced. Change of chlorine, in the *para*-position for different substituent's like fluoro, bromo, iodo led to decrease in potency while unsubstituted analogue (**28**) had higher affinity. Two fluorine substituent's at 2- and 6-positions (**29d**) were less beneficial than two (**29e**) or three atoms (**29f**) at 3,5- and 3,4,5-positions respectively.

Westwel and co-workers[44] has been synthesized 4-amino-*N*-phenyl-6-(arylamino)-1,3,5-triazin-2-carbohydrazides (**30**) and 4-amino-*N*-benzyl-6-(arylamino)-1,3,5-triazin-2-carboxamides (**31**) as anticancer agents in Rad6B expressing human cancer cell lines MDA-MB-231 and MCF-7. Compounds **31a**, **31b** and **31d** were found to be essentially inactive in the MDA-MB-231 cell line but **31a** and **31b** were inactive in MCF-7 cells. In contrast, compound **31c** was found to be the most active compound tested against the MCF-7 cell line with IC_{50} value of 1.97 µM, with moderate activity against MDAMB-231 with IC_{50} value of 32.9 µM.

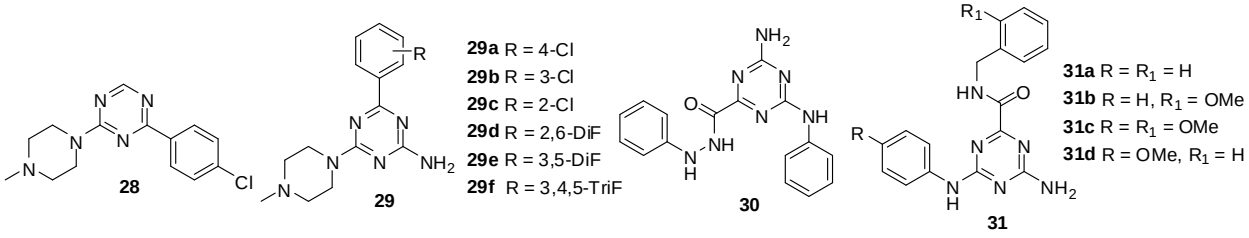

1.2. FUSED HETEROCYCLIC BASED MOLECULES

Fused heterocyclic compounds have provided a platform for the rapid exchange of research in the areas of organic, pharmaceutical, analytical, and medicinal chemistry. Every year large number of drugs being introduced in pharmacopeias is fused heterocyclic based molecules to improve the quality of life for humankind.

1.2.1. Pyrrolopyridine

Small substitution at 3-position of phenyl ring of urea (**32a**) like methyl, nitro or methoxy group (**32b-d**) gave upto 1000-fold increase in activity by targeting the lipophilic sub pocket. Excellent potency was maintained to both biochemical ADP-Glo and cellular assays by substitution with 6-fluoro-3-(trifluoromethyl)phenyl ring at the urea with phenyl ring (**32e**) pyridyl ring (**33**) at 5-position of pyrrolopyridine.[45] Introduction of phenyl moiety at 6-position of pyrrolo[2,3-*b*]pyridine-1-carboxamides resulted in ten-fold increase in activity (**34a**). Substitution of pyridine ring with 4-fluoro or 4-methoxyphenyl groups (**34b**) showed good inhibitory activity against PARP-1, whereas substitution with 2-fluorophenyl ring (**34c**) led to decrease in the inhibitory activity but substitution with 4-phenyl at phenyl ring (**34d**) resulted in complete loss of the enzymatic activity.[46]

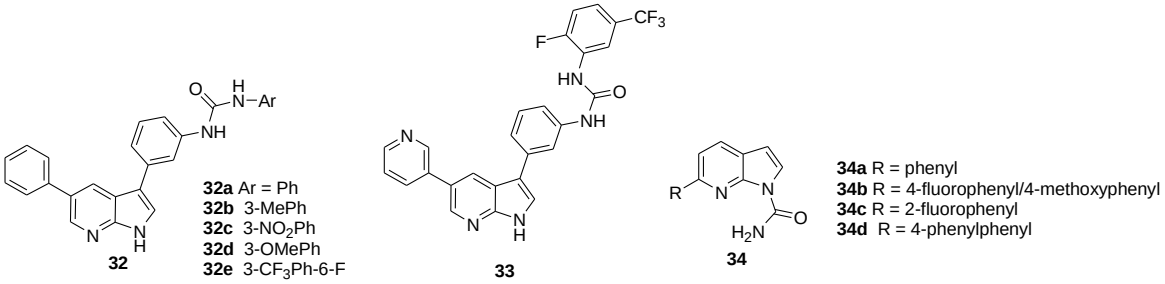

Replacement of *N*-acylurea moiety in pyrrolopyridine **35a** with conformationally constrained 2-pyridone, 4-pyridone, and pyridine *N*-oxide analogues **35(b-g)** resulted in potent Met kinase inhibitory activity.[47] Compound with *p*-fluorophenyl (**35c)**, in case of 2-pyridone, possessed potent inhibitory activity against Flt-3 and VEGFR-2 kinases while replacement of the phenyl ring with *tert*-butyl (**35d)** or cyclopropyl groups (**35e)**, significantly reduced the kinase inhibitory activity. The cycloalkyl ring at 4-position of 1*H*-pyrrolo[2,3-*b*]pyridine-5-carboxamide derivatives was important for JAK3 inhibitory activity, due to the interaction with the hydrophobic cavity of JAK3.[48]

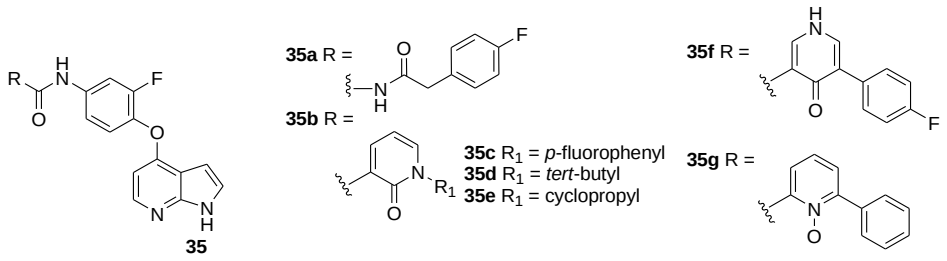

Substitution of cycloalkyl ring with piperidine modulates lipophilicity and metabolic stability, and polar functional groups like acetyl (**36a**) and mesyl (**36b**) at piperidine led to weak JAK3 inhibitory activity due to unfavorable for binding to JAK3 while *N*-benzyl piperidine analogue **36c** exhibited 4-fold increase in JAK3 inhibitory activity as compared to *N*-methylpiperidine **36d**. Optimization of excellent binding and cellular potencies was performed by keeping the trifluoromethyl substituent at 4-position of *N*-phenyl ring in compounds **37a** and **37b** while small methyl substituent led to major changes in receptor dissociation half-life with similar binding potency (**37b**).[49] Isoxazolol, **38b** was explored by isosteric replacement of carboxylic group of **38a** (VX-787), with improved potency and selectivity that depends on orientation of negative charge against influenza A.[50]

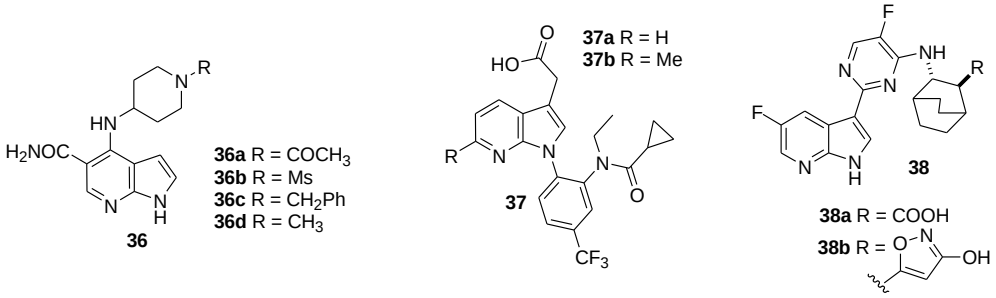

Exploration of pyrrolopyridine substituted with 3-(trifluoromethyl)-1*H*-pyrazol-5-yl group at 5-position along with 2-chloro-6-fluorophenyl substitution at 2-position (**39a)**, provided the best potency and inhibiting activity of calcium influx and IL2. The potency was dropped dramatically by introducing polar groups like tetrahydropyran (**39b**) or benzyl group (**39c**).[51] Zafforoni *et. al.*[52] synthesized and evaluated 1*H*-pyrrolo[2,3-*b*]pyridine derivatives in which the spacer is constituted by thiazole ring between pyrrolopyridine and substituted indole for their biological effects in experimental models of diffuse malignant peritoneal mesothelioma. Among this series, three most active compounds **40(a-c)** acted as cyclin-dependent kinase 1 inhibitors that consistently reduced DMPM cell proliferation and induced a caspase-dependent apoptotic response. Substitution of methyl substituent at pyrrole nitrogen in compound **40c** was the most

active compound. Fluorine substitution at 5-position of indole had no significant influence on the biological activity whereas chlorine substitution brought about a decrease in the activity (**40b**).

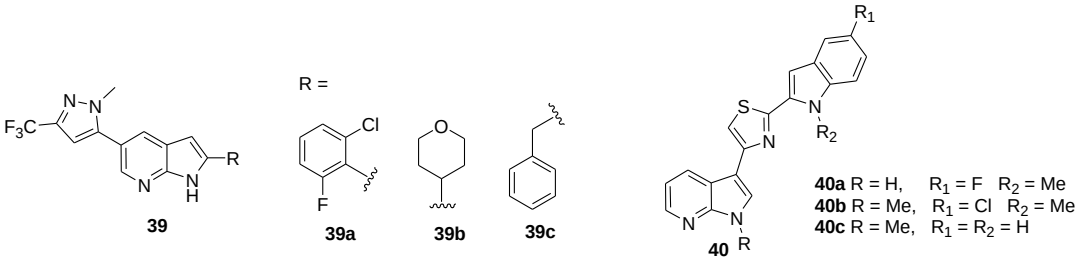

Dodd *et. al.*[53] optimized a series of 3,5-diaryl-1*H*-pyrrolo[2,3-*b*]pyridine having hydroxy groups (**41a**), showed high inhibitory potencies for inhibition of DYRKIA kinase as compared to their methoxy analogue (**41b**). Substitution on aryl moieties demonstrated that 4-OH function on C5 phenyl (**42a**) afforded a slight improvement in inhibitory potency as compared to 3-OH (**42b**) and 2-OH (**42c**) derivatives. Addition of 3,4-dihydroxy group (**42e)** doubled the DYRK1A inhibitory potencies with respect to the 4-OH derivative **42a**. Compounds in which both aryl rings were substituted with various patterns of mono- and/or dimethoxy groups found to be less potent than their corresponding hydroxy derivatives while the trimethoxy derivative **43b** was considerably more active than their corresponding dimethoxy derivative (**43a**). The presence of di 4-hydroxy groups was found to be essential for high activity (**43c**). A 2,4-dihydroxyphenyl group at C5 led to lowering the activity (**43d**), while the closely related 3,4-dihydroxy analogue (**43e**) displayed an even higher inhibitory potency.

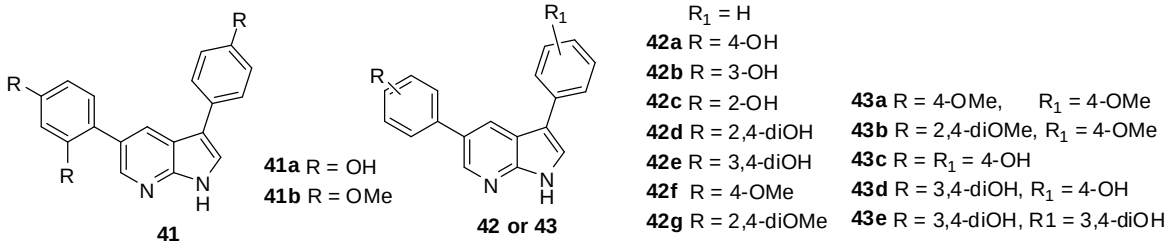

1.2.2. Quinazolinone

A series of 3,5-diaryl isoxazoline and isoxazole linked 2,3-dihydro quinazolin-4-one hybrids with different linker architectures were evaluated for their anticancer activity. Among the series, compound **44** exhibited significant anticancer activity against human cancer cell lines and also identified as an effective cyclin B1 inhibitor as well as CDK1 inhibitor.[54] A multi-step solid phase approach was developed for the parallel synthesis of structurally diverse

aminobenzimidazole that is separately tethered with a variety of biologically important heterocycles, such as quinazoline-2,4-diones (**45a**) and thioxoquinazolin-4-ones (**45b**), and tested for IKK and TBK-1 inhibition at concentration of 10 μM. Amongst the series, benzimidazole tethered thioxoquinazolin-4-one (**45b)** elicited significant inhibition to IKK2, IKKε and TBK-1 respectively, while rest of compounds showed activity less than 10%.[55]

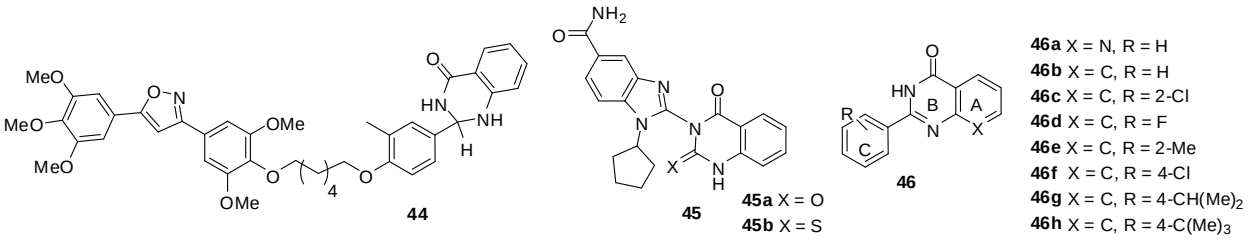

Lehtio *et. al.*[56] identified potent tankyrase inhibitors by replacement of A-ring from **46a**, yielded **46b** that is twofold more active. The ortho-chlorine substitution at the C-ring in **46c** caused lower potency and other small substituents like fluoro (**46d)** and methyl (**46e)** in this position did not improve the potency. The increased potency of para-chlorine (**46f)** was preserved by highlighting the importance of the hydrophobic substituent at this position as compared to the chlorine substitution at ortho-position in **46c**. Replacement of the para-chlorine with a larger aliphatic substituent like isopropyl (**46g)** and *tert*-butyl (**46h)** increased the hydrophobic interaction that caused 2-fold increase in potency. Increasing the size and hydrophobicity of the aliphatic para-substituent from methyl, to isopropyl and to *tert*-butyl enhanced the potency of the compound.

Despite the poor physico-chemical properties of hit compound **47a**, Nencini *et. al.*[57] has decided to modify the substituent on the piperazine ring that provided structural novelty to scaffold with improved activity in glioblastoma, gastric and sarcoma tumors. Replacement of NH group in compound **47a** with *N*-methyl analogue (**47b**) had a comparable IC_{50} that suggested hydrogen bond donor in this position is not essential for the activity. Compounds bearing *N*-benzyl (**47c**) and *N*-alkyl (**47d**) derivatives were inactive suggesting that presence of basic nitrogen on the piperazine ring were not tolerated for the activity, while beneficial effects on solubility were achieved with the complete removal of the aromatic portions (**47d)**. However, replacement of the carbonyl group in 2-position of the quinazoline ring gave inactive compound (**48**) that indicates hydrogen bond acceptor in this position was important for activity but removal of the carbonyl at 4-position (**49**) did not affect potency.

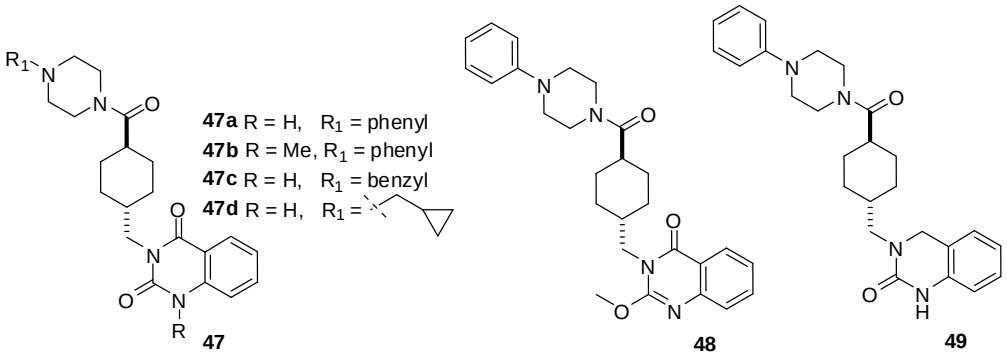

Compound **50a** with 6-nitro-3-allyl at quinazolinone showed very good inhibitory activity[58] but 6-nitro-3-benzyl (**50b)** exhibited moderate activity. Among all, 6-methyl-3-allyl and 6-methyl-3-benzyl derivatives (**50c** and **50d)** were very strong inhibitor of hCA II and VchCA along with a medium potency inhibitors of the cytosolic isoform hCA I. Scaffold optimization of quinazolinedione *N*-benzyl entity (**51a**), by increasing steric bulk at the 4-position of phenyl ring by methyl (**51b**) to ethyl (**51d**) to iso-propyl (**51e**) resulted in improved potency. Consequently, the 4-nitro (**51c)** and the 4-isopropyl (**51e)** groups showed the best potency to viral titer assay efficacy and cytotoxicity profile.[59] Generally, 5-HT7R selectivity and 5-HT1AR affinity for both receptors is influenced by arylpiperazine moiety with respect to elongation of the alkyl chain spacer and nature of the terminal amide fragment.[60] Elongation of chain linker from four (**52a**) to five methylene (**52d**), lower affinity towards both 5-HT1A and 5-HT7 receptors were observed. The 3-chlorophenyl derivatives **52b** and **52e** displayed the highest affinity values for 5-HT1AR and 5-HT7R, whereas the corresponding 4-chlorophenyl derivatives **52c** and **52f** showed a decrease in affinity towards both receptors. Introduction of 2-ethoxyphenyl group (**52g**) acted as dual ligand that led to the highest affinity values for 5-HT7R and 5-HT1AR.

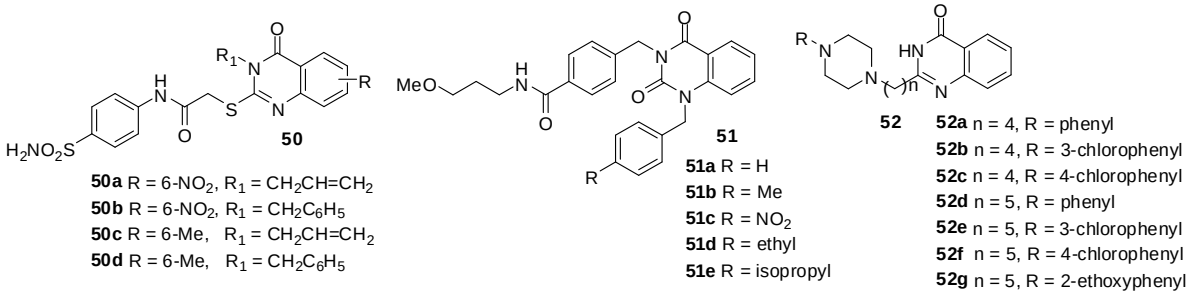

A series of 2-(1,3,4-thiadiazolyl)thio-6-substituted-quinazolin-4-one analogues (**53a-h**) and 2-(1,3,4-thiadiazolyl)thio-6-substituted-quinazolin-4-one analogues (**54a-g**) were evaluated for *in vitro* DHFR inhibition, antimicrobial, and antitumor activities.[61] Compounds **53d, 53g** and **53h** proved to be the most active DHFR inhibitors while compounds **53a**,**b**, **54c,d**,**f**, **55**, **56a,b** were

shown moderate activity and the rest of compounds were inactive. Compounds **53c, 53e** and **53f** showed remarkable broad-spectrum antimicrobial activity against gram negative bacteria while compounds **54c, 54e** and **56a-c** appeared to be selective and active against gram positive bacteria. Compounds **53(a**,**f**,**h**), **54(a**,**e**,**g)** and **56a** also showed broad spectrum antitumor activities.

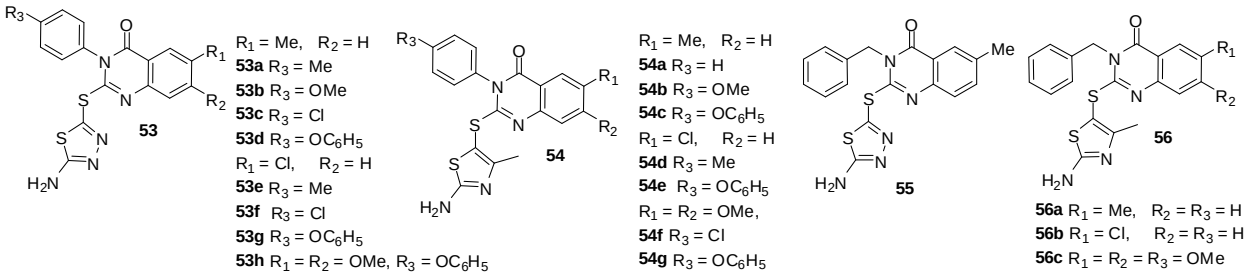

1.2.3. Pyrazolopyrimidine

A series of pyrazolo[3,4-*d*]pyrimidine analogues were synthesized with various amine and ester groups at N-1 and C-4 positions for evaluation of antitumor activities. Compound **57a** exhibited good antitumor activity against human hepatoma carcinoma cells 7402 and 7221 that exerted its cell growth inhibitory effect through partial disruption or suppressed dynamics of microtubules or even through interactions with other cellular targets. Presence of an ester group at N1 in compound **57a** showed more active antitumor agent than acid group **57b** due to increase in lipid/water partition coefficient. Presence of aminoanilino group at 4-position in **57d** enhanced the antitumor effect in comparison to compound **57c**.[62] The hERG activity of **58a** may be due to the presence of a NH_2 group present at 4-position of cyclohexylmethyl group. Replacement of NH_2 group (**58b**) with a hydroxyl group (**58c**) decreased the activity by 6-fold. Increasing the length of the linker between the pyrazole and the cyclohexyl methyl group (**58d**) also decreased the activity whereas by decreasing the length of the linker (**58e**) enhanced Mer activity.[63]

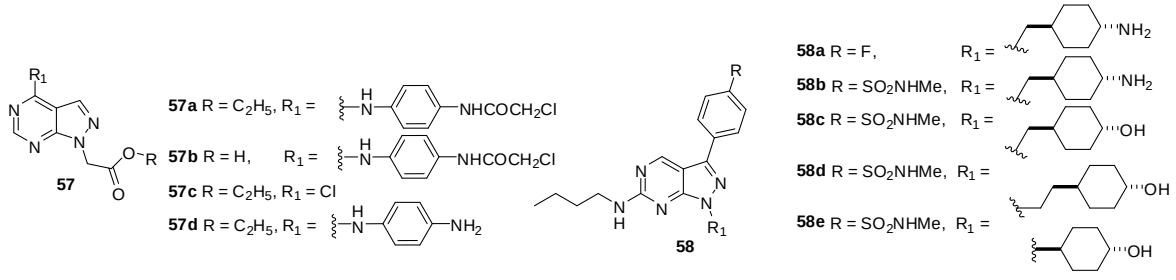

The aliphatic compounds with different carbon-chain lengths have shown good enzyme inhibitory activity (**59a**). The aliphatic chain with –OH at the terminal end was found slightly

more active (**59b**). However, when the terminal –OH was replaced with *tert*-amines (**59c**), there was significant loss of activity. In alicyclic compounds, spacing between the amino group of sulfonamide and the cyclic aliphatic ring showed inverse effect on activity (**59d**) whereas activity was reduced upon replacement of oxygen with $–CH_2$ in cyclic ring (**59e**).[64,65] The (4-methylpiperazin-1-yl)methyl was fixed as R_2 and varied R_1 by substitution of trifluoromethyl group (**60a**) with hydrogen (**60b**) led to a slight drop in bioactivities in both enzymatic and cellular assays. Then, trifluoromethyl group was fixed as R and varied R_2 with different substituent's like 4-methylenemorpholine (**60c**), decreased the enzymatic activity and the antiviability potency against MDA-MB-231 cells while with 1-ethyl-4-methylenepiperidine (**60d**), enzymatic and cellular potencies remained same. However, introduction of 2-(4-methylpiperazin-1-yl)ethanol (**60e**), slightly increased the antiviability against HepG2. Substitution of ethyl group at R_1 (**60f)** showed the highest inhibitory potency against the Src kinase and the most potent antiviability activity against the typical TNBC cell lines MDA-MB-231 and MDA-MB-435. Larger size hydrophobic group like isopropyl (**60a**) at the R_1 position afforded a slightly lower bioactivity as compared to **60f**.[66]

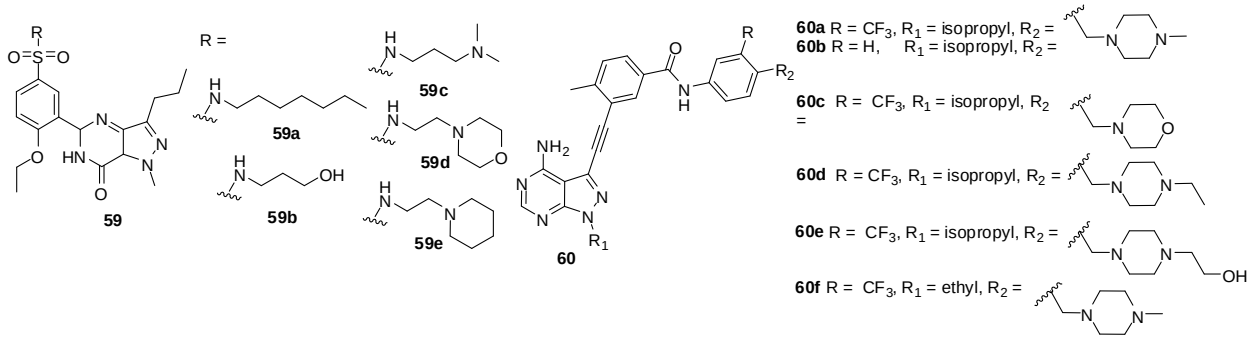

The isopropyl group conferred weak activity against AKA, AKB and CDK1 in **61b** but showed an improvement in metabolic stability. Increasing the size and the lipophilicity by replacement of isopropyl with monocyclic (**61c**), spirobicyclic (**61d**) and fused bicyclic (**61a**) led to dramatic potency enhancement accompanied with significant loss in metabolic stability. Switching from primary amide to substituted secondary amide like pyrrolidine gave rise to **62(a-c)** that exhibited the desired AKA/CDK1 inhibition whereas dimethylaminocarbonyl (**62a)** or methylaminomethylene substituents (**62b**) led to weak activity against CDK1 and AKA as compared to **62c**.[67] For Mer activity, the 4-aminocylcohexylmethylene selected as an optimized group at NH position of pyrazole on the basis of *in vitro* potency, the effect of substitution on the phenyl ring at 3-position of pyrazole was then explored and *para*-methoxy substituted analogue

(**63a)** was 5-fold more potent than *ortho* (**63b)** and *meta* (**63c)**. Electron withdrawing group such as *para*-CF_3 (**63d**) decreased activity, whereas electron donating group like *para*-methoxy (**63a**) increased activity.[68]

A series of highly potent and selective morpholine substituted pyrazolopyrimidine[69] as mTOR inhibitors has been synthesized that contain water-solubilizing groups attached to the 6-arylureidophenyl moiety and displayed superior potency and selectivity over PI3K. Introduction of basic amine at N-1 position of pyrazole ring gave dimethylamino-substituted analogue (**64b)**, significant decrease in mTOR and cellular activity was observed as compared to **64a**. Incorporation of basic amine at *para* position of arylureidophenyl group (**64d-f)** led to inhibitors with sub-nanomolar mTOR and cellular potency while PI3Ka activity was less affected by the addition of basic amines than mTOR activity in the case of dimethylaminoethyl urea (**64c)**.

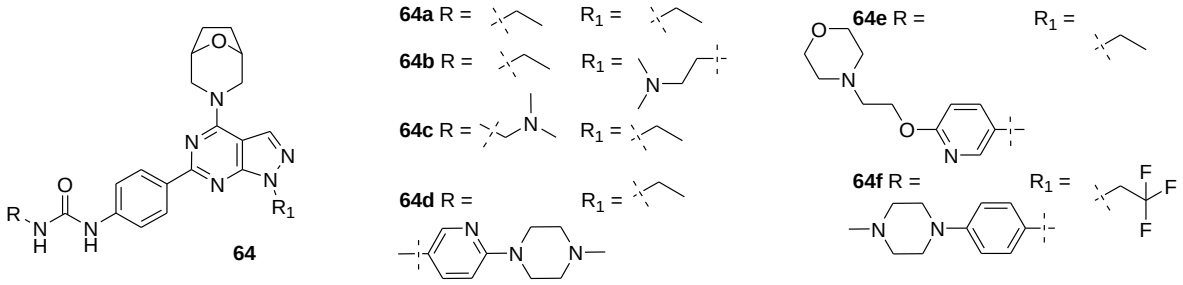

1.2.4. Benzimidazole

A new series of acridinyl-benzimidazole analogues for cyclin-dependent kinase (CDK-1 and CDK-5) has been reported by Sondhi *et. al.*[70] Nature of the substituents on benzimidazole ring of acridinyl-benzimidazoles have major impact on CDK inhibitory activity. The structures of the active compounds indicated that substitution with chloro (**69a)** and nitro (**69b)** groups have enhanced the potency due to the presence of hydrogen bonding acceptor and donor groups in benzimidazole that probably favours interaction with the active site of the CDK enzymes, whereas other analogues have lost their potency. Sharad Verma *et. al.*[71] has been reported the activity pattern of substituted benzimidazole at C-2 and C-4 positions of pyrimidine. The presence of aminobenzimidazole group at either C-2 and/or C-4 positions of pyrimidine **(70)** are critical for CDK1 inhibitory activity. Trifluoromethyl or bromo groups have been shown optimal at C-5 position of pyrimidine ring, while substitution with hydrogen and fluorine results in 200- and 10-fold decrease in potency, respectively.

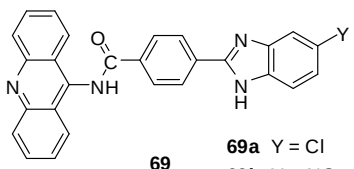

69

69a Y = Cl
69b Y = NO_2

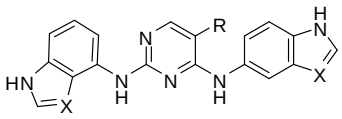

70

70a X = N, R = CF_3
70b X = N, R = Br
70c X = N, R = F
70d X = N, R = H
70e X = CH, R = CF_3
70f X = CH, R = Br
70g X = CH, R = F
70h X = CH, R = H

Bamford and co-workers[72] modified 2-[3-amino-1,2,5-oxadiazol-5-yl] benzimidazole (**71)** (MSK-1 IC_{50}=140 nM), to highly potent (1*H*-imidazo[4,5-*c*]pyridin-2-yl)-1,2,5-oxadiazol-3-ylamine derivative (**72)** (MSK-1, IC_{50}= 3 nM). Compound **72** showed improved potency with respect to compound **71** due to H-bonding interactions of amino-oxadiazole with the hinge region protein backbone and N5 of imidazopyridine with amino acid residue. Compound **73** had low nanomolar activity in both ATP competitive enzyme binding and inhibition of TNFα release in macrophages. Substitution at N1 with lipophilic functionality such as cyclohexyl or cyclopentyl afforded potent MSK-1 inhibitory compounds.[73] Introduction of substituents containing basic nitrogen such as piperidin-4-yl and 4-butylamino derivatives retain MSK-1 potency, advantage from straight alkyl chain analogue, although the shorter chain show some improved selectivity over RSK-1. However, the more bulky piperidin-4-yl compound (**74a**) combined the improved MSK-1 potency, and modest RSK-1 selectivity of cyclohexyl derivative (**74b**) with the modest GSK-3 selectivity.

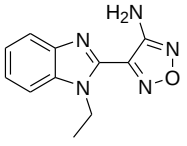

71

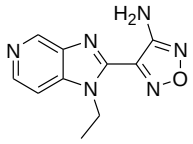

72

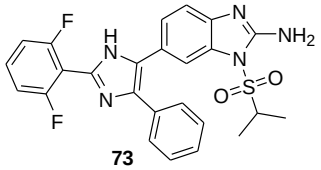

73

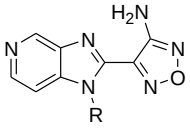

74

74a R = Piperidin-4-yl
74b R = Cyclohexyl

Compound **75** has been found as a potent inhibitor of both PLK1 and PLK3 and moderately inhibited the growth of tumor cells and also has a desirable *in vitro* activity. Compound **76** was more than 300-fold selective for inhibition of PLK1 over PLK3, for evaluating inhibition of polo-like kinase as an approach to cancer treatment. In turn, aqueous solubility has dramatically improved in **76** with heterocyclic substitution at 5- or 6-position of the benzimidazole while maintaining potency as inhibition of PLK1 and PLK3. However, 5-substituted benzimidazoles exhibited 2–3 fold increased cellular potency over 6-substituted counterparts. Several examples have also displayed potent activity against PLK3, although this activity is reduced in the presence of a heteroatom at the *ortho*-position of the heteroaryl ring.[74] Difference in enzyme

potency between compounds with 2-CF_3 or 2-Cl substitution on the benzyl ether **(77a-c),** 2-Cl benzyl ether **(77b)** has shown slightly more potency at the cellular level.

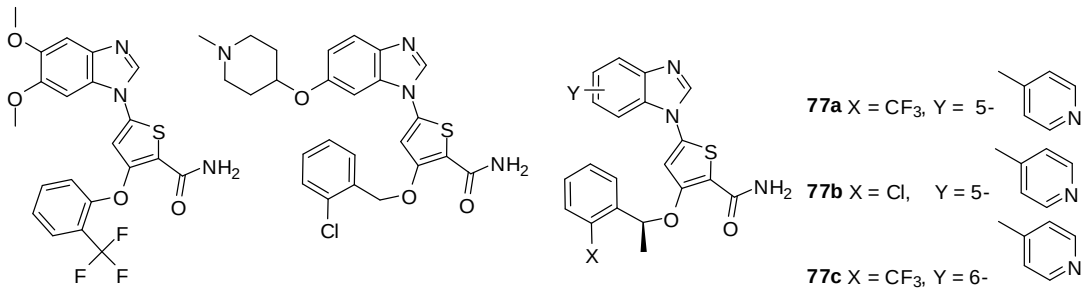

75 **76** **77**

Compound **78** showed *in vivo* efficacy in IGF and having potential for drug–drug interactions due to potent CYP3A4 inhibition (0.5 µM) and poor aqueous solubility (<1 µg/mL). The unsubstituted piperazine **(79)** showed three-fold improvement in enzymatic potency while cell-based activity is maintained relative to morpholine. To improve the overall profile of **78**, modification was done by changing substitution at C-5 position[75] with more polar *N*-substituted piperazines **80**.

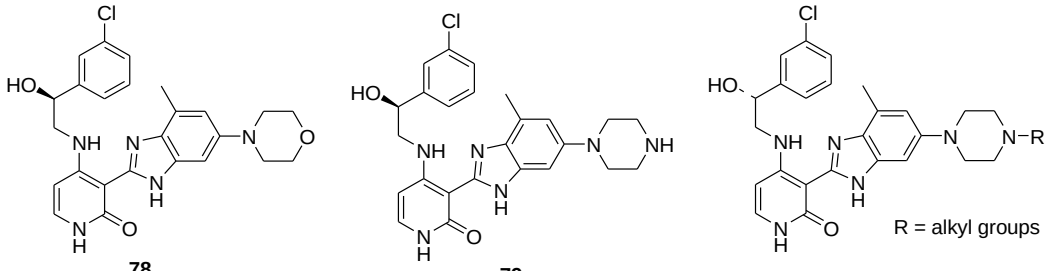

78 **79** **80**

Compounds **81** and **82** exhibited good selectivity and non toxicity against a panel of protein kinase with IC_{50} value in the range of 12 nM. Substitution with 2-methoxyethyl group (**83d**) resulted in four-fold loss in potency whereas no effect was observed with removal of methyl group. Large hydrophobic groups afforded a slight increase in potency like cyclopentylmethyl group (**83c**) with respect to cyclohexyl **(83a)**.[76]

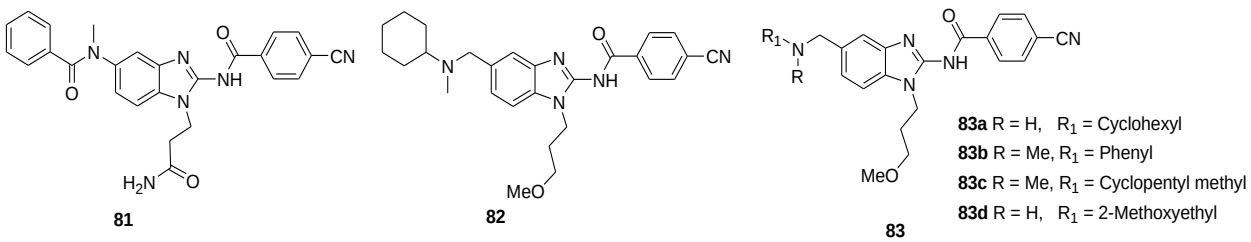

81 **82** **83**

Thus, research on triazine and fused heterocyclic moieties have revealed wide range of

biological activities. It was our interest to make novel derivatives of the benzimidazole with triazine and fused heterocyclic nucleus and evaluate their *in vitro* anticancer activities. Therefore, in the present research programme, we have combined the structures of triazine and fused heterocyclic moieties like pyrrolopyridine, quinazolinone, pyrazolopyrimidine with benzimidazole to develop new hybrid compounds which could act more effectively for human cancer cell lines and DHFR kinase inhibitors that help in finding the availability of anticancer agents. The work has also been extended for studied the interaction of hybrid compounds with calf thymus (ct)-DNA and bovine serum albumin.

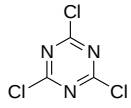

2,4,6-Trichloro-[1,3,5]triazine

1*H*-Pyrrolo[2,3-*b*]pyridine

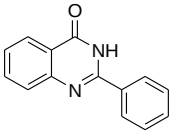

2-Phenyl-3*H*-quinazolin-4-one

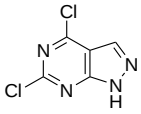

4,6-Dichloro-1*H*-pyrazolo[3,4-*d*]pyrimidine

Benzimidazole

CHAPTER 2
TRIAZINE-BENZIMIDAZOLE ANALOGUES

2.1. INTRODUCTION

Triazine bearing amino groups at C2- and C4-positions has been attracted considerable attention due to their chemotherapeutic potential.[77,78] The synthetic utility and much of the biological importance of triazine heterocycle arises because of their ease of nucleophilic substitutions on halogenated 1,3,5-triazines at 2-, 4- and 6-positions that are controlled by temperature, allows the sequential introduction of various substitutes for the preparation of mono-, di- and tri-substituted triazines.[79,80] Owing to enormous synthetic significance and diverse bioactivities of 1,3,5-triazine derivatives, several attempts have been made from time to time to generate libraries of modified triazine derivatives with improved biological activities.

OBJECTIVE

Benzimidazoles are known that have substitution on the imidazole ring and showed significant antitumor activities but amine at C-5 or C-6 positions of aromatic ring of benzimidazole and their substitution to triazine is not known. Here, we have designed a series of triazine substituted benzimidazoles along with substitution of primary and secondary amines as well as arylation through palladium catalyzed Suzuki reaction. These compounds were then evaluated for their *in vitro* 60 human cancer cell lines, dihydrofolate reductase inhibitory activity as well as ct-DNA interactions.

2.2. DESIGNING OF TRIAZINE-BENZIMIDAZOLE HYBRIDS

Encouraged by the activity profile of triazine and benzimidazole, we have combined the structural artifacts of 1,2,3-triazine and benzimidazole moieties as hybrid that is enriched with electronic environment to get single molecular framework. These hybrid molecules consisted of a heterocyclic ring (triazine) as central core that can act as a scaffold to carry three functionalized branches at 2-, 4- and 6-positions. The regioisomeric aminobenzimidazole ring has been accommodated at 2-position, *p*-fluoroaniline or morpholine at 4-position and different primary and secondary amines as well as aromatic rings at 6-position of triazine in order to observe the

effect of donors and acceptors within the moieties (Figure 1). Introduction of different orientations of benzyl group at 1- or 3-position of regioisomeric aminobenzimidazole moiety can also affect the activity of the hybrids. These compounds were screened for their *in vitro* antitumor activities in full NCI 60 cell lines panel assay and DHFR immunoassay. Binding interactions of compounds with DNA were also studied using UV-visible and fluorescence spectroscopy as well as NMR spectrometry.

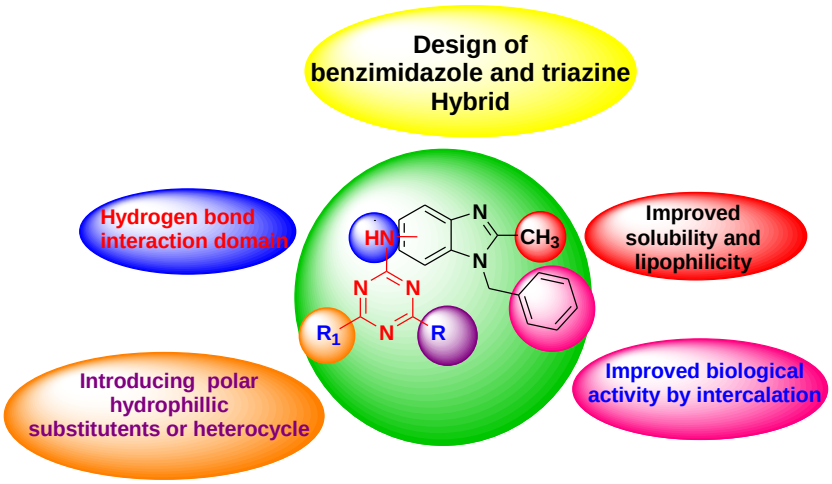

Figure 1. Triazine-benzimidazole hybrid

2.2.1. CHEMISTRY

The regioisomeric amino benzimidazoles (**4a** and **4b)** were prepared by alkylation of 2-methyl-5-nitro-1*H*-benzimidazole (**2**) with benzyl chloride in the presence of potassium carbonate at 80 ^{o}C to give mixtures of **3a** and **3b** followed by reduction with stannous chloride in 2N HCl at 110 ^{0}C (Scheme 1).

Scheme 1[a]. Synthesis of substituted amino benzimidazole

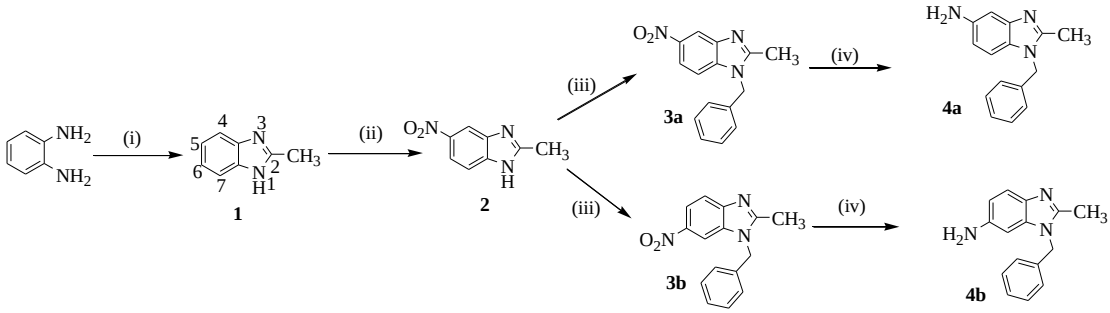

[a]Reagents and Conditions : (i) CH_3COOH, 100 ^{o}C, 98%; (ii) H_2SO_4, HNO_3, 0 ^{o}C, 75%; (iii) Benzyl chloride, K_2CO_3, C_2H_5OH, reflux, 75%; (iv) $SnCl_4.2H_2O$, 2N HCl, 110 ^{o}C, 25-65%.

Complete and unambiguous assignments for all ^{1}H and ^{13}C resonances could be achieved on the basis of chemical shift considerations, coupling information and NOE spectra (Figure 2). Discrimination between *N*-substitution products **4a** and **4b** was achieved by considering 2D NOE difference experiments (positive NOE's on signals of N-CH_2 protons due to the benzyl chain and doublet of phenyl ring of benzimidazole with compound **4a**, and positive NOE's on signal of N-CH_2 protons due to the benzyl chain and singlet of aromatic ring of benzimidazole and negative NOE with doublet of compound **4b**).

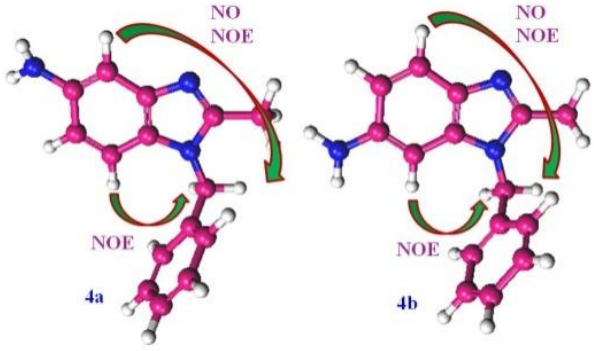

Figure 2. ^{1}H-^{1}H correlations used for structural assignment of compounds **4a** and **4b**.

Compounds **7-49** were synthesized by nucleophilic substitution reactions of amino benzimidazole with cyanuric chloride followed by displacement with different primary and secondary amines as well as substituted boronic acids. Thus, compound **4a** was treated with cyanuric chloride in the presence of 10% sodium bicarbonate at 0-5 ^{o}C for 6 h to give (1-benzyl-2-methyl-1*H*-benzimidazol-5-yl)-(4,6-dichloro-[1,3,5]triazin-2-yl)-amine (**5a)** in 96% yield followed by stirring with 4-fluoroaniline and morpholine at room temperature in the presence of 10% sodium bicarbonate for 4 h gave compounds **6a** and **6b** respectively (Scheme 2).

Similarly, compound **4b** was treated with cynauric chloride in the same reaction conditions to obtain (3-benzyl-2-methyl-3*H*-benzimidazol-5-yl)-(4,6-dichloro-[1,3,5]triazin-2-yl)-amine (**5b**) in 90% yield followed nucleophilic substitution with 4-fluoroaniline and morpholine to obtain compounds **6c** and **6d** respectively. Alternatively, poor overall yields of **6a-d** were obtained with first nucleophilic displacement of cynauric chloride with 4-fluoroaniline or morpholine and then second nucleophilic substitution with amino benzimidazoles (**4**). Finally, treatment of compound **6a-d** with different primary and secondary amines in the presence of potassium carbonate in 1,4-dioxane at 110 ^{o}C for 8 h gave compounds **7-40** in moderate to good

yields (Scheme 3, 4). Compound **18** was well characterized by single X-ray crystallography (Figure 3).

Scheme 2[a]. Synthesis of monosubstituted and disubstituted triazine

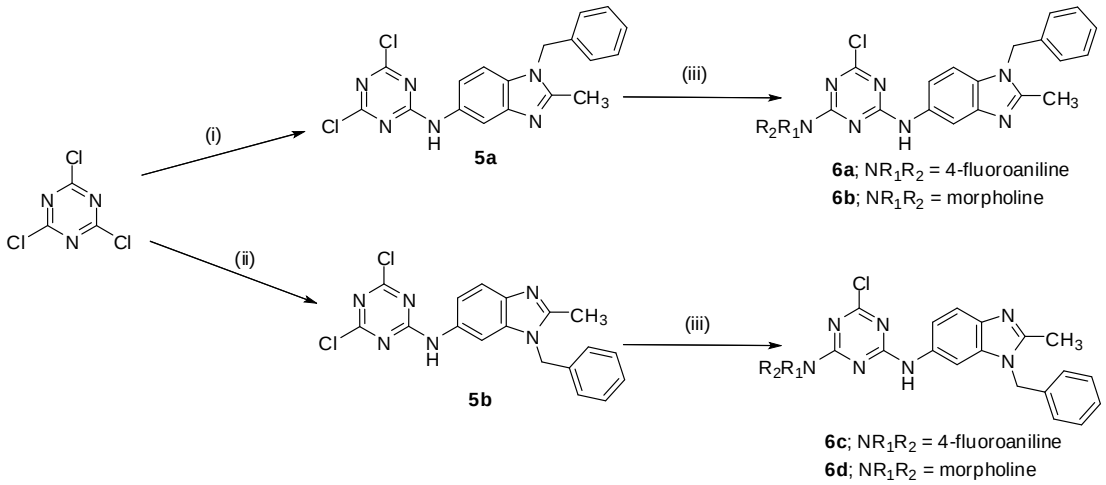

[a]Reagents and conditions: (i) **4a**, $NaHCO_3$, THF, 0−5 °C, 96%; (ii) **4b**, $NaHCO_3$, THF, 0−5 °C, 90%; (iii) 4-fluoroaniline/morpholine, $NaHCO_3$, THF, rt, 70-80%.

Scheme 3[a]. Synthesis of 2,4,6-trisubstituted triazines with respect to 5-aminobenzimidazole

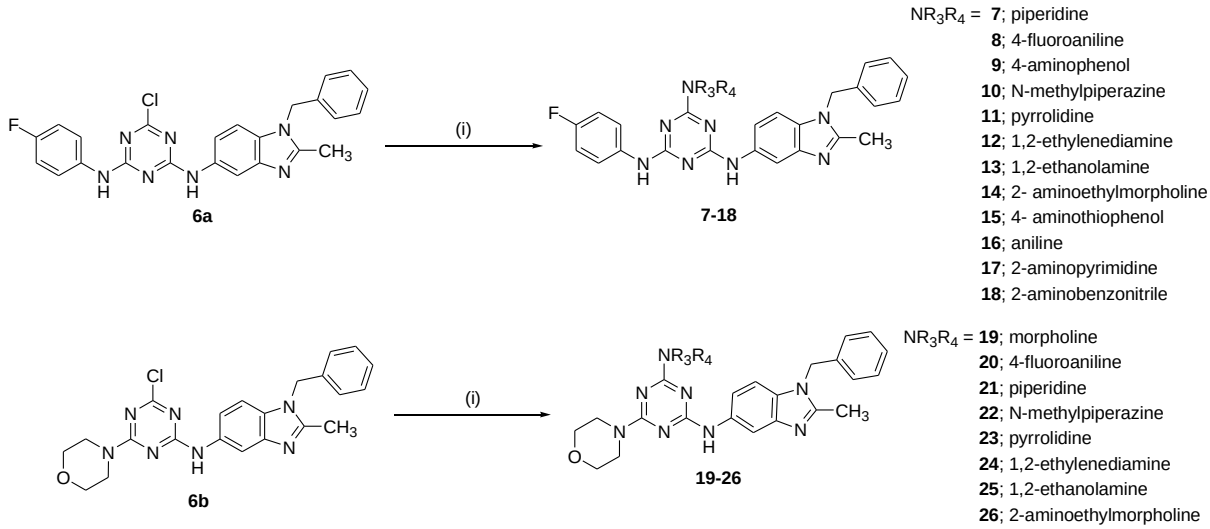

[a]Reagents and conditions: (i) HNR_3R_4, K_2CO_3, 1,4-dioxane, 110 ^{0}C, 55-88%.

Scheme 4[a]. Synthesis of 2,4,6-trisubstituted triazines with respect to 6-aminobenzimidazole

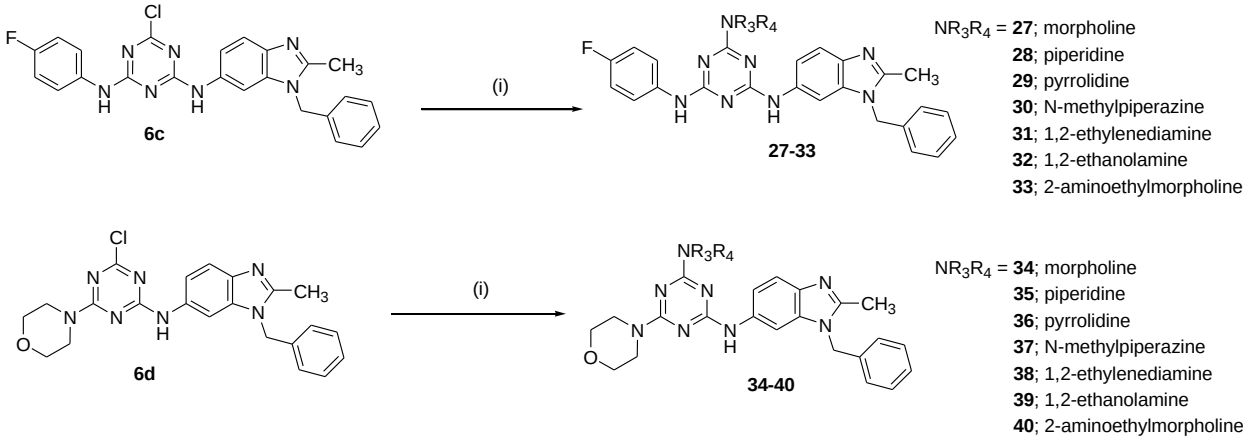

[a]Reagents and conditions: (i) HNR_3R_4, K_2CO_3, 1,4-dioxane, 110 ^{0}C, 68-88%.

Compounds **6a** and **6b** were also underwent Suzuki-Miyaura cross coupling reactions with varieties of aryl boronic acids in the presence of $Pd(PPh_3)_4$ and K_2CO_3 in 1,4-dioxane to give compounds **41-49** in 60-78% yields (Scheme 5).

Scheme 5[a]. Synthesis of trisubstituted triazine with Suzuki-Miyaura reaction

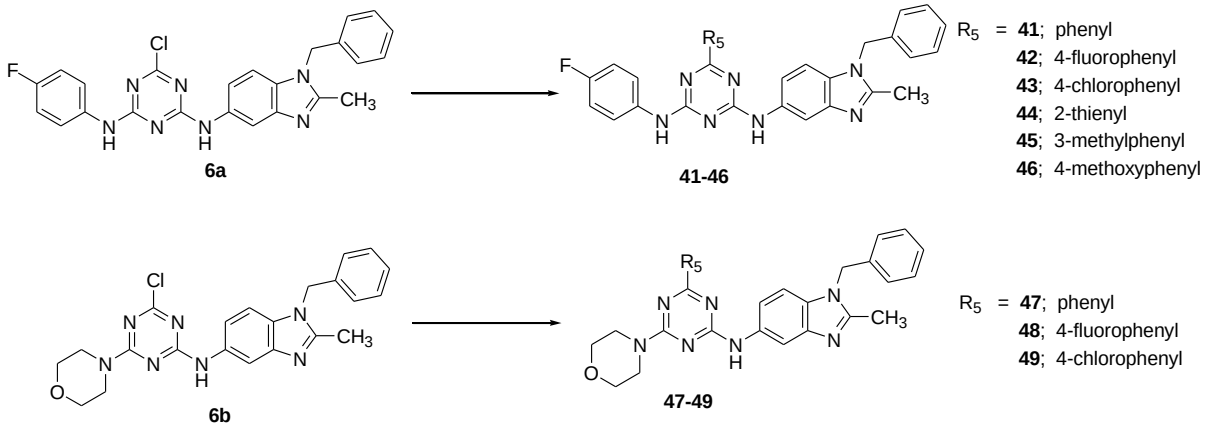

[a]Reagents and conditions: $R_5B(OH)_2$, $Pd(PPh_3)_4$, K_2CO_3, 1,4-dioxane, reflux, 59-78%.

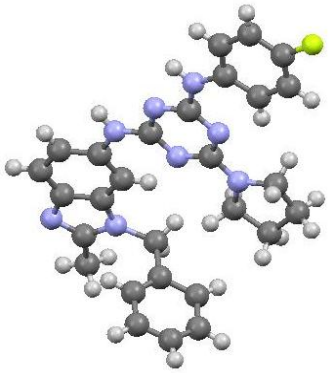

Figure 3. Crystal structure of compound **18** (CCDC No. 1009017).[81]

2.2.2. BIOLOGY

2.2.2.1. *In vitro* Anticancer Evaluation

All the synthesized compounds were submitted to National Cancer Institute (NCI) disease-oriented human cell lines for their evaluation of *in-vitro* antitumor activities. Thirty compounds (**6a, 6c-6d**, **8-13, 17, 19-22, 25, 28, 31-34, 36-41, 43, 44, 46** and **49**) were selected and evaluated against 60 human cell lines at one dose concentration level i.e. 10^{-5} M which included nine tumor subpanels namely; leukemia, non-small lung, colon, central nervous system, melanoma, ovarian, renal, prostate and breast cancer cells and their outputs were reported as mean graph of the percent growth of treated cells, and presented as percentage growth inhibition (GI %) as shown in tables 1-3. Compounds **6c**, **6d**, **10**, **11**, **20**, **21**, **33, 43, 44** and **46** were further screened against a panel of 60 different tumor cell lines at 5 dose concentration levels: 10^{-4}, 10^{-5}, 10^{-6}, 10^{-7} and 10^{-8} M as these have shown prominent cell growth inhibition at 10^{-5} M concentration against variety of cell lines (Table 4). Three response parameters like median growth inhibitory (GI_{50}, μM), total growth inhibitory (TGI, μM) and median lethal concentrations (LC_{50}, μM) were monitoring for each cell line. MG MID GI_{50} value (over all the 60 cancer cell lines) of compound **6c** was found to be 6.09 μM and also showed specificity towards leukemia, colon and breast cancer cell lines with GI_{50} values in the range of 3.34-4.91 μM. Nucleophilic displacement with primary and secondary amines enhanced the antitumor activity by 2 to 4 folds. MG MID GI_{50}, TGI and LC_{50} values of compound **6d** has been shown to be 9.79, 28.3 and 35.2 μM respectively. These are more specific towards colon, melanoma, ovarian and breast cancer cell lines with GI_{50} values in the range of 3.31-5.61 μM. Compounds **10**, **11** and **33** showed broad spectrum antitumor activities with GI_{50}, TGI and LC_{50} values of 1.77, 1.94 and 2.87 μM; 3.96, 5.59 and 16.6 μM and 10.3, 8.59 and 35.2 μM respectively. Compound **10** showed activity towards leukemia cancer cell lines K-562 and MOLT-4, non small lung cancer cell lines A549/ATCC, HOP-92 and NCI-H460, melanoma cancer cell line MDA-MB-435, ovarian cancer cell line OVCAR-8 and renal cancer cell line ACHN. Compound **33** showed specificity towards leukemia, colon, CNS, melanoma and breast cancer cell lines with GI_{50} in the range of 1.91-2.72 μM. Compound **20** exhibited remarkable anticancer activity against CNS cancer and renal cancer cell lines with GI_{50} values of 1.86 and 1.89 μM respectively. Similarly, compound **21** showed potency against leukemia, colon and renal cancer cell lines with GI_{50} values ranging from 2.50-

2.96 µM. Compounds **43**, **44** and **46** also showed excellent antitumor activities with MG MID GI_{50} values over all 60 human tumor cell lines of 7.67, 5.18 and 4.28 µM respectively. Compound **10** was almost three and tenfolds; compound **11** three and ninefolds; and compound **33** was two and six folds more active than respective triazine[82] and benzimidazole[83] analogues respectively (Table 4).

Table 1. Percent growth promotion of *in vitro* subpanel tumor cell lines at 10 µM concentration of compounds **6a, 6c, 6d, 8-13** and **17**.

Subpanel tumor cell lines	**6a**	**6c**	**6d**	**8**	**9**	**10**	**11**	**12**	**13**	**17**
Leukemia										
CCRF-CEM	21.46	77.11	54.31	10.61	8.15	**L**	**L**	**L**	98.07	63.24
HL-60(TB)	46.84	Nt	Nt	-	6.96	**L**	**L**	**L**	**L**	30.10
K-562	14.84	63.13	74.26	18.63	21.28	99.61	99.97	**L**	80.78	41.28
MOLT-4	9.41	41.07	74.20	15.19	19.80	98.894	**L**	**L**	nt	44.58
RPMI-8226	84.70	87.49	25.63	14.27	26.73	**L**	**L**	**L**	85.80	57.39
SR	42.49	63.93	81.49	18.58	20.78	**L**	**L**	**L**	85.06	51.61
Non-small cell lung cancer										
A549/ATCC	13.29	23.83	7.99	8.48	22.17	92.79	**L**	16.10	25.86	17.77
HOP-62	11.56	56.13	49.88	8.91	3.47	41.84	**L**	20.88	6.05	2.38
HOP-92	49.29	21.19	63.88	37.63	17.75	97.50	**L**	51.48	50.14	18.38
NCI-H226	19.55	26.80	17.55	13.78	12.75	35.02	**L**	4.61	8.37	11.51
NCI-H23	nt	11.76	83.50	nt	nt	nt	nt	nt	nt	Nt
NCI-H322M	nt	11.92	48.97	nt	nt	nt	78.59	0.32	1.09	5.47
NCI-H460	12.02	20.15	9.75	-	18.23	96.58	**L**	17.43	16.54	5.20
NCI-H522	**L**	77.52	**L**	14.16	15.10	**L**	**L**	14.09	14.35	22.51
Colon cancer										
COLO 205	-	8.82	0.01	2.84	-	**L**	**L**	18.03	5.46	10.54
HCC-2998	5.54	-	99.33	-	4.67	**L**	**L**	29.37	-	-
HCT-116	96.12	55.77	18.76	12.18	10.55	**L**	**L**	39.74	23.45	15.80
HCT-15	27.94	44.22	23.10	10.75	17.34	**L**	**L**	-	-	12.65
HT29	5.46	15.76	3.96	1.30	4.80	**L**	**L**	64.93	28.11	14.75
KM12	30.77	27.21	4.25	-	17.65	82.97	**L**	29.39	19.74	11.61
SW-620	15.25	17.19	29.58	3.96	18.75	84.44	**L**	26.05	-	-
CNS cancer										
SF-268	8.93	24.62	22.98	3.68	11.24	85.37	**L**	28.18	7.77	11.25
SF-295	3.61	21.83	12.69	8.21	5.35	**L**	**L**	20.23	13.61	15.58
SF-539	29.80	1.83	15.27	10.38	6.34	**L**	**L**	3.98	5.61	-
SNB-19	7.64	12.03	5.43	3.99	-	55.84	66.44	8.37	-	7.38
SNB-75	10.01	4.24	48.82	24.81	15.06	**L**	**L**	15.76	-	15.64
U251	Nt	30.91	9.52	-	nt	nt	**L**	22.64	13.66	13.25
Melanoma										
LOX IMVI	56.68	64.79	32.32	7.80	3.79	**L**	**L**	41.84	18.11	3.01
MALME-3M	-	11.46	3.17	-	0.89	**L**	**L**	6.46	-	7.94
M14	-	17.68	-	-	-	**L**	**L**	18.39	6.95	5.65
MDA-MB-435	4.44	11.25	-	0.94	4.26	99.81	**L**	19.61	8.37	9.24

SK-MEL-2	-	nt	-	-	-	**L**	**L**	9.54	-	-
SK-MEL-28	-	8.45	17.24	-	-	**L**	**L**	-	-	-
SK-MEL-5	7.59	30.78	10.51	1.09	5.60	29.09	**L**	13.36	19.70	6.35
UACC-257	10.33	-	-	3.11	3.73	**L**	**L**	9.53	1.20	-
UACC-62	17.62	48.63	48.63	10.18	3.94	**L**	**L**	nt	nt	Nt
Ovarian cancer										
IGORV1	16.99	33.34	**L**	16.86	2.23	75.36	**L**	18.57	11.11	23.97
OVCAR-3	5.75	5.09	1.59	4.79	8.38	**L**	**L**	13.34	9.84	9.64
OVCAR-4	14.18	-	-	14.36	12.82	**L**	95.21	22.98	4.73	20.21
OVCAR-5	3.73	-	-	4.24	3.66	57.10	**L**	-	-	-
OVCAR-8	18.46	57.71	56.00	9.21	22.25	99.44	**L**	10.87	20.04	8.83
NCI/ADR-RES	4.36	nt	-	10.63	-	56.85	**L**	-	2.28	10.50
SK-OV-3	4.12	2.61	6.31	-	-	31.28	**L**	4.49	-	2.64
Renal cancer										
786-0	67.01	20.42	31.70	13.16	6.04	**L**	**L**	17.59	5.33	-
A498	30.65	22.18	8.26	21.95	13.41	70.79	**L**	32.64	33.83	11.51
ACHN	63.79	28.42	20.63	7.88	8.70	90.31	88.51	3.22	1.72	1.60
CAKI-1	12.30	13.07	-	10.13	4.53	81.36	**L**	5.83	-	-
RXF 393	22.91	15.39	34.94	-	18.75	**L**	**L**	28.00	9.82	-
SN12C	22.10	53.32	21.78	5.75	2.54	65.11	**L**	14.88	8.89	8.42
TK-10	41.53	7.64	55.28	-	-	**L**	**L**	-	-	-
UO-31	19.30	62.88	26.21	39.28	6.02	**L**	**L**	10.74	21.19	26.97
Prostate cancer										
PC-3	21.18	19.20	12.86	23.25	10.68	80.27	nt	nt	nt	Nt
DU-145	35.96	5.78	5.83	-	41.57	83.26	**L**	17.77	11.46	4.12
Breast cancer										
MCF7	38.52	37.38	35.29	11.50	16.02	82.08	96.95	31.21	8.72	20.10
MDA-MB-231/ATCC	17.92	25.91	35.55	24.51	11.30	**L**	**L**	39.57	19.67	7.37
HS 578T	20.49	11.12	18.60	10.44	1.42	**L**	69.44	-	-	20.89
BT-549	9.39	39.84	16.27	5.26	-	**L**	**L**	9.96	-	-
T-47D	42.98	63.16	59.37	10.69	-	**L**	**L**	30.86	34.71	25.13
MDA-MB-468	23.76	30.32	37.82	9.45	13.36	**L**	**L**	26.83	0.84	-

Table 2. Percent growth promotion of *in vitro* subpanel tumor cell lines at 10 μM concentration of compounds **19-22, 25, 28** and **31-34**.

Subpanel tumor cell lines	**19**	**20**	**21**	**22**	**25**	**28**	**31**	**32**	**33**	**34**
Leukemia										
CCRF-CEM	-	53.35	37.81	3.80	**L**	20.52	51.94	25.27	70.53	4.80
HL-60(TB)	9.73	43.59	25.02	-	nt	nt	nt	nt	nt	Nt
K-562	4.18	42.12	15.68	9.72	2.77	26.52	61.30	25.67	96.96	6.32
MOLT-4	9.66	66.96	63.58	8.19	nt	30.69	40.69	27.46	77.27	25.02
RPMI-8226	25.25	60.37	82.31	-	12.18	25.24	46.20	33.68	96.89	5.41
SR	22.78	82.23	74.79	7.01	-	50.70	88.93	28.28	99.85	19.53
Non-small cell lung cancer										
A549/ATCC	3.58	32.96	**L**	-	2.27	29.20	13.23	13.78	53.72	9.63
HOP-62	8.85	-	55.47	5.05	16.34	-	20.59	0.23	52.16	4.56

HOP-92	73.53	80.20	**L**	17.15	18.81	24.70	56.77	19.38	69.74	14.75
NCI-H226	23.54	21.70	71.63	28.74	21.30	12.32	13.76	11.08	27.92	10.44
NCI-H23	nt	nt	nt	nt	-	5.43	10.37	6.24	32.98	-
NCI-H322	nt	nt	nt	nt	15.26	-	7.76	-	35.85	-
NCI-H460	6.85	33.42	95.13	-	-	17.67	21.75	4.15	70.59	3.20
NCI-H522	17.58	6.88	62.08	7.38	-	30.10	30.98	20.36	41.31	30.42
Colon cancer										
COLO 205	-	66.80	58.96	-	3.84	2.32	33.57	6.67	98.81	-
HCC-2998	-	6.08	5.67	-	0.15	-	-	-	55.41	-
HCT-116	7	52.44	**L**	1.82	3.50	26.52	39.72	13.33	72.10	-
HCT-15	20.79	53.36	78.73	3.97	4.18	16.55	-	8.36	**L**	-
HT29	5.71	78.39	**L**	-	-	28.90	55.46	-	**L**	-
KM12	4.92	8.07	91.68	-	-	8.36	26.84	7.50	56.62	-
SW-620	41.13	19.68	55.90	-	-	5.34	1.71	0.58	57.58	-
CNS cancer										
SF-268	14.92	27.69	31.02	3.76	10.35	4.31	19.17	-	37.22	8.79
SF-295	4.61	-	21.10	4.81	0.25	9.64	11.59	11.00	**L**	-
SF-539	19.30	32.61	18.39	8.66	11.04	2.48	0.19	3.59	70.24	-
SNB-19	-	9.49	34.67	-	-	17.50	10.08	2.43	21.27	4.14
SNB-75	29.22	14.42	nt	28.79	15.17	4.31	19.99	8.89	49.41	7.94
U251			**L**		-	21.47	46.54	6.96	71.27	8.73
Melanoma										
LOX IMVI	2.27	-	98.56	2.83	4.76	-	29.99	-	94.30	-
MALME-3M	-	9.73	**L**	-	4.19	-	25.97	6.95	**L**	-
M14	-	33.93	51.58	-	-	7.86	16.39	6.68	**L**	-
MDA-MB-435	-	-	47.19	-	nt	3.66	9.38	2.54	47.79	-
SK-MEL-2	0.88	15.00	81.03	-	nt	nt	19.94	nt	nt	-
SK-MEL-28	-	17.76	53.43	-	5.99	3.66		-	**L**	-
SK-MEL-5	8.02	21.35	45.11	2.45	12.46	22.87	25.48	26.04	85.81	17.96
UACC-257	-	36.94	39.62	0.84	7.76	-	15.87	-	**L**	0.45
UACC-62	13.70	19.91	67.88	-	5.81	9.98	9.33	6.56	**L**	-
Ovarian cancer										
IGORV1	12.52	28.60	52.99	-	0.90	nt	0.38	-	30.96	-
OVCAR-3	11.04	25.32	**L**	-	-	0.84	6.85	3.09	26.28	-
OVCAR-4	-	19.77	**L**	-	-	-	-	-	1.85	-
OVCAR-5	9.05	-	44.17	3.31	12.30	-	6.17		15.88	-
OVCAR-8	13.91	24.56	72.41	1.75	6.52	6.90	17.69	4.04	49.85	11.29
NCI/ADR-RES	10.09	22.44	72.96	-	nt	nt	nt	18.13	nt	Nt
SK-OV-3	-	-	60.19	-	-	2.27	13.16	-	20.97	-
Renal cancer										
786-0	18.71	67.59	89.06	2.49	0.66	11.83	20.52	11.90	95.83	13.79
A498	25.10	59.66	61.23	7.61	22.06	24.93	25.46	25.34	**L**	40.26
ACHN	10.63	40.24	**L**	3.40	9.49	3.60	8.19	4.66	47.84	-
CAKI-1	15.07	-	36.69	6.70	6.18	1.51	1.79	-	44.43	3.62
RXF 393	28.04	73.05	**L**	-	9.20	13.80	25.76	26.06	87.99	13.72
SN12C	8.69	20.15	47.77	-	-	3.75	24.80	1.60	38.15	-
TK-10	8.12	14.84	**L**	-	6.50	7.88	26.14	-	39.43	-
UO-31	56.12	45.70	98.39	18.32	28.40	15.65	13.69	13.16	62.71	23.67
Prostate cancer										
PC-3	9.01	38.02	52.90	3.31	11.62	21.34	26.95	0.89	28.48	-
DU-145	38.08	21.60	94.64	-	50.98	-	8.56	-	40.78	-
Breast cancer										
MCF7	2.21	35.55	34.50	1.21	10.26	38.84	39.07	19.76	66.43	9.52

MDA-MB-231/ATCC	19.97	16.07	90.40	-	14.30	-	42.88	7.95	66.68	7.46
HS 578T	20.15	22.58	65.43	-	4.97	0.58	20.53	8.56	59.44	2.02
BT-549	7.34	15.45	36.83	-	8.38	5.37	17.04	20.63	50.15	8.71
T-47D	17.51	30.02	**L**	0.38	36.69	34.66	23.18	39.28	47.00	19.23
MDA-MB-468	17.51	58.21	29.93	-	28.11	17.23	49.49	23.02	86.03	6.18

Table 3. Percent growth promotion of *in vitro* subpanel tumor cell lines at 10 μM concentration of compounds **36-41, 43, 44, 46** and **49**.

Subpanel tumor cell lines	**36**	**37**	**38**	**39**	**40**	**41**	**43**	**44**	**46**	**49**
Leukemia										
CCRF-CEM	11.27	20.13	5.33	-	2.33	-	96.12	72.84	**L**	Nt
HL-60(TB)	21.36	nt	nt	nt	nt	36.26	**L**	71.91	**L**	32.83
K-562	22.06	70.72	9.61	1.48	7.20	38.16	66.35	56.89	83.37	6.54
MOLT-4	22.53	nt	11.53	nt	22.71	41.75	99.16	76.49	**L**	9.83
RPMI-8226	36.91	34.60	6.93	1.88	-	53.00	99.81	**L**	**L**	32.52
SR	32.70	75.13	21.70	-	10.45	68.16	**L**	81.96	**L**	33.40
Non-small cell lung cancer										
A549/ATCC	15.62	14.87	-	2.38	2.61	32.53	42.62	56.91	67.99	13.79
HOP-62	1.08	13.41	0.97	3.31	-	5.32	19.39	7.68	46.67	1.49
HOP-92	73.72	35.48	27.62	18.92	21.22	35.58	64.95	78.03	60.27	25.17
NCI-H226	15.61	4.23	11.62	9.28	8.78	19.27	13.47	34.96	33.39	5.33
NCI-H23	nt	nt	-	0.07	0.59	nt	nt	nt	nt	nt
NCI-H322	nt	7.95	-	-	-	nt	5.98	nt	17.58	-
NCI-H460	9.40	23.91	1.16	1.18	-	16.83	28.86	60.41	69.67	2.42
NCI-H522	11.21	6.77	11.24	7.50	7.61	24.14	17.19	46.54	44.64	0.77
Colon cancer										
COLO 205	5.78	26.80	-	-	-	29.49	38.20	43.20	71.76	14.44
HCC-2998	-	3.67	-	-	-	11.99	18.36	27.88	54.47	-
HCT-116	37.75	28.69	9.66	0.24	-	39.66	49.72	75.82	76.61	22.71
HCT-15	43.06	12.64	2.79	0.27	-	32.39	35.56	69.71	66.63	10.83
HT29	33.02	47.02	-	-	-	40.57	44.18	79.52	91.13	18.57
KM12	24.32	6.81	-	-	-	39.81	62.81	74.82	74.05	3.10
SW-620	-	3.11	1.34	3.01	-	15.41	31.93	31.93	54.34	-
CNS cancer										
SF-268	5.31	31.24	4.01	8.14	1.49	23.76	45.07	36.32	53.08	-
SF-295	8.04	9.95	3.72	-	-	17.30	9.63	48.11	51.05	-
SF-539	22.90	23.50	-	-	-	0.21	7.42	40.09	32.19	-
SNB-19	-	-	4.05	7.90	-	31.50	16.60	33.28	39.32	1.10
SNB-75	-	37.60	-	7.73	7.08	28.42	34.76	47.76	31.99	12.30
U251		26.54	8.22	-	12.37	36.60	30.34		60.79	12.13
Melanoma										
LOX IMVI	5.80	25.26	0.54	-	-	12.26	23.45	35.15	61.06	-
MALME-3M	-	34.32	-	0.71	-	11.44	27.53	22.37	47.18	-
M14	-	16.59	5.56	-	-	34.08	41.73	46.92	61.08	3.50
MDA-MB-435	-	8.97	-	-	-	40.00	33.83	56.19	65.89	3.72
SK-MEL-2	1.38	nt		-	-	25.40	16.44	27.12	51.82	7.08
SK-MEL-28	-	35.86	-	-	-	5.63	7.37	25.70	43.45	-
SK-MEL-5	12.00	28.60	12.28	-	13.03	14.49	16.62	23.50	52.93	15.20
UACC-257	-	17.45	-	-	-	18.71	31.10	42.54	56.20	2.52

UACC-62	9.16	-	-	3.39	-	nt	nt	38.46	nt	nt
Ovarian cancer										
IGORV1	12.59	1.82	-	8.66	-	31.00	51.27	51.73	63.58	2.94
OVCAR-3	4.19	5.26	-	-	-	18.80	42.74	33.34	49.54	-
OVCAR-4	-	-	-	-	-	39.75	41.39	48.99	57.40	11.63
OVCAR-5	4.30	-	2.77	-	-	-	7.71	7.98	11.89	-
OVCAR-8	23.90	6.37	1.79	9.21	-	32.25	37.21	62.97	82.07	10.96
NCI/ADR-RES	10.83	nt	-	nt	-	29.49	40.95	42.68	73.43	6.93
SK-OV-3	-	3.82	-	-	-	1.78	7.08	4.89	23.18	1.14
Renal cancer										
786-0	22.50	27.23	8.02	5.60	2.84	18.37	8.96	62.45	53.33	16.68
A498	32.86	59.42	10.55	20.22	17.30	23.21	29.70	44.00	27.28	-
ACHN	7.95	5.31	-	2.57	1.04	23.62	28.37	54.43	62.85	-
CAKI-1	5.12	-	-	-	5.61	-	9.60	29.82	16.76	-
RXF 393	28.89	38.87	4.80	15.88	0.45	30.91	31.49	74.14	64.33	5.07
SN12C	9.28	-	-	15.14	-	21.89	22.91	29.74	51.61	-
TK-10	-	12.79	-	-	-	0.81	-	37.29	25.08	-
UO-31	45.20	37.34	11.37	15.75	13.27	43.41	55.55	63.55	70.72	23.53
Prostate cancer										
PC-3	30.81	9.97	-	-	-	nt	nt	70.56	nt	Nt
DU-145	8.23	1.56	-	-	-	2.93	18.56	24.80	45.28	-
Breast cancer										
MCF7	-	17.40	14.06	11.41	6.32	54.93	57.58	67.06	77.38	16.82
MDA-MB-231/ATCC	10.98	31.46	-	12.76	-	9.76	33.97	30.86	68.85	3.85
HS 578T	24.39	30.71	2.22	4.59	12.17	20.36	24.65	49.74	45.53	0.42
BT-549	15.84	33.90	3.35	9.63	7.60	4.60	-	30.49	29.34	-
T-47D	31.18	8.14	10.61	9.91	9.43	55.48	69.27	76.65	88.45	12.53
MDA-MB-468	17.79	33.21	15.53	14.42	7.58	27.62	25.71	66.79	71.63	-

- Inactive, nt- not tested

Table 4. Average GI_{50} (μM), TGI (μM) and LC_{50} (μM) over 60 cancer cell lines for compounds **6c, 6d, 10, 11, 20, 21, 33, 43, 44** and **46** at 5 dose concentration levels.

Compds.	Activity	I	II	III	IV	V	VI	VII	VIII	IX	MIG-MID[a]
6c	GI_{50}	3.34	6.23	4.91	6.39	5.92	8.10	7.49	8.27	4.21	6.09
	TGI	8.68	20.3	18.1	24.3	18.4	29.8	30.0	27.7	11.9	21.0
	LC_{50}	[b]	69.6	54.6	43.5	53.9	78.8	55.5	52.5	75.8	60.5
6d	GI_{50}	18.6	11.9	3.31	10.3	3.81	3.56	12.1	19.0	5.61	9.79
	TGI	[b]	17.4	35.6	53.0	16.2	21.2	40.0	[b]	15.3	28.3
	LC_{50}	[b]	7.89	7.22	[b]	6.18	[b]	45.7	[b]	67.9	35.3
10	GI_{50}	1.43	1.84	1.66	1.77	1.81	2.16	1.77	1.89	1.61	1.77
	TGI	4.04	3.86	3.44	3.94	3.37	5.25	3.81	4.38	3.60	3.96
	LC_{50}	8.47	7.52	7.15	10.8	6.27	15.5	9.66	20.5	7.54	10.3
11	GI_{50}	2.54	1.82	1.81	2.08	1.81	1.9	1.75	1.82	1.98	1.94
	TGI	5.28	4.02	3.54	17.6	3.68	4.01	3.56	3.82	4.88	5.59
	LC_{50}	[b]	14.5	6.93	8.64	13.7	11.0	1.26	6.00	6.69	8.59
20	GI_{50}	3.71	2.56	2.76	1.86	2.70	2.41	1.89	2.75	2.58	2.58
	TGI	5.49	4.02	3.65	[b]	4.18	3.98	3.18	[b]	5.47	4.28
	LC_{50}	[b]	[b]	[b]	[b]	[b]	[b]	5.88	[b]	[b]	5.88
21	GI_{50}	2.50	5.57	2.61	3.73	3.15	5.98	2.96	3.86	4.00	3.81

	TGI	7.65	22.1	10.2	19.5	10.7	25.3	13.5	17.8	23.3	16.6
	LC_{50}	[b]	75.6	19.6	38.7	46.9	58.6	30.9	61.2	59.1	48.8
33	GI_{50}	1.96	3.21	2.60	2.72	1.91	4.01	3.03	4.41	2.04	2.87
	TGI	6.82	18.5	8.51	12.0	4.08	27.4	19.3	43.9	8.99	16.6
	LC_{50}	55.0	38.5	24.0	15.3	24.2	62.3	14.6	62.5	20.6	35.2
43	GI_{50}	3.39	8.37	4.97	8.44	6.36	6.10	11.5	13.5	6.46	7.67
	TGI	9.55	38.6	59.8	48.6	31.7	24.4	45.4	[b]	50.8	38.6
	LC_{50}	[b]	83.8	[b]	61.4	80.6	65.4	[b]	[b]	[b]	72.8
44	GI_{50}	2.59	7.62	3.23	4.66	4.72	8.83	4.54	5.20	5.24	5.18
	TGI	9.49	33.1	17.0	14.4	19.7	27.3	43.5	52.2	21.9	26.5
	LC_{50}	B	55.4	25.3	43.0	39.0	75.7	[b]	[b]	79.2	52.9
46	GI_{50}	3.37	5.14	3.52	4.98	4.43	4.79	3.40	5.35	3.60	4.28
	TGI	67.9	20.9	14.4	[b]	31.2	40.5	27.7	[b]	23.4	32.2
	LC_{50}	[b]	[b]	18.2	[b]	[b]	[b]	[b]	[b]	[b]	18.2
Triazine	GI_{50}	1.18	3.84	4.47	7.05	20.42	6.82	1.46	3.31	1.48	5.49
Analogue[82]	TGI	2.92	11.5	14.6	18.9	14.0	19.5	12.0	4.63	22.4	15.4
	LC_{50}	3.46	27.1	44.3	44.2	35.5	48.0	36.3	13.0	49.4	42.6
Benzimidazole	GI_{50}	17.4	62.0	6.32	6.80	17.5	21.8	11.2	7.90	12.1	18.1
Analogue[83]	TGI	[b]	38.2	[b]	34.8	[b]	[b]	36.8	23.8	[b]	33.4
	LC_{50}	[b]	[b]	[b]	51.5	[b]	[b]	[b]	61.8	[b]	56.7

I, leukemia; II, non-small cell lung cancer; III, colon cancer; IV, CNS cancer; V, melanoma; VI, ovarian cancer; VII, renal cancer; VIII, prostate cancer; IX, breast cancer, [a] Full panel mean-graph midpoint (μM), [b] Compounds showed values >100 μM

Based on these *in vitro* studies, number of cell lines proved sensitive towards individual compound. It has been revealed that the benzimidazole and 4-fluoroaniline or morphine at triazine moiety improve biological function. Due to the presence of aromatic ring systems and protonated amine sites in triazine-benzimidazole hybrids, enzyme inhibition or DNA interaction may participate for tumor growth inhibitory activities of these compounds. This has led us to check the interaction of these compounds with dihydrofolate reductase (DHFR, enzyme involved in the process of propagation of cancer). UV-Visible and fluorescence studies along with thermal denaturation experiments have also been done with calf thymus (ct)-DNA which is responsible for polymerase for protein synthesis. It was envisaged that these studies may help in further refinement of the compounds for increasing their drug efficacy and also to check if the compounds exhibit promiscuity or not.

2.2.2.2. Dihydrofolate Reductase Inhibition Assay

Dihydrofolate reductase inhibition assay kit was used to investigate the inhibition of DHFR in the presence of triazine-benzimidazole analogues. It involves the DHFR mediated conversion of dihydrofolate to tetrahydrofolate in the presence of NADPH. It was observed that these compounds showed excellent inhibitory activity with IC_{50} values ranging from 0.002 μM to 42.4 μM (Table 5). Most of these compounds (**6d**, **10** and **11**) are comparable to that of methotrexate,

while compound **33** exhibited more inhibition of DHFR activity as evident from its IC_{50} value of 2.0 ± 0.01 nM and exhibited almost tenfold higher DHFR inhibitory activity than methotrexate (MTX). The inhibition of DHFR activities of compounds **44** and **46** showed IC_{50} values of 0.72 ± 0.2 µM and 0.32 ± 0.05 µM respectively, indicating slightly lower activity than that of compounds **10** and **11** while compound **43** revealed least active member with IC_{50} value of 42.4 ± 0.7 µM. However, compound **20** showed inactivity in DHFR enzymatic assay.

Table 5. DHFR inhibitory activity of compounds **6c, 6d, 10, 11, 20, 21, 33, 43, 44** and **46** with their binding constants and ligand efficiency.

Compounds	IC_{50} ()	K_a (M^{-1})	K_i (μM)	LE (M)[a]
6c	0.31 µM ± 0.03	--	--	0.28
6d	1.05 µM ± 0.07	4.03×10^4	0.470	0.27
10	0.31 µM ± 0.02	--	--	0.23
11	0.11 µM ± 0.07	8.51×10^4	0.041	0.26
20	--	--	--	--
21	2.07 µM ± 0.02	--	--	0.22
33	2.23 nM ± 0.01	1.77×10^5	0.031	0.30
43	42.4 µM ± 0.7	--	--	0.16
44	0.72 µM ± 0.2	--	--	0.23
46	0.32 µM ± 0.05	--	--	0.23
MTX	0.02 µM ± 0.03	--	--	0.23

[a]Ligand Efficiency (LE) = [-1.4× $\log_{10}$ (IC_{50} (M))]/(number of non hydrogen atoms).

2.2.2.3. UV−Visible Spectral Studies for Interaction of Compounds with DHFR

In order to support the enzyme immunoassay for DHFR inhibitory activity of compounds, UV-Visible studies in the presence of DHFR were performed. A solution of DHFR in HEPES buffer (10^{-3} M) at *p*H 7.2 exhibited UV−Vis absorption band at 269 nm. An appreciable change in the UV-Vis spectrum was observed on stepwise addition of compound **33** (20 µM, 10−40 µL) into DHFR solution. The presence of compound **33** caused hyperchromic shift in absorption maxima (Figure 4a). On the other hand, hyperchromic effect at λ_{max} = 285 nm in absorption band was

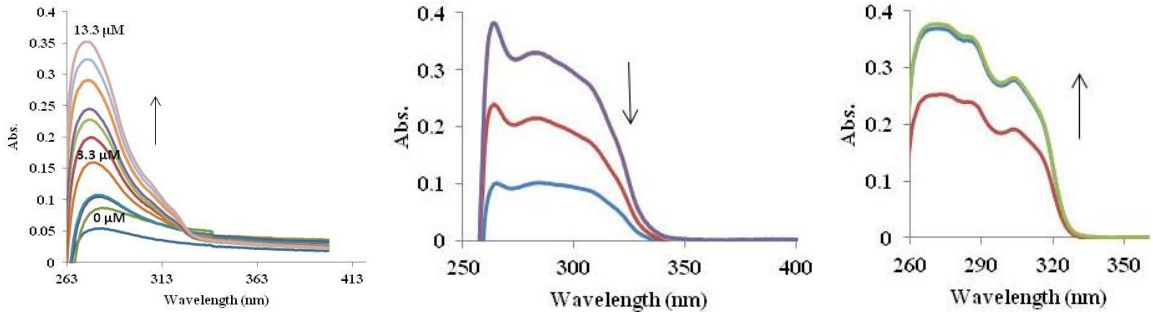

Figure 4. UV-Vis spectrum of DHFR in the presence of increasing concentration of (a) compound **33;** (b) compound **6d;** (c) compound **11** (20 µM, *p*H = 7.2).

observed with the addition of compound **11** into DHFR solution (5-50 μL) (Figure 4c). Therefore, changes in absorption spectra of compounds **11** and **33** in the presence of DHFR clearly indicated their binding capacities with the enzyme. The association constant (K_a) and inhibition constant (K_i) obtained from UV-Vis titrations are in parallel with the results of DHFR enzyme immunoassay (Table 5). Compound **33** with K_a = 1.77 x 10^5 M^{-1}, K_i = 0.031 μM and Ligand Efficiency = 0.30 clearly predicted the higher inhibitory activity of DHFR amongst other compounds. K_i of these compounds was calculated through following equation 1.[84]

$$K_i = IC_{50}/1+ [L]/K_d \text{ --------- } 1$$

where K_i is inhibition constant required to produce half maximum inhibition, L is ligand concentration and K_d is dissociation constant.

Similar results were observed in the presence of DHFR (5-50 μL) in case of compound **6d** that resulted in a hypochromic effect in absorption band (Figure 4b). However, compounds **6c**, **10**, **20**, **21**, **43**, **44** and **46** caused no significant change in absorption band in the presence of DHFR. Therefore, changes in absorption spectra of these compounds with increasing concentration of DHFR clearly indicated binding capacities of the molecules with DHFR. The association and inhibition constants obtained through UV-Vis titration experiments with DHFR are in parallel with the results obtained through DHFR enzyme immunoassay.

2.2.2.4. ^{1}H NMR Spectral Investigations

To find out the site of interaction of compounds with DHFR, ^{1}H NMR spectral studies have been performed. ^{1}H NMR spectra of compound **33** (30 mM), **10** (41 mM), and DHFR (6 μl) were recorded in 0.7 mL of DMSO-d_6 at 25 °C. In the ^{1}H NMR spectrum of compound **33** (lower trace, Figure 5), signals at δ 7.45, 6.80 and 5.60 correspond to exchangeable protons (NH) as confirmed by their D_2O exchange (middle trace, Figure 5). On addition of 6 μL of DHFR solution to compound **33** (DMSO-d_6), NH signal at δ 5.60 ppm has been diminished and signal due to NH at δ 7.45 ppm shifted downfield while signal at δ 6.90 ppm shifted upfield. Shifting of NH signals clearly predicted the interaction of compound **33** with residues of DHFR. A change in chemical shift and linewidth of some of the peaks of DHFR in the region 3−4 ppm (the region most distinctively visible in ^{1}H NMR spectrum of enzyme) (pink trace, Figure 5) also indicated interactions of compound **33** with DHFR.

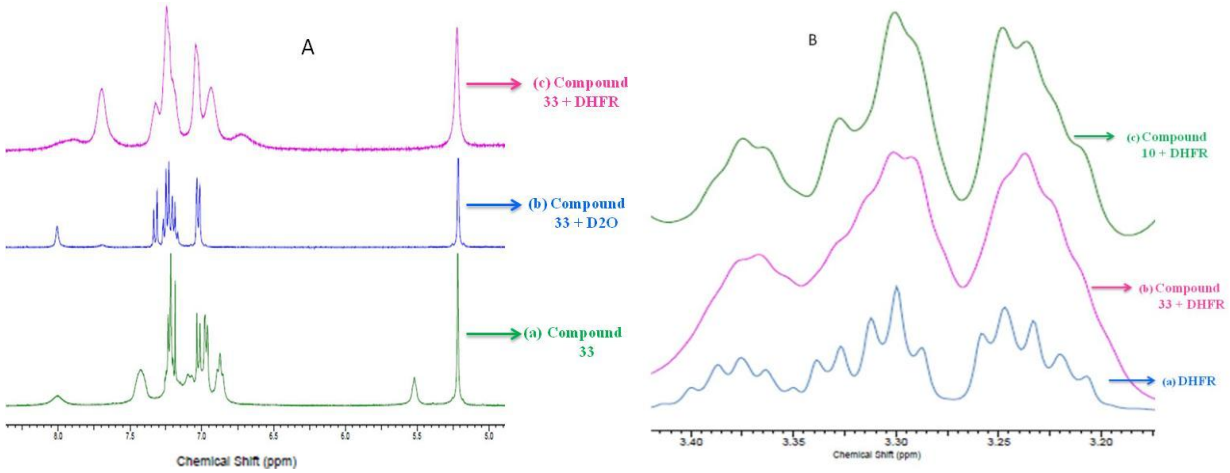

Figure 5. (**A**) (a) Part of ^{1}H NMR spectrum of compound **33**. (b) D_2O exchange showing exchangeable protons NH at δ 7.5, 6.9 and 5.6. (c) Compound **33** in presence of DHFR; (**B**) (a) Part of ^{1}H NMR spectrum of DHFR in region of δ 3.14-3.42 (6 µl in 0.7 mL of DMSO-d_6). (b) Changes in resonance in presence of compound **33**. (c) Changes in resonance in presence of compound **10**.

Addition of 6 µL of DHFR to solution of compound **10** (41 mM, DMSO-d_6) also showed changes in splitting pattern of DHFR signals in the region δ 3−4 ppm (green trace, Figure 5). However, compounds **6c, 6d, 11, 20, 21, 43, 44** and **46** did not exhibit appreciable change either in the spectrum of compounds or dihydrofolate reductase. Hence, results of NMR spectral investigations are in parallel with those of UV−Vis studies, supporting significant interactions of compound **33** with DHFR.

2.2.2.5. DNA Binding Studies

We therefore investigated the binding of the most active series, 5 dose compounds viz., **6c, 6d, 10, 11, 20, 21, 33, 43, 44** and **46** towards ct-DNA, through stepwise addition of DNA to a solution of compound at constant concentration and physiological *p*H. Compound **33** (25 µM) showed absorption maxima at 276 nm (Figure 6a). Upon incremental addition of ct-DNA caused tailing in absorption intensity between 325 nm and 1000 nm that might be due to aggregation in the presence of DNA. In emission spectra, the incremental addition of ct-DNA to compound **33** did not show any significant change in emission band at 340 nm but cause emission enhancement between 370 nm–500 nm (Figure 6b).

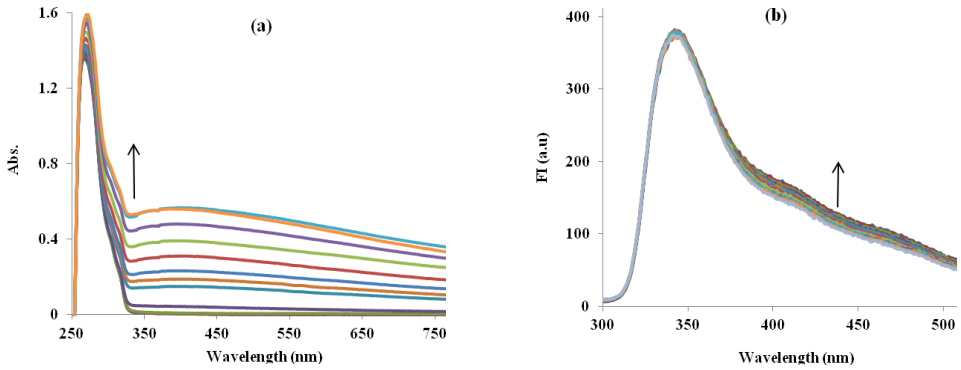

Figure 6. Effect of addition of ct-DNA on **(a)** absorption **(b)** emission spectra of compound **33** (25 μM, *p*H 7.0) in phosphate buffer.

In order to confirm the aggregation, UV-Vis experiment was performed on compound **33**.DNA complex with increasing H_2O ratio from 0-100% in ethanol which showed, upon increasing the water ratio up to 60%, tailing in absorption was formed whereas further increase in H_2O ratio did not affect the absorption intensity. However, compound **33**, in the absence of DNA, with increasing H_2O ratio, did not cause any tailing in the region 325-1000 nm. These aggregations in the presence of DNA were also confirmed through fluorescence spectroscopy (Figure **7**). Compound **33**.DNA complex with increasing H_2O ratio upto 60% caused emission enhancement at 340 nm, which clearly predicts the aggregation induced emission phenomenon in the presence of DNA.

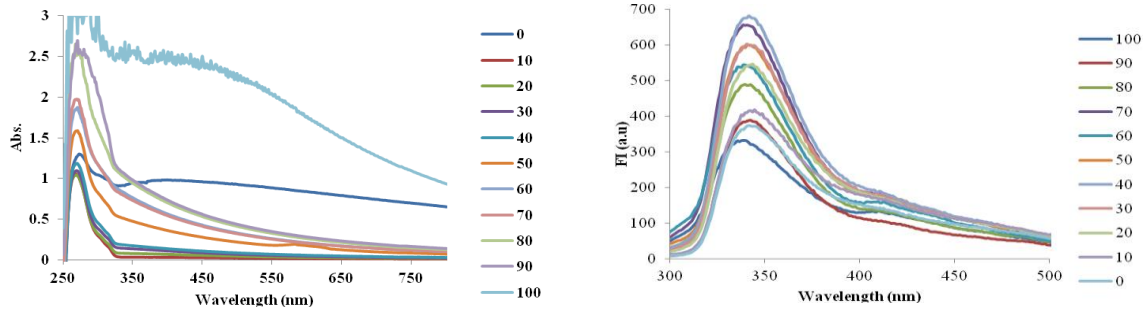

Figure 7. Effect of changing H_2O (0-100 %) ratio on **(a)** absorption and **(b)** emission spectra of compound **33**.

Similarly, we investigated the binding behavior of compounds **6c, 6d 10, 11, 20, 21, 43, 44** and **46** towards ct-DNA. There is increase in the absorption intensity upon incremental addition of ct-DNA to the solution of compound **6c, 10** and **43** (Figures 8a, 10a and 14a) while compounds **11, 44** and **46** (Figures 11a, 15a and 16a) showed decrease in the absorption

intensity. Compound **20** (25 µM) showed absorption maxima at 255 nm and 306 nm as shown in Figure 12a. Upon incremental addition of ct-DNA to the solution of compound **20**, there is increase in the absorption intensity at λ_{max} 255 nm with concomitant decrease in the absorption intensity at λ_{max} 306 nm with isobestic point at 294 nm. The presence of isobestic point during titration with compound **20** and DNA revealed that different species are in equilibrium and there is no stepwise formation of the complex species. In case of emission spectra, compound **6c**, **10, 20** and **46** (Figures 8b, 10b, 12b and 16b) caused emission quenching while compounds **11, 43** and **44** (Figures 11b, 14b and 15b) caused emission enhancement in the presence of DNA.

The stepwise increase in concentration of DNA in compound **6d** also caused increase in absorption intensity along with tailing in absorption intensity between 325 nm-1000 nm which indicated the aggregation of compound in the presence of DNA (Figure 9) whereas compound **21** caused decrease in absorption intensity at their respective λ_{max} (Figure 13). In case of emission spectra, compound **6d** caused fluorescence enhancement typically due to aggregation whereas compound **21** showed emission quenching in the presence of DNA. The binding constant K_a for ligand–DNA binding was determined from the Benesi–Hildebrand[85] equation-2 for UV-Vis and fluorescence titrations, suggested strong interaction of ct-DNA with compounds.

$$1/(A_f - A_{obs}) = 1/(A_f - A_{fc}) + \{1/[K_a(A_f - A_{fc})]\}[\text{ligand}] \quad \ldots\ldots 2$$

where K_a is the binding constant, A_f is the absorbance of the free host, A_{obs} is the absorbance observed, and A_{fc} is the absorbance at saturation.

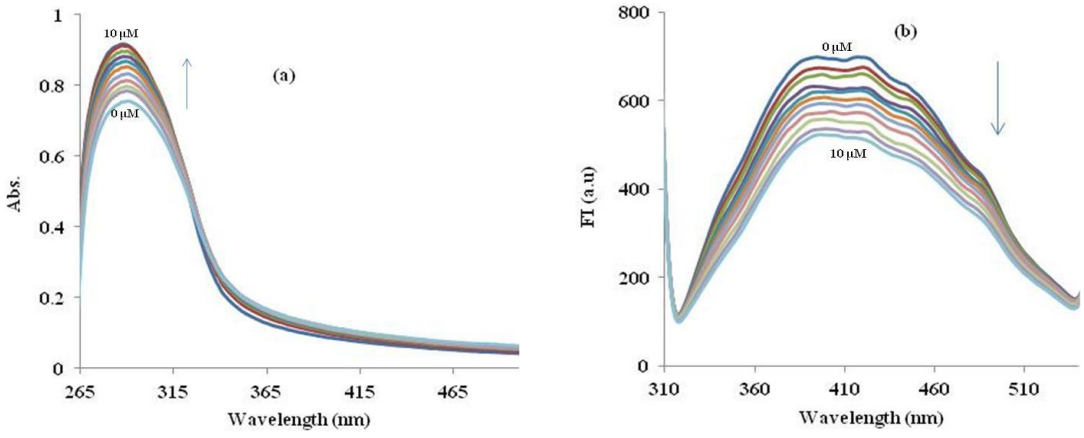

Figure 8. Effect of addition of ct-DNA on **(a)** absorption **(b)** emission spectra of compound **6c** in phosphate buffer.

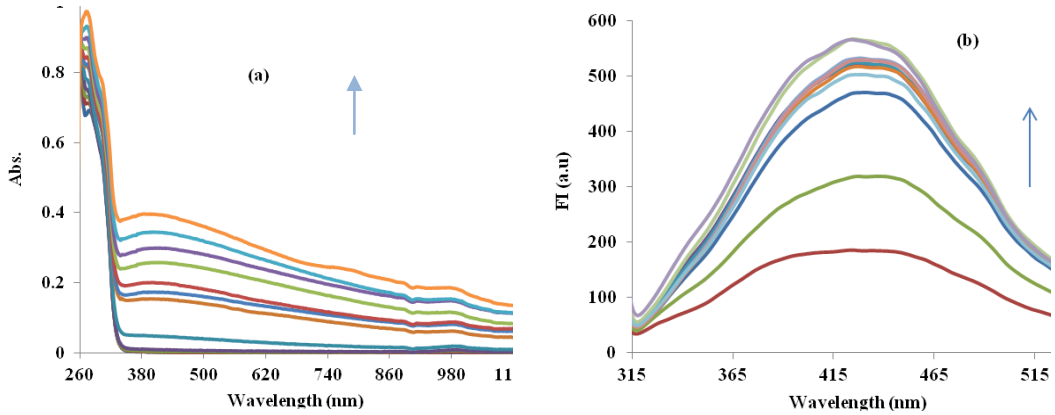

Figure 9. Effect of addition of ct-DNA on **(a)** absorption **(b)** emission spectra of compound **6d** in phosphate buffer.

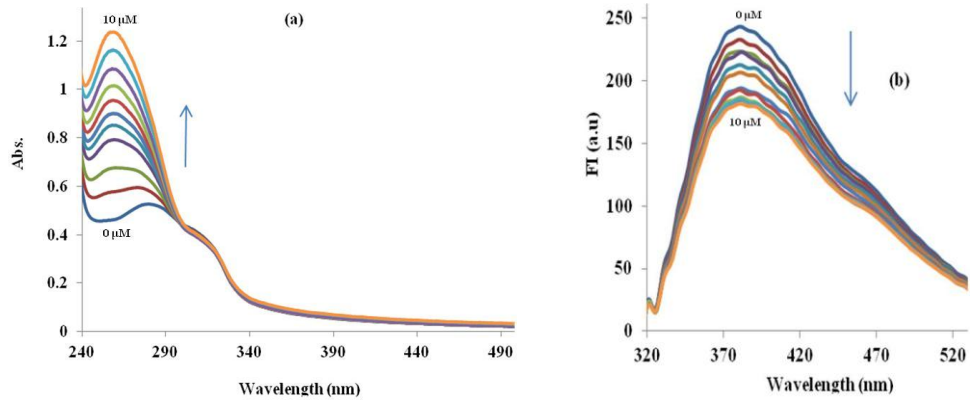

Figure 10. Effect of addition of ct-DNA on **(a)** absorption **(b)** emission spectra of compound **10** in phosphate buffer.

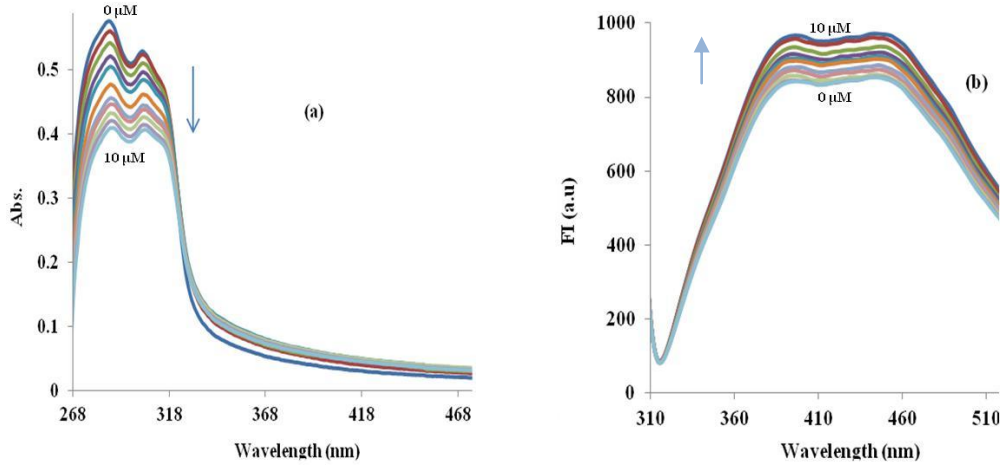

Figure 11. Effect of addition of ct-DNA on **(a)** absorption **(b)** emission spectra of compound **11** in phosphate buffer.

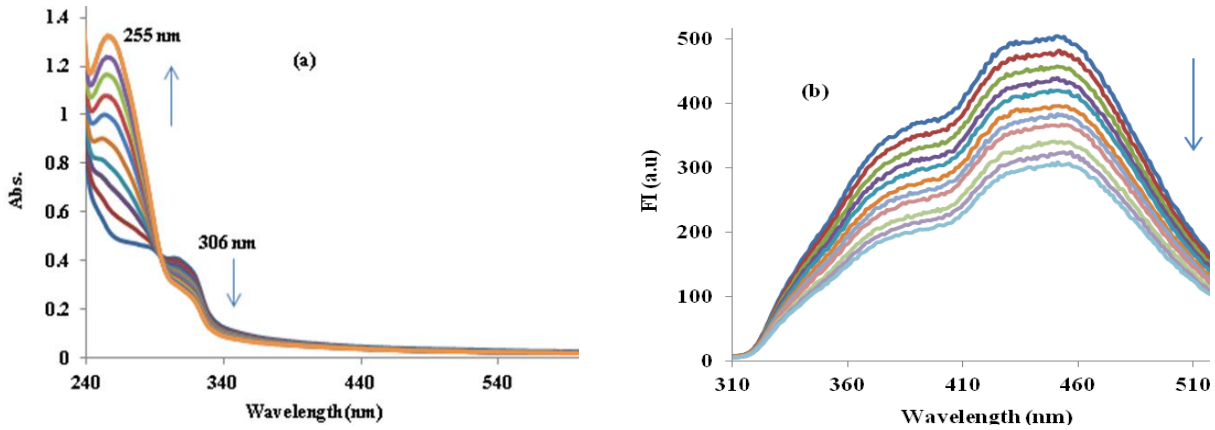

Figure 12. Effect of addition of ct-DNA on **(a)** absorption **(b)** emission spectra of compound **20** in phosphate buffer (pH 7.0).

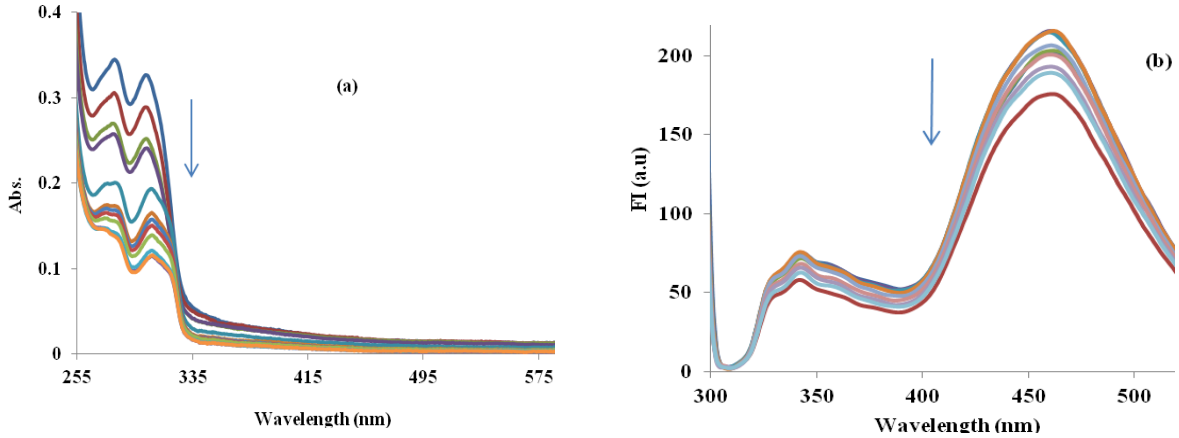

Figure 13. Effect of addition of ct-DNA on **(a)** absorption **(b)** emission spectra of compound **21** in phosphate buffer.

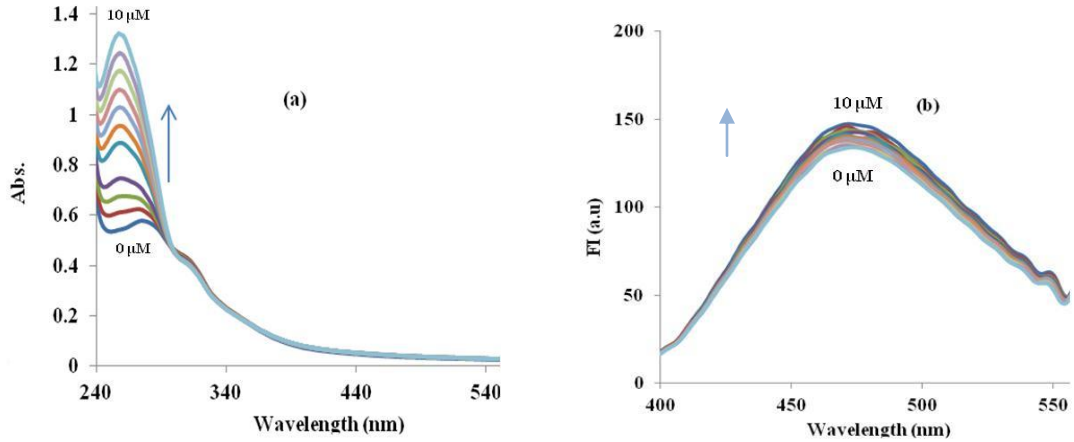

Figure 14. Effect of addition of ct-DNA on **(a)** absorption **(b)** emission spectra of compound **43** in phosphate buffer.

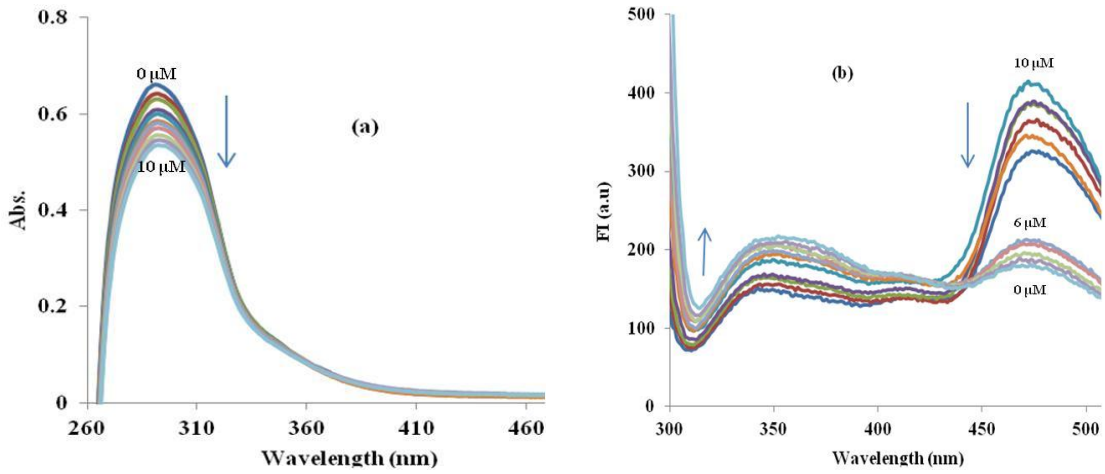

Figure 15. Effect of addition of ct-DNA on **(a)** absorption **(b)** emission spectra of compound **44** in phosphate buffer.

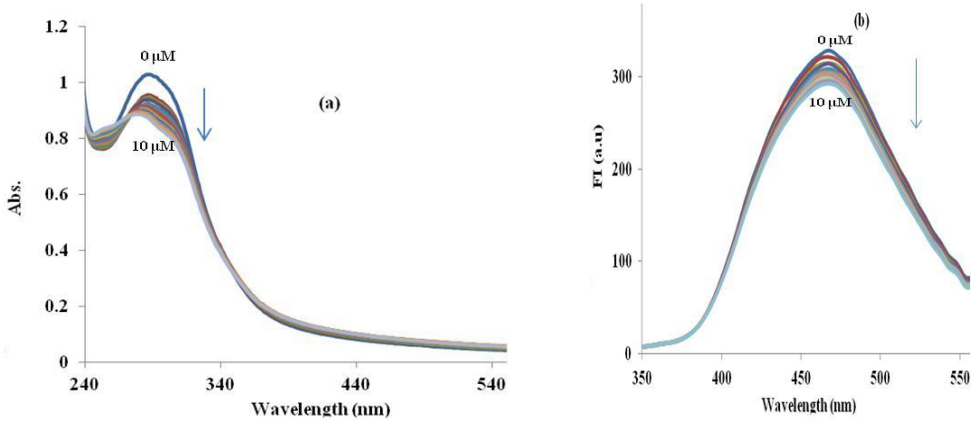

Figure 16. Effect of addition of ct-DNA on **(a)** absorption **(b)** emission spectra of compound **46** in phosphate buffer.

Table 6. Binding constant of compounds with ct-DNA**.**

Compd	K_a (UV studies) in M^{-1}	K_a (Fluorescent studies) in M^{-1}	T_m (^{0}C)
6c	6.03×10^4	2.97×10^4	57.0
6d	1.01×10^5	7.84×10^4	Nd
10	2.92×10^4	3.36×10^4	65.6
11	5.23×10^4	5.46×10^4	71.5
20	3.06×10^4	5.46×10^4	62.6
21	3.75×10^4	2.6×10^4	85.0
33	7.19×10^4	8.58×10^4	80.1
43	3.39×10^4	1.97×10^4	Nd
44	3.19×10^4	4.21×10^4	68.5
46	2.96×10^4	1.50×10^4	67.5

nd- not determined

In order to evaluate strength of intercalative nature of compounds with DNA, thermal behaviour of ct-DNA in the presence of hybrids was also determined. Intercalation of molecules into the double helix is known to stabilize the DNA against thermal strand separation and thus increases thermal melting temperature (T_m). The thermal denaturation temperature of ct- DNA (60 ^oC), increased significantly in the presence of compounds **21** (85.0 ^oC) and **33** (80.1 ^oC) which showed strong intercalation properties of these compounds with DNA (Table 6).

2.2.2.6. Physicochemical Parameters

As a part of our study; variation of fragments to the triazine and benzimidazole have allowed us to evaluate the influence of different parameters at the pharmacophoric part of the molecules. The compliance of compounds **6c, 6d, 10, 11, 20, 21, 33, 43, 44** and **46** were evaluated with different physicochemical descriptors, favouring their drug like properties (Table 7). Within the series of compounds, it has been observed that descriptors like total polar surface area (TPSA), molar refractivity, polarizability and solvent accessibility surface area showed great influence on the DHFR activity. Thus, the lipophilicity does not exert any effect on activity in all compounds but hydrophilicity produces an important parameter for the activity. Compound **33**, most active in DHFR interaction, showed higher values in all these parameters that also supported the inhibitory activity.

Table 7. Physicochemical parameters for compounds **6c, 6d, 10, 11, 20, 21, 33, 43, 44** and **46**.

Compd	log P	TPSA (Å^2)	nON	nOHNH	molar refractivity	dipole moment (debye)	polarizability	solvent accessibility surface area(Å^2)
6c	5.94	80.55	7	2	128.30	6.14	51.96	454.81
6d	4.47	81.00	8	1	123.11	5.31	52.83	436.57
10	5.82	87.03	9	2	153.23	5.89	63.18	529.91
11	6.34	83.79	8	2	144.72	5.77	59.95	499.74
20	4.88	84.23	9	1	139.24	4.83	57.17	491.32
21	5.27	93.02	9	2	144.12	5.50	58.76	494.69
33	4.96	105.05	10	3	160.04	6.41	65.60	550.42
43	7.65	80.55	7	2	152.97	4.22	63.84	519.11
44	5.96	80.55	7	2	147.03	5.24	58.70	498.16
46	6.88	89.79	8	2	154.63	5.66	64.33	531.90

2.2.2.7. Structure Activity Relationship

Structure-activity correlation, based upon the cancer cell lines and dihydrofolate reductase revealed that the nature of the substituents at C2- and C6-positions of triazine significantly affected the biological activity. Regarding 60 human tumor cell line studies; compounds with 1-benzyl-2-methyl-1*H*-benzimidazol-5-yl at C2-position of triazine (**7-26**) showed comparatively higher activity than their isomers, 3-benzyl-2-methyl-3*H*-benzimidazol-5-yl (**27-40**), suggested that there is much difference in antitumor activity with orientation of benzyl group of benzimidazole. In the first series of fluorophenyl compounds (**7-18**), substitution of chloro group **6a** with primary/secondary amines and aryl groups improved the inhibitory activity of compounds. Secondary amine substitutions at this position showed higher activity, as illustrated by 4-methylpiperazine (**10**) and pyrrolidine (**11**) groups in comparison to primary amines (**8, 9**, **12, 13** and **17**). Similarly, in case of Pd catalyzed arylation reaction of **6a** with aryl boronic acids (compounds **43, 44** and **46**), the activities were slightly decreased due to hydrophobic aryl groups. In another series of fluorophenyl compounds (**27-33**), substitution of **6c** with 4-aminoethylmorpholine (**33**) enhanced the antitumor activity in comparison to other primary and secondary amines. Similarly, with the series of morpholine substituted compounds, it has been observed that compounds **6b** and **19-26** showed comparatively higher activity than their isomers **6d** and **34-40**. Regarding 60 human tumor cell lines, in the series of compounds **6b** and **19-26** substitution at C6 position of triazine, 4-fluoroaniline (**20**) showed higher activity. In another series of compounds (**6d** and **19-26**), chloro substitution at C6 position of triazine, showed selectivity as compared to substitution of primary and secondary amines.

The dihydrofolate reductase inhibitory activity results revealed that substitution of **6c** with secondary amine 4-methylpiperazine did not effect the reactivity but substitution with pyrrolidine (**11**), showed almost three fold increase in activity while hydrophobic aryl groups like 2-thienyl (**44**) and 4-methoxyphenyl (**46**) showed slightly decrease in affinity. However, much higher activity was observed with small alkyl group linker, 2-aminoethylmorpholine (**33**) in the nanomolar range. These studies indicated that the substitution of the triazine-benzimidazole heterocycles with various primary and secondary amines led to highly potency towards 60 human cancer cell line activities as well as dihydrofolate reductase inhibition. The structure-activity relationship emerged from the activity towards cancer cell lines, DHFR and

DNA revealed that permutation of triazine and benzimidazole hybrid was well tolerated for *in vitro* anticancer and DHFR inhibitory activity.

2.2.2.8. Molecular Modeling

In order to have an insight into the molecular interaction of compounds with DHFR, their docking was planned to scrutinize the mode of interaction of compound with amino acids in the active site of the enzyme.[86] Molecular docking was carried out with compound **33**, which has been proven to be the most active in DHFR enzyme immunoassay. Compound **33** (Figure 17) sits in the active site of the enzyme (PDB ID 3GHW), interacting through H-bonding between oxygen atom of morphoine with α-helix of A124 (*d* = 2.87 Å) and M125 (*d* = 2.78 Å) amino acid residues. Nitrogen atom of morpholine (*d* = 0.98 Å), NH group of aminoethylmorpholine (*d* = 2.41 Å) and nitrogen atoms of triazine (*d* = 2.47 Å and *d* = 2.14 Å) showed hydrogen bonding with β-strand of C6 amino acid residue.

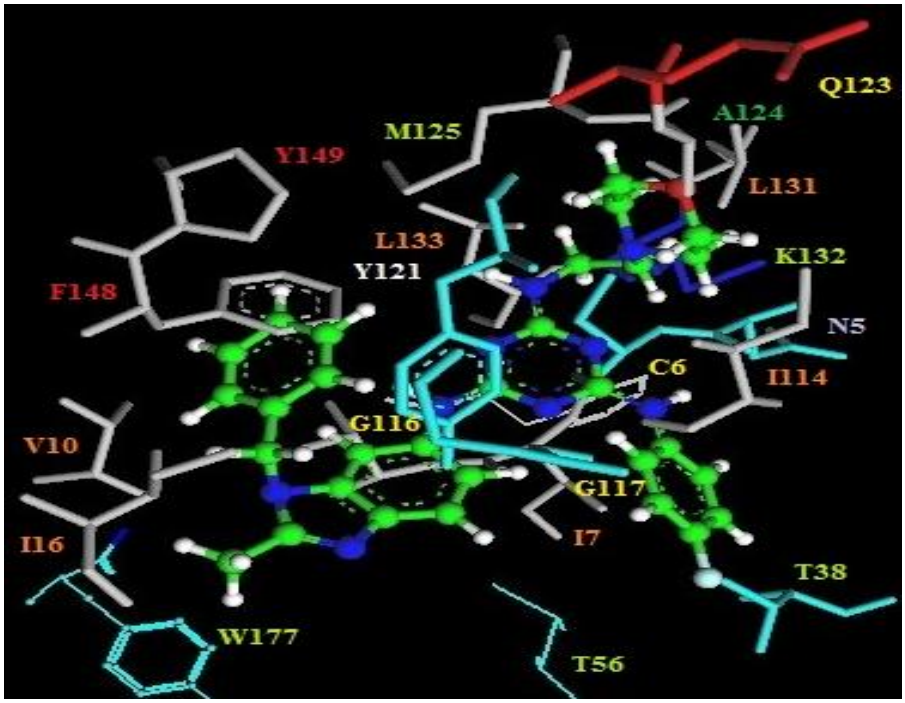

Figure 17. Compound **33** docked in the active site of DHFR (3GHW).[87]

Nitrogen atoms of triazine (*d* = 2.39 Å and *d* = 1.73 Å) and NH group of benzimidazole (*d* = 2.40 Å) showed hydrogen bonding interaction with β-strand of I7 amino acid residue. NH group of benzimidazole (*d* = 2.40 Å) also showed hydrogen bonding interaction with α-helix of Y121

amino acid residue. NH group of 4-fluorophenylamine (NH…O=C, *d* = 1.62 Å) and nitrogen atom of triazine (N…O=C, *d* = 2.26 Å) showed hydrogen bonding interaction with β-strand of N5 and I114 amino acid residues respectively. Therefore, the crystal coordinates of the DHFR in association with compound **33** supported the experimental results, as these compounds exhibited interactions with active site of enzymes.

2.2.3. CONCLUSION

The present work has led to the development of novel triazine-benzimidazole hybrids bearing 4-fluoroaniline and morpholine with different substitution of primary and secondary amines as well as substituted aryl groups. The anticancer activity profile of these hybrid compounds towards 60 human cancer lines indicated effective inhibition towards tumor growth for most of the cancer cell lines. As per the results of enzyme immunoassay (DHFR), these compounds exhibited significant inhibition towards DHFR with IC_{50} values in micromolar range while compound **33** showed highest activity with IC_{50} value of 2.0 nM. These interactions have also been confirmed by UV-Visible and NMR experiments. These compounds also showed strong intercalating properties with ct-DNA, determined by UV-Visible and fluorescence spectroscopy as well as thermal denaturation experiment. Moreover, molecular docking analysis of most active compound **33** in the active site of DHFR also supported the experimental results for their interactions. Overall results revealed that: (i) regioisomeric aminobenzimidazoles at triazine ring play a key role in varying the efficiency of antitumor activities, (ii) fluoroaniline or morpholine at one of position of triazine ring positively influences the antitumor effectiveness, inducing good activity against most of the cancer cell lines, (iii) chloro substitution at C6-position of triazine ring also imparts antitumor activity, (iv) introduction of 4-fluoroaniline (**8**), piperidine (**9**) and aminoethylmorpholine (**33**) at the C6 position of triazine ring led to a broad spectrum of selectivity with respect to other primary and secondary amines, thus essential for activity, (v) linker between triazine and benzimidazole is essential as H-bond region.These preliminary encouraging results of biological screening could offer an excellent framework in medicinal field.

2.2.4. EXPERIMENTAL SECTION

All materials were obtained from commercial suppliers and used without further purification unless otherwise noted. Melting points were determined in open capillaries and are uncorrected. ^{1}H NMR and ^{13}C NMR spectra were recorded on a Bruker Avance 400 (^{1}H, 400 MHz; ^{13}C, 100 MHz) or Jeol-400 (^{1}H, 400 MHz; ^{13}C, 100 MHz) spectrometer at ambient temperature, using $CDCl_3$ and DMSO-d_6 as solvents. Chemical shifts are reported in ppm. Data are reported as follows: chemical shift, multiplicity (s = singlet, d = doublet, t = triplet, q = quartet, b = broad, m = multiplet), coupling constants and number of protons. Mass spectrometric data were recorded at Waters Micromass Q-Tof Micro. Elemental analysis was done with Thermo Scientific (Flash 2000) analyzer. UV-Visible studies were carried out Shimadzu-2400 PC spectrometer. The fluorescence spectra were determined on a Varian Cary Eclipse fluorescence spectrometer. The crystal structure was collected on Bruker AXS KAPPA APEX II CCD diffractometer. Reactions were monitored by thin-layer chromatography (TLC) carried out on silica gel plates (GF 254) using UV light as visualizing agents. Silica gel 60-120 mesh was used for column chromatography. Hexane:ethyl acetate and chloroform:methanol were adopted solvent systems.

Chemicals and Solvents

o-Phenylenediamine, acetic acid, nitric acid, hydrochloric acid, sulphuric acid, benzyl chloride, potassium carbonate, sodium bicarbonate, ethanol, sodium hydroxide, stannous chloride, cyanuric chloride, tetrahydrofuran, 1,4-dioxane, chloroform, methanol, ethyl acetate, hexane, *p*-fluoroaniline, morpholine, piperidine, pyrrolidine, *N*-methylpiperazine, *p*-aminophenol, *p*-aminothiophenol, 1,2-ethylenediamine, 1,2-ethanolamine, aminoethylmorpholine, aniline, 2-aminopyrimidine, 2-aminobenzonitrile, phenylboronic acid, *p*-fluorophenylboronic acid, *p*-chlorophenylboronic acid, *p*-methoxyphenylboronic acid, *m*-methylphenylboronic acid and thiophene-2-boronic acid.

Procedure for synthesis of 1-benzyl-2-methyl-1*H*-benzimidazol-5-ylamine (4a) and 3-benzyl-2-methyl-3*H*-benzimidazol-5-ylamine (4b)

o-Phenylenediamine (1.08 g, 10.0 mmol) and acetic acid (0.52ml, 13.6 mmol) was refluxed on a water bath for 2 hr at 100 ^{0}C, cooled and 10% NaOH solution was added slowly with constant rotation of the flask, until the mixture was just alkaline to litmus. Crude benzimidazole was

filtered off at the pump, washed with ice cooled water and dried to give pure 2-methyl-1*H*-benzimidazole (**1**) in 98% yield. To a stirring solution of 2-methyl-1*H*-benzimidazole **(1)** (3.50 g, 24.1 mmol) in conc. H_2SO_4 (15 mL) at -5 ºC, was added conc. HNO_3 (15 mL) dropwise ensuring the reaction temperature was < 20 ºC. The solution was stirred at -5 °C for 30 min and then poured onto ice. The precipitate that formed was filtered and washed with water to give 2-methyl-5-nitro-1*H*-benzimidazole **(2)** (75%) as a light yellow solid. To a solution of 2-methyl-5-nitro-1*H*-benzimidazole **(2)** (9.0 g, 0.05 mol) in ethanol (50 mL), K_2CO_3 (6.98 g, 0.075 mol) and benzyl chloride (9.63 g, 0.075 mol) were refluxed for 8 h. After the completion of the reaction (monitored by TLC), the reaction mixture was filtered and concentrated to get yellow solid. The residual mass was crystallized from ethanol to give mixture of 1-benzyl-2-methyl-5-nitro-1*H*-benzimidazole and 3-benzyl-2-methyl-5-nitro-3*H*-benzimidazole **(3)** in 75% yield. To a suspension of $SnCl_2.2H_2O$ (15.45 g, 0.067 mol) in 2N HCl (47.6 mL), 1/3-benzyl-2-methyl-5-nitro-1*H/*3*H*-benzimidazole **(3)** (4.25 g, 0.019 mol) was heated at 110 ^oC for 7 h. After completion of the reaction, the suspension was neutralized with 2N NaOH and diluted with ethanol. Filtered the solid product and extracted the filtrate with chloroform, dried over Na_2SO_4, filtered and concentrated to get mixture of products which were separated through column chromatography using ethylacetate:methanol (19:1) as eluent to get solid compounds **4a** and **4b**.

1-Benzyl-2-methyl-1*H*-benzimidazol-5-ylamine (4a)

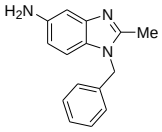

Brownish powder; (2.6 g, 69%); M.p. 137-139 ^oC; ^1H NMR (400 MHz, $CDCl_3$): δ = 7.48 (d, 1H, *J* = 8.24 Hz, ArH), 7.30-7.24 (m, 3H, ArH), 7.03 (d, 2H, *J* = 6.88 Hz, ArH), 6.63 (dd, 1H, ^2J = 8.24, ^3J = 1.84 Hz, ArH), 6.47 (d, 1H, *J* = 1.36 Hz, ArH), 5.19 (s, 2H, N-CH_2), 2.51 (s, 3H, CH_3); ^{13}C NMR (100 MHz, $CDCl_3$): δ = 149.2, 142.3, 136.7, 136.0, 129.0, 127.9, 127.8, 126.2, 119.5, 119.4, 112.0, 111.1, 95.1 (ArC), 47.0 (N-CH_2), 13.9 (CH_3); MS(ESI), m/z: 238.2 (M^++1).

3-Benzyl-2-methyl-3*H*-benzimidazol-5-ylamine (4b).

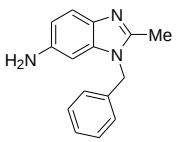

Brownish powder; (1.0 g, 26%); M.p. 137-139 ^oC; ^1H NMR (400 MHz, $CDCl_3$): δ = 7.28-7.24 (m, 3H, ArH), 7.02 (s, 1H, ArH), 7.01 (d, 2H, *J* = 5.52 Hz, ArH), 6.97 (d, 1H, *J* = 8.24 Hz, ArH), 6.60 (d, 1H, *J* = 8.24 Hz, ArH), 5.22 (s, 2H, N-CH_2), 2.52 (s, 3H, CH_3); ^{13}C NMR (100 MHz, $CDCl_3$): δ = 151.7, 143.2, 142.1, 135.9, 129.3, 129.0, 127.9, 126.2, 112.3, 109.8, 104.3 (ArC), 47.1 (N-CH_2), 13.8 (CH_3); MS(ESI), m/z: 238.2 (M^++1).

General procedure for the preparation of (1/3-Benzyl-2-methyl-1*H*/3*H*-benzimidazol-5-yl)-(4,6-dichloro-[1,3,5]triazin-2-yl)-amine (5a, 5b).

To a stirred solution of cyanuric chloride (10.0 g, 0.054 mol) in anhydrous THF (150 mL) was added 1/3-benzyl-2-methyl-1*H*/3*H*-benzimidazol-5-ylamine **(4a/4b)** (11.56 g, 0.048 mol) at 0-5 ^{o}C. To this mixture, 10% $NaHCO_3$ was added drop wise and stirred at the same temperature for 6 h. The resulted reaction mixture was then poured into crushed ice and filtered, dried and then column chromatographed on silica gel in chloroform:methanol (50:1) as eluents to give (1/3-benzyl-2-methyl-1*H*/3*H*-benzimidazol-5-yl)-(4,6-dichloro-[1,3,5]triazin-2-yl)-amine (**5a/5b**).

(1-Benzyl-2-methyl-1*H*-benzimidazol-5-yl)-(4,6-dichloro-[1,3,5]triazin-2-yl)-amine (5a).

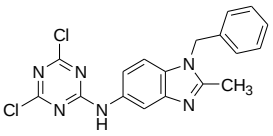

Yellow powder; (20.02 g, 96%); M.p. > 300 ^{o}C;^{1}H NMR (400 MHz, DMSO-d_6): δ = 11.22 (s, 1H, NH), 7.98 (s, 1H, ArH), 7.60 (d, 1H, *J* = 3.60 Hz, ArH), 7.42 (dd, 1H, ^{2}J = 8.72 Hz, ^{3}J = 1.92 Hz, ArH), 7.34-7.29 (m, 5H, ArH), 5.49 (s, 2H, N-CH_2), 2.50 (s, 3H, CH_3); ^{13}C NMR (100 MHz, DMSO-d_6): δ = 154.8, 152.2, 150.4, 134.3, 132.3, 129.5, 128.9, 128.5, 128.3, 120.6, 114.8, 105.3 (ArC), 48.3 (N-CH_2), 12.4 (CH_3); MS(ESI), m/z: 385.1 (M^++1); Anal. Calcd for $C_{18}H_{14}Cl_2N_6$: C, 56.12; H, 3.66; N, 21.81, Found: C, 56.42; H, 3.60; N, 21.44.

(3-Benzyl-2-methyl-3*H*-benzimidazol-5-yl)-(4,6-dichloro-[1,3,5]triazin-2-yl)-amine (5b).

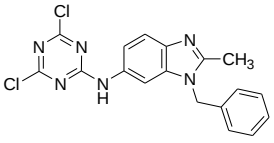

Yellow powder; (18.78 g, 90%); M.p. > 300 ^{o}C; ^{1}H NMR (400 MHz, DMSO-d_6): δ = 8.60 (bs, 1H, NH), 8.07 (d, 1H, *J* = 1.84 Hz, ArH), 7.36 (d, 1H, *J* = 8.72 Hz, ArH), 7.29-7.21 (m, 3H, ArH), 7.16 (d, 1H, *J* = 8.68 Hz, ArH), 7.05 (d, 1H, *J* = 5.96 Hz, ArH), 6.85 (d, 1H, *J* = 8.68 Hz, ArH), 5.31 (s, 2H, CH_2), 2.57 (s, 3H, CH_3); ^{13}C NMR (100 MHz, DMSO-d_6): δ = 154.8, 152.2, 150.4, 136.4, 134.2, 132.2, 129.5, 129.0, 128.3, 126.8, 120.7, 114.9, 105.0 (ArC), 48.4 (N-CH_2), 12.0 (CH_3); MS(ESI), m/z: 385.1 (M^++1); Anal. Calcd for $C_{18}H_{14}Cl_2N_6$: C, 56.12; H, 3.66; N, 21.81, Found: C, 56.37; H, 3.41; N, 21.87.

General procedure for the preparation of compounds 6a-d.

To a stirred solution of (1/3-benzyl-2-methyl-1*H*/3*H*-benzimidazol-5-yl)-(4,6-dichloro-[1,3,5]triazin-2-yl)-amine **(5a/5b)** (10 g, 0.026 mol) in anhydrous THF (150 mL) was added 4-fluoroaniline/morpholine (3.46 g, 0.031 mol) at room temperature. To this mixture, 10% $NaHCO_3$ was added drop wise and stirred for 4 h. The resulted reaction mixture was then poured into

crushed ice, filtered, dried and column chromatographed on silica gel in chloroform:methanol (50:1) to afford the desired products.

***N*-(1-benzyl-2-methyl-1*H*-benzimidazol-5-yl)-6-chloro-*N*'-(4-fluoro-phenyl)-[1,3,5]triazine-2,4-diamine (6a).**

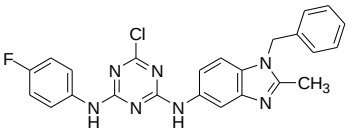

White powder; (8.35 g, 70%); M.p. > 300 ^{o}C; ^{1}H NMR (400 MHz, DMSO-d_6): δ = 10.15 (s, 1H, NH), 10.11 (s, 1H, NH), 7.90-7.84 (m, 2H, ArH), 7.72-7.57 (m, 2H, ArH), 7.47 (d, 1H, *J* = 8.52 Hz, ArH), 7.37 (d, 1H, *J* = 8.44 Hz, ArH), 7.47 (d, 1H, *J* = 8.52 Hz, ArH), 7.37 (d, 1H, *J* = 8.44 Hz, ArH), 7.29-7.20 (m, 3H, ArH), 7.09-6.90 (m, 3H, ArH), 5.19 (s, 2H, N-CH_2), 2.50 (s, 3H, CH_3); ^{13}C NMR (100 MHz, DMSO-d_6): δ = 163.6, 151.5, 138.4, 134.9, 132.9, 128.3, 127.2, 126.5, 125.9, 122.4, 117.6, 116.1, 114.7, 114.5, 101.8 (ArC), 46.4 (N-CH_2), 13.5 (CH_3); MS(ESI), m/z: 460.2 (M^++1); Anal. Calcd for $C_{24}H_{19}ClFN_7$: C, 62.68; H, 4.16; N, 21.32, Found: C, 62.92; H, 4.56; N, 21.47.

(1-Benzyl-2-methyl-1*H*-benzimidazol-5-yl)-(4-chloro-6-morpholin-4-yl-[1,3,5]triazin-2-yl)-amine (6b).

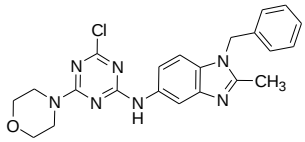

White powder; (9.07 g, 80%); M.p. > 300 ^{o} C; ^{1}H NMR (400 MHz, $CDCl_3$): δ = 7.76 (bs, 1H, NH), 7.66 (d, 1H, *J* = 8.72 Hz, ArH), 7.32-7.26 (m, 5H, ArH), 7.10 (d, 1H, *J* = 8.24 Hz, ArH), 7.02 (s, 1H, ArH), 5.30 (s, 2H, N-CH_2), 3.80 (s, 2H, mor-CH_2), 3.67 (s, 2H, mor-CH_2), 3.50 (s, 2H, mor-CH_2), 3.40 (s, 2H, mor-CH_2), 2.55 (s, 3H, CH_3); ^{13}C NMR (100 MHz, $CDCl_3$): δ = 164.6, 163.8, 152.4, 139.4, 135.6, 132.8, 129.2, 128.1, 125.7, 119.2, 116.2, 102.1 (ArC), 66.7 (O-CH_2), 66.5 (O-CH_2), 46.9 (N-CH_2), 44.0 (N-CH_2), 14.0 (CH_3); MS(ESI), m/z: 436.2 (M^++1); Anal. Calcd for $C_{22}H_{22}ClON_7$: C, 60.62; H, 5.09; N, 22.49, Found: C, 61.01; H, 5.41; N, 22.14.

***N*-(3-benzyl-2-methyl-3*H*-benzimidazol-5-yl)-6-chloro-*N*'-(4-fluoro-phenyl)-[1,3,5]triazine-2,4-diamine (6c).**

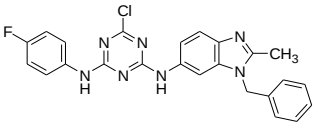

White powder; (9.21 g, 77%); M.p. > 300 ^{o} C; ^{1}H NMR (400 MHz, $CDCl_3$): δ = 7.73 (bs, 1H, NH), 7.51-7.26 (m, 7H, ArH), 7.17 (d, 1H, *J* = 8.28 Hz, ArH), 7.08 (d, 4H, *J* = 1.36 Hz, ArH), 6.86 (bs, 1H, NH), 5.34 (s, 2H, N-CH_2), 2.61 (s, 3H, CH_3); ^{13}C NMR (100 MHz, $CDCl_3$): δ = 153.2, 142.9, 135.6, 133.4, 129.2, 128.3, 128.2, 126.8, 126.3, 125.4, 124.5, 122.4, 115.7, 114.6, 109.4 (ArC), 47.4 (N-

CH_2), 14.2 (CH_3); MS(ESI), m/z: 460.2 (M^++1); Anal. Calcd for $C_{24}H_{19}ClFN_7$: C, 62.68; H, 4.16; N, 21.32, Found: C, 63.04; H, 4.43; N, 21.37.

(3-Benzyl-2-methyl-3*H*-benzimidazol-5-yl)-(4-chloro-6-morpholin-4-yl-[1,3,5]triazin-2-yl)-amine (6d).

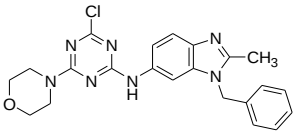

White powder; (8.38 g, 74%); M.p. > 300 ^oC; ^1H NMR (400 MHz, $CDCl_3$): δ = 8.08 (s, 1H, NH), 7.34-7.30 (m, 3H, ArH), 7.23 (d, 1H, *J* = 3.68 Hz, ArH), 7.17 (d, 2H, *J* = 8.72 Hz, ArH), 7.06 (d, 1H, *J* = 7.80 Hz, ArH), 7.04 (d, 1H, *J* = 1.40 Hz, ArH), 5.32 (s, 2H, N-CH_2), 3.85 (t, 4H, *J* = 9.16 Hz, mor-CH_2), 3.74-3.73 (m, 4H, mor-CH_2), 2.58 (s, 3H, CH_3); ^{13}C NMR (100 MHz, $CDCl_3$): δ = 163.8, 152.9, 142.8, 135.6, 132.5, 129.3, 129.1, 128.1, 128.0, 126.2, 125.9, 122.9, 116.6, 116.5, 111.6, 109.4 (ArC), 66.7 (O-CH_2), 47.3 (N-CH_2), 44.1 (N-CH_2), 14.1 (CH_3); MS(ESI), m/z: 436.2 (M^++1); Anal. Calcd for $C_{22}H_{22}ClON_7$: C, 60.62; H, 5.09; N, 22.49, Found: C, 60.65; H, 5.36; N, 22.30.

General procedure for the preparation of compounds 7-40.

To a stirred solution of *N*-(1/3-benzyl-2-methyl-1*H*/3*H*-benzimidazol-5-yl)-6-chloro-*N*'-(4-fluoro-phenyl)-[1,3,5]triazine-2,4-diamine (**6a/6b**) (0.200 g, 0.435 mmol) in 1,4-dioxane (20 ml) piperidine (0.147 g, 1.74 mmol) and potassium carbonate (0.076 g, 0.551 mmol) was added and refluxed for 8 h. Extracted the reaction mixture with chloroform, dried over Na_2SO_4, filtered and concentrated to get crude product which was then purified through column chromatography using chloroform:methanol (50:1) as eluents to give the desired products.

***N*-(1-benzyl-2-methyl-1*H*-benzimidazol-5-yl)-*N*'-(4-fluoro-phenyl)-6-piperidin-1-yl-[1,3,5]triazine-2,4-diamine (7).**

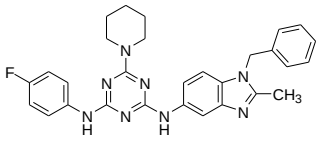

White powder; (0.179 g, 81%); M.p. > 300 ^oC; ^1H NMR (400 MHz, $CDCl_3$): δ = 7.85 (bs, 1H, NH), 7.60 (d, 1H, *J* = 8.68 Hz, ArH), 7.45 (d, 1H, *J* = 4.60 Hz, ArH), 7.43 (d, 1H, *J* = 4.56 Hz, ArH), 7.29-7.26 (m, 3H, ArH), 7.10 (d, 1H, *J* = 2.28 Hz, ArH), 7.08 (d, 1H, *J* = 1.84 Hz, ArH), 7.05 (s, 1H, ArH), 7.01 (d, 1H, *J* = 5.96 Hz, ArH), 6.94 (t, 2H, *J* = 8.72 Hz, ArH), 5.20 (s, 2H, N-CH_2), 3.68 (s, 4H, pip-CH_2), 2.49 (s, 3H, CH_3), 1.61 (t, 2H, *J* = 3.64 Hz, pip-CH_2), 1.49 (s, 4H, pip-CH_2); ^{13}C NMR (100 MHz, $CDCl_3$): δ = 164.7, 164.3, 151.7, 138.4, 135.9, 135.8, 135.3, 129.0, 127.9, 126.1, 121.9, 118.9, 115.4, 115.1, 101.4 (ArC), 46.8 (N-CH_2), 44.5 (N-CH_2), 29.7 (CH_2), 25.7 (CH_2), 24.8 (CH_2), 14.0 (CH_3); MS(ESI), m/z: 509.3 (M^++1); Anal. Calcd for $C_{29}H_{29}FN_8$: C, 68.49; H, 5.75; N, 22.03, Found: C, 68.84; H, 5.70; N, 21.88.

***N*-(1-benzyl-2-methyl-1*H*-benzimidazol-5-yl)-*N*',*N*''-bis-(4-fluoro-phenyl)-[1,3,5]triazine-2,4,6-triamine (8).**

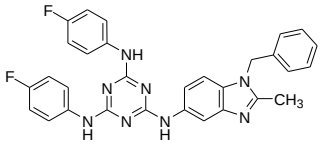

White powder; (0.154 g, 66.5%); M.p. > 300 ^{o}C; ^{1}H NMR (400 MHz, $CDCl_3$): δ = 7.61 (d, 2H, *J* = 8.72 Hz, ArH), 7.57 (bs, 1H, NH), 7.41 (d, 2H, *J* = 4.60 Hz, ArH), 7.39 (d, 2H, *J* = 4.60 Hz, ArH), 7.26-7.24 (m, 3H, ArH), 7.18 (s, 1H, ArH), 7.16 (d, 1H, *J* = 1.40 Hz, ArH), 7.13 (d, 1H, *J* = 1.80 Hz, ArH), 6.95-6.93 (m, 4H, ArH), 6.90 (bs, 1H, NH), 5.13 (s, 2H, N-CH_2), 2.50 (s, 3H, CH_3); ^{13}C NMR (100 MHz, $CDCl_3$): δ = 164.5, 160.2, 157.8, 152.2, 139.2, 135.8, 135.7, 134.4, 133.4, 129.0, 127.9, 126.3, 122.9, 119.0, 116.7, 115.5, 115.3 (ArC), 47.0 (N-CH_2), 14.1 (CH_3); MS(ESI), m/z: 535.3 (M^++1); Anal. Calcd for $C_{30}H_{24}F_2N_8$: C, 67.40; H, 4.53; N, 20.96, Found: C, 66.00; H, 4.50; N, 20.87.

4-[4-(1-Benzyl-2-methyl-1*H*-benzimidazol-5-ylamino)-6-(4-fluoro-phenylamino)-[1,3,5]triazin-2-ylamino]-phenol (9).

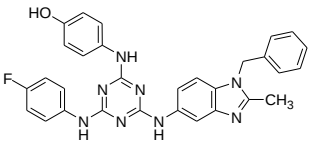

White powder; (0.162 g, 70%); m.p. > 300 ^{o}C; ^{1}H NMR (400 MHz, DMSO-d_6): δ = 9.42 (bs, 1H, NH), 8.96 (bs, 1H, NH), 7.74-7.70 (m, 4H, ArH), 7.44 (d, 2H, *J* = 13.96 Hz, ArH), 7.37 (d, 3H, *J* = 7.52 Hz, ArH), 7.21-7.11 (m, 3H, ArH), 7.01 (d, 3H, *J* = 7.12 Hz, ArH), 6.67 (d, 1H, *J* = 8.80 Hz, ArH), 5.11 (s, 2H, N-CH_2), 2.50 (s, 3H, CH_3); ^{13}C NMR (100 MHz, $CDCl_3$): δ = 164.4, 164.2, 152.7, 140.9, 135.6, 133.2, 129.1, 128.1, 126.2, 123.9, 119.2, 115.8, 115.6, 101.9 (ArC), 47.0 (N-CH_2), 14.2 (CH_3); MS(ESI), m/z: 533.3 (M^++1); Anal. Calcd for $C_{30}H_{25}FN_8O$: C, 67.66; H, 4.73; N, 21.04, Found: C, 67.46; H, 4.42; N, 21.42.

***N*-(1-benzyl-2-methyl-1*H*-benzimidazol-5-yl)-*N*'-(4-fluoro-phenyl)-6-(4-methyl-piperazin-1-yl)-[1,3,5]triazine-2,4-diamine (10).**

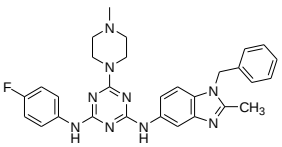

White powder; (0.193 g, 85%); M.p. > 300 ^{o}C; ^{1}H NMR (400 MHz, $CDCl_3$): δ = 7.82 (bs, 1H, NH), 7.63 (d, 1H, *J* = 8.52 Hz, ArH), 7.48-7.45 (m, 2H, ArH), 7.32-7.29 (m, 3H, ArH), 7.16 (d, 1H, *J* = 12.36 Hz, ArH) , 7.09-7.04 (m, 4H, ArH), 6.90 (d, 1H, *J* = 7.88 Hz, ArH), 6.69 (s, 1H, NH), 5.31 (s, 2H, N-CH_2), 3.75 (s, 4H, pip-CH_2), 2.58 (s, 3H, CH_3), 2.35 (s, 3H, N-CH_3), 2.30 (s, 4H, pip-CH_2); ^{13}C NMR (100 MHz, $CDCl_3$): δ = 164.9, 164.3, 159.9, 157.5, 151.8, 139.9, 135.8, 135.7, 129.1, 127.9, 126.0, 122.1, 118.9, 115.5, 115.2, 101.7 (ArC), 54.7 (N-CH_2), 46.2 (N-CH_2), 43.1 (N-CH_2), 31.3 (N-CH_3), 14.2 (CH_3); MS(ESI), m/z: 524.3 (M^++1); Anal. Calcd for $C_{29}H_{30}FN_9$: C, 66.52; H,

5.77; N, 24.08, Found: C, 66.37; H, 5.51; N, 24.07.

_N_-(1-benzyl-2-methyl-1_H_-benzimidazol-5-yl)-_N_'-(4-fluoro-phenyl)-6-pyrrolidin-1-yl-[1,3,5]triazine-2,4-diamine (11).

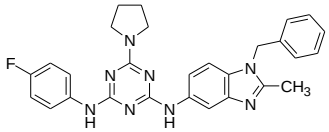

White powder; (0.180 g, 84%); M.p. > 300 ^{o}C; ^{1}H NMR (400 MHz, $CDCl_3$): δ = 8.19 (bs, 1H, NH), 7.57-7.55 (m, 2H, ArH), 7.31-7.26 (m, 3H, ArH), 7.11 (d, 2H, *J* = 8.72 Hz, ArH), 7.06 (d, 2H, *J* = 6.44 Hz, ArH), 6.98 (d, 2H, *J* =8.72 Hz, ArH), 6.89 (s, 1H, ArH), 5.30 (s, 2H, N-CH_2), 3.64 (d, 4H, *J* = 16.52 Hz, pyrr.-CH_2), 2.56 (s, 3H, CH_3), 1.95 (s, 4H, pyrr.-CH_2); ^{13}C NMR (100 MHz, $CDCl_3$): δ = 163.9, 163.6, 152.4, 152.2, 143.0, 135.9, 135.5, 131.5, 129.1, 128.0, 126.2, 121.3, 115.4, 115.2, 109.1, 108.8 (ArC), 47.2 (N-CH_2), 46.3 (N-CH_2), 25.3 (N-CH_2), 14.1 (CH_3); MS(ESI), m/z: 495.3 (M^++1); Anal. Calcd for $C_{28}H_{27}FN_8$: C, 68.00; H, 5.50; N, 22.66, Found: C, 67.66; H, 5.59; N, 22.43.

_N_-(2-amino-ethyl)-_N_'-(1-benzyl-2-methyl-1_H_-benzimidazol-5-yl)-_N_''-(4-fluoro-phenyl)-[1,3,5]triazine-2,4,6-triamine (12).

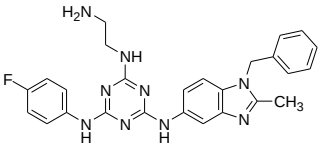

White powder; (0.185 g, 88%); M.p. > 300 ^{o}C; ^{1}H NMR (400 MHz, $CDCl_3$): δ = 8.01 (bs, 1H, NH), 7.50-7.48 (m, 3H, ArH), 7.31-7.26 (m, 4H, ArH), 7.11 (d, 2H, *J* = 8.24 Hz, ArH), 7.06 (d, 1H, *J* = 7.32 Hz, ArH), 6.95 (d, 2H, *J* = 7.36 Hz, ArH), 5.29 (s, 2H, N-CH_2), 3.49 (s, 2H, aliphatic-CH_2), 2.91 (s, 2H, aliphatic-CH_2), 2.56 (s, 3H, CH_3), 1.80 (bs, 2H, NH_2); ^{13}C NMR (100 MHz, $CDCl_3$): δ = 166.4, 166.3, 164.4, 163.4, 152.3, 151.9, 136.1, 136.0, 129.0, 127.9, 119.0, 115.5, 115.3, 115.2 (ArC), 43.5 (N-CH_2), 43.4 (N-CH_2), 41.4 (N-CH_2), 14.1 (CH_3); MS(ESI), m/z: 484.3 (M^++1); Anal. Calcd for $C_{26}H_{26}FN_9$: C, 64.58; H, 5.42; N, 26.07, Found: C, 64.47; H, 5.21; N, 25.87.

2-[4-(1-Benzyl-2-methyl-1_H_-benzimidazol-5-ylamino)-6-(4-fluoro-phenylamino)-[1,3,5]triazin-2-ylamino]-ethanol (13).

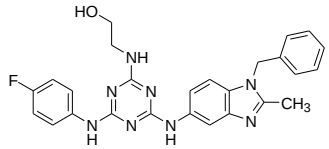

White powder; (0.181 g, 86%); M.p. > 300 ^{o}C; ^{1}H NMR (400 MHz, $CDCl_3$): δ = 7.62 (d, 1H, *J* = 6.88 Hz, ArH), 7.44 (d, 3H, *J* = 7.80 Hz, ArH), 7.34-7.26 (m, 6H, ArH), 7.03-6.94 (m, 3H, ArH, NH), 5.20 (s, 2H, N-CH_2), 3.78 (m, 2H, aliphatic-CH_2), 3.55 (m, 2H, aliphatic-CH_2), 2.54 (s, 3H, CH_3); ^{13}C NMR (100 MHz, $CDCl_3$): δ = 167.0, 163.8, 152.4, 152.2, 141.8, 133.1, 131.5, 129.1, 128.8, 128.0, 126.3, 121.6, 114.7, 108.4 (ArC), 47.5 (O-CH_2), 43.5 (N-CH_2), 43.3 (N-CH_2), 13.8 (CH_3); MS(ESI), m/z: 485.3 (M^++1); Anal. Calcd for $C_{26}H_{25}FN_8O$: C, 64.45; H, 5.20; N, 23.13, Found:

C, 64.35; H, 5.12; N, 23.49.

_N_-(1-benzyl-2-methyl-1_H_-benzimidazol-5-yl)-_N_'-(4-fluoro-phenyl)-_N_''-(2-morpholin-4-yl-ethyl)-[1,3,5]triazine-2,4,6-triamine (14).

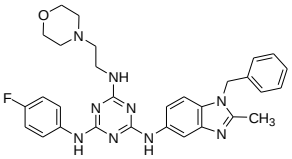

White powder; (0.209 g, 87%); M.p. > 300 ^{o}C; ^{1}H NMR (400 MHz, $CDCl_3$): δ = 8.08 (bs, 1H, NH), 7.50-7.45 (m, 2H, ArH), 7.31-7.26 (m, 3H, ArH), 7.17 (d, 1H, *J* = 9.64 Hz, ArH), 7.11 (d, 2H, *J* = 8.72 Hz, ArH), 7.05 (d, 2H, *J* = 7.80 Hz, ArH), 6.97 (t, 2H, *J* = 15.60 Hz, ArH), 5.59 (bs, 1H, NH), 5.29 (s, 2H, N-CH_2), 3.69 (s, 6H, mor.-CH_2), 3.51 (s, 2H, mor.-CH_2), 2.56 (s, 3H, CH_3), 2.55 (t, 2H, *J* = 11.88 Hz, aliphatic-CH_2), 2.44-2.40 (m, 2H, aliphatic-CH_2); ^{13}C NMR (100 MHz, $CDCl_3$): δ = 165.8, 164.4, 152.0, 151.9, 135.9, 135.7, 129.1, 129.0, 127.9, 126.3, 119.0, 115.5, 115.3 (ArC), 66.9 (O-CH_2), 57.2 (N-CH_2), 53.4 (N-CH_2), 46.9 (N-CH_2), 37.1 (N-CH_2), 22.8 (N-CH_2), 14.2 (CH_3); MS(ESI), m/z: 554.5 (M^++1); Anal. Calcd. for $C_{30}H_{32}FN_9O$: C, 65.08; H, 5.83; N, 22.77, Found: C, 65.47; H, 5.44; N, 23.14.

6-(4-Amino-phenylsulfanyl)-_N_-(1-benzyl-2-methyl-1_H_-benzimidazol-5-yl)-_N_'-(4-fluoro-phenyl)-[1,3,5]triazine-2,4-diamine (15).

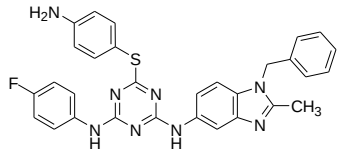

White powder; (0.143 g, 60%); M.p. > 300 ^{o}C; ^{1}H NMR (400 MHz, $CDCl_3$): δ = 7.52 (bs, 1H, NH), 7.33-7.30 (m, 4H, ArH), 7.29-7.26 (m, 5H, ArH), 7.14-7.03 (m, 4H, ArH), 6.84 (d, 2H, *J* = 6.88 Hz, ArH), 6.67 (bs, NH, ArH), 6.57 (d, 1H, *J* = 8.72 Hz, ArH), 5.14 (s, 2H, N-CH_2), 4.01 (bs, 2H, NH_2), 2.48 (s, 3H, CH_3); ^{13}C NMR (100 MHz, $CDCl_3$): δ = 162.3, 152.4, 148.0, 135.8, 134.4, 129.1, 129.0, 128.0, 127.9, 126.4, 126.3, 118.8, 118.5, 115.4, 115.1 (ArC), 49.9 (N-CH_2), 14.0 (CH_3); MS(ESI), m/z: 549.3 (M^++1); Anal. Calcd for $C_{30}H_{25}FN_8S$: C, 65.68; H, 4.59; N, 20.42; S, 5.84, Found: C, 65.32; H, 4.85; N, 20.82; S, 5.47.

_N_-(1-benzyl-2-methyl-1_H_-benzimidazol-5-yl)-_N_'-(4-fluoro-phenyl)-_N_''-phenyl-[1,3,5]triazine-2,4,6-triamine (16).

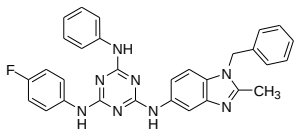

White powder; (0.139 g, 62%); M.p. > 300 ^{o}C; ^{1}H NMR (400 MHz, $CDCl_3$): δ = 7.61 (d, 2H, *J* = 8.24 Hz, ArH), 7.49 (d, 2H, *J* = 8.24 Hz, ArH), 7.42-7.41 (m, 2H, ArH), 7.26-7.24 (m, 6H, ArH), 7.23 (s, 1H, NH), 7.16 (d, 1H, *J* = 8.72 Hz, ArH), 7.05 (d, 1H, *J* = 6.92 Hz, ArH), 6.95-6.90 (m, 3H, ArH, NH), 5.12 (s, 2H, N-CH_2), 2.49 (s, 3H, CH_3); ^{13}C NMR (100 MHz, $CDCl_3$): δ = 164.5, 164.4, 157.6, 152.1, 140.0, 135.9, 129.0, 128.8, 127.9, 126.3, 123.5, 122.9, 122.8, 120.9, 119.0, 115.5,

115.3 (ArC), 47.0 (N-CH_2), 14.1 (CH_3); MS(ESI), m/z: 517.3 (M^++1); Anal. Calcd for $C_{30}H_{25}FN_8$: C, 69.75; H, 4.88; N, 21.69, Found: C, 69.47; H, 4.44; N, 21.97.

_N_-(1-benzyl-2-methyl-1_H_-benzimidazol-5-yl)-_N_'-(4-fluoro-phenyl)-_N_''-pyrimidin-2-yl-[1,3,5]triazine-2,4,6-triamine (17).

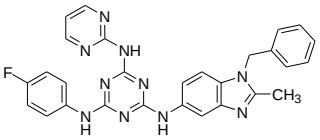

White powder; (0.124 g, 55%); M.p. > 300 ^oC; ^1H NMR (400 MHz, $CDCl_3$): δ = 7.65 (d, 1H, *J* = 8.24 Hz, ArH), 7.48-7.46 (m, 3H, ArH), 7.28-7.26 (m, 6H, ArH), 7.02 (d, 5H, *J* = 8.24 Hz, ArH), 6.80 (bs, 1H, NH), 5.21 (s, 2H, N- CH_2), 2.55 (s, 3H, CH_3); ^{13}C NMR (100 MHz, $CDCl_3$): δ = 164.5, 164.6, 160.3, 157.9, 152.1, 140.0, 135.9, 135.7, 134.4, 129.0, 127.9, 126.3, 122.9, 122.8, 119.1, 116.7, 115.6, 115.3 (ArC), 47.0 (N-CH_2), 14.1 (CH_3). MS(ESI), m/z: 519.3 (M^++1). Anal. Calcd for $C_{28}H_{23}FN_{10}$: C, 64.85; H, 4.47; N, 27.01, Found: C, 64.73; H, 4.41; N, 27.44.

2-[4-(1-Benzyl-2-methyl-1_H_-benzimidazol-5-ylamino)-6-(4-fluoro-phenylamino)-[1,3,5]triazin-2-ylamino]-benzonitrile (18).

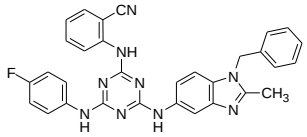

White powder; (0.143 g, 61%); M.p. > 300 ^oC; ^1H NMR (400 MHz, $CDCl_3$): δ = 7.90 (bs, 1H, NH), 7.64 (d, 2H, *J* = 8.68 Hz, ArH), 7.59 (s, 1H, ArH), 7.44-7.42 (m, 3H, ArH), 7.26-7.20 (m, 4H, ArH), 7.15-7.13 (m, 2H, ArH), 7.02-6.90 (m, 4H, ArH), 5.28 (s, 1H, N-CH_2), 5.08 (s, 1H, N-CH_2), 2.53 (s, 3H, CH_3); ^{13}C NMR (100 MHz, $CDCl_3$): δ = 164.5, 160.3, 157.9, 152.1, 150.2, 150.0, 142.4, 136.5, 136.0, 134.5, 129.0, 127.9, 126.3, 126.2, 119.6, 116.3, 115.6, 115.3, 113.0 (ArC), 95.2 (CN), 47.1 (N-CH_2), 14.1 (CH_3); MS(ESI), m/z: 542.4 (M^++1); Anal. Calcd for $C_{31}H_{24}FN_9$: C, 68.75; H, 4.47; N, 23.28, Found: C, 68.52; H, 4.20; N, 23.20.

(1-Benzyl-2-methyl-1_H_-benzimidazol-5-yl)-(4,6-di-morpholin-4-yl-[1,3,5]triazin-2-yl)-amine (19).

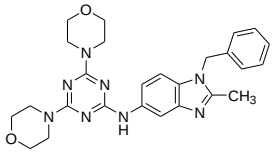

White powder; (0.158 g, 71%); M.p. > 300 ^oC; ^1H NMR (400 MHz, $CDCl_3$): δ = 7.94 (d, 1H, *J* = 1.8 Hz, ArH), 7.62 (d, 1H, *J* = 8.52 Hz, ArH), 7.32-7.26 (m, 3H, ArH), 7.07 (d, 3H, *J* = 1.92 Hz, ArH), 7.03 (s, 1H, NH), 5.29 (s, 2H, N-CH_2), 3.75-3.61 (m, 16H, mor-CH_2), 2.51 (s, 3H, CH_3); ^{13}C NMR (100 MHz, $CDCl_3$): δ = 165.1, 164.2, 151.6, 138.1, 135.8, 134.8, 129.2, 128.0, 125.7, 118.9, 115.5, 101.1 (ArC), 66.8 (O-CH_2), 46.7 (N-CH_2), 43.6 (N-CH_2), 13.9 (CH_3); MS(ESI), m/z: 487.3 (M^++1); Anal. Calcd for $C_{26}H_{30}N_8O_2$: C, 64.18; H, 6.21; N, 23.03, Found: C, 64.33; H, 6.29; N, 23.40.

***N*-(1-benzyl-2-methyl-1*H*-benzimidazol-5-yl)-*N*'-(4-fluoro-phenyl)-6-morpholin-4-yl-[1,3,5]triazine-2,4-diamine (20).**

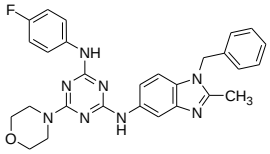

White powder; (0.159 g, 68%); M.p. > 300 ^{o}C; ^{1}H NMR (400 MHz, $CDCl_3$): δ = 7.81 (bs, 1H, NH), 7.64 (d, 1H, *J* = 8.56 Hz, ArH), 7.47-7.32 (m, 2H, ArH), 7.31-7.26 (m, 3H, ArH), 7.13 (dd, 1H, ^{2}J = 1.84 Hz, ^{3}J = 8.56 Hz, ArH), 7.03-7.01 (m, 4H, ArH, NH), 6.98 (d, 1H, *J* = 8.6 Hz, ArH), 6.67 (s, 1H, ArH), 5.26 (s, 2H, N-CH_2), 3.69 (m, 8H, mor-CH_2), 2.53 (s, 3H, CH_3); ^{13}C NMR (100 MHz, $CDCl_3$): δ = 165.1, 159.9, 151.5, 138.4, 135.8, 134.9, 134.0, 132.9, 129.1, 128.0, 126.0, 122.1, 119.1, 115.5, 115.3, 101.7 (ArC), 66.7 (O-CH_2), 46.9 (N-CH_2), 43.7 (N-CH_2), 14.1 (CH_3); MS(ESI), m/z: 511.3 (M^++1); Anal. Calcd for $C_{28}H_{27}FN_8O$: C, 65.87; H, 5.33; N, 21.95, Found: C, 65.37; H, 5.30; N, 21.77.

(1-Benzyl-2-methyl-1*H*-benzimidazol-5-yl)-(4-morpholin-4-yl-6-piperidin-1-yl)-[1,3,5]triazin-2-yl)-amine (21).

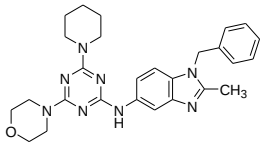

White powder; (0.172 g, 77.5%); M.p. > 300 ^{o}C; ^{1}H NMR (400 MHz, $CDCl_3$): δ = 8.01 (s, 1H, ArH), 7.61 (d, 1H, *J* = 8.56 Hz, ArH), 7.32-7.25 (m, 3H, ArH), 7.06 (d, 3H, *J* = 1.84 Hz, ArH), 6.78 (bs, 1H, NH), 5.28 (s, 2H, N-CH_2), 3.75-3.61 (m, 12H, mor- CH_2, pip-CH_2), 2.51 (s, 3H, CH_3), 1.56 (t, 4H, *J* = 7.44 Hz, pip-CH_2), 1.27 (t, 2H, *J* = 7.56 Hz, pip-CH_2); ^{13}C NMR (100 MHz, $CDCl_3$): δ = 165.3, 164.8, 164.4, 151.5, 138.2, 135.9, 135.8, 135.1, 129.1, 127.9, 125.9, 118.9, 115.2, 100.8 (ArC), 66.7 (O-CH_2), 46.8 (N-CH_2), 44.2 (N-CH_2), 43.6 (N-CH_2), 25.8 (CH_2), 24.9 (CH_2), 14.0 (CH_3); MS(ESI), m/z: 485.3 (M^++1); Anal. Calcd for $C_{27}H_{32}ON_8$: C, 66.92; H, 6.66; N, 23.12, Found: C, 66.95; H, 6.48; N, 23.29.

(1-Benzyl-2-methyl-1*H*-benzimidazol-5-yl)-[4-(4-methyl-piperazin-1-yl)-6-morpholin-4-yl-[1,3,5]triazin-2-yl]-amine (22).

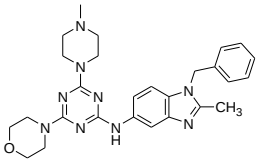

White powder; (0.176 g, 77%); M.p. > 300 ^{o}C; ^{1}H NMR (400 MHz, DMSO-d_6): δ = 9.12 (bs, 1H, NH), 8.51 (s, 1H, ArH), 8.02 (d, 1H, *J* = 7.20 Hz, ArH), 7.49 (dd, 1H, ^{2}J = 29.84 Hz, ^{3}J = 7.28 Hz, ArH), 7.25-7.18 (m, 3H, ArH), 6.97-6.95 (m, 2H, ArH), 5.31 (s, 2H, N-CH_2), 3.69-3.44 (m, 12H, mor-CH_2, pip-CH_2), 2.51 (s, 3H, CH_3), 2.45 (t, 4H, *J* = 4.36 Hz, pip-CH_2), 2.26 (s, 3H, N-CH_3); ^{13}C NMR (100 MHz, $CDCl_3$): δ = 164.9, 164.8, 151.8, 138.6, 135.9, 135.7, 135.0, 134.2, 129.2, 129.1, 127.9, 126.0, 122.1, 119.0, 115.4, 115.2 (ArC), 54.7 (O-CH_2), 46.8 (N-CH_2), 46.2 (N-CH_2), 43.2 (N-CH_2), 29.7

(N-CH_3), 14.0 (CH_3); MS(ESI), m/z: 500.3 (M^++1); Anal. Calcd for $C_{27}H_{33}N_9O$: C, 64.91; H, 6.66; N, 25.23, Found: C, 64.65; H, 6.41; N, 25.34.

(1-Benzyl-2-methyl-1*H*-benzimidazol-5-yl)-(4-morpholin-4-yl-6-pyrrolidin-1-yl-[1,3,5]triazin-2-yl)-amine (23).

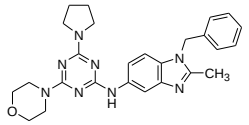

White powder; (0.159 g, 74%); M.p. > 300 ^oC; ^1H NMR (400 MHz, $CDCl_3$): δ = 8.11 (s, 1H, NH), 7.61 (d, 1H, *J* = 8.52 Hz, ArH), 7.32-7.03 (m, 3H, ArH), 7.04 (dd, 2H, ^2J = 1.72 Hz, ^3J = 8.36 Hz, ArH), 7.02 (d, 1H, *J* = 9.28 Hz, ArH), 6.79 (s, 1H, ArH), 5.30 (s, 2H, N-CH_2), 3.75-3.73 (m, 6H, mor-CH_2), 3.72-3.69 (m, 4H, pyrr-CH_2), 3.61-3.59 (m, 2H, mor-CH_2), 2.52 (s, 3H, CH_3), 1.95 (s, 4H, pyrr-CH_2); ^{13}C NMR (100 MHz, $CDCl_3$): δ = 151.4, 151.3, 138.0, 135.9, 135.6, 135.2, 129.1, 127.8, 125.8, 118.9, 118.7, 115.1, 115.0, 100.8 (ArC), 66.8 (O-CH_2), 46.8 (N-CH_2), 46.0 (N-CH_2), 43.6 (N-CH_2), 29.7 (CH_2), 25.4 (CH_2), 14.0 (CH_3); MS(ESI), m/z: 471.3 (M^++1); Anal. Calcd for $C_{26}H_{30}N_8O$: C, 66.36; H, 6.43; N, 23.81, Found: C, 66.37; H, 6.47; N, 23.76.

***N*-(2-amino-ethyl)-*N*'-(1-benzyl-2-methyl-1*H*-benzimidazol-5-yl)-6-morpholin-4-yl-[1,3,5]triazine-2,4-diamine (24).**

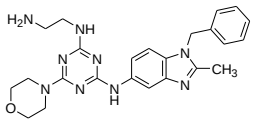

White powder; (0.172 g, 82%); M.p. > 300 ^oC; ^1H NMR (400 MHz, $CDCl_3$): δ = 7.93 (d, 1H, *J* = 8.72 Hz, ArH), 7.75 (bs, 1H, NH), 7.61 (d, 1H, *J* = 4.32 Hz, ArH), 7.28-7.26 (m, 3H, ArH), 7.08-6.99 (m, 3H, ArH), 5.25 (s, 2H, N-CH_2), 3.67 (s, 12H, mor-CH_2, aliphatic-CH_2), 2.49 (s, 3H, CH_3), 1.91 (bs, 2H, NH_2); ^{13}C NMR (100 MHz, $CDCl_3$): δ = 165.1, 164.3, 151.8, 151.7, 135.8, 129.1, 127.9, 126.2, 126.0, 125.7, 119.0, 115.4, 101.0 (ArC), 66.8 (O-CH_2), 46.9 (N-CH_2), 46.7 (N-CH_2), 43.6 (N-CH_2), 29.7 (CH_2), 14.0 (CH_3); MS(ESI), m/z: 460.3 (M^++1); Anal. Calcd for $C_{24}H_{29}N_9O$: C, 62.73; H, 6.36; N, 27.43, Found: C, 62.37; H, 6.41; N, 27.63.

2-[4-(1-Benzyl-2-methyl-1*H*-benzimidazol-5-ylamino)-6-morpholin-4-yl-[1,3,5]triazin-2-ylamino]-ethanol (25).

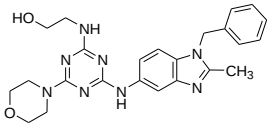

White powder; (0.173 g, 82%); M.p. > 300 ^oC; ^1H NMR (400 MHz, $CDCl_3$): δ = 8.07 (bs, 1H, NH), 7.61 (d, 2H, *J* = 8.68 Hz, ArH), 7.32-7.26 (m, 3H, ArH), 7.07-7.05 (m, 1H, ArH), 6.85 (d, 2H, *J* = 8.28 Hz, ArH), 5.59 (bs, 1H, NH), 5.29 (s, 2H, N-CH_2), 3.69 (s, 6H, mor-CH_2), 3.51 (s, 2H, mor-CH_2), 2.56 (t, 2H, *J* = 5.60 Hz, aliphatic-CH_2), 2.50 (m, 2H, aliphatic-CH_2), 2.44 (s, 3H, CH_3), 2.04 (bs, 1H, OH); ^{13}C NMR (100 MHz, $CDCl_3$): δ = 166.8, 164.9, 151.8, 138.7, 135.9, 134.1, 129.1, 127.9,

125.9, 119.0, 116.2, 101.8 (ArC), 67.8 (O-CH_2), 46.9 (N-CH_2), 43.8 (N-CH_2), 43.6 (N-CH_2), 14.0 (CH_3); MS(ESI), m/z: 461.3 (M^++1); Anal. Calcd for $C_{24}H_{28}N_8O_2$: C, 62.59; H, 6.13; N, 24.33, Found: C, 62.70; H, 6.31; N, 24.65.

***N*-(1-benzyl-2-methyl-1*H*-benzimidazol-5-yl)-6-morpholin-4-yl-*N*'-(2-morpholin-4-yl-ethyl)-[1,3,5]triazine-2,4-diamine (26).**

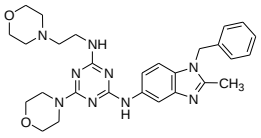

White powder; (0.191 g, 83%); M.p. > 300 ^oC; ^1H NMR (400 MHz, $CDCl_3$): δ = 7.91 (bs, 1H, NH), 7.60 (d, 1H, *J* = 8.72 Hz, ArH), 7.30-7.27 (m, 3H, ArH), 7.17 (s, 1H, ArH), 7.08 (d, 1H, *J* = 8.72 Hz, ArH), 7.03 (d, 2H, *J* = 6.40 Hz, ArH), 5.41 (t, 1H, *J* = 6.40 Hz, NH), 5.28 (s, 2H, N-CH_2), 3.67-3.47 (m, 20H, mor-CH_2, aliphatic-CH_2), 2.50 (s, 3H, CH_3); ^{13}C NMR (100 MHz, $CDCl_3$): δ = 165.2, 164.3, 151.7, 138.4, 135.9, 135.8, 134.7, 129.1, 127.9, 125.9, 118.9, 115.5, 101.4, 101.1 (ArC), 66.9 (O-CH_2), 66.7 (O-CH_2), 57.3 (N-CH_2), 53.4 (N-CH_2), 46.8 (N-CH_2), 43.6 (N-CH_2), 36.9 (N-CH_2), 14.0 (CH_3); MS(ESI), m/z: 530.3 (M^++1); Anal. Calcd for $C_{28}H_{35}N_9O_2$: C, 63.50; H, 6.66; N, 23.80, Found: C, 63.90; H, 6.32; N, 23.60.

***N*-(3-benzyl-2-methyl-3*H*-benzimidazol-5-yl)-*N*'-(4-fluoro-phenyl)-6-morpholin-4-yl-[1,3,5]triazine-2,4-diamine (27).**

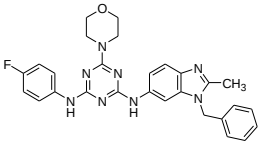

White powder; (0.159 g, 68%); M.p. > 300 ^oC; ^1H NMR (400 MHz, $CDCl_3$): δ = 8.03 (bs, 1H, NH), 7.50 (d, 1H, *J* = 4.60 Hz, ArH), 7.48 (d, 1H, *J* = 4.60 Hz, ArH), 7.31-7.26 (m, 4H, ArH), 7.13 (d, 2H, *J* = 8.72 Hz, ArH), 7.06 (d, 2H, *J* = 6.88 Hz, ArH), 6.99-6.98 (m, 2H, ArH), 6.88 (s, 1H, NH), 5.30 (s, 2H, N-CH_2), 3.81 (d, 4H, *J* = 8.72 Hz, mor-CH_2), 3.74 (d, 4H, *J* = 5.12 Hz, mor-CH_2), 2.57 (s, 3H, CH_3); ^{13}C NMR (100 MHz, $CDCl_3$): δ = 165.3, 164.6, 164.3, 159.8, 157.4, 152.6, 143.0, 135.8, 135.1, 133.6, 132.0, 129.1, 128.0, 126.2, 121.7, 115.5, 115.3, 109.1 (ArC), 66.9 (O-CH_2), 47.2 (N-CH_2), 43.8 (N-CH_2), 14.1 (CH_3); MS(ESI), m/z: 511.3 (M^++1); Anal. Calcd for $C_{28}H_{27}FN_8O$: C, 65.87; H, 5.33; N, 21.95, Found: C, 65.97; H, 5.76; N, 21.80.

***N*-(3-benzyl-2-methyl-3*H*-benzimidazol-5-yl)-*N*'-(4-fluoro-phenyl)-6-piperidin-1-yl-[1,3,5]triazine-2,4-diamine (28).**

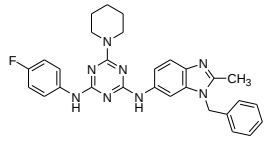

White powder; (0.179 g, 81%); M.p. > 300 ^oC; ^1H NMR (400 MHz, $CDCl_3$): δ = 8.01 (bs, 1H, NH), 7.53 (d, 1H, *J* = 4.60 Hz, ArH), 7.50 (d, 1H, *J* = 5.04 Hz, ArH), 7.32-7.26 (m, 4H, ArH), 7.13 (d, 1H, *J* = 2.40 Hz, ArH), 7.07 (d, 2H, *J* = 1.84 Hz, ArH), 6.99 (t, 2H, *J* = 8.72 Hz, ArH), 6.84 (s, 1H, ArH), 6.76 (s,

1H, NH), 5.31 (s, 2H, N-CH_2), 3.79 (d, 4H, *J* = 5.48 Hz, pip-CH_2), 2.57 (s, 3H, CH_3), 1.72-1.70 (m, 2H, pip-CH_2), 1.61 (d, 2H, *J* = 4.12 Hz, pip-CH_2), 1.53 (s, 2H, Pip-CH_2); ^{13}C NMR (100 MHz, $CDCl_3$): δ = 164.9, 164.8, 164.3, 159.6, 152.4, 143.0, 135.9, 135.4, 133.9, 129.1, 128.0, 126.3, 121.4, 115.4, 115.2, 111.4, 109.1 (ArC), 47.4 (N-CH_2), 47.2 (N-CH_2), 44.5 (N-CH_2), 27.1 (CH_2), 25.9 (CH_2), 24.9 (CH_2), 14.1 (CH_3); MS(ESI), m/z: 509.3 (M^++1); Anal. Calcd for $C_{29}H_{29}FN_8$: C, 68.49; H, 5.75; N, 22.03, Found: C, 68.67; H, 5.75; N, 22.00.

_N_-(3-benzyl-2-methyl-3_H_-benzimidazol-5-yl)-_N_'-(4-fluoro-phenyl)-6-pyrrolidin-1-yl-[1,3,5]triazine-2,4-diamine (29).

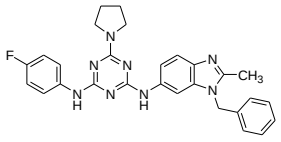

White powder; (0.180 g, 84%); M.p. > 300 ^{o}C; ^{1}H NMR (400 MHz, $CDCl_3$): δ = 8.19 (bs, 1H, NH), 7.57 (m, 2H, ArH), 7.31-7.26 (m, 5H, ArH), 7.06 (dd, 2H, ^2J = 6.44 Hz, ^3J = 12.04 Hz, ArH), 6.98 (d, 3H, *J* = 8.72 Hz, ArH), 6.89 (s, 1H, NH), 5.30 (s, 2H, N-CH_2), 3.64 (d, 4H, *J* = 16.52 Hz, pyrr-CH_2), 2.56 (s, 3H, CH_3), 1.95 (s, 2H, pyrr-CH_2), 1.80 (s, 2H, pyrr-CH_2); ^{13}C NMR (100 MHz, $CDCl_3$): δ = 163.9, 163.6, 152.4, 152.2, 143.0, 135.9, 135.5, 131.5, 129.1, 128.0, 126.2, 121.3, 115.4, 115.2, 109.1, 108.8 (ArC), 47.2 (N-CH_2), 46.3 (N-CH_2), 25.3 (CH_2), 14.1 (CH_3); MS(ESI), m/z: 495.3 (M^++1); Anal. Calcd for $C_{28}H_{27}FN_8$: C, 68.00; H, 5.50; N, 22.66, Found: C, 68.27; H, 5.55; N, 22.59.

_N_-(3-benzyl-2-methyl-3_H_-benzimidazol-5-yl)-_N_'-(4-fluoro-phenyl)-6-(4-methyl-piperazin-1-yl)-[1,3,5]triazine-2,4-diamine (30).

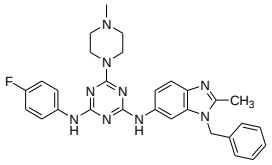

White powder; (0.193 g, 85%); M.p. > 300 ^{o}C; ^{1}H NMR (400 MHz, $CDCl_3$): δ = 8.02 (bs, 1H, NH), 7.49 (d, 2H, *J* = 4.62 Hz, ArH), 7.30-7.27 (m, 4H, ArH), 7.10 (d, 2H, *J* = 8.68 Hz, ArH), 7.05 (d, 2H, *J* = 7.80 Hz, ArH), 6.97 (m, 2H, ArH), 5.28 (s, 2H, N-CH_2), 3.84 (s, 4H, pip-CH_2), 2.55 (s, 3H, CH_3), 2.44 (s, 3H, N-CH_3), 2.31 (s, 4H, pip-CH_2); ^{13}C NMR (100 MHz, $CDCl_3$): δ = 165.1, 164.3, 160.0, 157.1, 152.5, 142.9, 135.8, 134.0, 133.5, 131.7, 129.1, 128.0, 126.2, 121.7, 115.5, 115.2, 109.1 (ArC), 56.3 (N-CH_2), 54.9 (N-CH_2), 47.2 (N-CH_2), 46.2 (N-CH_2), 46.0 (N-CH_2), 43.3 (N-CH_3), 14.1 (CH_3); MS(ESI), m/z: 524.3 (M^++1); Anal. Calcd for $C_{29}H_{30}FN_9$: C, 66.52; H, 5.77; N, 24.08, Found: C, 66.65; H, 5.99; N, 23.78.

***N*-(2-Amino-ethyl)-*N*'-(3-benzyl-2-methyl-3*H*-benzimidazol-5-yl)-*N*''-(4-fluoro-phenyl)-[1,3,5]triazine-2,4,6-triamine (31).**

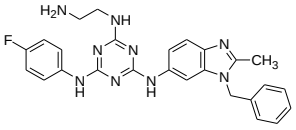

White powder; (0.185 g, 88%); M.p. > 300 ^{o}C; ^{1}H NMR (400 MHz, $CDCl_3$): δ = 8.04 (bs, 1H, NH), 7.50-7.46 (m, 2H, ArH), 7.31-7.28 (m, 4H, ArH), 7.11 (d, 2H, *J* = 8.24 Hz, ArH), 7.06 (d, 2H, *J* = 7.32 Hz, ArH), 6.95 (d, 2H, *J* = 7.36 Hz, ArH), 6.90 (bs, 1H, NH), 5.29 (s, 2H, N-CH_2), 3.49-3.45 (m, 2H, aliphatic-CH_2), 2.91-2.88 (m, 2H, aliphatic-CH_2), 2.56 (s, 3H, CH_3), 1.80 (bs, 2H, NH_2); ^{13}C NMR (100 MHz, $CDCl_3$): δ = 166.5, 166.4, 163.8, 152.5, 142.9, 136.0, 135.8, 129.1, 128.0, 126.4, 126.3, 115.4, 115.2, 109.1 (ArC), 47.2 (N-CH_2), 43.5 (N-CH_2), 41.4 (N-CH_2), 14.1 (CH_3); MS(ESI), m/z: 484.3 (M^++1); Anal. Calcd for $C_{26}H_{26}FN_9$: C, 64.58; H, 5.42; N, 26.07, Found: C, 64.88; H, 5.41; N, 25.68.

2-[4-(3-benzyl-2-methyl-3*H*-benzimidazol-5-ylamino)-6-(4-fluoro-phenylamino)-[1,3,5]triazin-2-ylamino]-ethanol (32).

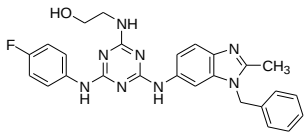

White powder; (0.181 g, 86%); M.p. > 300 ^{o}C; ^{1}H NMR (400 MHz, $CDCl_3$): δ = 8.08 (bs, 1H, NH), 7.44 (d, 2H, *J* = 4.60 Hz, ArH), 7.29-7.26 (m, 5H, ArH), 7.03-7.02 (m, 3H, ArH), 6.89-6.88 (m, 2H, ArH), 5.24 (s, 2H, N-CH_2), 3.80 (m, 2H, aliphatic-CH_2), 3.56 (m, 2H, aliphatic-CH_2), 2.52 (s, 3H, CH_3), 1.84 (s, 1H, OH); ^{13}C NMR (100 MHz $CDCl_3$): δ = 167.0, 163.9, 163.8, 152.4, 152.2, 141.8, 133.1, 131.5, 129.1, 128.8, 128.0, 126.3, 121.6, 121.2, 114.7, 108.4 (ArC), 47.5 (O-CH_2), 43.5 (N-CH_2), 43.3 (N-CH_2), 13.6 (CH_3); MS(ESI), m/z: 485.3 (M^++1); Anal. Calcd for $C_{26}H_{25}FN_8O$: C, 64.45; H, 5.20; N, 23.13, Found: C, 64.47; H, 5.42; N, 23.01.

***N*-(3-benzyl-2-methyl-3*H*-benzimidazol-5-yl)-*N*'-(4-fluoro-phenyl)-*N*''-(2-morpholin-4-yl-ethyl)-[1,3,5]triazine-2,4,6-triamine (33).**

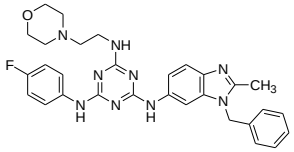

White powder; (0.209 g, 87%); M.p. > 300 ^{o}C; ^{1}H NMR (400 MHz, $CDCl_3$): δ = 8.08 (s, 1H, ArH), 7.50-7.46 (m, 3H, NH, ArH), 7.33-7.26 (m, 4H, ArH), 7.11 (d, 2H, *J* = 8.72 Hz, ArH), 7.05 (d, 2H, *J* = 7.80 Hz, ArH), 6.97-6.95 (m, 2H, ArH), 5.60 (bs, 1H, NH), 5.29 (s, 2H, N-CH_2), 3.69 (s, 6H, mor-CH_2), 3.51 (s, 2H, mor-CH_2), 2.56-2.53 (m, 4H, aliphatic-CH_2), 2.50 (s, 3H, CH_3); ^{13}C NMR (100 MHz, $CDCl_3$): δ = 166.0, 164.6, 152.5, 142.9, 135.8, 129.1, 129.0, 128.0, 127.5, 126.3, 122.1, 121.7, 115.5, 115.2, 109.1, 108.1 (ArC), 66.9 (O-CH_2), 57.2 (N-CH_2), 53.4 (N-CH_2), 47.2 (N-CH_2), 37.1 (N-CH_2), 14.1 (CH_3); MS(ESI), m/z: 554.3 (M^++1); Anal. Calcd. for $C_{30}H_{32}FN_9O$: C, 65.08; H,

5.83; N, 22.77, Found: C, 64.87; H, 5.44; N, 22.78.

(3-Benzyl-2-methyl-3*H*-benzimidazol-5-yl)-(4,6-di-morpholin-4-yl-[1,3,5]triazin-2-yl)-amine (34).

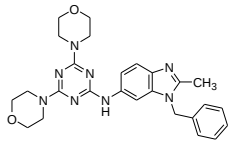

White powder; (0.158 g, 71%); M.p. > 300 ^{o}C; ^{1}H NMR (400 MHz, $CDCl_3$): δ = 8.04 (d, 1H, *J* = 1.80 Hz, ArH), 7.30-7.26 (m, 4H, ArH), 7.11 (d, 1H, *J* = 8.72 Hz, ArH), 7.05 (d, 3H, *J* = 7.80 Hz, ArH, NH), 5.28 (s, 2H, N-CH_2), 3.79 (s, 8H, mor-CH_2), 3.72 (s, 8H, mor-CH_2), 2.57 (s, 3H, CH_3); ^{13}C NMR (100 MHz, $CDCl_3$): δ = 165.3, 164.5, 152.4, 143.0, 135.9, 134.3, 131.6, 129.0, 128.0, 126.2, 116.2, 110.7, 109.1 (ArC), 67.0 (O-CH_2), 66.9 (O-CH_2), 47.1 (N-CH_2), 47.0 (N-CH_2), 43.7 (N-CH_2), 14.1 (CH_3); MS(ESI), m/z: 487.3 (M^++1); Anal. Calcd for $C_{26}H_{30}N_8O_2$: C, 64.18; H, 6.21; N, 23.03, Found: C, 64.32; H, 6.12; N, 22.69.

(3-Benzyl-2-methyl-3*H*-benzimidazol-5-yl)-(4-morpholin-4-yl-6-piperidin-1-yl)-[1,3,5]triazin-2-yl)-amine (35).

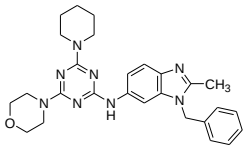

White powder; (0.172 g, 77.5%): M.p. > 300 ^{o}C; ^{1}H NMR (400 MHz, $CDCl_3$): δ = 8.03 (d, 1H, *J* = 1.84 Hz, ArH), 7.31-7.26 (m, 4H, ArH), 7.11 (d, 1H, *J* = 8.72 Hz, ArH), 7.04 (d, 2H, *J* = 6.88 Hz, ArH), 6.90 (bs, 1H, NH), 5.28 (s, 2H, N-CH_2), 3.79-3.71 (m, 12H, mor-CH_2, pip-CH_2), 2.54 (s, 3H, CH_3), 1.64 (d, 2H, *J* = 4.60 Hz, pip-CH_2), 1.57 (d, 4H, *J* = 5.12 Hz, pip-CH_2); ^{13}C NMR (100 MHz, $CDCl_3$): δ = 165.5, 164.9, 164.6, 152.3, 143.0, 135.9, 134.6, 131.4, 129.0, 127.9, 126.2, 116.1, 110.5, 109.0 (ArC), 67.0 (O-CH_2), 47.1 (N-CH_2), 44.2 (N-CH_2), 43.7 (N-CH_2), 31.0 (CH_2), 25.9 (CH_2), 25.0 (CH_2), 14.1 (CH_3); MS(ESI), m/z: 485.3 (M^++1); Anal. Calcd for $C_{27}H_{32}N_8O$: C, 66.92; H, 6.66; N, 23.12, Found: C, 66.68; H, 6.43; N, 23.52.

(3-Benzyl-2-methyl-3*H*-benzimidazol-5-yl)-(4-morpholin-4-yl-6-pyrrolidin-1-yl-[1,3,5]triazin-2-yl)-amine (36).

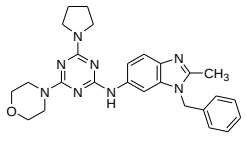

White powder; (0.159 g, 74%); M.p. > 300 ^{o} C; ^{1}H NMR (400 MHz, $CDCl_3$): δ = 8.15 (s, 1H, ArH), 7.30-7.26 (m, 4H, ArH), 7.11 (d, 1H, *J* = 8.72 Hz, ArH), 7.05 (d, 2H, *J* = 7.76 Hz, ArH), 6.83 (s, 1H, NH), 5.29 (s, 2H, N-CH_2), 3.80 (t, 4H, *J* = 9.16 Hz, mor-CH_2), 3.73 (t, 4H, *J* = 9.20 Hz, mor-CH_2), 3.60 (s, 2H, pyrr-CH_2), 3.58 (s, 2H, pyrr-CH_2), 2.55 (s, 3H, CH_3), 1.92 (s, 4H, pyrr-CH_2); ^{13}C NMR (100 MHz, $CDCl_3$): δ = 165.1, 164.2, 163.7, 152.2, 143.0, 136.0, 134.8, 131.3, 129.0, 127.9, 126.2, 115.8, 110.3, 109.0 (ArC), 67.0 (O-CH_2), 47.1 (N-CH_2), 46.1 (N-CH_2), 43.7 (N-CH_2), 25.4 (CH_2), 25.3

(CH_2), 14.1 (CH_3); MS(ESI), m/z: 471.3 (M^++1); Anal. Calcd for $C_{26}H_{30}N_8O$: C, 66.36; H, 6.43; N, 23.81, Found: C, 66.37; H, 6.49; N, 23.77.

(3-Benzyl-2-methyl-3*H*-benzimidazol-5-yl)-[4-(4-methyl-piperazin-1-yl)-6-morpholin-4-yl-[1,3,5]triazin-2-yl]-amine (37).

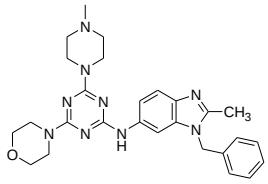

White powder; (0.176 g, 77%); M.p. > 300 ^oC; ^1H NMR (400 MHz, $CDCl_3$): δ = 8.02 (d, 1H, *J* =1.84 Hz, ArH), 7.32-7.26 (m, 4H, ArH), 7.12 (d, 1H, *J* = 8.24 Hz, ArH), 7.05 (d, 2H, *J* = 7.80 Hz, ArH), 6.85 (bs, 1H, NH), 5.29 (s, 2H, N-CH_2), 3.82-3.78 (m, 8H, mor-CH_2, pip-CH_2), 3.73 (t, 4H, *J* = 8.72 Hz, mor-CH_2), 2.55 (s, 3H, CH_3), 2.44 (t, 4H, *J* = 10.08 Hz, pip-CH_2), 2.39 (s, 3H, N-CH_3); ^{13}C NMR (100 MHz, $CDCl_3$): δ = 165.4, 165.1, 165.0, 164.5, 152.5, 152.1, 143.0, 142.7, 135.9, 134.4, 131.1, 129.0, 127.9, 126.2, 116.1, 110.6, 109.1 (ArC), 66.9 (O-CH_2), 56.3 (N-CH_2), 55.0 (N-CH_2), 47.1 (N-CH_2), 46.3 (N-CH_2), 43.7 (N-CH_2), 43.1 (N-CH_3), 14.1 (CH_3). MS(ESI), m/z: 500.3 (M^++1). Anal. Calcd for $C_{27}H_{33}N_9O$: C, 64.91; H, 6.66; N, 25.23, Found: C, 64.70; H, 6.53; N, 25.31.

***N*-(2-Amino-ethyl)-*N*'-(3-benzyl-2-methyl-3*H*-benzimidazol-5-yl)-6-morpholin-4-yl-[1,3,5]triazine-2,4-diamine (38).**

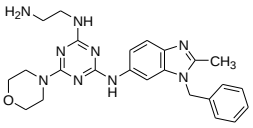

White powder; (0.172g, 82%); M.p. > 300 ^oC; ^1H NMR (400 MHz, $CDCl_3$): δ = 8.05 (bs, 1H, NH), 7.31-7.26 (m, 5H, ArH), 7.11-7.08 (m, 3H, ArH), 5.29 (s, 2H, N-CH_2), 3.79 (s, 4H, mor-CH_2), 3.72 (s, 4H, mor-CH_2), 3.48 (t, 2H, *J* = 5.48 Hz, aliphatic-CH_2), 2.91 (t, 2H, *J* = 5.52 Hz, aliphatic-CH_2), 2.55 (s, 3H, CH_3), 1.65 (bs, 2H, NH_2); ^{13}C NMR (100 MHz, $CDCl_3$): δ = 166.2, 165.8, 164.5, 152.4, 143.0, 135.9, 134.9, 132.9, 131.7, 129.1, 128.0, 126.2, 109.1 (ArC), 69.1 (O-CH_2), 47.2 (N-CH_2), 43.7 (N-CH_2), 43.6 (N-CH_2), 41.8 (N-CH_2), 14.1 (CH_3); MS(ESI), m/z: 460.3 (M^++1); Anal. Calcd for $C_{24}H_{29}ON_9$: C, 62.73; H, 6.36; N, 27.43, Found: C, 62.33; H, 6.40; N, 27.87.

2-[4-(3-Benzyl-2-methyl-3*H*-benzimidazol-5-ylamino)-6-morpholin-4-yl-[1,3,5]triazin-2-ylamino]-ethanol (39).

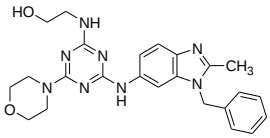

White powder; (0.173 g, 82%); M.p. > 300 ^oC; ^1H NMR (400 MHz, $CDCl_3$): δ = 8.14 (bs, 1H, NH), 7.30-7.27 (m, 4H, ArH), 7.04-7.02 (m, 4H, ArH), 6.40 (bs, 1H, NH), 5.21 (s, 2H, N-CH_2), 3.76-3.70 (m, 8H, mor-CH_2), 3.63-3.62 (m, 2H, aliphatic-CH_2), 2.86 (t, 2H, *J* = 10.08 Hz, aliphatic-CH_2), 2.54 (s, 3H, CH_3); ^{13}C NMR (100 MHz, $CDCl_3$): δ = 166.8, 165.0, 152.5, 142.8, 135.8, 133.9, 131.8, 129.1,

128.0, 126.2, 116.6, 111.4, 109.1 (ArC), 69.1 (O-CH_2), 66.9 (O-CH_2), 47.2 (N-CH_2), 43.7 (N-CH_2), 43.6 (N-CH_2), 14.1 (CH_3); MS(ESI), m/z: 461 (M^++1); Anal. Calcd for $C_{24}H_{28}N_8O_2$: C, 62.59; H, 6.13; N, 24.33, Found: C, 62.50; H, 6.31; N, 24.47.

***N*-(3-benzyl-2-methyl-1*H*-benzimidazol-5-yl)-6-morpholin-4-yl-*N*'-(2-morpholin-4-yl-ethyl)-[1,3,5]triazine-2,4-diamine (40).**

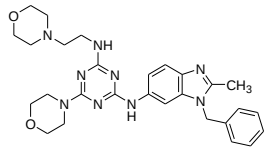

White powder; (0.191 g, 79%); M.p. > 300 ^oC; ^1H NMR (400 MHz, $CDCl_3$): δ = 8.08 (s, 1H, NH), 7.30 (d, 4H, *J* = 7.36 Hz, ArH), 7.10-7.05 (m, 4H, ArH), 5.42 (bs, 1H, NH), 5.29 (s, 2H, N-CH_2), 3.80 (s, 8H, mor-CH_2), 3.71 (s, 8H, mor-CH_2), 3.50 (s, 2H, aliphatic-CH_2), 2.53 (s, 3H, CH_3), 2.45 (s, 2H, aliphatic-CH_2); ^{13}C NMR (100 MHz, $CDCl_3$): δ = 167.8, 167.2, 166.9, 152.4, 143.0, 135.9, 134.8, 132.9, 129.1, 128.0, 127.5, 126.2, 118.9, 109.1 (ArC), 69.1 (O-CH_2), 57.4 (N-CH_2), 53.4 (N-CH_2), 47.2 (N-CH_2), 43.7 (CH_2), 37.0 (CH_2), 14.1 (CH_3); MS(ESI), m/z: 530 (M^++1); Anal. Calcd for $C_{28}H_{35}N_9O_2$: C, 63.50; H, 6.66; N, 23.80, Found: C, 63.55; H, 6.92; N, 23.88.

General procedure for the preparation of compounds 41-49.

To a stirred solution of *N*-(1-benzyl-2-methyl-1*H*-benzimidazol-5-yl)-6-chloro-*N'*-(4-fluoro-phenyl)-[1,3,5]triazine-2,4-diamine (**6a**) (0.200 g, 0.435 mmol) in 1,4-dioxane (20 ml) was added boronic acid (0.516 mmol), $Pd(PPh_3)_4$ (10 mol%) and potassium carbonate (0.076g, 0.516 mmol) and refluxed for 8 h in an inert atmosphere. After completion of reaction, extracted the reaction mixture with chloroform, dried over Na_2SO_4, filtered and concentrated to get crude product which were purified through column chromatography using chloroform:methanol (50:1) as eluents to give desired products.

***N*-(1-benzyl-2-methyl-1*H*-benzimidazol-5-yl)-*N*'-(4-fluoro-phenyl)-6-phenyl-[1,3,5]triazine-2,4-diamine (41).**

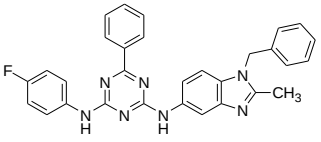

White powder; (0.162 g, 74%); M.p. > 300 ^oC; ^1H NMR (400 MHz, $CDCl_3$): δ = 8.37 (bs, 1H, NH), 8.33 (d, 2H, *J* = 7.36 Hz, ArH), 7.55-7.53 (m, 4H, ArH), 7.48-7.43 (m, 5H, ArH), 7.28-7.06 (m, 2H, ArH), 7.22 (d, 1H, *J* = 8.72 Hz, ArH), 7.04-7.01 (m, 3H, ArH), 5.25 (s, 2H, N-CH_2), 2.55 (s, 3H, CH_3); ^{13}C NMR (100 MHz, $CDCl_3$): δ = 171.7, 164.6, 160.3, 157.9, 152.2, 138.9, 136.5, 136.4, 133.8, 132.9, 132.2, 132.1, 129.1, 128.6, 128.5, 128.4, 128.0, 126.2, 115.7, 115.4, 102.9 (ArC), 47.0 (N-CH_2), 14.2 (CH_3); MS(ESI), m/z: 502.2 (M^++1); Anal. Calcd for $C_{30}H_{24}FN_7$: C, 71.84; H, 4.82; N, 19.55, Found: C, 71.94; H, 4.48; N, 19.52.

***N*-(1-benzyl-2-methyl-1*H*-benzimidazol-5-yl)-6-(4-fluoro-phenyl)-*N*'-(4-fluoro-phenyl)-[1,3,5]triazine-2,4-diamine (42).**

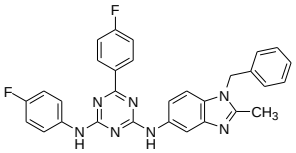

White powder; (0.162 g, 72%); M.p. > 300 ^{o}C; ^{1}H NMR (400 MHz, $CDCl_3$): δ = 8.33 (bs, 1H, NH), 7.83 (bs, 1H, NH), 7.68 (d, 2H, *J* = 8.72 Hz, ArH), 7.54 (d, 2H, *J* = 2.76 Hz, ArH), 7.29-7.25 (m, 7H, ArH), 7.04-7.02 (m, 5H, ArH), 5.27 (s, 2H, N-CH_2), 2.54 (s, 3H, CH_3); ^{13}C NMR (100 MHz, $CDCl_3$): δ = 170.6, 164.7, 152.2, 139.5, 135.9, 134.3, 133.4, 132.5, 130.6, 129.1, 126.2, 122.8, 119.2, 115.7, 115.5, 102.2 (ArC), 46.9 (N-CH_2), 14.0 (CH_3); MS(ESI), m/z: 520.3 (M^++1); Anal. Calcd for $C_{30}H_{23}F_2N_7$: C, 69.35; H, 4.46; N, 18.87, Found: C, 69.37; H, 4.40; N, 18.88.

***N*-(1-benzyl-2-methyl-1*H*-benzimidazol-5-yl)-6-(4-chloro-phenyl)-*N*'-(4-fluoro-phenyl)-[1,3,5]triazine-2,4-diamine (43).**

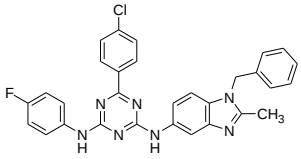

White powder; (0.152 g, 66%); M.p. > 300 ^{o}C; ^{1}H NMR (400 MHz, $CDCl_3$): δ = 8.23 (bs, 1H, NH), 7.90 (d, 2H, *J* = 9.60 Hz, ArH), 7.67-7.65 (m, 3H, ArH), 7.48-7.46 (m, 9H, ArH), 7.26-7.25 (m, 2H, ArH), 7.08 (bs, 1H, NH), 5.27 (s, 2H, N-CH_2), 2.63 (s, 3H, CH_3); ^{13}C NMR (100 MHz, $CDCl_3$): δ = 164.5, 151.9, 138.1, 135.6, 135.1, 135.0, 134.7, 132.8, 132.2, 132.1, 131.1, 129.7, 129.3, 128.7, 128.5, 128.3, 127.8, 127.2, 115.7, 115.5 (ArC), 47.1 (N-CH_2), 13.9 (CH_3); MS(ESI), m/z: 536.3 (M^++1); Anal. Calcd for $C_{30}H_{23}ClFN_7$: C, 67.22; H, 4.33; N, 18.29, Found: C, 66.89; H, 4.44; N, 18.67.

***N*-(1-benzyl-2-methyl-1*H*-benzimidazol-5-yl)-*N'*-(4-fluoro-phenyl)-6-thiophen-2-yl-[1,3,5]triazine-2,4-diamine (44).**

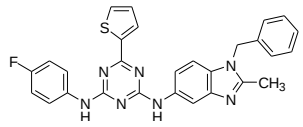

White powder; (0.132 g, 60%); M.p. > 300 ^{o}C; ^{1}H NMR (400 MHz, $CDCl_3$): δ = 7.90 (bs, 1H, NH), 7.69 (d, 2H, *J* = 6.88 Hz, ArH), 7.54 (d, 4H, *J* = 5.96 Hz, ArH), 7.30-7.25 (m, 4H, ArH), 7.05-7.02 (m, 5H, ArH), 5.39 (s, 2H, N-CH_2), 2.55 (s, 3H, CH_3); ^{13}C NMR (100 MHz, $CDCl_3$): δ = 152.2, 135.9, 135.8, 132.9, 132.2, 131.6, 129.1, 128.6, 128.5, 128.2, 128.1, 127.9, 127.8, 127.5, 126.2, 125.7, 125.4, 119.2, 119.1, 115.7, 115.5 (ArC), 46.9 (N-CH_2), 13.4 (CH_3); MS(ESI), m/z: 508.3 (M^++1); Anal. Calcd for $C_{28}H_{22}FN_7S$: C, 66.25; H, 4.37; N, 19.32; S, 6.32, Found: C, 66.47; H, 4.60; N, 19.21; S, 6.10.

***N*-(1-benzyl-2-methyl-1*H*-benzimidazol-5-yl)-*N'*-(4-fluoro-phenyl)-6-m-tolyl-[1,3,5]triazine-2,4-diamine (45).**

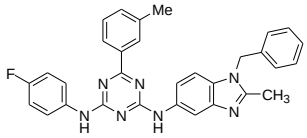

White powder; (0.155 g, 69%); M.p. > 300 ^{o}C; ^{1}H NMR (400 MHz, $CDCl_3$): δ = 8.18 (s, 1H, NH), 8.13 (d, 1H, *J* = 7.32 Hz, ArH), 7.68 (d, 1H, *J* = 8.72 Hz, ArH), 7.56 (bs, 1H, NH), 7.50 (s, 1H, ArH), 7.31-7.26 (m, 9H, ArH), 7.22-7.22 (m, 4H, ArH), 5.26 (s, 2H, N-CH_2), 2.54 (s, 3H, CH_3), 2.40 (s, 3H, CH_3); ^{13}C NMR (100 MHz, $CDCl_3$): δ = 163.6, 151.0, 136.7, 136.0, 133.2, 131.5, 127.8, 125.3, 125.0, 124.5, 121.2, 118.0, 114.2, 113.1 (ArC), 46.2 (N-CH_2), 20.8 (CH_3), 13.2 (CH_3); MS(ESI), m/z: 516.3 (M^++1); Anal. Calcd for $C_{31}H_{26}FN_7$: C, 72.22; H, 5.08; N, 19.02, Found: C, 72.01; H, 5.10; N, 18.93.

***N*-(1-benzyl-2-methyl-1*H*-benzimidazol-5-yl)-*N'*-(4-fluoro-phenyl)-6-(4-methoxy-phenyl)-[1,3,5]triazine-2,4-diamine (46).**

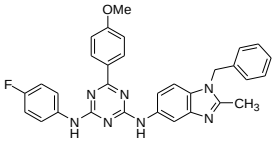

White powder; (0.172 g, 74%); M.p. > 300 ^{o}C; ^{1}H NMR (400 MHz, $CDCl_3$): δ = 8.29 (d, 1H, *J* = 6.88 Hz, ArH), 7.69 (d, 1H, *J* = 6.88 Hz, ArH), 7.66 (d, 1H, *J* = 6.84 Hz, ArH), 7.54 (d, 2H, *J* = 5.96 Hz, ArH), 7.48 (d, 2H, *J* = 7.76 Hz, ArH), 7.28-7.26 (m, 3H, ArH), 7.20 (d, 1H, *J* = 6.88 Hz, ArH), 7.11-7.08 (m, 5H, ArH), 7.06 (bs, 1H, NH), 5.24 (s, 2H, N-CH_2), 3.83 (s, 3H, OCH_3) 2.53 (s, 3H, CH_3); ^{13}C NMR (100 MHz, $CDCl_3$): δ = 164.6, 164.5, 160.3, 157.9, 152.1, 135.9, 135.7, 134.4, 133.3, 129.0, 128.0, 126.3, 122.8, 119.0, 116.7, 115.6, 115.4 (ArC), 47.1 (N-CH_2), 29.8 (O-CH_3), 14.1 (CH_3); MS(ESI), m/z: 532.3 (M^++1); Anal. Calcd for $C_{31}H_{26}FN_7O$: C, 70.04; H, 4.93; N, 18.44, Found: C, 70.27; H, 4.78; N, 18.77.

(1-Benzyl-2-methyl-1*H*-benzimidazol-5-yl)-(4-morpholin-4-yl-6-phenyl-[1,3,5]triazin-2-yl)-amine (47).

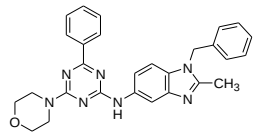

White powder; (0.150 g, 69%); M.p. > 300 ^{o}C; ^{1}H NMR (400 MHz, $CDCl_3$): δ = 8.34 (d, 2H, *J* = 7.32 Hz, ArH), 8.02 (bs, 1H, NH), 7.67 (d, 1H, *J* = 6.28 Hz, ArH), 7.48 (d, 1H, *J* = 7.32 Hz, ArH), 7.35 (d, 1H, *J* = 3.20 Hz, ArH), 7.34-7.30 (m, 3H, ArH), 7.16 (d, 2H, *J* = 8.24 Hz, ArH), 7.07 (d, 2H, *J* = 6.40 Hz, ArH), 5.33 (s, 2H, N-CH_2), 3.98 (s, 4H, mor-CH_2), 3.73 (s, 4H, mor-CH_2), 2.55 (s, 3H, CH_3); ^{13}C NMR (100 MHz, $CDCl_3$): δ = 170.9, 165.1, 165.0, 152.0, 138.7, 136.8, 135.8, 134.1, 131.6, 129.6, 129.2, 128.3, 128.0, 125.9, 119.1, 115.6, 101.4 (ArC), 66.9 (O- CH_2), 46.9 (N-CH_2), 43.7 (N-CH_2), 14.0 (CH_3); MS(ESI), m/z: 478.3 (M^++1); Anal. Calcd for $C_{28}H_{27}N_7O$: C, 70.42; H,

5.70; N, 20.53, Found: C, 70.26; H, 5.62; N, 20.29.

(1-Benzyl-2-methyl-1*H*-benzimidazol-5-yl)-[4-(4-fluoro-phenyl)-6-morpholin-4-yl-[1,3,5]triazin-2-yl]-amine (48).

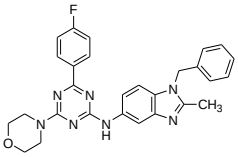

White powder; (0.162 g, 71%); M.p. > 300 ^{o}C; ^{1}H NMR (400 MHz, $CDCl_3$): δ = 8.34 (t, 2H, *J* = 7.32 Hz, ArH), 7.98 (bs, 1H, NH), 7.66 (d, 2H, *J* = 8.68 Hz, ArH), 7.32-7.26 (m, 4H, ArH), 7.05 (d, 4H, *J* = 5.96 Hz, ArH), 5.30 (s, 2H, N-CH_2), 3.95 (s, 4H, mor-CH_2), 3.72 (s, 4H, mor-CH_2), 2.52 (s, 3H, CH_3); ^{13}C NMR (100 MHz, $CDCl_3$): δ = 170.0, 165.1, 164.4, 152.0, 138.9, 137.7, 135.8, 134.0, 132.1, 132.0, 129.7, 129.2, 128.6, 128.5, 128.0, 125.8, 119.2, 115.7, 101.5 (ArC), 66.8 (O-CH_2), 46.9 (N-CH_2), 43.7 (N-CH_2), 14.0 (CH_3); MS(ESI), m/z: 496.3 (M^++1); Anal. Calcd for $C_{28}H_{26}FN_7O$: C, 67.86; H, 5.29; N, 19.79, Found: C, 67.67; H, 4.99; N, 19.80.

(1-Benzyl-2-methyl-1*H*-benzimidazol-5-yl)-[4-(4-chloro-phenyl)-6-morpholin-4-yl-[1,3,5]triazin-2-yl]-amine (49).

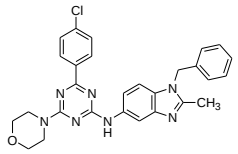

White powder; (0.184 g, 78%); M.p. > 300 ^{o}C; ^{1}H NMR (400 MHz, $CDCl_3$): δ = 8.33 (t, 2H, *J* = 7.32 Hz, ArH), 8.00 (bs, 1H, NH), 7.66 (d, 2H, *J* = 8.68 Hz, ArH), 7.34-7.26 (m, 3H, ArH), 7.15 (dd, 1H, ^{2}J = 1.84 Hz, ^{3}J = 8.72 Hz, ArH), 7.05 (d, 4H, *J* = 5.96 Hz, ArH), 5.30 (s, 2H, N-CH_2), 3.95 (s, 4H, mor-CH_2), 3.72 (s, 4H, mor-CH_2), 2.52 (s, 3H, CH_3); ^{13}C NMR (100 MHz, $CDCl_3$): δ = 170.0, 165.1, 164.4, 152.0, 138.9, 137.7, 135.8, 135.4, 134.0, 132.2, 132.1, 132.0, 129.7, 129.2, 128.6, 128.5, 128.0, 125.8, 119.2, 115.7, 101.5 (ArC), 66.8 (O-CH_2), 46.9 (N-CH_2), 43.7 (N-CH_2), 14.1 (CH_3); MS(ESI), m/z: 512.3 (M^++1); Anal. Calcd for $C_{28}H_{26}ClN_7O$: C, 65.68; H, 5.12; N, 19.15, Found: C, 65.88; H, 5.21; N, 19.10.

2.3. TRIAZINE-BENZIMIDAZOLE WITH PHENYL LINKER (4-FLUOROANILINE)

DNA is the molecule present in all cellular forms of life that contains the genetic information for biological development. DNA is a major drug target because of its vital role in the cell. New and more effective drugs are designed which recognize a specific site or conformation of DNA. The ability to identify structural elements of a drug, responsible for specificity of binding to DNA, may improve the screening process for new drugs. Small molecules targeting DNA have attracted significant scientific interest due to their medicinal, biochemical and biological applications. These molecules interact with DNA through three different non-covalent modes such as intercalation,[88]

groove binding,[89] and electrostatic interactions.[90] These interactions are helpful in understanding the mechanisms of DNA damage and planning the design of more efficient compounds. Generally, drug upon binding to DNA are stabilized through a series of weak interactions such as π-stacking interactions of aromatic heterocyclic groups between the base pairs (intercalation), hydrogen bonding and van der Waals interactions of functional groups bound along the groove of the DNA helix.[91] Hybrid or conjugate molecules have also been studied for the interaction with DNA.[92,93] Biological applications associated with triazine and benzimidazole, prompted us to investigate the corresponding structure as a potential new molecular probe for interaction with calf thymus DNA by *in vitro* experiments.

2.3.1. CHEMISTRY

2,4,6-Trisubstituted triazines (**4-21**) were prepared in moderate to good yields using nucleophilic substitution and Suzuki-Miyaura cross coupling reactions (Scheme 6). Cyanuric chloride was reacted with 4-fluoroaniline in the presence of 10% $NaHCO_3$ in THF at 0-5 ^{0}C for 6 h to obtain (4,6-dichloro-[1,3,5]triazin-2-yl)-(4-fluoro-phenyl)-amine (**1**) in 85% yield. Compound **1** was treated with 4-(1*H*-benzimidazol-2-yl)-phenylamine (**2**) (synthesized by the condensation of 4-aminobenzoic acid and *o*- phenylenediamine in the presence of polyphosphoric acid at 200 ^{o}C for 5 h) in the presence of potassium carbonate and THF at room temperature for 24 h to provide the *N*-[4-(1*H*-benzimidazol-2-yl)-phenyl]-6-chloro-*N*'-(4-fluoro-phenyl)-[1,3,5]triazine-2,4-diamine **(3)** in 82 % yield.

Scheme 6[a]. Synthesis of triazine-benzimidazole analogues.

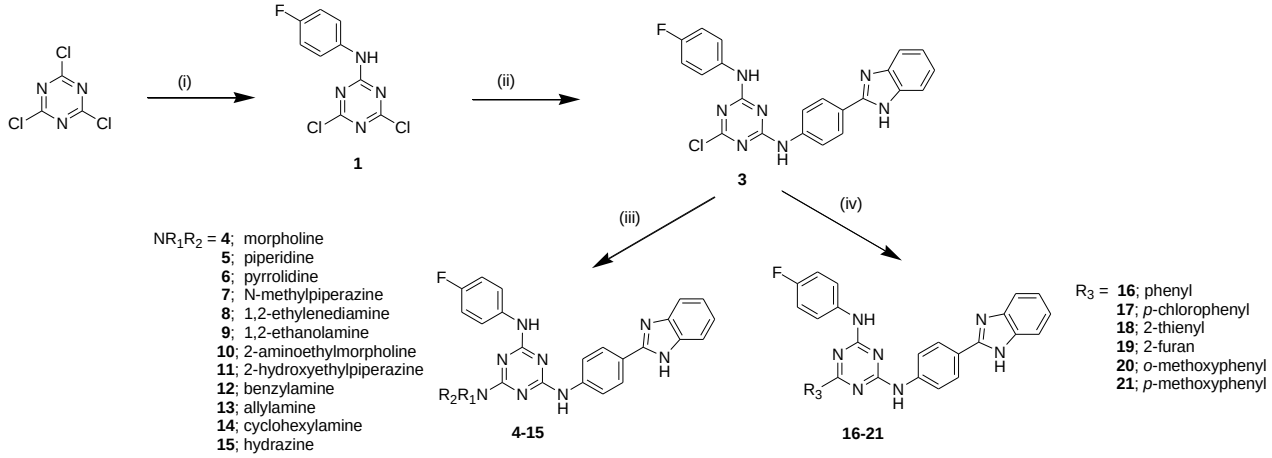

[a]Reagents and conditions: (i) fluoroaniline, $NaHCO_3$, THF, 0−5 °C; (ii) **2**, K_2CO_3, THF, rt; (iii) NHR_1R_2, K_2CO_3, 1,4-dioxane, reflux; (iv) $R_3B(OH)_2$, $Pd(PPh_3)_4$, K_2CO_3, 1,4-dioxane, reflux.

Further, treatment of **3** with different primary and secondary amines in the presence of 10% potassium carbonate in 1,4-dioxane at 110 ^{o}C for 6-8 hrs gave compounds **4-15** in 66-78% yields. Compound **3** was also treated with five and six membered aryl boronic acids through Suzuki coupling, in the presence of 10 mol % of $Pd(PPh_3)_4$ and 1.5 equivalents of K_2CO_3 in 1,4-dioxane afforded compounds **16-21** in 65-71% yields.

2.3.2. BIOLOGY

2.3.2.1. *In vitro* Anticancer Evaluation

All the synthesized compounds were submitted to National Cancer Institute (NCI) disease-oriented human cell lines for their evaluation of *in-vitro* antitumor activities. One compound (**6**) was selected and evaluated against 60 human cell lines at one dose concentration level i.e. 10^{-5} M (Table 8). Compound **6** showed activity towards leukemia cancer cell lines CCRF-CEM, HL-60(TB), K-562, SR and RPMI-8226, melanoma cancer cell lines LOXIMVI and colon cancer cell line SW-620. Compound **6** was further screened against a panel of 60 different tumor cell lines at 5 dose concentration levels: 10^{-4}, 10^{-5}, 10^{-6}, 10^{-7} and 10^{-8} M as these have shown prominent cell growth inhibition at 10^{-5} M concentration against variety of cell lines. Three response parameters like median growth inhibitory (GI_{50}, µM), total growth inhibitory (TGI, µM) and median lethal concentrations (LC_{50}, µM) were monitoring for each cell line. MG MID GI_{50} value (over all the 60 cancer cell lines) of compound **6** showed specificity towards leukemia, colon and CNS cancer cell lines with GI_{50} values in the range of 2.22-2.45 µM. MG MID GI_{50}, TGI and LC_{50} values of compound **6** has been shown to be 3.58, 9.87 and 35.5 µM respectively (Table 9).

Table 8. Percent growth promotion of *in vitro* subpanel tumor cell lines at 10 µM concentration of compound **6**.

Leukemia		**CNS cancer**		**Breast cancer**		**Colon cancer**	
CCRF-CEM	**5.35**	SF-268	91.23	MCF7	**32.73**	COLO 205	85.97
HL-60(TB)	**5.97**	SF-295	90.89	MDA-MB-231/ATCC	**61.57**	HCC-2998	**55.65**
K-562	-38.79	SF-539	81.60	HS 578T	84.57	HCT-116	-53.56
MOLT-4	**48.23**	SNB-19	102.59	BT-549	85.13	HCT-15	-8.99
RPMI-8226	-11.63	SNB-75	**65.38**	T-47D	**44.60**	HT29	**36.12**
SR	**10.72**	U251	**55.81**	MDA-MB-468	83.64	KM12	83.80
						SW-620	**0.69**
Ovarian cancer		**Melanoma**		**Renal cancer**		**Non-small cell lung cancer**	
IGORV1	83.05	LOX IMVI	**3.18**	786-0	85.22	A549/ATCC	**61.16**

OVCAR-3	94.41	MALME-3M	85.71	A498	**75.28**	EKVX	**71.93**
OVCAR-4	88.61	M14	-58.32	ACHN	**73.15**	HOP-62	**78.61**
OVCAR-5	97.39	MDA-MB-435	98.12	CAKI-1	88.01	HOP-92	**64.38**
OVCAR-8	81.70	SK-MEL-2	95.20	RXF 393	**77.78**	NCI-H226	**79.93**
NCI/ADR- RES	**62.99**	SK-MEL-28	**47.66**	SN12C	81.20	NCI-H23	**75.10**
SK-OV-3	**75.10**	SK-MEL-5	87.00	TK-10	151.24	NCI-H322M	96.03
Prostate cancer		UACC-257	97.47	UO-31	**68.13**	NCI-H460	70.39
PC-3	**33.80**					NCI-H522	**78.80**
DU-145	93.29						

30-40% growth inhibition; 40-50% growth inhibition; 50-70% growth inhibition; 90-100% growth inhibition; highly potent

Table 9. Average GI_{50} (μM), TGI (μM) and LC_{50} (μM) over 60 cancer cell lines for compound **6.**

Compound	Activity	I	II	III	IV	V	VI	VII	VIII	IX	MIG-MID[a]
6	GI_{50}	2.22	3.85	2.23	2.45	4.71	5.08	5.68	3.48	2.48	3.58
	TGI	6.82	12.1	5.55	7.57	10.4	13.2	13.4	11.7	8.07	9.87
	LC_{50}	[b]	38.8	28.2	30.5	23.8	46.5	35.7	38.8	42.0	35.5

I, leukemia; II, non-small cell lung cancer; III, colon cancer; IV, CNS cancer; V, melanoma; VI, ovarian cancer; VII, renal cancer; VIII, prostate cancer; IX, breast cancer; [a] Full panel mean-graph midpoint (μM); [b] Compounds showed values >100 μM

2.3.2.2. DNA Binding Study

These synthesized compounds were further screened for their interaction with DNA. Absorption and emission spectroscopies are extensively used as effective methods for monitoring complex formation between DNA and small molecules. The interaction of compounds **4-21** (20 μM) towards ct-DNA were investigated by UV-Visible spectroscopy in phosphate buffer (10 mM, pH 7.4). The electronic spectra of all the tested compounds showed intense band at the range of 300-335 nm due to the transitions between π-π* energy levels. Addition of ct-DNA to the solution of compounds **7**, **9-11**, **16** and **21** in phosphate buffer resulted in gradual decrease in the absorption intensity. These compounds showed comparatively more hypochromicity in the respective percentage of 58.3%, 51%, 63%, 58.9%, 62.5% and 64.5% (Figure 18) as compared to compounds **4-6**, **8**, **12**, **14**, **15**, **18** and **20** which showed hypochromicity in the range of 21% - 49.3% (Figures 20-28). Compounds **13**, **17** and **19** did not show any significant change in the presence of ct-DNA. As there is no change in position of the absorption band (bathochromic or hypsochromic shift) of conjugates, it can be inferred that these compounds exhibit groove binding interactions to ct-DNA.[94]

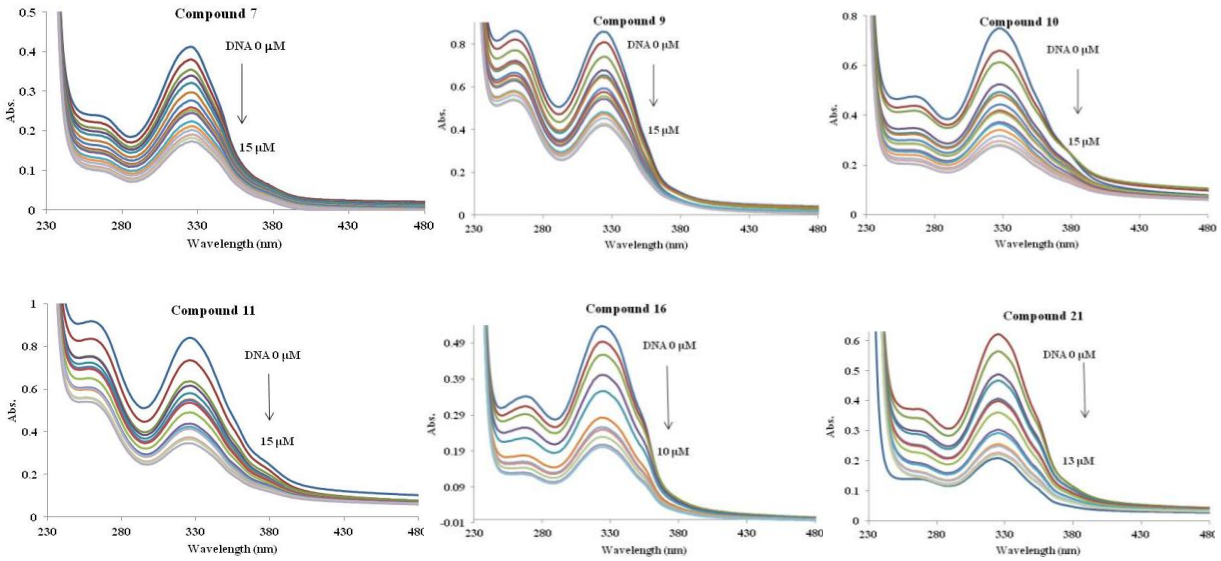

Figure 18. UV-vis spectral changes of compounds **7**, **9-11**, **16** and **21** (20 µM) upon addition of ct-DNA (0 µM-15 µM) in phosphate buffer (10 mM, pH 7.4).

In order to further investigate the interaction between triazine-benzimidazole analogs, fluorescence titration experiments were performed. On exciting the compounds **7**, **9-11**, **16** and **21**, the emission spectra showed intense band between 375-473 nm. The fluorescence intensity of compounds regularly decreased while maximum emission wavelength did not apparently shifts with increase of ct-DNA concentration. As shown in Figure 19, addition of ct-DNA (0–17

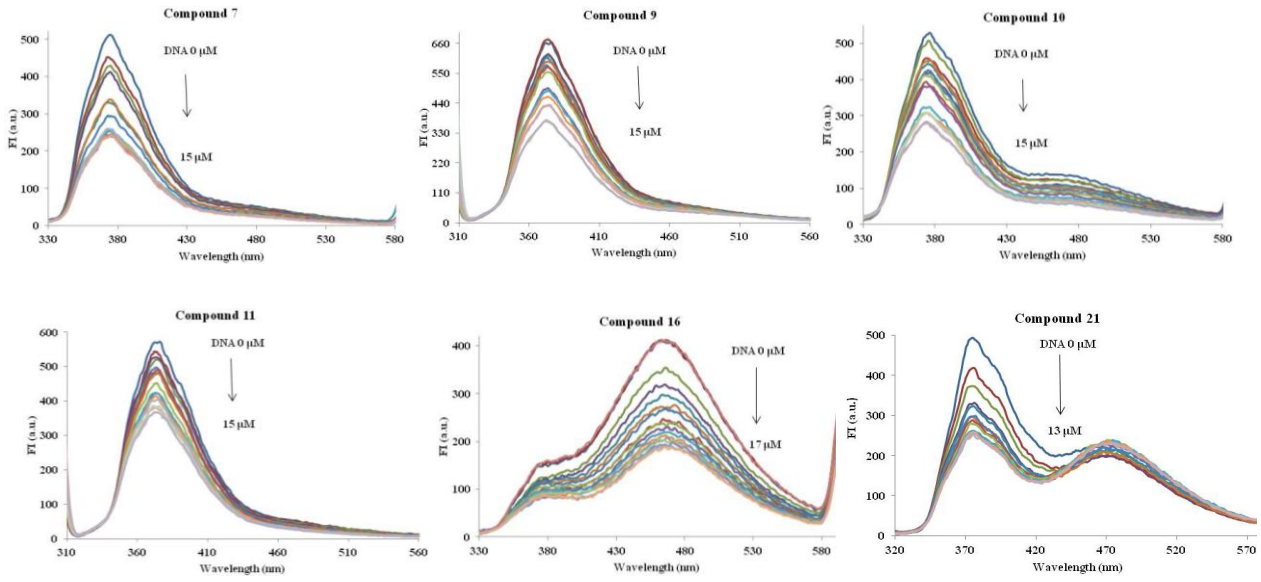

Figure 19. Fluorescence spectral changes of **7**, **9-11**, **16** and **21** (20 µM) upon addition of ct-DNA (0 µM-17 µM) in phosphate buffer (10 mM, pH 7.4).

μM), compounds **7**, **9- 11**, **16** and **21** showed quenching of 52.4%, 44.3%, 46.0%, 35.4%, 54.3% and 48.0% respectively while the intensities of compounds **4-6, 8, 12, 14, 15, 18** and **20** were quenched in the range of 20-58% (Figures 20-28). Compounds **13, 17** and **19** did not show any significant change in the presence of ct-DNA in emission spectroscopy. The change in absorption and fluorescence intensities clearly indicated the interacting properties of compounds **7**, **9-11**, **16** and **21** with DNA.

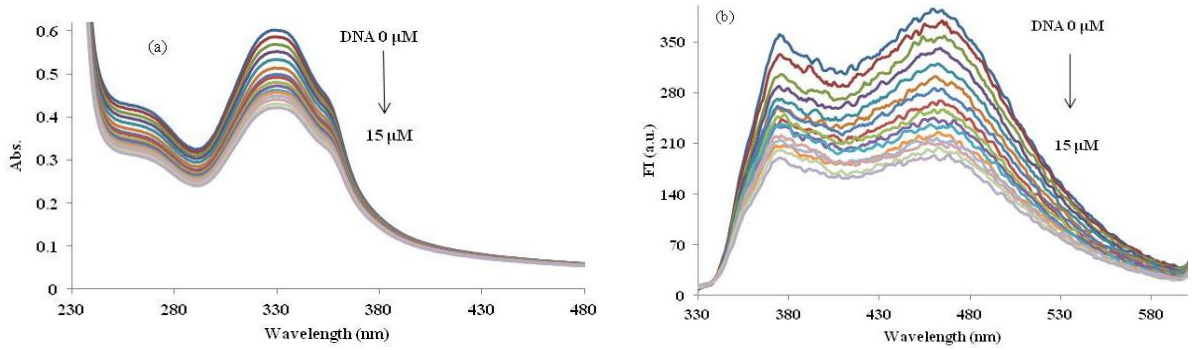

Figure 20. (a) Absorption (b) emission spectra of compound **4** (20.0 μM) with increasing concentration of ct-DNA in phosphate buffer.

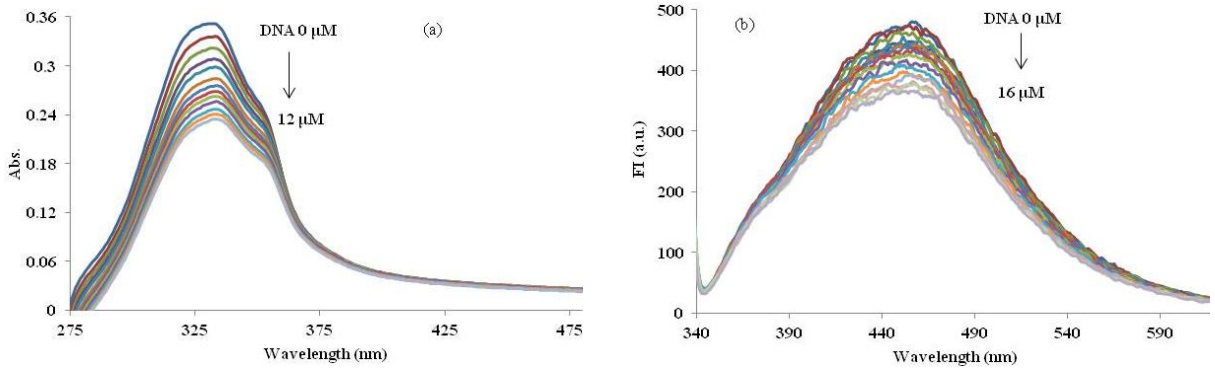

Figure 21. (a) Absorption (b) emission spectra of compound **5** (20.0 μM) with increasing concentration of ct-DNA in phosphate buffer.

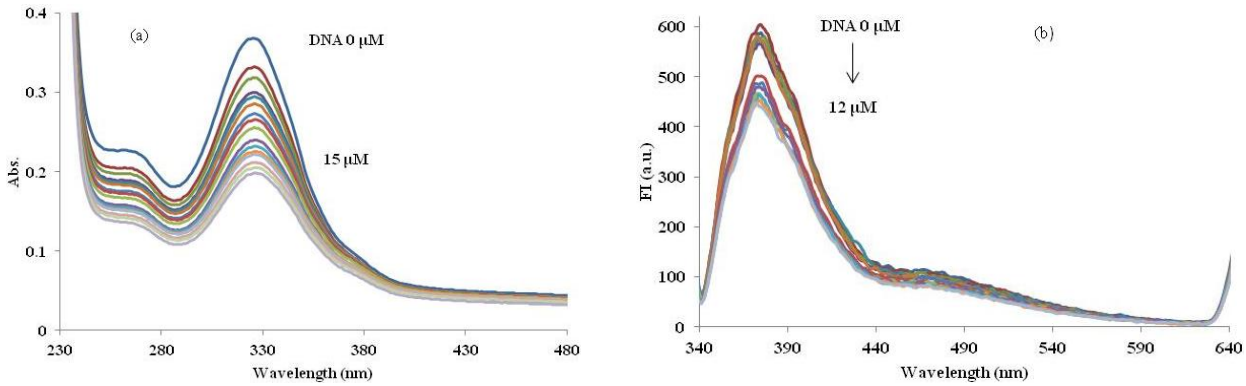

Figure 22. (a) Absorption (b) emission spectra of compound **6** (20.0 µM) with increasing concentration of ct-DNA in phosphate buffer.

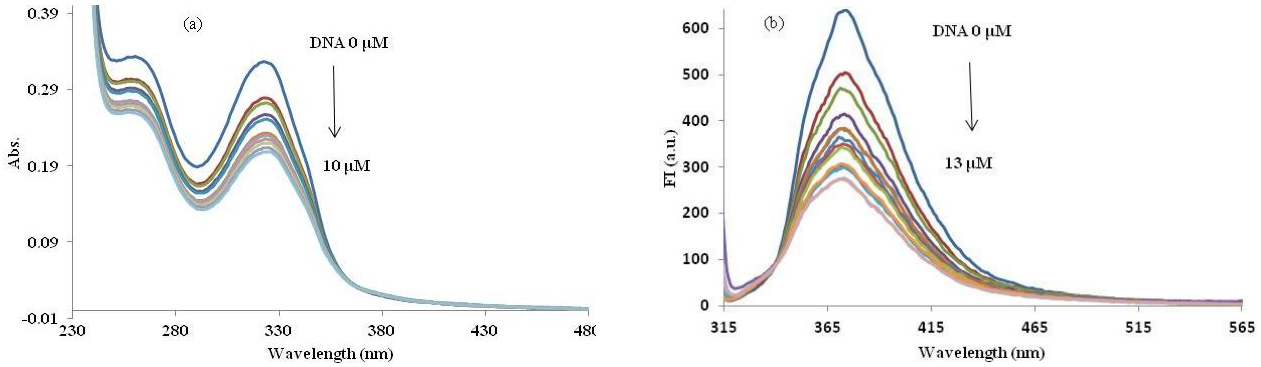

Figure 23. (a) Absorption (b) emission spectra of compound **8** (20.0 µM) with increasing concentration of ct-DNA in phosphate buffer.

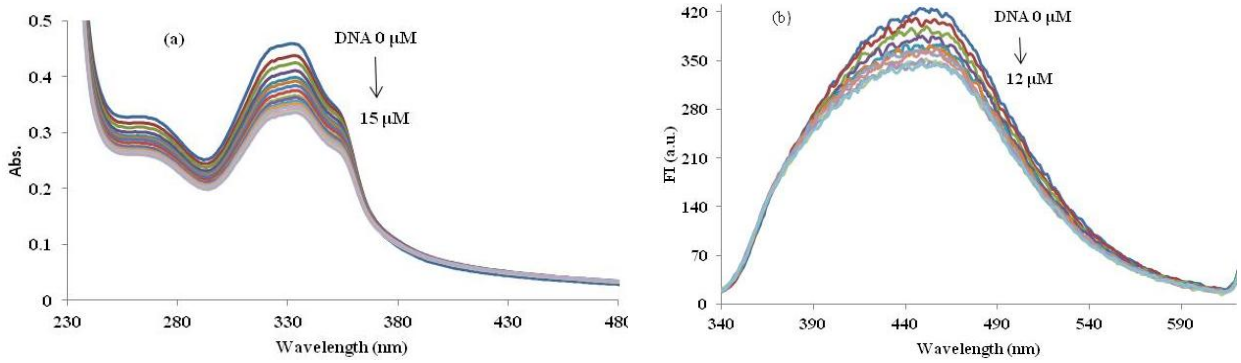

Figure 24. (a) Absorption (b) emission spectra of compound **12** (20.0 µM) with increasing concentration of ct-DNA in phosphate buffer.

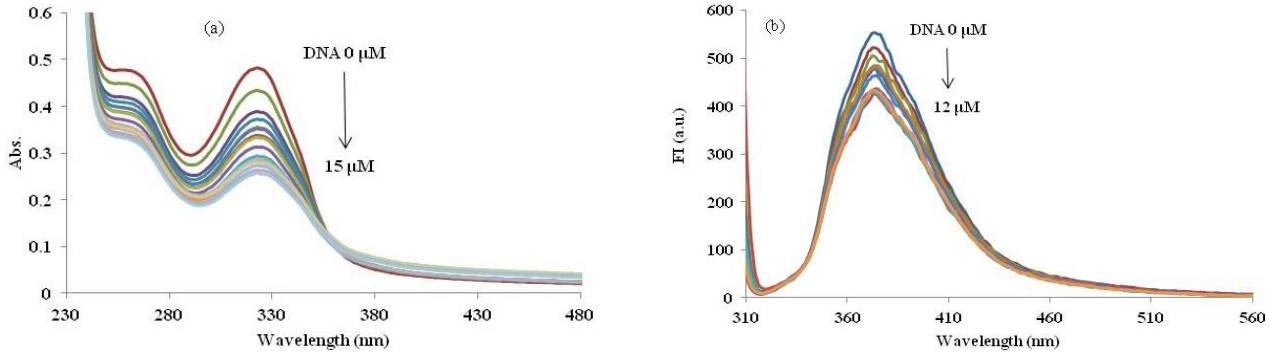

Figure 25. (a) Absorption (b) emission spectra of compound **14** (20.0 µM) with increasing concentration of ct-DNA in phosphate buffer.

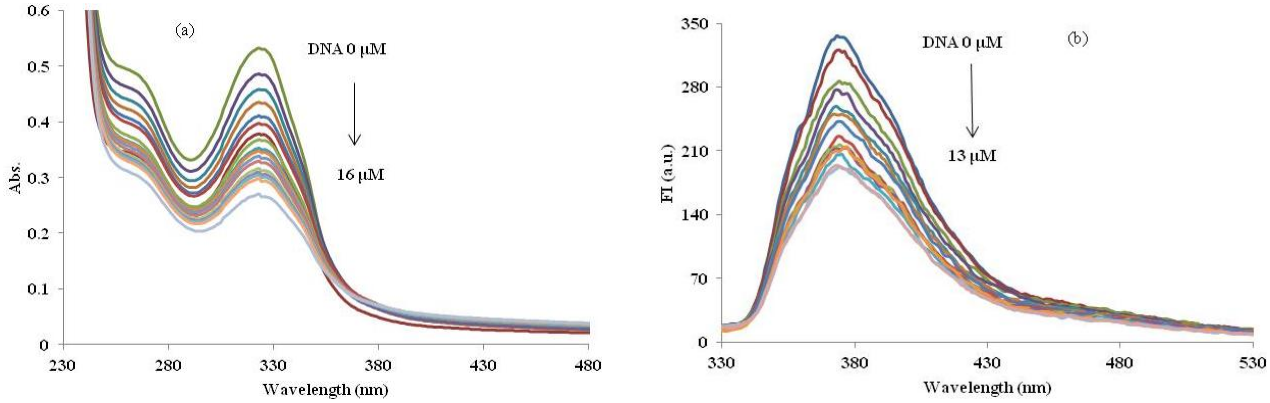

Figure 26. (a) Absorption (b) emission spectra of compound **15** (20.0 µM) with increasing concentration of ct-DNA in phosphate buffer.

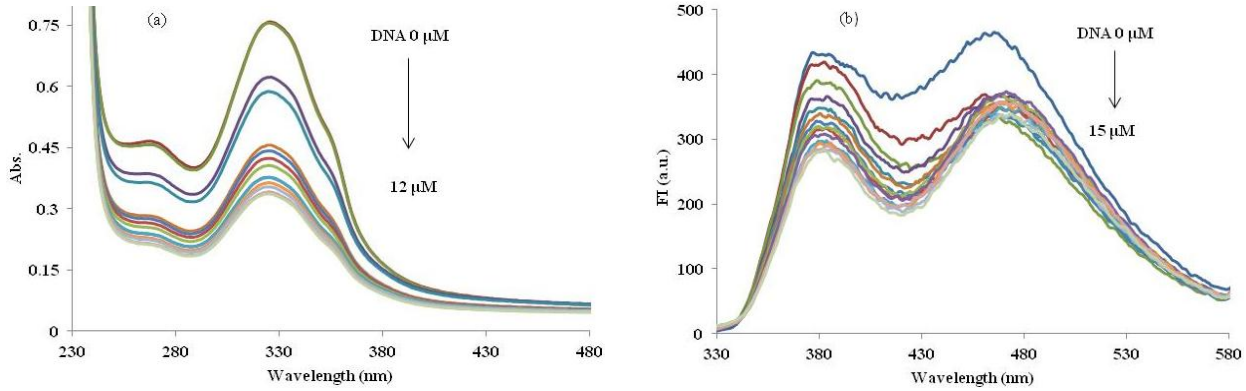

Figure 27. (a) Absorption (b) emission spectra of compound **18** (20.0 µM) with increasing concentration of ct-DNA in phosphate buffer.

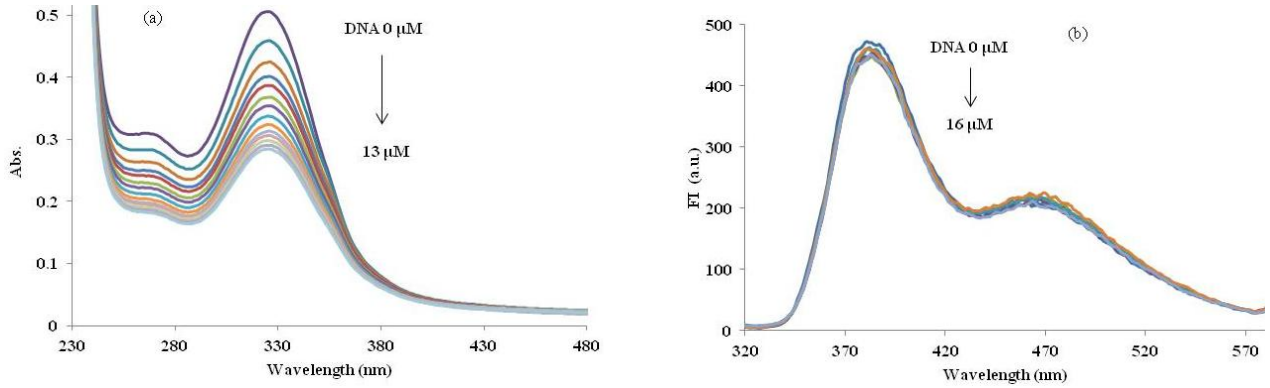

Figure 28. (a) Absorption (b) emission spectra of compound **20** (20.0 µM) with increasing concentration of ct-DNA in phosphate buffer.

For the quantitative investigation of binding strength, the binding constants of these compounds with ct-DNA were determined from UV-Visible and fluorescence titration data using Benesi–Hildebrand equation[85] (Figure 29 and Figure 30). The K values indicated that there is strong binding interaction between triazine-benzimidazole analogs and ct-DNA as shown in table 10.

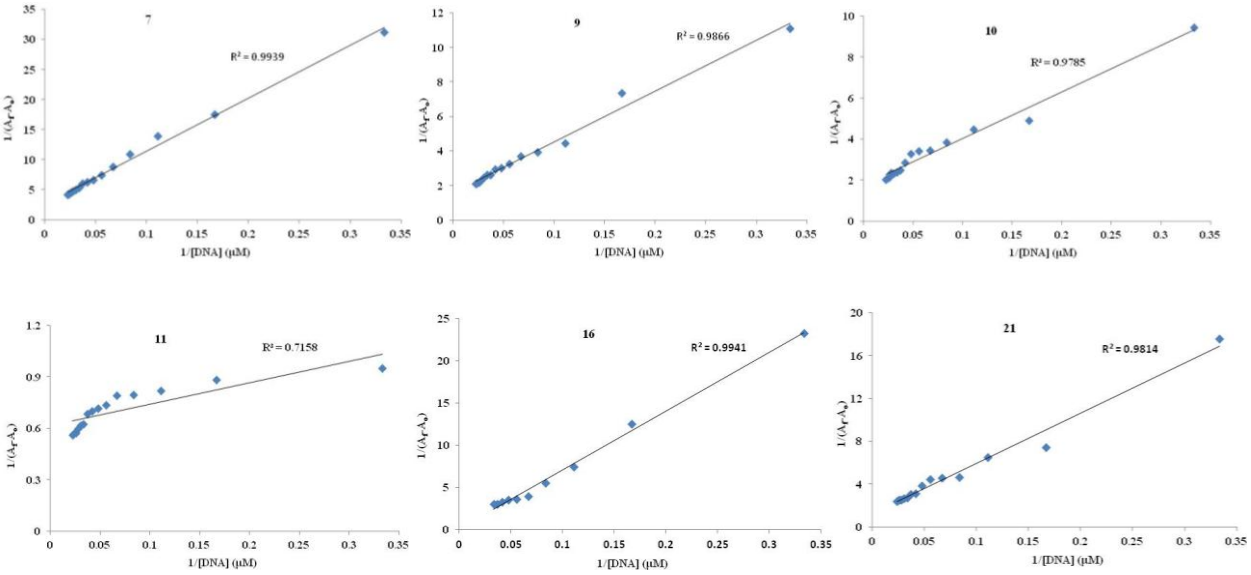

Figure 29. Plot of $1/(A_f - A_0)$ vs. 1/[DNA] for absorption spectra of compounds **7, 9-11, 16** and **21** in the presence of ct-DNA.

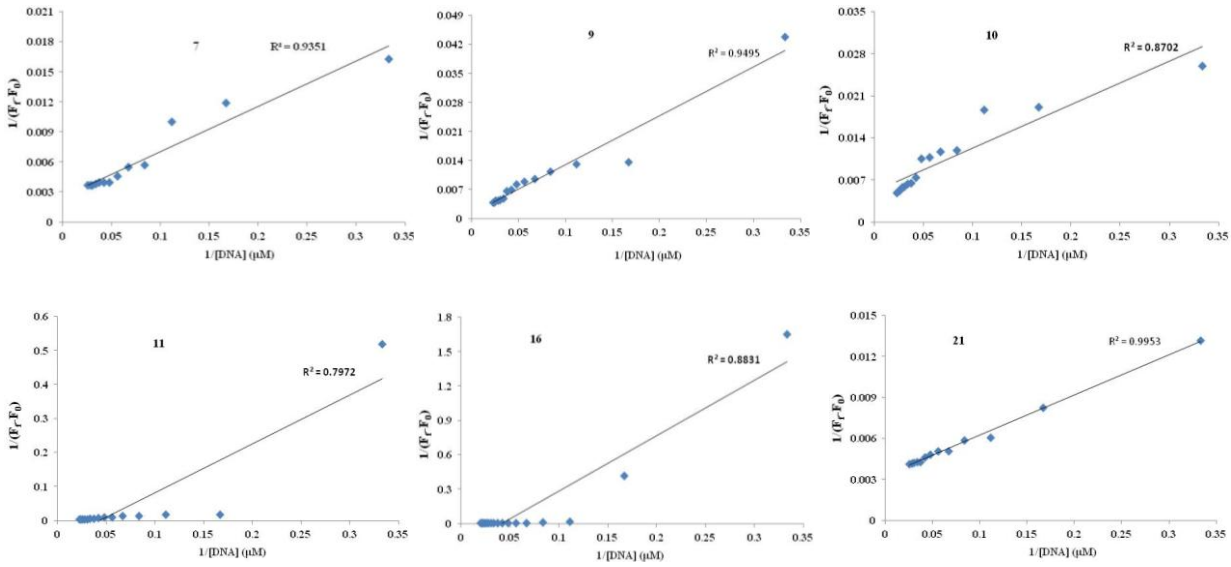

Figure 30. Plot of $1/(F_f - F_0)$ vs. 1/[DNA] for emission spectra of compounds **7, 9-11, 16** and **21** in the presence of ct-DNA.

To evaluate the possible mode of binding of compounds **7**, **9-11**, **16** and **21** with DNA, thermal denaturation study was performed. Stabilization of the double helix is commonly observed for intercalating ligands, whereas groove binders may lead to stabilization or destabilization in the melting temperature (T_m) of double standard DNA.[95] The T_m value for free ct-DNA has been found to be 65.6 ^oC whereas complexes of compounds **7**, **9-11**, **16** and **21** with DNA, the T_m was measured in the range of 57.0-64.4 ^oC. It has been found that triazine-benzimidazole analogues destabilize DNA double helix by 1.2-8.6 degrees (Table 10). This indicated that the mode of binding of compounds with DNA is not due to intercalation but some other interactions are responsible for their binding.

Table 10. Photophysical properties, binding constants (K), T_m and ΔT_m of compounds with ct-DNA.

Compds	Hypochromicity (%) in absorption spectra	Quenching (%) in emission spectra	K of absorption spectra (M^{-1})	K of emission spectra (M^{-1})	T_m (^0C) (ct-DNA = 65.6)	ΔT_m (^0C)
7	58.3	52.4	1.7×10^4	2.3×10^3	60.1	-5.5
9	51.0	44.3	5.4×10^3	9.7×10^4	57.0	-8.6
10	63.0	46.0	1.8×10^4	2.8×10^4	58.8	-6.8
11	58.9	35.4	1.3×10^4	2.7×10^4	62.4	-3.2
16	62.5	54.3	4.1×10^4	4.8×10^4	64.4	-1.2
21	64.5	48.0	2.3×10^4	2.8×10^4	59.3	-6.3

In order to rationalize the binding mode, a competitive binding experiment was performed with compounds **7**, **9-11**, **16** and **21** and DNA in the presence of minor groove binder (Hoechst 33258) and an intercalator (ethidium bromide).[96,97] DNA (0 μM- 30 μM) was added to Hoechst 33258 (20 μM) solution and the fluorescence emission spectra were recorded when saturation was reached. In this case, the emission intensity gradually increased and reached a maximum (saturation). With increasing concentration of compounds **7**, **9-11** and **16**, the emission intensity of Hoechst.DNA complex was enhanced to a significant level while in case of compound **21** the emission intensity of Hoechst.DNA complex was quenched (Figure 31). This indicated that the Hoechst dye was replaced with compounds **7**, **9-11**, **16** and **21** from the minor groove of DNA. A similar experiment was performed with addition of DNA to a solution of ethidium bromide (EB) that provided an increase in emission intensity of ethidium bromide to saturation. Ethidium bromide is one of the most sensitive fluorescent probes having a planar structure that binds to DNA *via* the intercalative mode. The extent of fluorescence quenching of the EB.DNA system can be used to determine the extent of intercalation between molecule and DNA.[98] However, in this case, on subsequent addition of compounds **7, 9-11, 16** and **21** to the ethidium bromide.DNA complex, there was no significant change in emission intensity of ethidium bromide.DNA complex, suggesting that triazine-benzimidazoles bind to DNA in the non-intercative mode. These results further supported the binding of compounds **7**, **9-11**, **16** and **21** through groove mode.

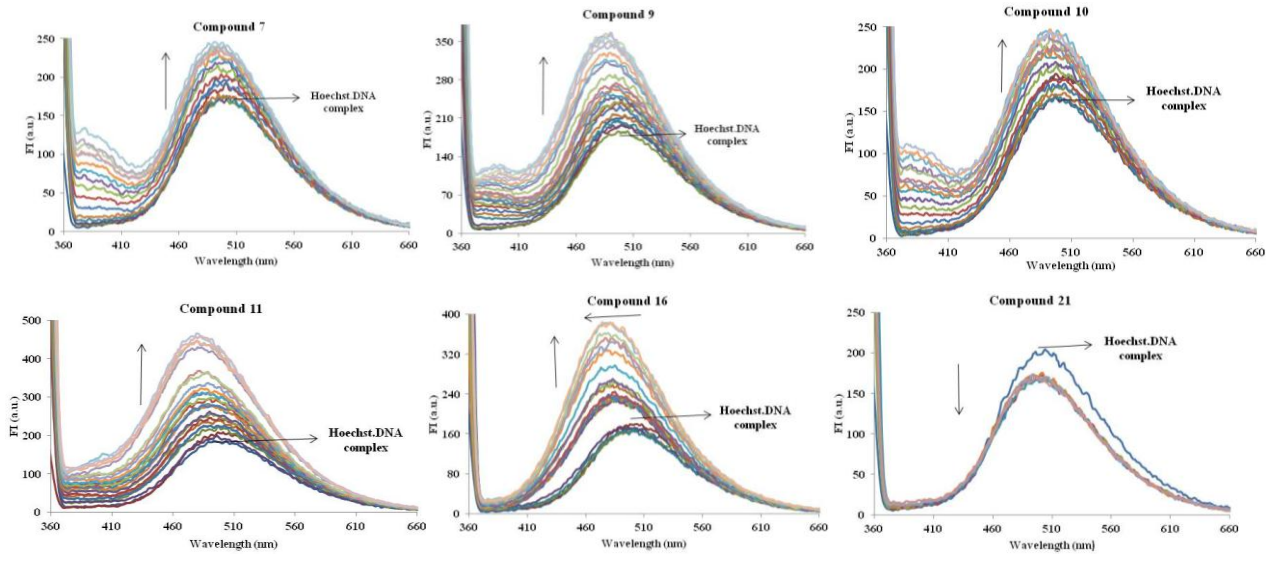

Figure 31. Gradual addition of ligands **7, 9-11, 16** and **21** (2–30 μM) results in significant changes in the fluorescence intensity of Hoechst bound ct-DNA.

Further, viscosity titration method was performed to confirm the binding mode between triazine-benzimidazoles and ct-DNA. The intercalation of compound into DNA causes a significant increase in viscosity due to increase in separation of base pairs at the intercalation site of DNA helix as the base pairs are pushed apart to accommodate the binding molecule. On the other hand, groove or electrostatic binding leads to minor or no increment in the DNA viscosity.[99] A viscosity plot of $(\eta/\eta_o)^{1/3}$ versus ligand.DNA ratio was obtained to study any change in the viscosity of ct-DNA solution in the presence of compounds. As shown in figure 32, with

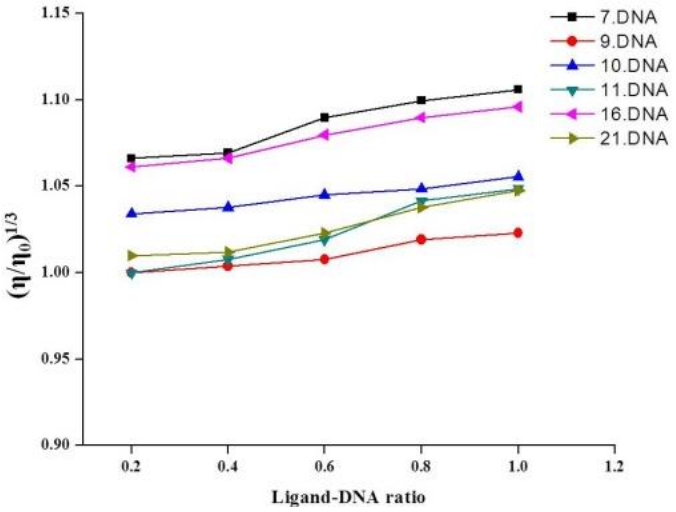

Figure 32. The relative specific viscosity of an aqueous solution of ct-DNA in the presence of ligands **7**, **9-11**, **16** and **21**.

continuous addition of compounds **7, 9-11, 16** and **21** to ct-DNA solution, small increase in viscosity was observed which was not as pronounced as observed for classical intercalators, thus confirming that these compounds interacts with minor groove of DNA and ruling out the possibility of intercalation.

The effect of ionic strength was determined to evaluate whether there is electrostatic binding between triazine-benzimidazoles and ct-DNA. The addition of NaCl weakens the surface-binding interactions because positively charged sodium ions can bind to negatively charged ct-DNA phosphate groups via electrostatic attractions, and then neutralize the negative charges of the helix backbone to ct-DNA. If there is no electrostatic binding, there is no effect on the ratio of fluorescence quenching.[100] An increase in NaCl concentration did not significantly change the slopes of F_o/F of the free compounds (Figure 33a) and compound.DNA complexes (Figure 33b), indicating that triazine-benzimidazoles do not bind to ct-DNA by electrostatic binding.

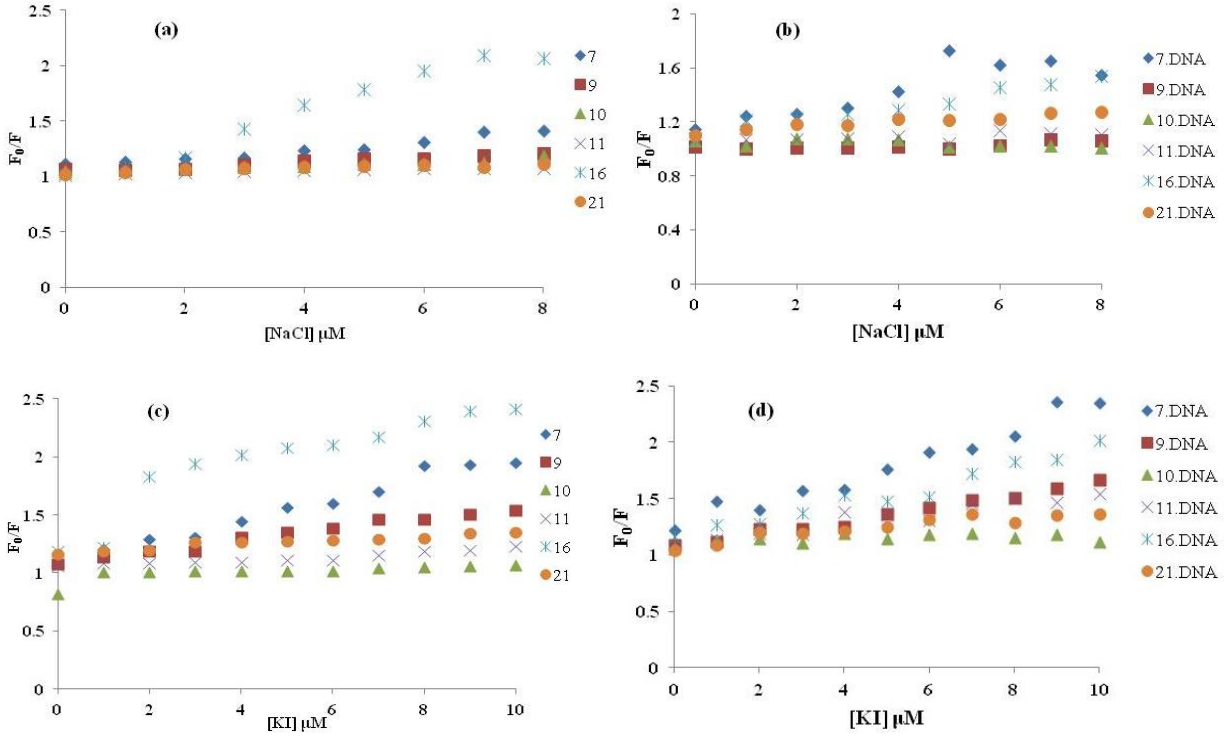

Figure 33. Fluorescence quenching plots of compounds **7, 9-11, 16** and **21** and compound.DNA complexes by (a,b) NaCl and (c,d) KI.

To further explore the binding mode between compounds and ct-DNA, iodine quenching experiments were performed. When small molecules intercalate into DNA base pairs, the bound molecules are protected by the double helix of DNA, thus it is difficult for the anionic quenchers to come into contact with small molecules. Therefore, the quenching constant of compound.DNA complex should be smaller than that of the free small molecules.[101] Potassium iodide is highly negative charged quencher, which is often used to determine the binding mode of compound with DNA.[96] The ratio of fluorescent intensity of compounds **7, 9-11, 16** and **21** and DNA complexes did not show any significant changes upon successive addition of iodide that further eliminated the possibility of intercalation. These results signified the interaction of compounds **7, 9-11, 16** and **21** with DNA through groove binding mode or/and electrostatic binding (Figure 33c-d).

2.3.2.3. Molecular Modeling

Docking experiments were performed to find the most stable and favourable orientation as blind dockings using Argus lab.[86] The structures of the ligands (**7, 9-11, 16** and **21**) were

optimized to true minima on the potential energy surface. The structural coordinates of DNA was obtained from the protein data bank (PDB ID: 1BNA).[102] Based on the energies and the number of occurrences of each conformation, the conformation with highest number of occurrences was obtained, and had the most optimal energy of all the clusters, and thus was chosen for the final binding orientation analysis (Figure 34). In the docking analysis, the binding site was assigned across the entire grooves of the DNA molecule. The docking studies of the synthesized ligands clearly showed the importance of mode of action through the interaction between the triazine derivatives and DNA. Moreover, hydrogen bonds were formed between compounds (**7, 9-11, 16** and **21**) with DNA base pairs (Table 11). Due to differences in the functional group, there are differences in their hydrogen bonding interaction with ct-DNA, and thus differences in the values of binding constants. The molecular modelling study shows that all the six ligands bind DNA preferably through the groove mode.

Table 11. H-bonding of compounds **7**, **9-11**, **16** and **21** with DNA base pairs.

Compds.	NH of fluoroaniline	NH of phenyl linker	NH of imidazole ring of benzimidazole	Variable substitutent	No. of H-bonding
7	7DT (2.26 Å), 6DA (1.86 Å), 7DA (1.74 Å)	18DA (3.35 Å), 18DA (1.69 Å)	17DA (2.78 Å), 8DT (2.89 Å), 16DG (2.16 Å), 9DC (2.38 Å)	-	9
9	22DG (2.28 Å), 23DC (2.75 Å)	5DA (1.46 Å), 5DA (1.38 Å)	22DG (0.76 Å), 3DC (2.95 Å), 22DG (2.81 Å)	NH of ethanolamine with DC (1.17 Å), DG (2.09 Å), 24DG (2.82 Å); OH of ethanolamine with 2DG (2.09 Å), 1DC (1.17 Å)	12
10	6DA (1.66 Å)	6DA (2.36 Å), 7DT (2.30 Å), 19DT (2.75 Å), 18DA (2.10 Å)	16DG (2.13 Å)	NH of aminoethylmorpholine with 5DA (2.66 Å), 6DA (2.40 Å), 5DA (1.21 Å)	9
11	5DA (2.58 Å), 5DA (1.51 Å), 5DC (2.87 Å)	20DT (2.38 Å), 5DA (2.61 Å)	18DA (1.54 Å), 7DT (1.73 Å), 5DA (2.65 Å)	OH of hydroxyethylpiperazine with 24DG (2.74 Å), 2DG (1.84 Å), 2DG (2.41 Å)	11
16	7DT (1.38 Å)	17DA (2.22 Å), 18DA (2.03 Å)	10DG (2.95 Å), 15DC (2.63 Å), 9DC (2.74 Å), 16DG (2.34 Å)	-	7
21	8DT (2.57 Å), 7DT (2.30 Å)	17DA (1.67 Å), 17DA (2.99 Å)	10DG (2.48 Å), 9DC (2.97 Å)	-	6

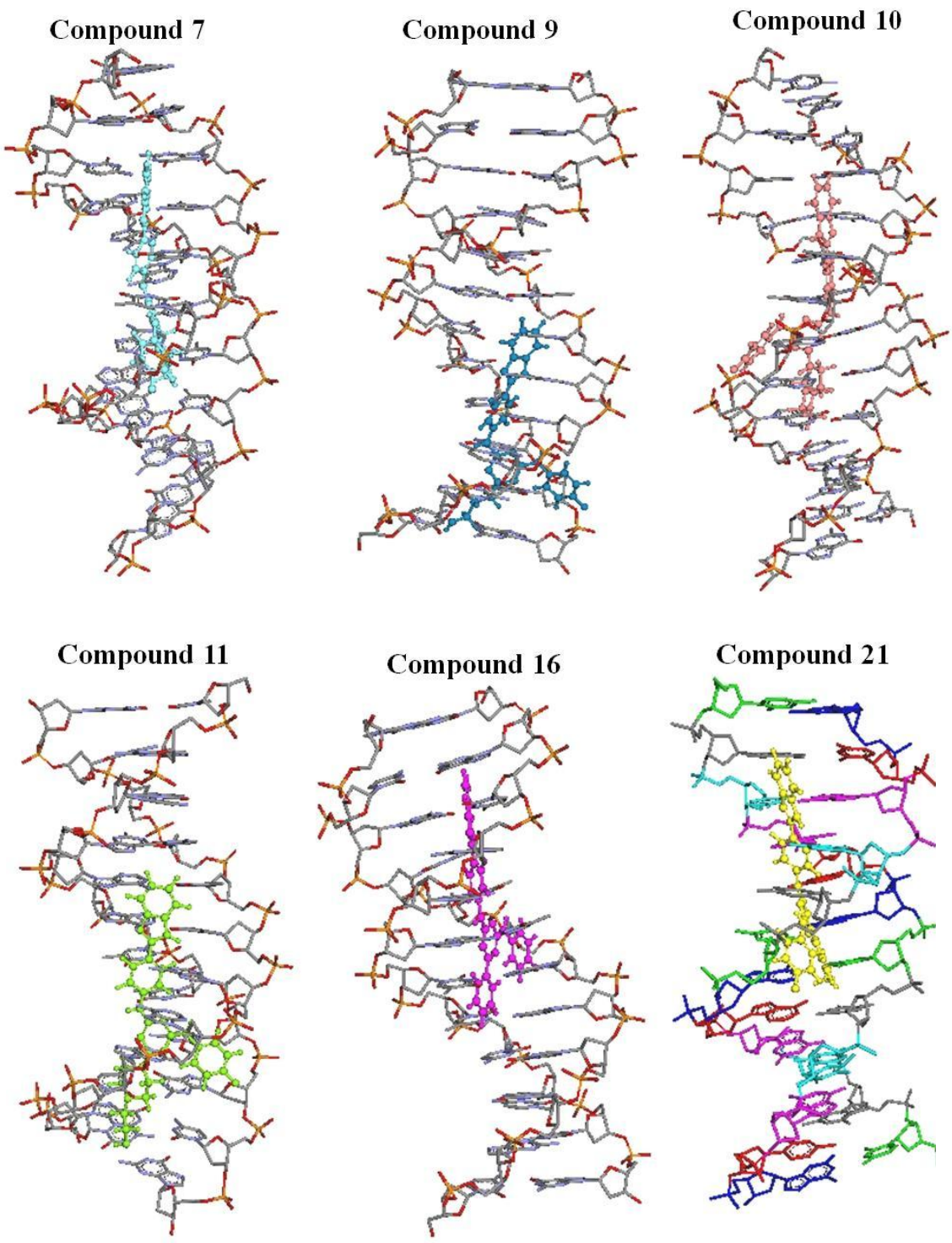

Figure 34. Docked poses of compounds (**7, 9-11, 16** and **21**) with DNA.

2.3.3. CONCLUSIONS

Triazine-benzimidazole analogues with different substitution of primary and secondary amines as well aryl groups were synthesized in moderate to good yields. These compounds were characterized by ^{1}H and ^{13}C NMR as well as mass spectrometry. The interaction of triazine-benzimidazole analogs with ct-DNA was carried out using various spectroscopic techniques. Through the analysis of UV absorbance and fluorescence spectra, formation of compound.DNA complexes was confirmed. Competitively displacement assay with ethidium bromide and Hoechst 33258 revealed that compounds interact with DNA through groove binding. Thermal denaturation experiments and viscosity techniques also supported the interaction of these compounds through groove binding mode. The effect of ionic strength and iodide quenching again confirmed the involvement of groove binding and not intercalation. Molecular docking experiments were further confirmed that triazine analogs bind to the groove of DNA. These results provide valuable information regarding drug-DNA interactions, which may be useful for the greater clinical efficacy of rational drug design.

2.3.4. EXPERIMENTAL SECTION

Synthesis of (4,6-dichloro-[1,3,5]triazin-2-yl)-(4-fluoro-phenyl)-amine (1).

To a stirred solution of cyanuric chloride (10 g, 0.054 mol) in anhydrous THF (150 mL), 4-fluoroaniline (7.21 g, 0.065 mol) was added at 0-5 ^{0}C. To this mixture, 10% $NaHCO_3$ was added and stirred at the same temperature for 6 h. The resulted reaction mixture was then poured into crushed ice, filtered, dried and column chromatographed on silica gel in ethylacetate:hexane (1:4) to afford the desired product (4,6-dichloro-[1,3,5]triazin-2-yl)-(4-fluoro-phenyl)-amine **(1)** as white solid; (11.93 g, 85%); mp: 222-224 ^{o}C.[103]

Synthesis of 4-(1*H*-benzimidazol-2-yl)-phenylamine (2).

A mixture of 4-aminobenzoic acid (5 g, 5.78 mmol) and *o*-phenylenediamine (3.9 g, 3.68 mmol) were stirred in a syrupy polyphosphoric acid (12.5 gm) at 200 ^{0}C for 5 h. The reaction was monitored with TLC. The reaction mixture was cooled and poured into crushed ice. The precipitate was then stirred in cold water. Ammonium hydroxide solution was added until pH 7 was achieved. The resulting solid was filtered and washed several times with methanol and column chromatographed on silica gel in ethylacetate:hexane (4:1) to afford the desired

product 4-(1*H*-benzimidazol-2-yl)-phenylamine (**2**).

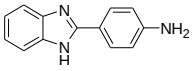

White solid; yield: 82%; mp: 207-209 ^{o}C[104]; ^{1}H NMR (400 MHz, DMSO-d_6): δ = 7.96 (d, 2H, *J* = 8.72 Hz, ArH), 7.55-7.51 (m, 2H, ArH), 7.16-7.14 (m, 2H, ArH), 6.75 (d, 2H, *J* = 8.24 Hz, ArH), 4.45 (bs, 2H, NH_2); ^{13}C NMR (100 MHz, $CDCl_3$ + DMSO-d_6): δ = 152.2, 148.4, 127.5, 120.9, 118.6, 113.8 (ArC); MS (ESI), m/z: 209.2 (M^{+}+1).

Synthesis of *N*-[4-(1*H*-benzimidazol-2-yl)-phenyl]-6-chloro-*N*'-(4-fluoro-phenyl)-[1,3,5]triazine-2,4-diamine (3).

To a stirred solution of (4,6-dichloro-[1,3,5]triazin-2-yl)-(4-fluoro-phenyl)-amine **(1)** (10 g, 0.026 mol) in anhydrous THF (150 mL), 4-(1*H*-benzimidazol-2-yl)-phenylamine (**2**) (8.06 g, 0.038 mol) was added at room temperature. To this mixture, 10% K_2CO_3 was added and stirred for 24 h. The resulted reaction mixture was then poured into crushed ice, filtered, dried and column chromatographed on silica gel using ethylacetate:hexane (4:1) to afford the desired product *N*-[4-(1*H*-benzimidazol-2-yl)-phenyl]-6-chloro-*N*'-(4-fluoro-phenyl)-[1,3,5]triazine-2,4-diamine **(3).**

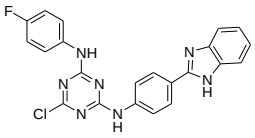

white solid; yield: 82%; mp: 249-251^{o}C; ^{1}H NMR (400 MHz, $CDCl_3$ + DMSO-d_6): δ = 10.12 (bs, 1H, NH), 9.97 (bs, 1H, NH), 8.19 (d, 1H, *J* = 8.72 Hz, ArH), 8.14 (d, 1H, *J* = 7.76 Hz, ArH), 8.00 (d, 1H, *J* = 3.20 Hz, ArH), 7.86 (d, 2H, *J* = 7.80 Hz, ArH), 7.71-7.67 (m, 2H, ArH), 7.60 (s, 1H, ArH), 7.22-7.19 (m, 2H, ArH), 7.10-7.06 (m, 2H, ArH); ^{13}C NMR (100 MHz, $CDCl_3$): δ = 169.4, 141.2, 134.9, 133.9, 133.6, 131.4, 129.1, 128.4, 126.3, 122.3, 119.8, 118.0, 110.3, 108.3 (ArC); MS (ESI), m/z: 431.8 (M^{+}+1); Anal. Calcd for $C_{22}H_{15}ClFN_7$: C, 61.19; H, 3.50; N, 22.70, Found: C, 61.18; H, 3.47; N, 22.71.

General procedure for the synthesis of compounds 4-15.

To a stirred solution of *N*-[4-(1*H*-benzimidazol-2-yl)-phenyl]-6-chloro-*N*'-(4-fluoro-phenyl)-[1,3,5]triazine-2,4-diamine **(3)** (0.200 g, 0.463 mmol) in 1,4-dioxane (20 mL), amines (0.556 mmol) and potassium carbonate (0.095g, 0.695 mmol) were added and heated at 110 ^{o}C for 6-8 hrs. Extracted the reaction mixture with chloroform, dried over Na_2SO_4, filtered and concentrated to get crude product which was then purified through column chromatography using chloroform:methanol (50:1) as eluents to give compounds **4-15**.

***N*-[4-(1*H*-Benzimidazol-2-yl)-phenyl]-*N*'-(4-fluoro-phenyl)-6-morpholin-4-yl-[1,3,5]triazine-2,4-diamine (4).**

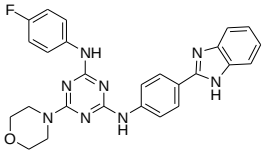

White solid; yield: 75%; mp: 248-250 ^{o}C; ^{1}H NMR (400 MHz, $CDCl_3$): δ = 8.00 (d, 2H, *J* = 4.72 Hz, ArH), 7.83 (s, 1H, NH), 7.72 (d, 2H, *J* = 8.24 Hz, ArH), 7.52-7.48 (m, 3H, ArH), 7.07 (t, 3H, *J* = 8.68 Hz, ArH), 6.96 (s, 1H, ArH), 6.80 (s, 1H, ArH), 3.82-3.76 (m, 4H, mor-CH_2), 3.70-3.69 (m, 4H, mor-CH_2); ^{13}C NMR (100 MHz, $CDCl_3$ + DMSO-d_6): δ = 163.7, 159.1, 148.6, 144.5, 134.8, 131.5, 128.2, 125.2, 122.1, 119.6, 114.9, 114.6, 114.4, 113.3 (ArC), 65.9 (O-CH_2), 43.4 (N-CH_2); MS (ESI), m/z: 482.5 (M^++1); Anal. Calcd for $C_{26}H_{23}FN_8O$: C, 64.72; H, 4.80; N, 23.22, Found: C, 64.65; H, 4.77; N, 23.18.

***N*-[4-(1*H*-Benzimidazol-2-yl)-phenyl]-*N*'-(4-fluoro-phenyl)-6-piperidin-1-yl-[1,3,5]triazine-2,4-diamine (5).**

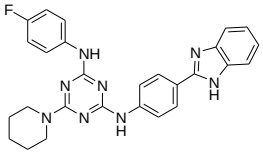

White solid; yield: 78%; mp: 252-254 ^{o}C; ^{1}H NMR (400 MHz, $CDCl_3$): δ = 8.00 (d, 2H, *J* = 8.28 Hz, ArH), 7.73 (bs, 1H, NH), 7.72 (d, 2H, *J* = 7.72 Hz, ArH), 7.53-7.49 (m, 3H, ArH), 7.05-7.00 (m, 4H, ArH), 6.85 (s, 1H, ArH), 3.79-3.78 (d, 4H, *J* = 5.04 Hz, N-CH_2), 1.55-1.51 (m, 6H, CH_2); ^{13}C NMR (100 MHz, $CDCl_3$ + DMSO-d_6): δ = 147.6, 131.1, 128.0, 125.1, 123.3, 120.8, 116.0, 114.7, 114.5, 113.1 (ArC), 43.5 (N-CH_2), 24.8 (CH_2), 21.6 (CH_2); MS (ESI), m/z: 480.5 (M^++1); Anal. Calcd for $C_{27}H_{25}FN_8$: C, 67.48; H, 5.24; N, 23.32, Found: C, 67.50; H, 5.20; N, 23.39.

***N*-[4-(1*H*-Benzimidazol-2-yl)-phenyl]-*N*'-(4-fluoro-phenyl)-6-pyrrolidin-1-yl-[1,3,5]triazine-2,4-diamine (6).**

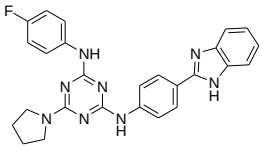

White solid; yield: 72%; mp: 242-244 ^{o}C; ^{1}H NMR (400 MHz, $CDCl_3$): δ = 7.96 (d, 1H, *J* = 8.68 Hz, ArH), 7.70 (d, 2H, *J* = 8.72 Hz, ArH), 7.59-7.52 (m, 4H, ArH), 7.25-7.22 (m, 1H, ArH), 7.10 (bs, 1H, NH), 7.02-6.97 (m, 4H, ArH), 3.59-3.57 (m, 4H, N-CH_2), 1.96-1.95 (m, 4H, CH_2); ^{13}C NMR (100 MHz, $CDCl_3$): δ = 163.9, 163.6, 152.4, 143.0, 135.9, 135.5, 134.2, 129.1, 128.0, 126.2, 121.3, 115.4, 115.2, 109.1 (ArC), 47.2 (N-CH_2), 25.3 (CH_2); MS (ESI), m/z: 466.5 (M^++1); Anal. Calcd for $C_{26}H_{23}FN_8$: C, 66.94; H, 4.97; N, 24.02, Found: C, 66.85; H, 4.93; N, 24.15.

***N*-[4-(1*H*-Benzimidazol-2-yl)-phenyl]-*N*'-(4-fluoro-phenyl)-6-(4-methyl-piperazin-1-yl)-[1,3,5]triazine-2,4-diamine (7).**

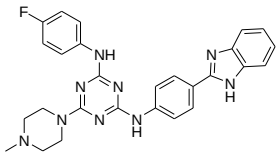

White solid; yield: 77%; mp: 268-270 ^{o}C; ^{1}H NMR (400 MHz, $CDCl_3$): δ = 7.97 (d, 2H, *J* = 8.72 Hz, ArH), 7.71 (bs, 1H, NH), 7.63 (d, 2H, *J* = 7.76 Hz, ArH), 7.48-7.45 (m, 2H, ArH), 7.25-7.23 (m, 3H, ArH), 7.13 (s, 1H, ArH), 7.02 (t, 2H, *J* = 8.24 Hz, ArH), 3.82-3.80 (m, 4H, N-CH_2), 2.43-2.41 (m, 4H, N-CH_2), 2.32 (s, 3H, CH_3); ^{13}C NMR (100 MHz, $CDCl_3$): δ = 164.9, 164.3, 151.8, 138.6, 138.5, 135.7, 135.0, 134.2, 129.1, 127.9, 126.2, 126.0, 122.1, 118.9, 116.4, 116.0, 115.5, 115.2 (ArC), 54.7 (N-CH_2), 43.1 (N-CH_2) 14.0 (N-CH_3); MS (ESI), m/z: 495.5 (M^++1); Anal. Calcd for $C_{27}H_{26}FN_9$: C, 65.44; H, 5.29; N, 25.44, Found: C, 65.35; H, 5.25; N, 25.50.

***N*-(2-Amino-ethyl)-*N*'-[4-(1*H*-benzimidazol-2-yl)-phenyl]-*N*''-(4-fluoro-phenyl)-[1,3,5]triazine-2,4,6-triamine (8).**

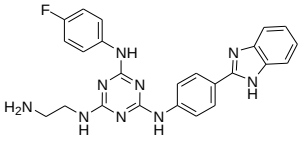

White solid; yield: 72%; mp: 273-275 ^{o}C; ^{1}H NMR (400 MHz, $CDCl_3$): δ = 8.02 (bs, 1H, NH), 7.50-7.48 (m, 3H, ArH), 7.31 (d, 3H, *J* = 7.32 Hz, ArH), 7.11 (d, 2H, *J* = 8.24 Hz, ArH), 7.06 (d, 2H, *J* = 7.32 Hz, ArH), 6.95 (d, 2H, *J* = 7.36 Hz, ArH), 3.50-3.48 (m, 2H, N-CH_2), 2.93 (t, 2H, *J* = 5.48 Hz, N-CH_2); ^{13}C NMR (100 MHz, $CDCl_3$): δ = 166.4, 152.5, 142.9, 135.9, 135.8, 129.1, 128.0, 126.3, 115.4, 115.2, 109.1 (ArC), 43.5 (N-CH_2), 41.4 (N-CH_2); MS (ESI), m/z: 455.4 (M^++1); Anal. Calcd for $C_{24}H_{22}FN_9$: C, 63.28; H, 4.87; N, 27.68, Found: C, 63.35; H, 4.80; N, 27.60.

2-[4-[4-(1*H*-Benzimidazol-2-yl)-phenylamino]-6-(4-fluoro-phenylamino)-[1,3,5]triazin-2-ylamino]-ethanol (9).

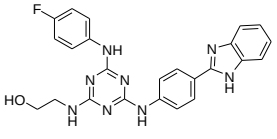

White solid; yield: 69%; mp: 261-263 ^{o}C; ^{1}H NMR (400 MHz, $CDCl_3$): δ = 8.02 (bs, 1H, NH), 7.44-7.42 (m, 2H, ArH), 7.29-7.26 (m, 5H, ArH), 7.03-6.98 (m, 3H, ArH), 6.90-6.84 (m, 2H, ArH), 3.81-3.79 (m, 2H, O-CH_2), 3.57-3.53 (m, 2H, N-CH_2), 1.84 (bs, 1H, OH); ^{13}C NMR (100 MHz, $CDCl_3$): δ = 166.5, 164.1, 152.5, 142.6, 135.7, 129.1, 128.0, 126.3, 122.0, 115.4, 115.1, 109.1 (ArC), 47.2 (O-CH_2), 43.7 (N-CH_2); MS (ESI), m/z: 456.4 (M^++1); Anal. Calcd for $C_{24}H_{21}FN_8O$: C, 63.15; H, 4.64; N, 24.55, Found: C, 63.05; H, 4.60; N, 24.65.

***N*-[4-(1*H*-Benzimidazol-2-yl)-phenyl]-*N*'-(4-fluoro-phenyl)-*N*''-(2-morpholin-4-yl-ethyl)-[1,3,5]triazine-2,4,6-triamine (10).**

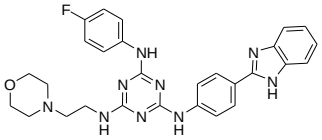

White solid; yield: 74%; mp: 278-280 ^{o}C; ^{1}H NMR (400 MHz, $CDCl_3$): δ = 7.94-7.90 (m, 2H, ArH), 7.61 (d, 1H, *J* = 9.16 Hz, ArH), 7.55-7.51 (m, 3H, ArH, NH), 7.50-7.43 (m, 3H, ArH), 7.23-7.21 (m, 1H, ArH), 7.02 (d, 1H, *J* = 6.40 Hz, ArH), 6.99 (d, 1H, *J* = 2.28 Hz, ArH), 6.97 (d, 1H, *J* = 1.84 Hz, ArH), 3.71-3.65 (m, 4H, O-CH_2), 3.53-3.46 (m, 2H, N-CH_2), 2.56-2.49 (m, 2H, N-CH_2), 2.46-2.42 (m, 4H, N-CH_2); ^{13}C NMR (100 MHz, $CDCl_3$): δ = 166.0, 164.6, 152.5, 142.9, 135.8, 129.1, 128.0, 126.3, 122.1, 121.7, 115.5, 115.2, 109.1 (ArC), 66.9 (O-CH_2), 53.4 (N-CH_2), 47.2 (N-CH_2), 37.1 (N-CH_2); MS (ESI), m/z: 525.5 (M^++1); Anal. Calcd for $C_{28}H_{28}FN_9O$: C, 63.99; H, 5.37; N, 23.98, Found: C, 64.10; H, 5.33; N, 24.05.

2-{4-[4-[4-(1*H*-Benzimidazol-2-yl)-phenylamino]-6-(4-fluoro-phenylamino)-[1,3,5]triazin-2-yl]-piperazin-1-yl}-ethanol (11).

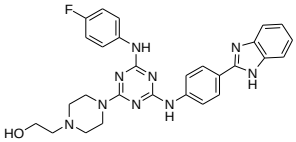

White solid; yield: 73%; mp: 274-276 ^{o}C; ^{1}H NMR (400 MHz, $CDCl_3$): δ = 7.97 (d, 1H, *J* = 8.28 Hz, ArH), 7.61 (d, 2H, *J* = 8.28 Hz, ArH), 7.50-7.44 (m, 3H, ArH), 7.26-7.24 (m, 3H, ArH), 7.03-6.97 (m, 3H, ArH), 6.81 (bs, 1H, NH), 3.92 (t, 2H, *J* = 0.44 Hz, O-CH_2), 3.83-3.79 (m, 4H, N-CH_2), 3.67 (t, 2H, *J* = 4.12 Hz, N-CH_2), 2.55-2.53 (m, 4H, N-CH_2), 1.83 (bs, 1H, OH); ^{13}C NMR (100 MHz, $CDCl_3$): δ = 152.4, 143.0, 135.9, 134.3, 131.6, 129.0, 128.0, 126.2, 116.2, 110.7, 109.1, 109.0 (ArC), 66.9 (O-CH_2), 47.1 (N-CH_2), 43.7 (N-CH_2), 43.6 (N-CH_2); MS (ESI), m/z: 525.5 (M^++1); Anal. Calcd for $C_{28}H_{28}FN_9O$: C, 63.99; H, 5.37; N, 23.98, Found: C, 64.11; H, 5.29; N, 23.91.

***N*-[4-(1*H*-Benzimidazol-2-yl)-phenyl]-*N*'-benzyl-*N*''-(4-fluoro-phenyl)-[1,3,5]triazine-2,4,6-triamine (12).**

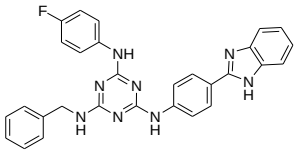

White solid; yield: 78%; mp: 247-249 ^{o}C; ^{1}H NMR (400 MHz, $CDCl_3$): δ = 9.09 (d, 1H, *J* = 6.88 Hz, ArH), 8.81 (d, 2H, *J* = 7.80 Hz, ArH), 8.52 (s, 1H, ArH), 8.45 (bs, 1H, NH), 8.06-8.04 (m, 3H, ArH), 7.99 (d, 1H, *J* = 7.76 Hz, ArH), 7.91 (d, 3H, *J* = 8.24 Hz, ArH), 7.86 (d, 1H, *J* = 7.76 Hz, ArH), 7.74 (d, 1H, *J* = 6.40 Hz, ArH), 7.35-7.28 (m, 3H, ArH), 7.16 (t, 1H, *J* = 7.36 Hz, ArH), 5.98 (s, 2H, N-CH_2); ^{13}C NMR (100 MHz, $CDCl_3$): δ = 168.7, 152.6, 142.1, 135.6, 133.4, 133.1, 132.7, 132.5, 129.1, 128.2, 128.1, 126.3, 116.9, 110.8, 109.5 (ArC), 47.3 (N-CH_2); MS (ESI), m/z:

502.5 (M^++1); Anal. Calcd for $C_{29}H_{23}FN_8$: C, 69.31; H, 4.61; N, 22.30, Found: C, 69.22; H, 4.58; N, 22.39.

_N_-Allyl-_N_'-[4-(1_H_-benzimidazol-2-yl)-phenyl]-_N_''-(4-fluoro-phenyl)-[1,3,5]triazine-2,4,6-triamine (13).

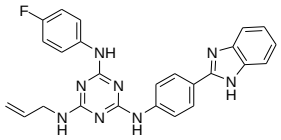

White solid; yield: 70%; mp: 288-290 ^oC; ^1H NMR (400 MHz, $CDCl_3$): δ = 9.04 (d, 1H, *J* = 7.36 Hz, ArH), 8.45 (m, 1H, ArH), 7.97 (d, 2H, *J* = 7.80 Hz, ArH), 7.83 (d, 1H, *J* = 7.76 Hz, ArH), 7.73 (d, 2H, *J* = 5.96 Hz, ArH), 7.43-7.39 (m, 2H, ArH), 7.29-7.25 (m, 2H, ArH, NH), 7.15-7.11 (m, 2H, ArH), 6.20-6.10 (m, 1H, allylic-CH), 5.40-5.29 (m, 4H, allylic-CH_2); ^{13}C NMR (100 MHz, $CDCl_3$): δ = 148.5, 144.5, 143.8, 142.7, 133.9, 130.8, 129.6, 129.5, 128.4, 122.7, 122.0, 120.6, 120.1, 110.0, 109.9, 108.8 (ArC), 54.6 (N-CH_2); MS (ESI), m/z: 452.4 (M^++1); Anal. Calcd for $C_{25}H_{21}FN_8$: C, 66.36; H, 4.68; N, 24.76, Found: C, 66.48; H, 4.64; N, 24.88.

_N_-[4-(1_H_-Benzimidazol-2-yl)-phenyl]-_N_'-cyclohexyl-_N_''-(4-fluoro-phenyl)-[1,3,5]triazine-2,4,6-triamine (14).

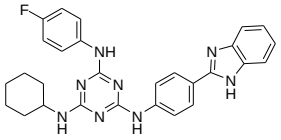

White solid; yield: 72%; mp: 281-283 ^oC; ^1H NMR (400 MHz, $CDCl_3$): δ = 7.98 (d, 2H, *J* = 7.60 Hz, ArH), 7.73-7.63 (m, 3H, ArH), 7.52-7.47 (m, 2H, ArH), 7.24-7.16 (m, 3H, ArH), 7.13 (bs, 1H, NH), 7.01 (t, 2H, *J* = 8.04 Hz, ArH), 5.05 (bs, 1H, NH), 3.81 (s, 1H, N-CH), 2.04-2.02 (m, 2H, CH_2), 1.76-1.63 (m, 4H, CH_2), 1.38-1.19 (m, 4H, CH_2); ^{13}C NMR (100 MHz, $CDCl_3$ + TFA): δ = 152.5, 147.6, 141.5, 130.8, 128.3, 126.7, 123.5, 123.4, 121.3, 116.7, 116.6, 115.8, 115.5, 113.6 (ArC), 51.7 (CH), 31.9 (CH_2), 25.0 (CH_2), 24.7 (CH_2); MS (ESI), m/z: 494.5 (M^++1); Anal. Calcd for $C_{28}H_{27}FN_8$: C, 68.00; H, 5.50; N, 22.66, Found: C, 68.19; H, 5.46; N, 22.75.

_N_-[4-(1_H_-Benzimidazol-2-yl)-phenyl]-_N_'-(4-fluoro-phenyl)-6-hydrazino-[1,3,5]triazine-2,4-diamine (15).

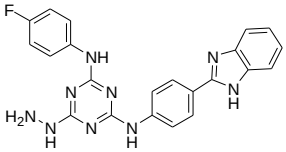

White solid; yield: 66%; mp: 289-291 ^oC; ^1H NMR (400 MHz, $CDCl_3$ + DMSO-d_6): δ = 8.30 (s, 1H, NH), 8.25-8.12 (m, 3H, ArH), 8.00-7.85 (m, 3H, ArH), 7.76-7.59 (m, 3H, ArH), 7.35-7.19 (m, 3H, ArH); ^{13}C NMR (100 MHz, $CDCl_3$ + DMSO-d_6): δ = 151.5, 138.4, 134.9, 132.9, 128.3, 127.2, 126.5, 125.9, 122.4, 117.6, 116.1, 114.7, 114.5 (ArC); MS (ESI), m/z: 427.4 (M^++1); Anal. Calcd for $C_{22}H_{18}FN_9$: C, 61.82; H, 4.24; N, 29.49, Found: C, 61.80; H, 4.21; N, 29.40.

General procedure for the synthesis of compounds 16-21.

To a stirred solution of *N*-[4-(1*H*-benzimidazol-2-yl)-phenyl]-6-chloro-*N*'-(4-fluoro-phenyl)-[1,3,5]triazine-2,4-diamine **(3)** (0.200 g, 0.463 mmol) in 1,4-dioxane (20 mL), arylboronic acids (0.556 mmol), $Pd(PPh_3)_4$ (10 mol%) and potassium carbonate (0.095g, 0.695 mmol) were added and refluxed for 8-10 hrs in an inert atmosphere. After the completion of reaction, extracted the reaction mixture with chloroform, dried over Na_2SO_4, filtered and concentrated to get crude product which was purified through column chromatography using chloroform:methanol (50:1) as eluents to give compounds **16-21**.

***N*-[4-(1*H*-Benzimidazol-2-yl)-phenyl]-*N*'-(4-fluoro-phenyl)-6-phenyl-[1,3,5]triazine-2,4-diamine (16).**

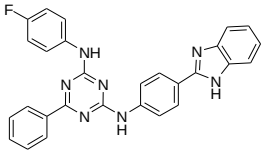

White solid; yield: 69%; mp: 246-248 ^oC; ^1H NMR (400 MHz, $CDCl_3$): δ = 7.92 (d, 2H, *J* = 6.84 Hz, ArH), 7.69-7.60 (m, 3H, ArH, NH), 7.52 (d, 3H, *J* = 5.96 Hz, ArH), 7.45 (d, 4H, *J* = 4.60 Hz, ArH), 7.21-7.20 (m, 3H, ArH), 6.96 (t, 3H, *J* = 8.24 Hz, ArH); ^{13}C NMR (100 MHz, $CDCl_3$): δ = 164.5, 160.3, 157.8, 152.2, 139.2, 135.8, 135.7, 134.4, 129.0, 127.9, 126.3, 122.9, 122.8, 119.0, 116.7, 115.5, 115.3 (ArC); MS (ESI), m/z: 473.5 (M^++1); Anal. Calcd for $C_{28}H_{20}FN_7$: C, 71.02; H, 4.26; N, 20.71, Found: C, 71.23; H, 4.22; N, 20.79.

***N*-[4-(1*H*-Benzimidazol-2-yl)-phenyl]-6-(4-chloro-phenyl)-*N*'-(4-fluoro-phenyl)-[1,3,5]triazine-2,4-diamine (17).**

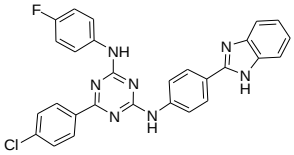

White solid; yield: 68%; mp: 262-264 ^oC; ^1H NMR (400 MHz, $CDCl_3$ + DMSO-d_6): δ = 8.69 (d, 2H, *J* = 7.76 Hz, ArH), 8.10-8.05 (m, 4H, ArH), 7.84-7.77 (m, 2H, ArH), 7.69-7.63 (m, 4H, ArH), 7.56 (d, 1H, *J* = 7.36 Hz, ArH), 7.50 (d, 1H, *J* = 6.88 Hz, ArH), 7.28 (t, 2H, *J* = 6.88 Hz, ArH); ^{13}C NMR (100 MHz, $CDCl_3$): δ = 170.0, 165.1, 164.4, 152.0, 138.8, 137.7, 135.8, 135.4, 134.0, 132.2, 132.1, 132.0, 129.7, 129.2, 128.6, 128.5, 128.0, 125.8, 119.2, 115.7, 101.5 (ArC); MS(ESI), m/z: 507.9 (M^++1); Anal. Calcd for $C_{28}H_{19}ClFN_7$: C, 66.21; H, 3.77; N, 19.30, Found: C, 66.11; H, 3.74; N, 19.38.

***N*-[4-(1*H*-Benzimidazol-2-yl)-phenyl]-*N*'-(4-fluoro-phenyl)-6-thiophen-2-yl-[1,3,5]triazine-2,4-diamine (18).**

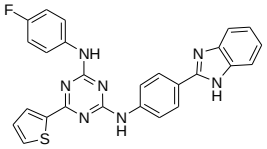

White solid; yield: 67%; mp: 274-276 ^{o}C; ^{1}H NMR (400 MHz, $CDCl_3$): δ = 7.98 (d, 3H, *J* = 8.72 Hz, ArH), 7.73-7.62 (m, 4H, ArH), 7.54-7.50 (m, 3H, ArH), 7.35 (d, 2H, *J* = 3.64 Hz, ArH), 7.06 (t, 3H, *J* = 9.16 Hz, ArH); ^{13}C NMR (100 MHz, $CDCl_3$): δ = 170.9, 165.1, 164.5, 152.0, 138.7, 136.8, 135.8, 134.1, 131.6, 129.2, 128.3, 128.0, 125.9, 119.1, 115.6, 101.4 (ArC); MS (ESI), m/z: 479.5 (M^++1); Anal. Calcd for $C_{26}H_{18}FN_7S$: C, 65.12; H, 3.78; N, 20.45; S, 6.69, Found: C, 65.29; H, 3.75; N, 20.42; S, 6.75.

***N*-[4-(1*H*-Benzimidazol-2-yl)-phenyl]-*N*'-(4-fluoro-phenyl)-6-furan-2-yl-[1,3,5]triazine-2,4-diamine (19).**

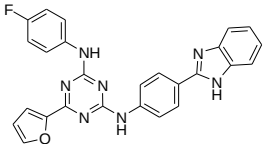

White solid; yield: 71%; mp: 248-250 ^{o}C; ^{1}H NMR (400 MHz, $CDCl_3$): δ = 7.95 (d, 2H, *J* = 8.24 Hz, ArH), 7.58-7.52 (m, 4H, ArH), 7.48-7.45 (m, 3H, ArH), 7.24-7.22 (m, 4H, ArH), 7.02-6.98 (m, 2H, ArH); ^{13}C NMR (100 MHz, $CDCl_3$): δ = 170.6, 164.7, 152.2, 139.5, 135.9, 134.3, 132.5, 130.6, 129.1, 126.2, 122.8, 119.2, 115.7, 115.5, 102.2 (ArC); MS (ESI), m/z: 463.4 (M^++1); Anal. Calcd for $C_{26}H_{18}FN_7O$: C, 67.38; H, 3.91; N, 21.16, Found: C, 67.46; H, 3.88; N, 21.29.

***N*-[4-(1*H*-Benzimidazol-2-yl)-phenyl]-*N*'-(4-fluoro-phenyl)-6-(2-methoxy-phenyl)-[1,3,5]triazine-2,4-diamine (20).**

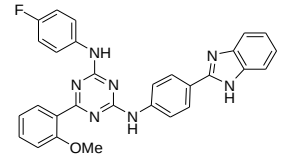

White solid; yield: 65%; mp: 288-290 ^{o}C; ^{1}H NMR (400 MHz, $CDCl_3$): δ 7.98 (d, 3H, *J* = 8.72 Hz, ArH), 7.81 (s, 1H, ArH), 7.67 (d, 3H, *J* = 8.00 Hz, ArH), 7.52-7.50 (m, 5H, ArH, NH), 7.27 (d, 2H, *J* = 2.76 Hz, ArH), 7.06 (t, 3H, *J* = 8.24 Hz, ArH), 3.96 (s, 3H, OCH_3); ^{13}C NMR (100 MHz, $CDCl_3$): δ = 152.7, 144.8, 139.2, 135.5, 132.6, 132.0, 129.2, 129.0, 127.9, 127.4, 126.7, 126.2, 122.5, 121.5, 117.0, 113.9, 111.9, 109.4 (ArC), 55.3 (OCH_3); MS (ESI), m/z: 503.5 (M^++1); Anal. Calcd for $C_{29}H_{22}FN_7O$: C, 69.17; H, 4.40; N, 19.47, Found: C, 69.03; H, 4.33; N, 19.41.

***N*-[4-(1*H*-Benzimidazol-2-yl)-phenyl]-*N*'-(4-fluoro-phenyl)-6-(4-methoxy-phenyl)-[1,3,5]triazine-2,4-diamine (21).**

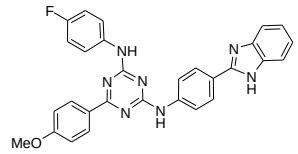

White solid; yield: 70%; mp: 266-268 ^{o}C; ^{1}H NMR (400 MHz, $CDCl_3$): δ = 7.97 (d, 3H, *J* = 8.72 Hz, ArH), 7.66 (d, 3H, *J* = 8.24 Hz, ArH), 7.52-7.50 (m, 3H, ArH), 7.32 (bs, 1H, NH), 7.28-7.27 (m, 3H,

ArH), 7.25 (s,1H, ArH), 7.05 (t, 3H, *J* = 8.72 Hz, ArH), 3.96 (s, 3H, OCH_3); ^{13}C NMR (100 MHz, $CDCl_3$): δ = 163.2, 159.7, 157.0, 147.2, 136.4, 132.2, 130.2, 128.5, 127.6, 126.8, 122.4, 116.6, 114.0, 113.6, (ArC), 55.4 (OCH_3); MS (ESI), m/z: 503.5 (M^++1); Anal. Calcd for $C_{29}H_{22}FN_7O$: C, 69.17; H, 4.40; N, 19.47, Found: C, 69.05; H, 4.37; N, 19.40.

2.4. TRIAZINE-BENZIMIDAZOLE WITH PHENYL LINKER (MORPHOLINE)

Bovine serum albumin is used as a promising drug delivery system owing to abundance in plasma and executing as transporter carriers of endogenous and exogenous compounds[105] including fatty acids, amino acids, drugs, and pharmaceuticals for prognosis of pharmacokinetic and pharmacodynamics behavior of several drugs. BSA has two tryptophan residues (Trp-134 and Trp-212) possess intrinsic fluorescence.[105,107] It provides a convenient mode for detecting structural changes upon ligand binding that significantly influences drug efficacy, the rate of drug delivery, and its elimination. In addition, owing to its biochemical and pharmacological properties, BSA has been used to target diseased and malignant cells as a versatile drug carrier; resulting in higher efficacy of treatment and reduced side effects.[108-110]

2.4.1. CHEMISTRY

The triazine-benzimidazole analogues were synthesized by their substitution with primary and secondary amines as well as aryl boronic acids (**5-21**), reported in Scheme 7. Cyanuric chloride was reacted with morpholine in the presence of sodium bicarbonate in THF at 0-5 ^oC for 6 h to obtain 4,6-dichloro-2-morpholin-4-yl-[1,3,5]triazine (**2**) in 89% yield. Condensation of 4-aminobenzoic acid with *o*-phenylenediamine in the presence of polyphosphoric acid at 200 ^oC for 5 h afforded 4-(1*H*-benzimidazol-2-yl)-phenylamine as white solid. Compound **2** was underwent nucleophilic substitution reaction with 4-(1*H*-benzimidazol-2-yl)-phenylamine (**3**) in the presence of potassium carbonate and THF at room temperature for 24 h provided [4-(3*H*-benzimidazol-5-yl)-phenyl]-(6-chloro-2-morpholin-4-yl-[1,3,5]triazin-2-yl)-amine (**4**) in 84 % yield. Further, treatment of compound **4** with different primary and secondary amines in the presence of potassium carbonate and 1,4-dioxane at 110 ^oC for 8 h gave compounds **5-15** in 66-75% yields. Compound **4** was also treated with five and six membered aryl boronic acids through Suzuki-Miyaura cross coupling reaction, in the presence of 10 mol % of $Pd(PPh_3)_4$ and 1.5 equivalents of K_2CO_3 in 1,4-dioxane to afford compounds **16-21** in 64-75% yields.

Scheme 7[a]. Synthesis of triazine-benzimidazole analogues.

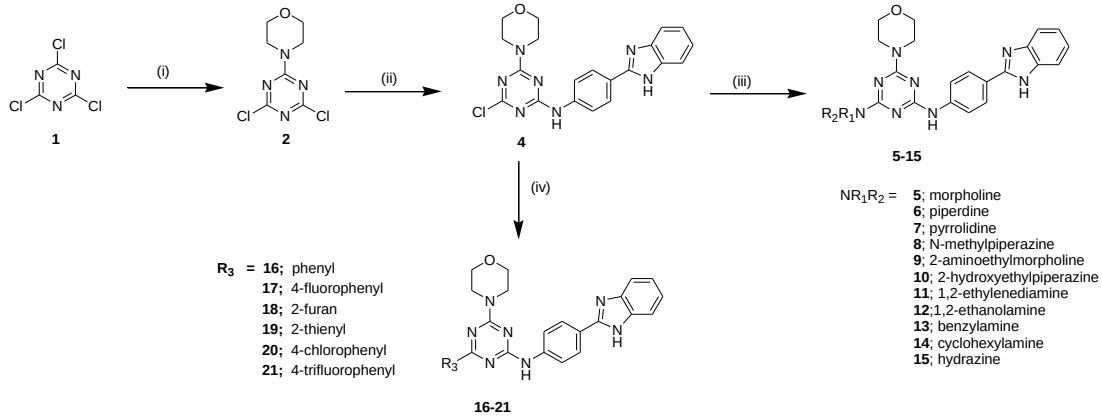

[a]Reagents and conditions: (i) morpholine, $NaHCO_3$, THF, 0−5 °C; (ii) **3**, K_2CO_3, THF, rt; (iii) NHR_1R_2, K_2CO_3, 1,4-dioxane, reflux; (iv) $R_3B(OH)_2$, $Pd(PPh_3)_4$, K_2CO_3, 1,4-dioxane, reflux.

2.4.2. BIOLOGY

2.4.2.1. *In vitro* Anticancer Evaluation

These compounds were submitted to the National Cancer Institute (NCI) disease oriented human cell lines for *in vitro* evaluation as antitumor activities. Four compounds (**6, 16, 17** and **20**) were selected for evaluation against 60 human cancer cell lines at one dose concentration of 10^{-5} M. *In vitro* antitumor screening data revealed that compounds with piperidine substitution and aryl groups such as phenyl, 4-fluorophenyl and 4-chlorophenyl showed significant activity for most of the cancer cell lines. The obtained results of the tested triazine-benzimidazole analogous showed distinctive potential pattern of selectivity. Compounds **6**, **16**, **17** and **20** were found to be broad spectrum against all nine subpanels of cancer cell lines at primary single dose (10 µM) with mean growth percent of 0.72, -56.41, -7.32 and -83.19 respectively. Close examination of the data presented in Table 12 indicated that compounds **16** and **20** are the most potent while **6** and **17** possessed moderate antitumor activity.

Table 12. Percent growth promotion of *in vitro* subpanel tumor cell lines at 10 µM concentration of compounds **6, 16, 17** and **20.**

Subpanel tumor cell lines	**6**	**16**	**17**	**20**	Subpanel tumor cell lines	**6**	**16**	**17**	**20**
Leukemia					SK-MEL-5	-90.75	-95.41	-90.65	-97.59
CCRF-CEM	**8.74**	-15.74	-1.84	-91.49	UACC-257	-19.30	-56.40	-27.63	-82.52
HL-60(TB)	-22.74	-32.69	-46.01	-81.44	**Ovarian cancer**				

K-562	-6.74	-30.14	-22.02	-100.0	IGORV1	51.34	-38.08	33.68	-71.16
MOLT-4	13.72	-37.78	1.78	-91.61	OVCAR-3	10.91	-73.44	5.15	-95.58
RPMI-8226	2.47	-22.64	-13.83	-73.43	OVCAR-4	61.19	-47.23	59.84	-73.91
SR	9.79	8.94	6.01	-83.32	OVCAR-5	73.94	0.63	66.34	-74.72
Non-small cell lung cancer					OVCAR-8	45.70	-50.44	39.24	-73.82
A549/ATCC	13.89	-68.45	11.23	-75.19	NCI/ADR-RES	45.64	-60.81	34.23	-87.53
EKVX	27.70	-66.92	7.91	-91.35					
HOP-62	-45.21	-64.49	-27.31	-73.89	SK-OV-3	22.49	-30.32	19.61	-89.89
HOP-92	43.35	-66.25	6.57	Nt	**Renal cancer**				
NCI-H226	32.70	-19.29	17.11	-64.52	786-0	-57.34	-88.93	-60.02	-94.51
NCI-H23	19.72	-59.05	11.34	-83.39	A498	-28.59	-83.40	-32.12	-81.51
NCI-H322M	35.03	-0.47	27.03	-92.85	ACHN	22.92	-58.90	9.00	-90.60
NCI-H460	0.81	-67.25	0.13	-80.31	CAKI-1	-46.89	-89.38	-56.60	-93.57
NCI-H522	9.25	-68.19	11.94	-73.93	RXF 393	-56.14	-75.14	-67.46	-91.12
Colon cancer					SN12C	52.41	-62.79	40.78	-79.48
COLO 205	-61.28	-68.80	-43.73	-68.39	TK-10	58.80	-58.06	43.87	-94.44
HCC-2998	-1.07	-80.71	-19.85	-89.86	UO-31	-37.82	-60.57	-43.52	-87.59
SF-295	-51.43	-76.36	-63.50	-94.37	**Prostate cancer**				
SF-539	7.95	-76.83	0.31	-92.73	PC-3	12.41	-35.46	2.31	-93.48
SNB-19	10.38	-18.63	17.47	-81.19	DU-145	38.96	-27.79	38.47	-93.96
SNB-75	-0.68	-89.65	-19.21	-92.64	**Breast cancer**				
U251	8.02	-67.51	6.38	-93.05	MCF7	3.49	-76.15	-44.29	-73.81
Melanoma					MDA-MB-231/ATCC	23.15	-63.34	5.74	-76.74
LOX IMVI	-77.07	-88.99	-75.60	-92.98	HS 578T	-12.59	-39.90	-11.86	-40.25
MALME-3M	-50.20	-77.26	-65.73	-73.43	BT-549	23.12	33.65	5.16	-73.63
M14	-24.53	-80.66	-7.64	-82.62	T-47D	23.39	-62.31	16.08	-64.77
MDA-MB-435	-27.26	-81.06	-38.01	-86.10	MDA-MB-468	-3.66	-62.73	-1.23	-83.99
SK-MEL-2	-20.55	-52.66	-19.20	-71.35					
SK-MEL-28	-30.22	-82.85	-34.04	-84.68					

nt, not tested; 30-40% growth inhibition; 40-50% growth inhibition; 50-70% growth inhibition; 90-100% growth inhibition; highly potent.

These four compounds were further screened for five dose concentration level (0.01-100 µM) as these have shown prominent cell growth inhibition at 10 µM concentration against variety of cell lines. Further evaluation of these compounds was very effective against two cancer cell line: HL-60 (TB) and SR, with GI_{50} values in the nanomolar range. Leukemia cancer cell line HL-60 (TB) appeared to be the most sensitive to the growth inhibition effects to compound **16**, exhibited GI_{50} value of 31 nM with TGI value of 601 nM against this cell type. Similarly, compounds **6**, **16**, **17** and **20** also showed effective growth inhibition against Leukemia cancer cell line SR with GI_{50} values of 731 nM, 125 nM, 539 nM and 31 nM respectively. All four compounds were active against renal cancer cell line RXF393 with GI_{50} values of 808 nM, 501 nM, 459 nM and 222 nM respectively. Compound **20** also showed specificity towards all subpanels with MG MID GI_{50}

value of 720 nM. Thus, compound **20** is almost four fold, more active than compounds **6**, **16** and **17** with MG MID GI_{50} values of 2680 nM, 1380 nM and 2370 nM respectively (Table 13).

Table 13. Compounds **6, 16, 17** and **20** with GI_{50} (μM), TGI (μM) and LC_{50} (μM) of *in vitro* subpanel tumor cell lines at five different concentrations.

Compds.	Activity	I	II	III	IV	V	VI	VII	VIII	IX	MIG-MID[a]
6	GI_{50}	2.37	2.85	2.43	2.54	1.95	3.46	2.46	3.67	2.36	2.68
	TGI	6.50	9.66	5.52	23.2	4.18	22.6	11.8	9.13	6.72	11.0
	LC_{50}	[b]	9.54	30.2	46.6	11.8	26.9	8.29	[b]	92.7	32.3
16	GI_{50}	0.57	1.74	0.99	1.41	1.56	1.85	1.20	1.51	1.63	1.38
	TGI	2.17	3.67	2.55	3.04	3.18	3.88	2.72	3.07	4.08	3.15
	LC_{50}	16.3	14.2	6.53	5.98	6.52	6.84	6.27	6.25	8.74	8.63
17	GI_{50}	2.02	2.68	2.15	2.23	1.91	2.74	2.03	3.46	2.09	2.37
	TGI	6.11	6.65	4.73	11.8	4.04	11.5	7.36	6.66	5.55	7.16
	LC_{50}	[b]	7.76	7.90	8.47	7.43	[b]	7.83	[b]	[b]	7.88
20	GI_{50}	0.19	1.15	0.26	0.77	1.07	0.92	1.11	0.41	0.62	0.72
	TGI	0.58	2.59	0.69	1.92	2.48	2.30	2.25	1.49	1.86	1.80
	LC_{50}	[b]	5.58	2.75	[b]	5.79	5.20	5.60	4.33	[b]	4.88

I, leukemia; II, non-small cell lung cancer; III, colon cancer; IV, CNS cancer; V, melanoma; VI, ovarian cancer; VII, renal cancer; VIII, prostate cancer; IX, breast cancer. [a] Full panel mean-graph midpoint (μM). [b] Compounds showed values >100 μM.

2.4.2.2. Structure Activity Relationship

Structure-activity correlation, based upon the cancer cell lines revealed that the nature of the substituents at C6-position of triazine significantly affected the biological activity. Regarding 60 human tumor cell line studies; substitution of chloro group (**4)** with secondary amines and aryl groups improved the inhibitory activity of compounds. Secondary amine substitutions at this position showed higher activity, as illustrated by piperdine (**6**) in comparison to other secondary and primary amines. Similarly, in case of Pd catalyzed arylation reaction of **4** with aryl boronic acids (compounds **16, 17** and **20**), the activities showed higher due to hydrophobic aryl groups. These studies indicated that the substitution of the triazine-benzimidazole heterocycles with various aryl groups led to highly potency as compared to primary and secondary amines towards 60 human cancer cell line activities.

2.4.2.3. Bovine serum albumin interactions

To examine the structural changes of BSA with these synthesized compounds **5-21**, absorbance and fluorescence spectral measurements were carried out. The binding properties of BSA (10 μM) towards compounds **5-21** were investigated by UV-Visible spectroscopy in phosphate buffer (10 mM, pH 7.4). The electronic spectrum of BSA showed an intense band at 279 nm that

arises due to presence of phenyl rings in Trp (tryptophan), Tyr (tyrosine), and Phe (phenylalanine) residues. However, subsequent addition of compounds **5-14, 16, 17** and **20** to BSA solution resulted in gradual increase in the intensity of peak at 279 nm to some extent, but with the appearance of a new band at 324 nm indicating the interaction of compounds with the protein by extending the peptide strands of BSA and leading to an increase of hydrophobicity in the vicinity of this residue (Figure 35).

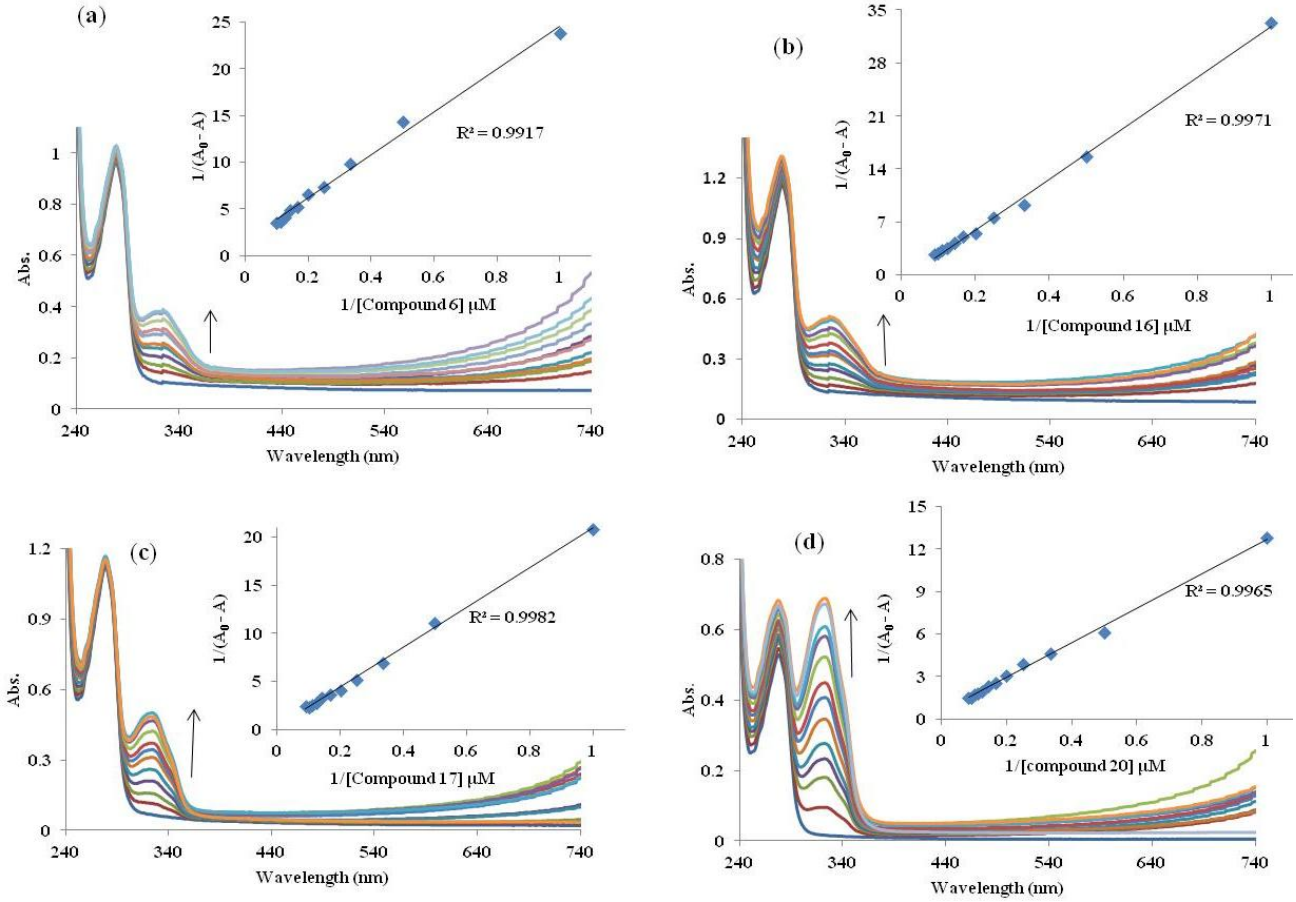

Figure 35. Absorption spectral change of BSA (10 µM) in phosphate buffer upon addition of compounds **6** (a), **16** (b), **17** (c) and **20** (d) at 0-20 µM; Inset shows Benesi–Hildebrand plot of $1/[A_0\text{-}A]$ vs. 1/[compounds] for binding of BSA with compounds through absorption spectral titrations.

As shown in Table 14, addition of compounds **5-14, 16, 17** and **20** to BSA showed hyperchromicity within range of 65.2% - 97.6% (Figures 37-45), while compounds **15, 18, 19** and **21** did not show any significant change. However, the maximum absorption wavelength of BSA remains unchanged, implying that the interaction between compounds and BSA is a

noncovalent in nature that occur through the $\pi-\pi$ stacking between aromatic rings of compounds and phenyl rings of Trp, Tyr and Phe residues located in the binding cavity of BSA.

The interaction studies were further investigated through emission spectroscopy. On exciting the BSA at 280 nm, the emission spectra showed an intense band at 350 nm. The emission is sensitive to the changes in local environment of the tryptophan and so can be attenuated by binding of a small molecule at or near this residue. In all cases the fluorescence intensities of the protein are decreased regularly with increasing concentration of compounds **5-14, 16, 17** and **20**, indicating the binding of compounds to the protein. On gradual addition of compounds **5-14, 16, 17** and **20**, a decrease in the fluorescence intensity of BSA at 350 nm accompanies the appearance of one peak within range of 370 nm and 373 nm, which can be attributed to the complexation between compounds and protein (Figures 36-45). Compounds **15, 18, 19** and **21** did not show any significant change in the conformation of BSA. The change in absorption and fluorescence intensities clearly indicated the interacting properties of compounds **5-14, 16, 17** and **20** with BSA.

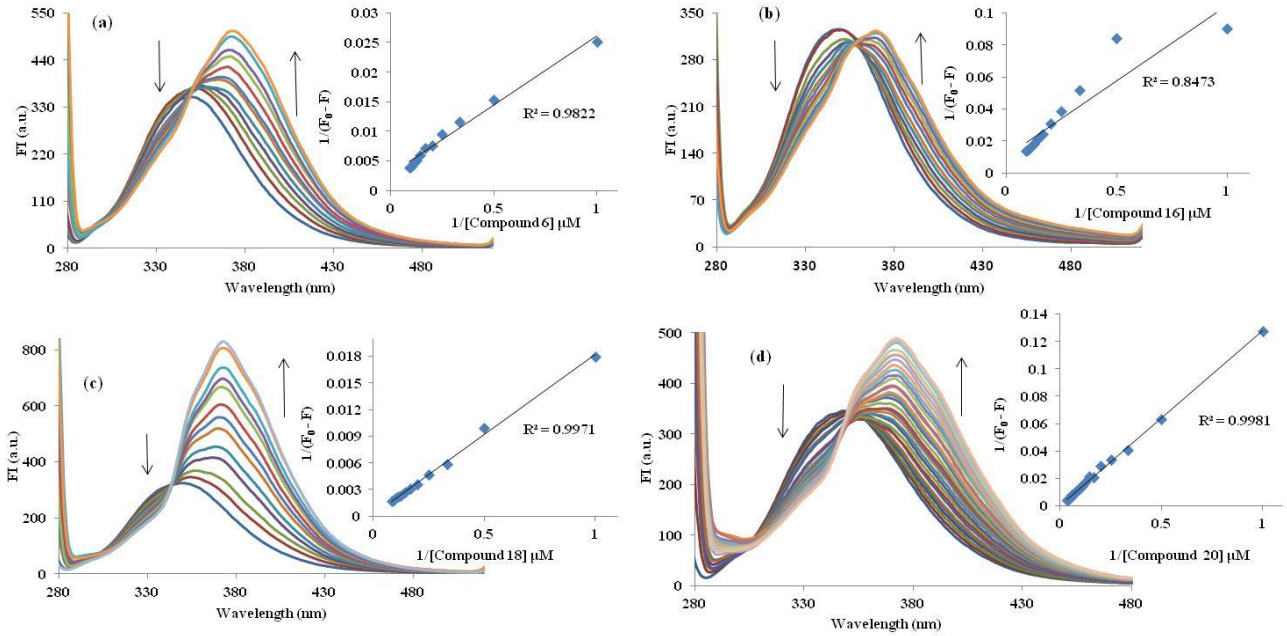

Figure 36. Fluorescence spectral change of BSA (10 µM) in phosphate buffer upon addition of **6** (a), **16** (b), **17** (c) and **20** (d) at 0-20 µM. Inset shows Benesi–Hildebrand plot of $1/[F_0\text{-}F]$ vs. 1/[compounds] for binding of BSA with compounds through emission spectral titrations.

When a small molecule bind independently to a set of equivalent sites on a macromolecule, the photophysical properties, binding constants (K) using Benesi–Hildebrand equation[85] and the numbers of binding sites (n) using double-logarithmic equation[111,112] can be determined for the

quantitative investigation of the binding strength between triazine-benzimidazole analogues and BSA. The binding constant of complexes confirmed the significant role of configuration of triazine-benzimidazole analogues around BSA as shown in Table 14. According to the absorbance and fluorescence titration results (Inset Figures 35 and 36), the linear fitting plots of $1/(F_0\text{-}F)$ vs. 1/[compounds] can be observed for the interaction between BSA and compounds **5-14, 16, 17** and **20** (Figures 37-45). The value of n is helpful to know the number of binding sites and to locate the binding site in BSA for the compounds **5-14, 16, 17** and **20**, which was nearly 1, indicating that there was one independent class of binding site on BSA for compounds and the molar ratio of protein to compounds **5-14, 16, 17** and **20** is 1:1 in the binding reactions.

Table 14. Photophysical properties and binding constants of BSA with compounds **5-14, 16, 17** and **20.**

Sr. No.	Hyperchromicity (%) in absorption spectra	Enhancement (%) in emission spectra	Isoemissive Point (nm)	Red Shift in emission intensity (nm)	K of absorption spectra (M^{-1})	K of emission spectra (M^{-1})	n
5	72.93	63.43	350	24	7.0×10^4	6.9×10^4	1.24
6	72.31	49.74	350	25	9.7×10^4	5.7×10^4	0.91
7	65.29	68.99	341	22	1.0×10^5	5.4×10^4	1.67
8	75.98	77.53	339	22	8.5×10^4	2.6×10^4	1.19
9	85.95	57.22	345	23	8.4×10^4	5.7×10^4	0.90
10	68.72	73.21	343	25	1.2×10^5	5.4×10^4	1.61
11	70.53	69.01	347	22	6.3×10^4	1.3×10^5	0.94
12	90.60	71.82	340	23	9.5×10^4	8.0×10^4	1.01
13	88.44	42.06	352	24	1.2×10^4	1.8×10^5	1.14
14	85.87	23.12	349	17	1.0×10^5	1.6×10^5	1.58
16	72.27	22.78	357	20	1.2×10^5	3.2×10^4	1.47
17	86.80	71.83	341	23	1.0×10^5	7.9×10^4	0.99
20	97.67	49.10	349	22	1.0×10^5	4.2×10^7	0.87

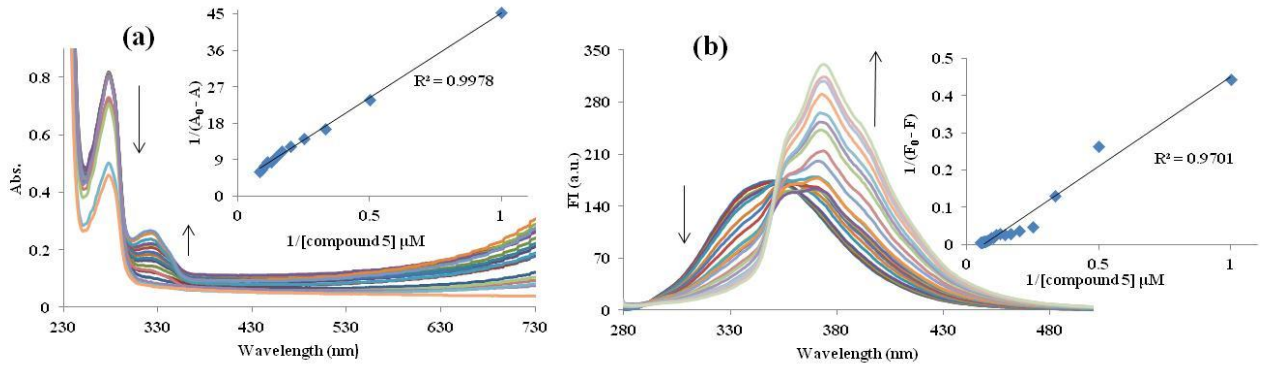

Figure 37. (a) Absorption and (b) Fluorescence spectra change of BSA (10 µM) in aqueous solution upon addition of compound **5.**

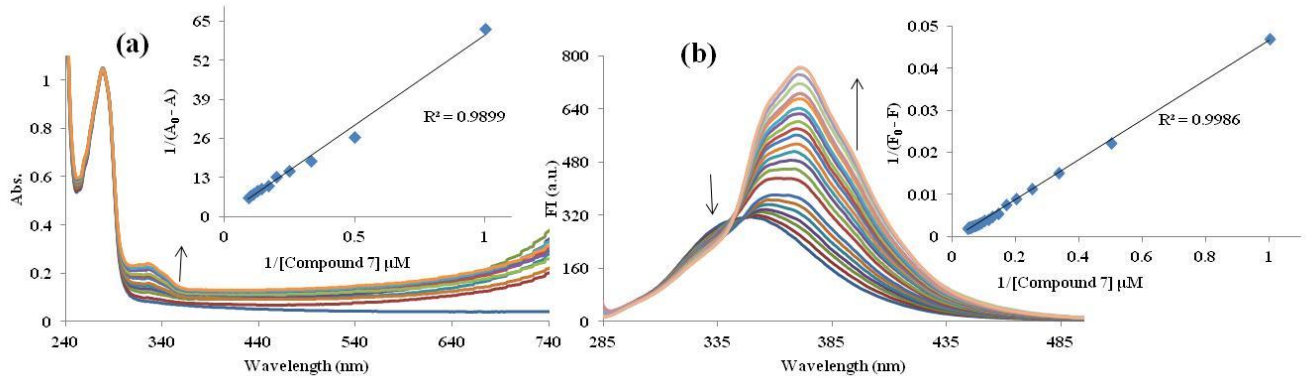

Figure 38. (a) Absorption and (b) Fluorescence spectra change of BSA (10 μM) in aqueous solution upon addition of compound **7.**

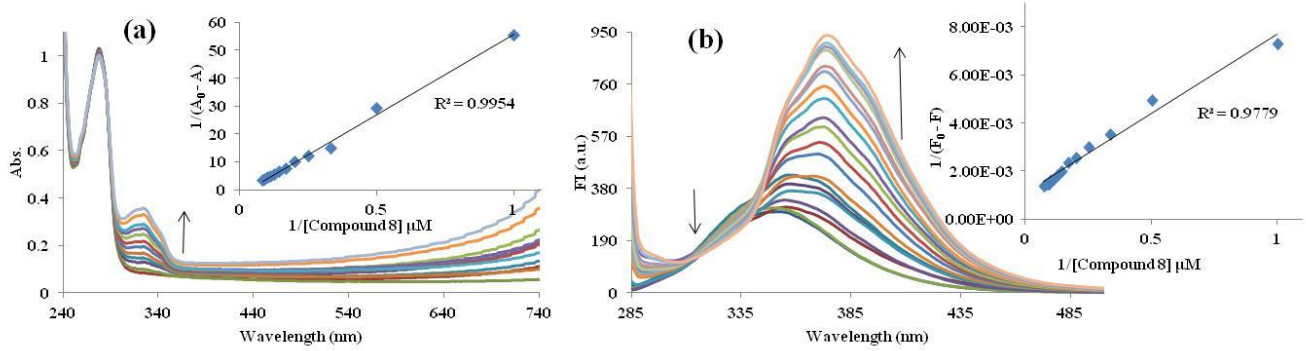

Figure 39. (a) Absorption and (b) Fluorescence spectra change of BSA (10 μM) in aqueous solution upon addition of compound **8.**

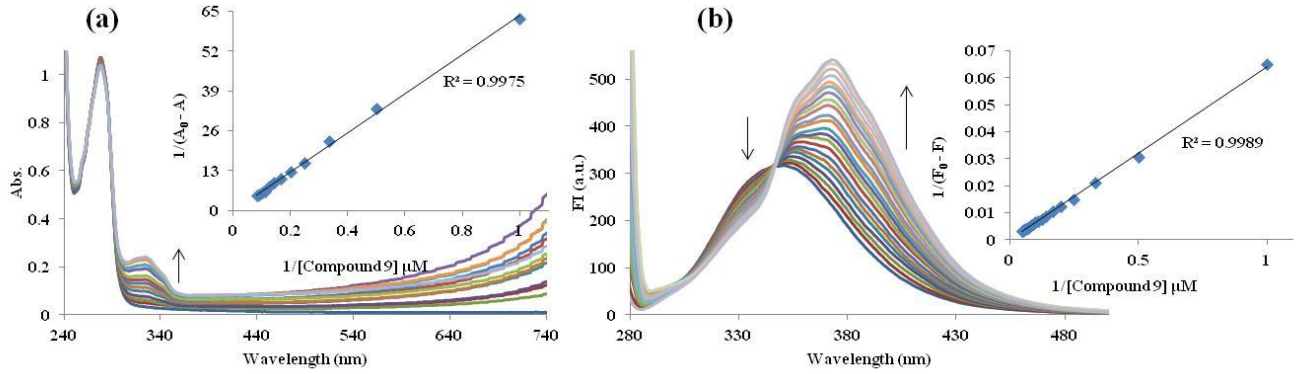

Figure 40. (a) Absorption and (b) Fluorescence spectra change of BSA (10 μM) in aqueous solution upon addition of compound **9.**

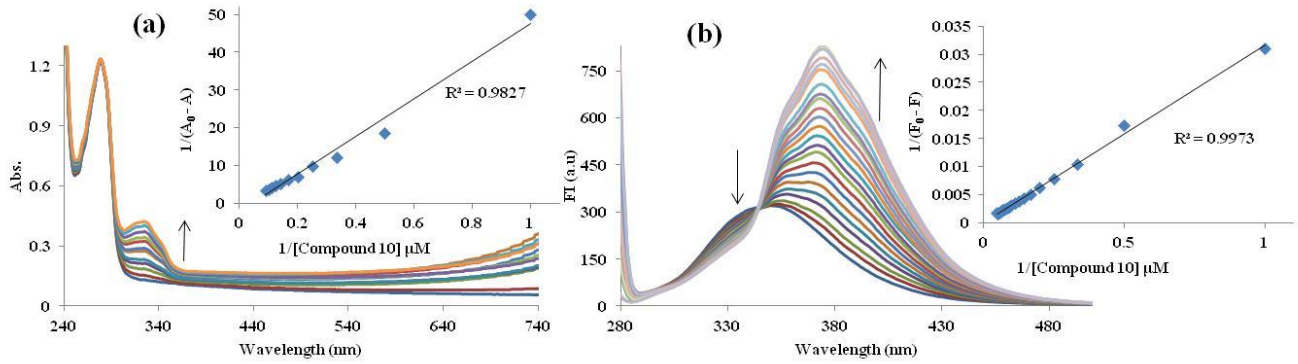

Figure 41. (a) Absorption and (b) Fluorescence spectra change of BSA (10 µM) in aqueous solution upon addition of compound **10.**

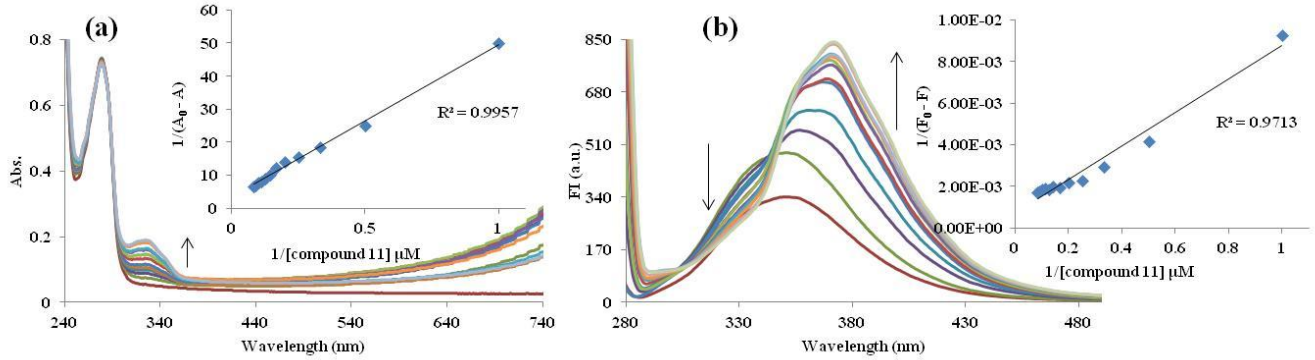

Figure 42. (a) Absorption and (b) Fluorescence spectra change of BSA (10 µM) in aqueous solution upon addition of compound **11.**

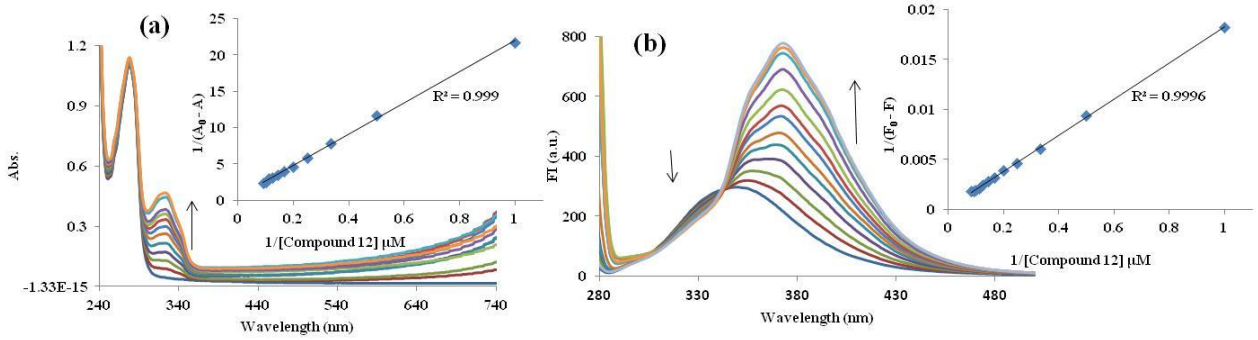

Figure 43. (a) Absorption and (b) Fluorescence spectra change of BSA (10 µM) in aqueous solution upon addition of compound **12.**

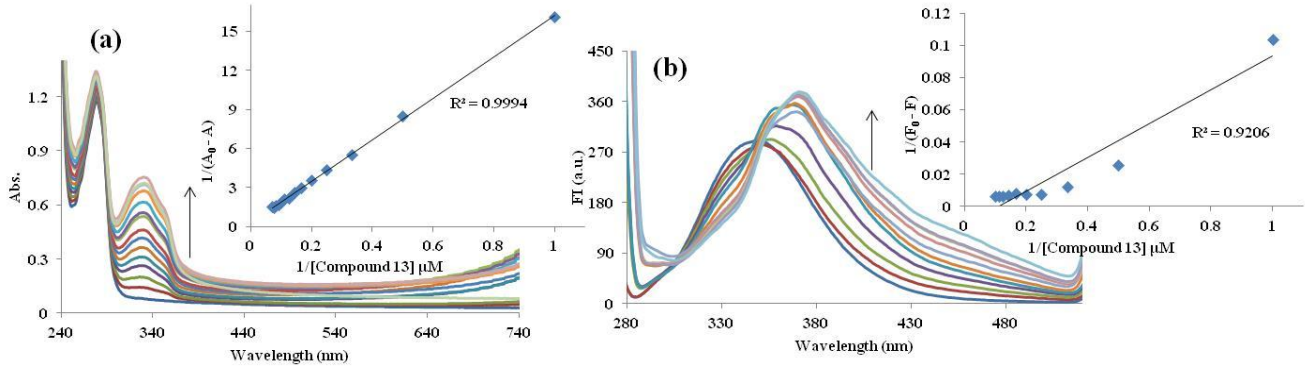

Figure 44. (a) Absorption and (b) Fluorescence spectra change of BSA (10 µM) in aqueous solution upon addition of compound **13.**

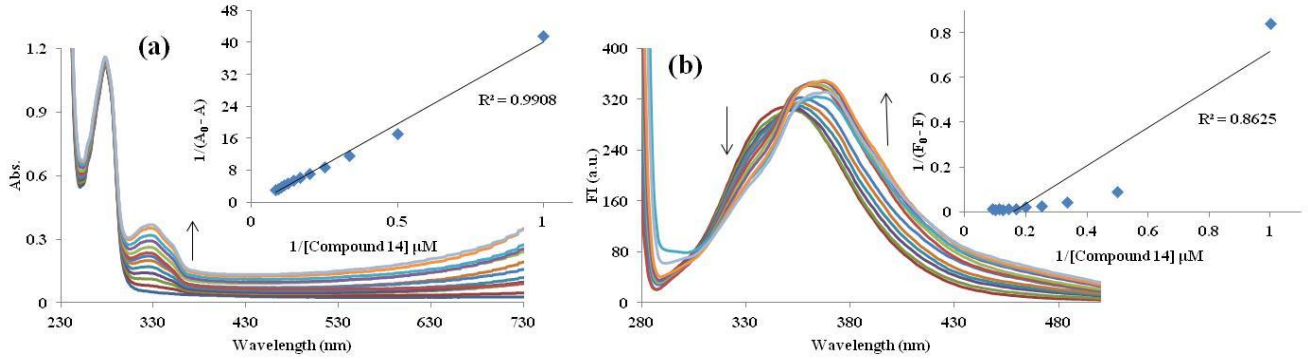

Figure 45. (a) Absorption and (b) Fluorescence spectra change of BSA (10 µM) in aqueous solution upon addition of compound **14.**

2.4.2.4. Fluorescence Resonance Energy Transfer (FRET)

The spectral studies suggested that the triazine-benzimidazole analogues form complexes with BSA. To further confirm the vicinity of the analogues to the fluorophore BSA (the drug binding site distance between the site and fluorophore),[113,114] fluorescence resonance energy transfer (FRET) from protein to ligands have been verified. According to the Förster theory of nonradioactive energy transfer, the transfer of energy can take place through a direct electrodynamic interaction between the primarily excited molecule and its neighbors. Using the fluorescence resonance energy transfer (FRET), the distance R of binding between triazine-benzimidazole analogues and BSA could be calculated by the equation.[115]

$$E = 1-(F/F_0) = R_0^6/(R_0^6 + R^6)$$

where E denotes the efficiency of energy transfer between the donor and acceptor, and r is the distance between the donor and acceptor. R_0, the critical distance at which the transfer efficiency equals to 50%, is given by the following equation.[116]

$$R_0^6 = 979\ (K^2 n^{-4} \phi J)^{1/6}\ \text{nm}$$

K^2 is the orientation factor to the donor and acceptor of dipoles and is equal to 2/3 for random orientation as in fluid solution, n is the refraction index of medium, Φ is the fluorescence quantum yield of the donor, and *J* expresses the degree of spectral overlap between the donor emission and the acceptor absorption, which could be calculated by the equation:

$$J = \frac{\int_0^\infty F(\lambda)\varepsilon(\lambda)\lambda^4 d\lambda}{\int_0^\infty F(\lambda) d\lambda}$$

where F(λ) is the normalized donor emission spectrum in the range from λ to λ + Δλ, and ε(λ) is the molar absorption coefficient of the acceptor at wavelength λ. In the present case, we took n = 1.36 and Φ = 0.32. According to the above equations and experimental data, *J*(λ), R_0, R, and E were evaluated (Table 15). On gradual addition of compounds **5-14, 16, 17** and **20**, fluorescence intensity of the tryptophan residue present in BSA decreased with a concomitant increase in the fluorescence intensity through an isoemissive point within range of 339 nm - 357 nm (Figure 46, Table 14).

This indicates an efficient energy transfer from the tryptophan residue present in BSA to compounds **5-14, 16, 17** and **20** (Figures 47-50). The overlap of the absorption spectrum of compounds **6**, **16, 17** and **20** and the emission spectrum of BSA are shown in figure **50**. It has been reported that the energy transfer will most probably take place when the average distance between a donor fluorescence and acceptor fluorescence is on the 2−8 nm scale and $0.5R_0 < R < 1.5R_0$. This is in accord with conditions of Forster's nonradioactive energy transfer theory which indicated again a static quenching interaction between triazine-benzimidazole analogues and BSA.

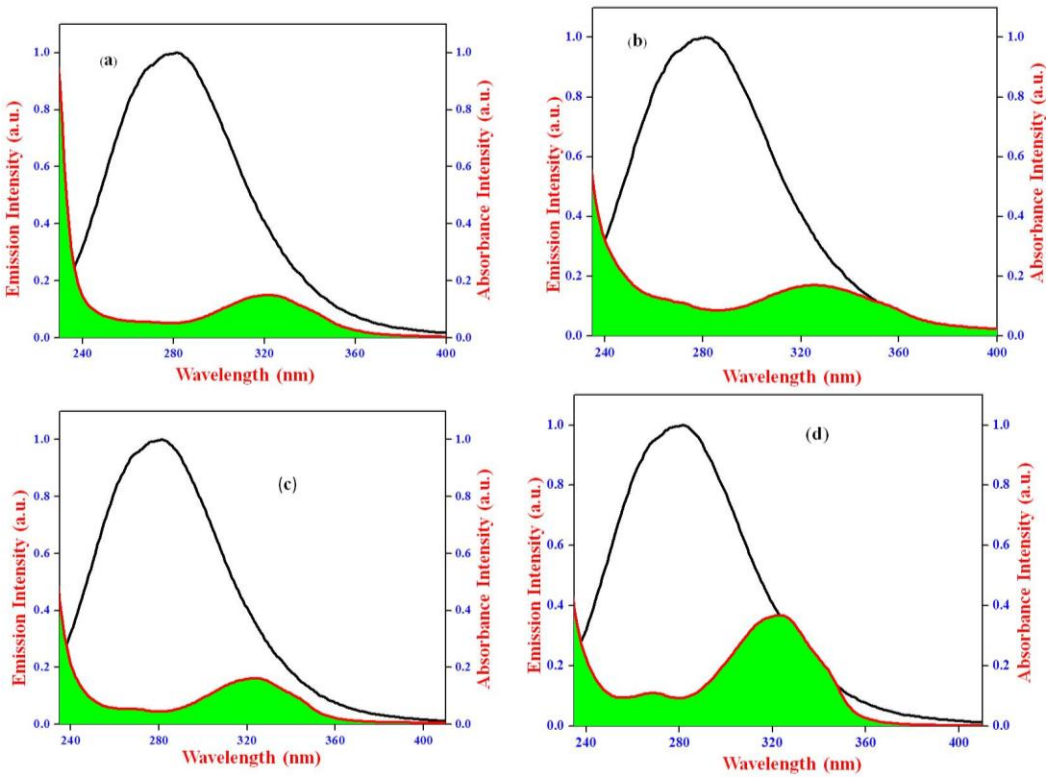

Figure 46. Normalized spectral overlap of emission and absorption spectra of (a) BSA.compound **6**, (b) BSA.compound **16**; (c) BSA.compound **17** and BSA.compound **20** complexes.

Table 15. Forster Energy Transfer Parameters for BSA.triazine-benzimidazole complexes **5-14, 16, 17** and **20**.

Sr. No.	$\Phi_{(ligands)}$	$\Phi_{(complex)}$	% Overlapping Area	Energy efficiency (E)	J (mol^{-1} cm^{-1} nm^4)	R (nm)	R_0 (nm)
5	0.31	0.20	24.98	37.50	1.25×10^{15}	4.41	4.78
6	0.24	0.29	30.29	2.63	1.28×10^{15}	4.43	7.90
7	0.23	0.23	9.60	26.86	1.35×10^{15}	4.47	5.28
8	0.30	0.25	2.30	21.62	1.21×10^{15}	4.40	5.45
9	0.36	0.24	14.50	24.41	1.29×10^{15}	4.44	5.38
10	0.34	0.22	19.35	29.30	1.28×10^{15}	4.43	5.14
11	0.23	0.27	19.46	15.58	1.24×10^{15}	4.41	5.81
12	0.32	0.22	10.78	31.71	1.46×10^{15}	4.53	5.13
13	0.38	0.29	26.74	7.39	1.42×10^{15}	4.51	6.94
14	0.28	0.28	18.57	11.28	1.44×10^{15}	4.52	6.40
16	0.22	0.29	27.55	9.56	1.59×10^{15}	4.59	6.61
17	0.31	0.20	23.80	3.74	1.39×10^{15}	4.49	7.62
20	0.30	0.31	37.63	3.10	1.63×10^{15}	4.61	7.98

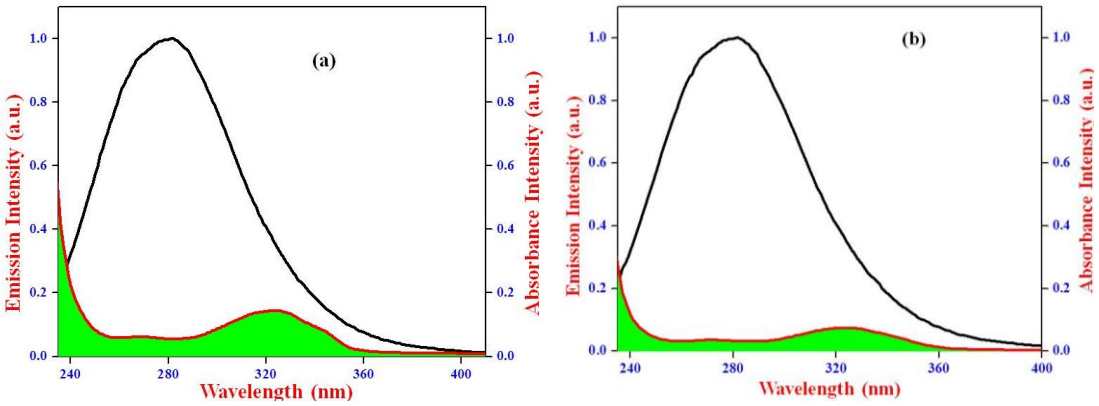

Figure 47. Spectral overlaps of fluorescence and absorption spectra of (a) BSA-compound **5** (b) BSA-compound **7.**

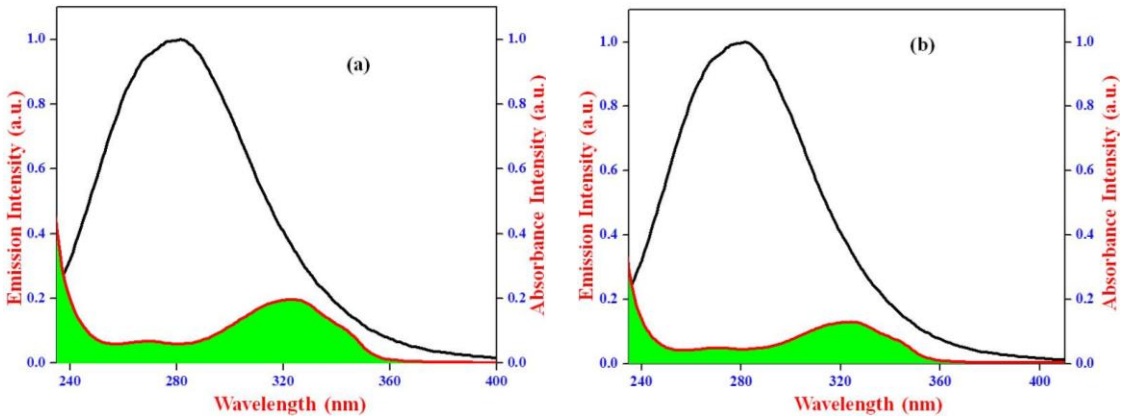

Figure 48. Spectral overlaps of fluorescence and absorption spectra of (a) BSA-compound **8** (b) BSA-compound **9.**

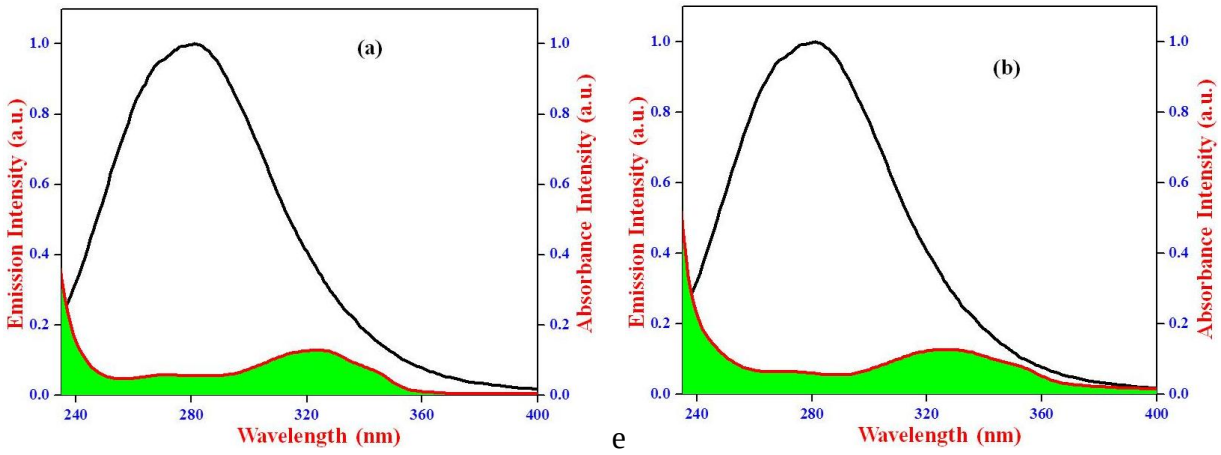

e

Figure 49. Spectral overlaps of fluorescence and absorption spectra of (a) BSA-compound **10** (b) BSA-compound **11.**

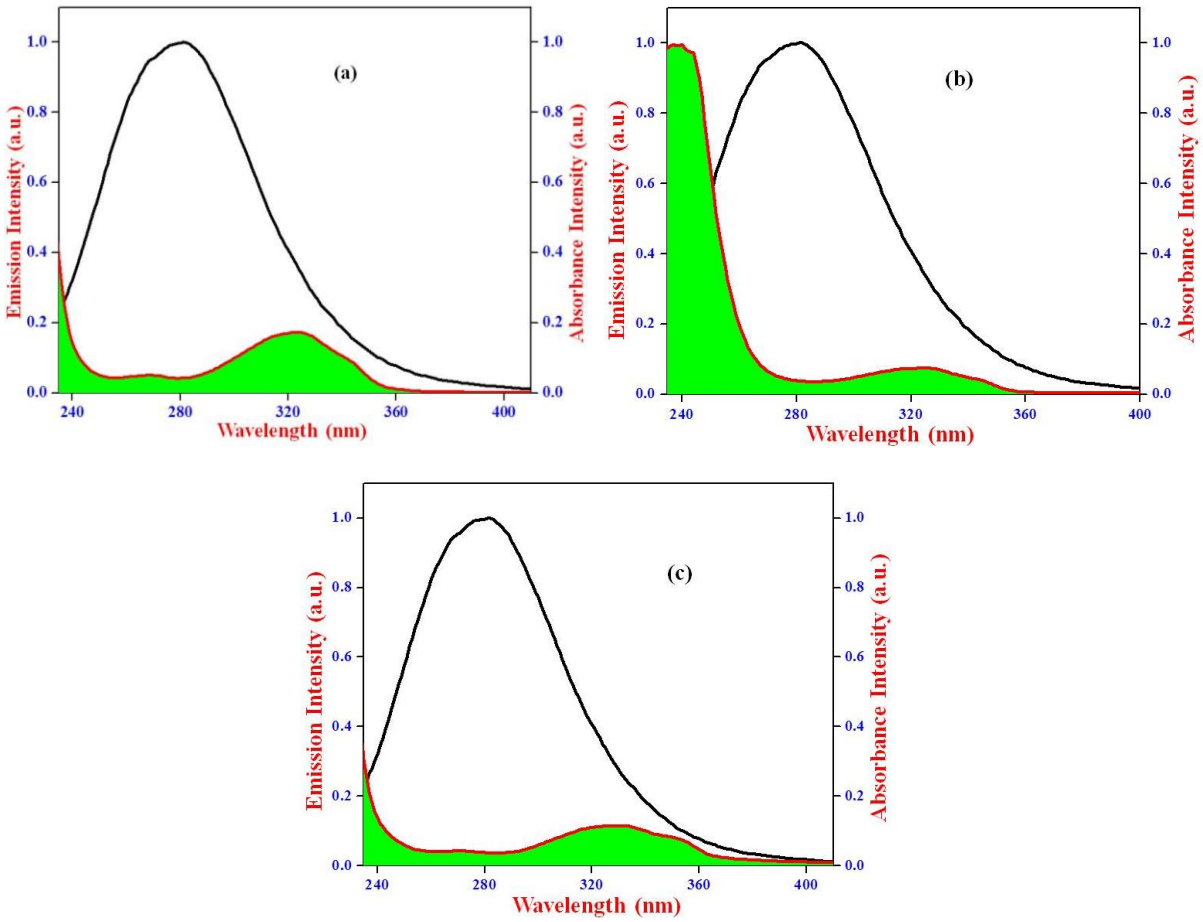

Figure 50. Spectral overlaps of fluorescence and absorption spectra of (a) BSA-compound **12** (b) BSA-compound **13** (c) BSA-compound **14.**

2.4.2.5. Molecular Docking Studies

To study the exact conformation of compounds **6**, **16**, **17** and **20** at the binding sites to BSA, we have run a docking program with the lowest binding free energy to stimulate the binding mode between compounds **6**, **16**, **17** and **20** and BSA (PDB: 4F5S).[117,118] The calculated free energy change between compounds **6**, **16**, **17** and **20** and BSA was found to be -6.74 kcal/mol, -8.29 kcal/mol, -8.30 kcal/mol and -7.47 kcal/mol respectively. These molecules bind to the site essentially via hydrophobic and Van der Waals forces (Figure 51). It has been reported that in some cases these amino acid residues undergo hydrogen bonding interactions as well. These results suggested that the formation of hydrogen bonds in BSA decrease the hydrophilicity and increased the hydrophobicity to stabilize the BSA.triazine-benzimidazole complexes. The

findings from docking studies provided a good structural basis to correlate the results with that of the emission quenching studies of BSA in presence of triazine-benzimidazole analogues.

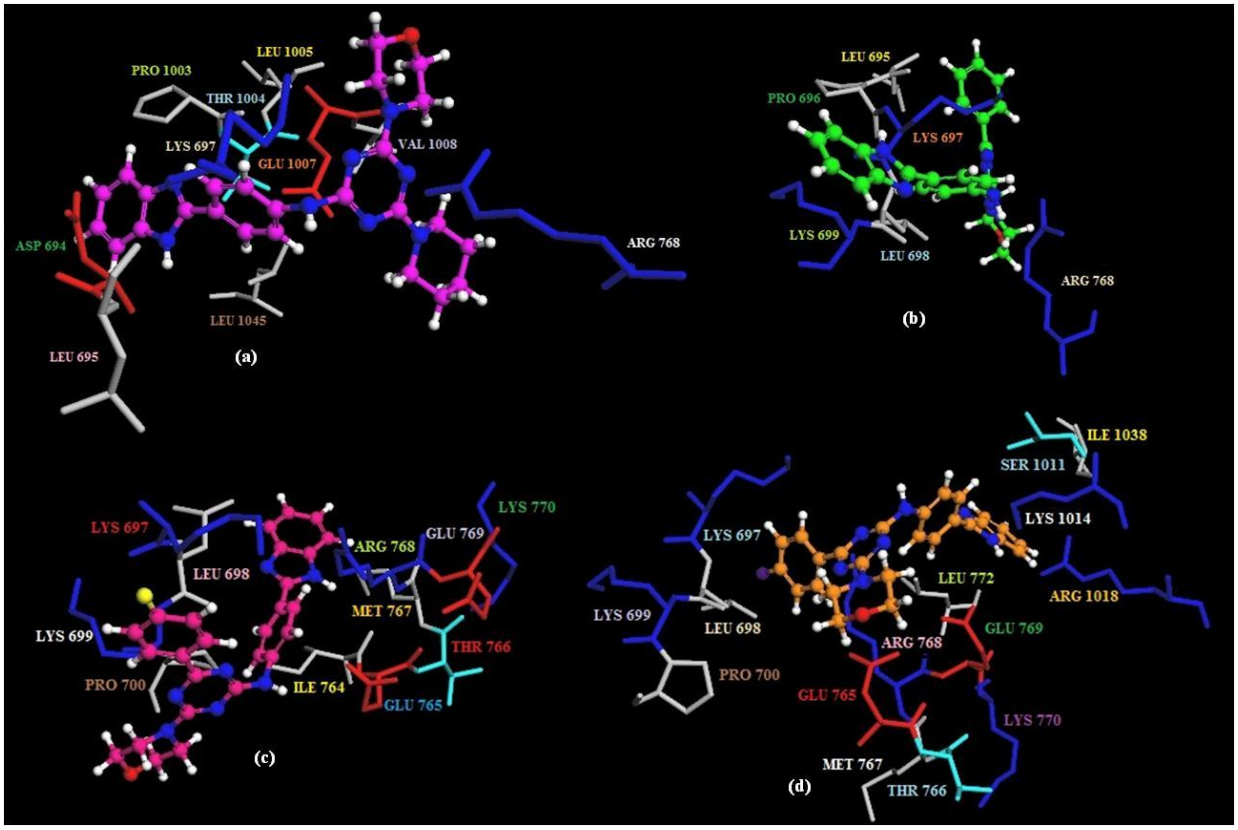

Figure 51. Docking of BSA with (a) compound **6;** (b) compound **16;** (c) compound **17** and (d) compound **20.**

2.4.3. CONCLUSIONS

A series of novel substituted triazine-benzimidazole analogs have been synthesized and evaluated for growth inhibition properties against a panel of 60 human cancer cell lines, and their GI_{50}, TGI and LC_{50} values have been determined. Four compounds (6, 16, 17 and 20) have been identified with GI_{50}'s in the nanomolar range for most of the cell lines. These compounds were also shown strong interacting properties with BSA, determined by UV-Visible and fluorescence spectroscopy. The experimental results demonstrated that fluorescence intensity of BSA was quenched with subsequent appearance of new band at the range of 370nm and 373 nm. The large binding constant values suggest that triazine-benzimidazole binds to the high affinity binding sites to albumin. These preliminary encouraging results of biological screening could offer an excellent framework in medicinal and pharmaceutical chemistry.

2.4.4. EXPERIMENTAL SECTION

Synthesis of 4,6-dichloro-2-morpholin-4-yl-[1,3,5]triazine (2).

To the stirred solution of cyanuric chloride (10 g, 0.054 mol) in anhydrous THF (150 mL), morpholine (5.65 g, 0.065 mol) was added at 0-5 ^{0}C. To this mixture, 10% $NaHCO_3$ was added and stirred at the same temperature for 6 h. The resulted reaction mixture was then poured into crushed ice, filtered, dried and column chromatographed on silica gel in ethylacetate:hexane (1:4) to afford the desired product 4,6-dichloro-2-morpholin-4-yl-[1,3,5]triazine **(2)** as white solid; (11.33 g, 89%); mp: 277-279 ^{o}C.

Synthesis of [4-(3*H*-benzimidazol-5-yl)-phenyl]-(6-chloro-2-morpholin-4-yl-[1,3,5]triazin-2-yl)-amine (4): To the stirred solution of 4,6-dichloro-2-morpholin-4-yl-[1,3,5]triazine (**2**) (10 g, 0.042 mol) in anhydrous THF (150 mL), 4-(1*H*-benzimidazol-2-yl)-phenylamine (**3)** (10.67 g, 0.051 mol) was added at room temperature. To this mixture, 10% K_2CO_3 was added and stirred for 24 h. The resulted reaction mixture was then poured into crushed ice, filtered, dried and column chromatographed on silica gel using ethylacetate:hexane (4:1) to afford the desired product [4-(3*H*-benzimidazol-5-yl)-phenyl]-(6-chloro-2-morpholin-4-yl-[1,3,5]triazin-2-yl)-amine **(4).**

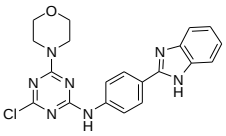

white solid; yield: 84%; mp: 277-279 ^{o}C; ^{1}H NMR (400 MHz, $CDCl_3$ + DMSO-d_6): δ = 9.94 (bs, 1H, NH), 8.14 (d, 2H, *J* = 8.68 Hz, ArH), 7.81 (d, 2H, *J* = 8.72 Hz, ArH), 7.62-7.56 (m, 2H, ArH), 7.21-7.18 (m, 2H, ArH), 3.87-3.86 (m, 4H, mor-CH_2), 3.77-3.75 (m, 4H, mor-CH_2); ^{13}C NMR (100 MHz, $CDCl_3$): δ = 152.9, 142.8, 135.6, 129.1, 128.1, 126.2, 109.4 (ArC), 66.7 (O-CH_2), 47.3 (N-CH_2); MS(ESI), m/z: 407.8 (M^++1); Anal. Calcd for $C_{20}H_{18}ClN_7O$: C, 58.90; H, 4.45; N, 24.04, Found: C, 58.99; H, 4.41; N, 24.20.

General procedure for the synthesis of compounds 5-15.

To the stirred solution of [4-(3*H*-benzimidazol-5-yl)-phenyl]-(6-chloro-2-morpholin-4-yl-[1,3,5]triazine-2,4-diamine **(4)** (0.200 g, 0.463 mmol) in 1,4-dioxane (20 mL), amine (0.556 mmol) and potassium carbonate (0.095g, 0.695 mmol) were added and heated at 110 ^{o}C for 8 h. Extracted the reaction mixture with chloroform, dried over Na_2SO_4, filtered and concentrated to get crude product which was then purified through column chromatography using chloroform:methanol (50:1) as eluents to give compounds **5-15**.

[4-(3*H*-Benzimidazol-5-yl)-phenyl]-(2,6-di-morpholin-4-yl-[1,3,5]triazin-2-yl)-amine (5).

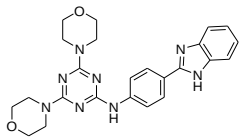

White solid; yield: 78%; mp: 268-270 ^{o}C; ^{1}H NMR (400 MHz, $CDCl_3$): δ = 8.00 (d, 2H, *J* = 7.76 Hz, ArH), 7.70 (d, 3H, *J* = 8.24 Hz, ArH), 7.27-7.25 (m, 3H, ArH), 6.87 (bs, 1H, NH), 3.81-3.76 (m, 8H, mor-CH_2), 3.74-3.70 (m, 8H, mor-CH_2); ^{13}C NMR (100 MHz, $CDCl_3$): δ = 165.1, 151.6, 135.8, 129.2, 128.2, 128.0, 125.7, 118.9, 115.5, 101.1 (ArC), 66.8 (O-CH_2), 43.6 (N-CH_2); MS(ESI), m/z: 458.5 (M^++1); Anal. Calcd for $C_{24}H_{26}N_8O_2$: C, 62.87; H, 5.72; N, 24.44, Found: C, 62.98; H, 5.67; N, 24.55.

[4-(3*H*-Benzimidazol-5-yl)-phenyl]-(2-morpholin-4-yl-6-piperidin-1-yl-[1,3,5]triazin-2-yl)-amine (6).

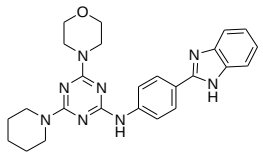

White solid; yield: 72%; mp: 271-273 ^{o}C; ^{1}H NMR (400 MHz, $CDCl_3$): δ = 8.00 (d, 2H, *J* = 8.72 Hz, ArH), 7.72 (d, 2H, *J* = 8.72 Hz, ArH), 7.62 (s, 1H, ArH), 7.26-7.24 (m, 3H, ArH), 6.88 (bs, 1H, NH), 3.79 (t, 4H, *J* = 5.42 Hz, mor-CH_2), 3.75-3.68 (m, 8H, mor-CH_2, N-CH_2), 1.68-1.59 (m, 6H, CH_2); ^{13}C NMR (100 MHz, $CDCl_3$): δ = 152.3, 143.0, 135.9, 134.6, 131.4, 129.0, 127.9, 126.2, 116.1, 110.5, 109.0, (ArC), 67.0 (O-CH_2), 44.2 (N-CH_2), 43.7 (N-CH_2), 25.9 (CH_2), 25.0 (CH_2); MS(ESI), m/z: 456.5 (M^++1); Anal. Calcd for $C_{25}H_{28}N_8O$: C, 65.77; H, 6.18; N, 24.54, Found: C, 65.65; H, 6.14; N, 24.62.

[4-(3*H*-Benzimidazol-5-yl)-phenyl]-(2-morpholin-4-yl-6-pyrrolidin-1-yl-[1,3,5]triazin-2-yl)-amine (7).

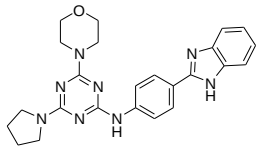

White solid; yield: 76%; mp: 277-279 ^{o}C; ^{1}H NMR (400 MHz, $CDCl_3$): δ = 7.99 (d, 2H, *J* = 8.68 Hz, ArH), 7.75 (d, 2H, *J* = 8.68 Hz, ArH), 7.61 (bs, 1H, NH), 7.25-7.23 (m, 4H, ArH), 6.94 (bs, 1H, NH), 3.82-3.79 (m, 4H, mor-CH_2), 3.74-3.72 (m, 4H, mor-CH_2), 3.57 (t, 4H, *J* = 5.04 Hz, N-CH_2), 1.96-1.94 (m, 4H, CH_2); ^{13}C NMR (100 MHz, $CDCl_3$): δ = 152.2, 143.0, 136.0, 134.8, 129.0, 127.9, 126.2, 115.8, 110.3, 109.0 (ArC), 67.0 (O-CH_2), 46.1 (N-CH_2), 43.7 (N-CH_2), 25.4 (CH_2); MS(ESI), m/z: 442.5 (M^++1); Anal. Calcd for $C_{24}H_{26}N_8O$: C, 65.14; H, 5.92; N, 25.32, Found: C, 65.25; H, 5.88; N, 25.39.

[4-(3*H*-Benzimidazol-5-yl)-phenyl]-[6-(4-methyl-piperazin-1-yl)-2-morpholin-4-yl-[1,3,5]triazin-2-yl]-amine (8).

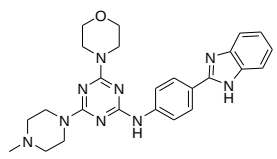

White solid; yield: 77%; mp: 282-284 ^{o}C; ^{1}H NMR (400 MHz, $CDCl_3$): δ = 8.01 (d, 2H, *J* = 8.72 Hz, ArH), 7.70 (d, 2H, *J* = 8.72 Hz, ArH), 7.63 (bs, 1H, NH), 7.27-7.24 (m, 4H, ArH), 6.87 (bs, 1H, NH), 3.84 (t, 4H, *J* = 4.12 Hz, mor-

CH_2), 3.80-3.78 (m, 4H, mor-CH_2), 3.75-3.72 (m, 4H, N-CH_2), 2.46 (t, 4H, *J* = 4.60 Hz, N-CH_2), 2.35 (s, 3H, N-CH_3); ^{13}C NMR (100 MHz, $CDCl_3$): δ = 138.2, 135.9, 135.8, 135.1, 129.1, 127.9, 125.9, 118.9, 115.2, 100.8 (ArC), 66.8 (O-CH_2), 46.8 (N-CH_2), 44.2 (N-CH_2), 43.6 (N-CH_2), 14.0 (N-CH_3); MS(ESI), m/z: 471.5 (M^++1); Anal. Calcd for $C_{25}H_{29}N_9O$: C, 63.68; H, 6.20; N, 26.73, Found: C, 63.79; H, 6.15; N, 26.66.

_N_-[4-(3_H_-Benzimidazol-5-yl)-phenyl]-2-morpholin-4-yl-_N_'-(6-morpholin-4-yl-ethyl)-[1,3,5]triazine-4,6-diamine (9).

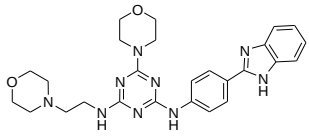

White solid; yield: 69%; mp: 289-291 ^{o}C; ^{1}H NMR (400 MHz, $CDCl_3$): δ = 8.05 (s, 1H, ArH), 7.30 (t, 4H, *J* = 7.36 Hz, ArH, NH), 7.10 (d, 2H, *J* = 8.24 Hz, ArH), 7.05 (d, 2H, *J* = 11.36 Hz, ArH), 3.82-3.80 (m, 8H, mor-CH_2), 3.72-3.69 (m, 8H, mor-CH_2), 3.51-3.49 (m, 2H, N-CH_2), 2.20-2.17 (m, 2H, N-CH_2); ^{13}C NMR (100 MHz, $CDCl_3$): δ = 166.0, 164.6, 152.5, 142.9, 135.8, 129.1, 128.0, 126.3, 122.1, 121.7, 115.5, 115.2, 109.1 (ArC), 66.9 (O-CH_2), 57.2 (N-CH_2), 53.4 (N-CH_2), 47.2 (N-CH_2), 37.1 (N-CH_2); MS(ESI), m/z: 501.5 (M^++1); Anal. Calcd for $C_{26}H_{31}N_9O_2$: C, 62.26; H, 6.23; N, 25.13, Found: C, 62.30; H, 6.18; N, 25.25.

2-(4-{4-[4-(3_H_-Benzimidazol-5-yl)-phenylamino]-2-morpholin-4-yl-[1,3,5]triazin-6-yl}-piperazin-1-yl)-ethanol (10).

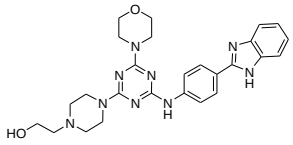

White solid; yield: 68%; mp: 287-289 ^{o}C; ^{1}H NMR (400 MHz, $CDCl_3$): δ = 7.60 (d, 1H, *J* = 8.72 Hz, ArH), 7.33-7.27 (m, 3H, ArH), 7.17 (s, 1H, ArH), 7.08 (d, 1H, *J* = 8.72 Hz, ArH), 7.03 (d, 2H, *J* = 6.40 Hz, ArH), 3.67-3.57 (m, 12H, mor-CH_2, N-CH_2), 3.47 (d, 2H, *J* = 8.28 Hz, O-CH_2), 2.43-2.42 (m, 2H, N-CH_2), 2.15-2.13 (m, 4H, N-CH_2); ^{13}C NMR (100 MHz, $CDCl_3$): δ = 151.7, 138.4, 135.9, 135.8, 134.7, 129.1, 127.9, 125.9, 118.9, 115.7, 115.5 (ArC), 66.9 (O-CH_2), 66.7 (O-CH_2), 57.3 (N-CH_2), 53.4 (N-CH_2), 43.6 (N-CH_2), 36.9 (N-CH_2); MS(ESI), m/z: 501.5 (M^++1); Anal. Calcd for $C_{26}H_{31}N_9O_2$: C, 62.26; H, 6.23; N, 25.13, Found: C, 62.15; H, 6.18; N, 25.24.

_N_-(6-Amino-ethyl)-_N_'-[4-(3_H_-benzimidazol-5-yl)-phenyl]-2-morpholin-4-yl-[1,3,5]triazine-4,6-diamine (11).

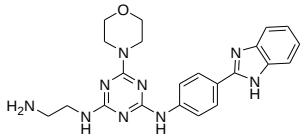

White solid; yield: 73%; mp: 265-267 ^{o}C; ^{1}H NMR (400 MHz, $CDCl_3$): δ = 7.95 (d, 2H, *J* = 7.76 Hz, ArH), 7.62-7.59 (m, 4H, ArH, NH), 7.25-7.22 (m,

3H, ArH), 3.75-3.73 (m, 4H, mor-CH_2), 3.71-3.67 (m, 4H, mor-CH_2), 3.46 (t, 2H, *J* = 5.96 Hz, N-CH_2), 2.91 (t, 2H, *J* = 5.48 Hz, N-CH_2); ^{13}C NMR (100 MHz, $CDCl_3$): δ = 152.4, 143.0, 135.9, 134.2, 131.7, 129.1, 128.0, 126.2, 109.1 (ArC), 66.9 (O-CH_2), 47.2 (N-CH_2), 43.7 (N-CH_2), 41.8 (N-CH_2); MS(ESI), m/z: 431.5 (M^++1); Anal. Calcd for $C_{22}H_{25}N_9O$: C, 61.24; H, 5.84; N, 29.21, Found: C, 61.39; H, 5.80; N, 29.14.

2-{4-[4-(3*H*-Benzimidazol-5-yl)-phenylamino]-2-morpholin-4-yl-[1,3,5]triazin-6-ylamino}-ethanol (12).

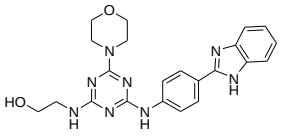

White solid; yield: 71%; mp: 262-264 ^{o}C; ^{1}H NMR (400 MHz, $CDCl_3$): δ = 8.05 (s, 1H, ArH), 7.31 (d, 3H, *J* = 7.36 Hz, ArH), 7.24-7.22 (m, 1H, ArH), 7.11 (d, 1H, *J* = 8.24 Hz, ArH), 7.05 (d, 2H, *J* = 6.88 Hz, ArH), 3.79-3.72 (m, 8H, mor-CH_2), 3.49 (t, 2H, *J* = 5.48 Hz, O-CH_2), 2.91-2.88 (m, 2H, N-CH_2); ^{13}C NMR (100 MHz, $CDCl_3$): δ = 152.5, 142.8, 135.8, 133.9, 131.8, 129.1, 128.0, 126.2, 116.6, 111.4, 109.1 (ArC), 66.8 (O-CH_2), 63.8 (O-CH_2), 47.2 (N-CH_2), 43.7 (N-CH_2); MS(ESI), m/z: 432.4 (M^++1); Anal. Calcd for $C_{22}H_{24}N_8O_2$: C, 61.10; H, 5.59; N, 25.91, Found: C, 61.01; H, 5.55; N, 25.99.

***N*-[4-(3*H*-Benzimidazol-5-yl)-phenyl]-*N*'-benzyl-2-morpholin-4-yl-[1,3,5]triazine-4,6-diamine (13).**

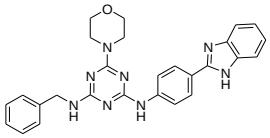

White solid; yield: 66%; mp: 275-277 ^{o}C; ^{1}H NMR (400 MHz, $CDCl_3$): δ = 8.04 (d, 1H, *J* = 1.80 Hz, ArH), 7.30-7.27 (m, 4H, ArH), 7.24 (d, 1H, *J* = 1.80 Hz, ArH), 7.22 (d, 1H, *J* = 2.28 Hz, ArH), 7.11 (d, 2H, *J* = 8.72 Hz, ArH), 7.05 (d, 2H, *J* = 1.84 Hz, ArH), 7.03 (d, 2H, *J* = 4.12 Hz, ArH), 5.28 (s, 2H, N-CH_2), 3.72 (t, 8H, *J* = 8.72 Hz, mor-CH_2); ^{13}C NMR (100 MHz, $CDCl_3$): δ = 151.9, 138.8, 135.8, 134.9, 134.0, 129.1, 128.0, 126.0, 122.1, 119.1, 115.5, 115.3, 101.7 (ArC), 66.7 (O-CH_2), 46.9 (N-CH_2), 43.7 (N-CH_2); MS(ESI), m/z: 478.5 (M^++1); Anal. Calcd for $C_{27}H_{26}N_8O$: C, 67.77; H, 5.48; N, 23.42, Found: C, 67.71; H, 5.43; N, 23.49.

***N*-[4-(3*H*-Benzimidazol-5-yl)-phenyl]-*N*'-cyclohexyl-2-morpholin-4-yl-[1,3,5]triazine-4,6-diamine (14).**

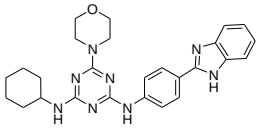

White solid; yield: 68%; mp: 283-285 ^{o}C; ^{1}H NMR (400 MHz, $CDCl_3$): δ = 8.00 (d, 2H, *J* = 7.76 Hz, ArH), 7.76 (d, 1H, *J* = 6.88 Hz, ArH), 7.67-7.62 (m, 2H, ArH), 7.25-7.23 (m, 2H, ArH), 6.95 (s, 1H, ArH), 4.95 (m, 1H, N-CH), 3.79-3.73 (m, 8H, mor-CH_2), 2.05-2.02 (m, 2H, CH_2), 1.77-1.74 (m, 2H, CH_2), 1.66-1.64 (m, 2H, CH_2), 1.41-1.38 (m, 2H, CH_2), 1.25-1.19 (m, 2H, CH_2); ^{13}C NMR (100 MHz, $CDCl_3$): δ = 165.8,

164.4, 152.0, 151.9, 135.9, 135.7, 129.0, 127.9, 126.3, 126.1, 119.0, 115.5, 115.3 (ArC), 66.9 (O-CH_2), 57.2 (N-CH), 53.4 (N-CH_2), 37.1 (CH_2), 32.0 (CH_2), 22.7 (CH_2); MS(ESI), m/z: 470.5 (M^++1); Anal. Calcd for $C_{26}H_{30}N_8O$: C, 66.36; H, 6.43; N, 23.81, Found: C, 66.48; H, 6.38; N, 23.89.

[4-(3*H*-Benzimidazol-5-yl)-phenyl]-(6-hydrazino-2-morpholin-4-yl-[1,3,5]triazin-4-yl)-amine (15).

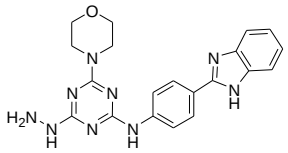

White solid; yield: 64%; mp: 296-298 ^oC; ^1H NMR (400 MHz, $CDCl_3$): δ = 7.67 (d, 1H, *J* = 8.60 Hz, ArH), 7.61 (d, 1H, *J* = 8.72 Hz, ArH), 7.48 (bs, 1H, NH), 7.25-7.23 (m, 2H, ArH), 7.11-6.98 (m, 4H, ArH), 3.67-3.65 (m, 4H, mor-CH_2), 3.50-3.47 (m, 4H, mor-CH_2); ^{13}C NMR (100 MHz, $CDCl_3$): δ = 152.4, 139.4, 135.6, 132.8, 129.2, 128.1, 125.7, 119.2, 116.2, 102.1 (ArC), 66.6 (O-CH_2), 43.9 (N-CH_2); MS(ESI), m/z: 403.4 (M^++1); Anal. Calcd for $C_{20}H_{21}N_9O$: C, 59.54; H, 5.25; N, 31.25, Found: C, 59.64; H, 5.21; N, 31.28.

General procedure for the synthesis of compounds 16-21.

To the stirred solution of [4-(3*H*-benzimidazol-5-yl)-phenyl]-(6-chloro-2-morpholin-4-yl-[1,3,5]triazin-2-yl)-amine **(4)** (0.200 g, 0.490 mmol) in 1,4-dioxane (20 mL), arylboronic acids (0.556 mmol), $Pd(PPh_3)_4$ (10 mol%) and potassium carbonate (0.101g, 0.736 mmol) were added and refluxed for 8-10 hrs in an inert atmosphere. After the completion of reaction, extracted the reaction mixture with chloroform, dried over Na_2SO_4, filtered and concentrated to get crude product which was purified through column chromatography using chloroform:methanol (50:1) as eluents to give compounds **16-21**.

[4-(3*H*-Benzimidazol-5-yl)-phenyl]-(2-morpholin-4-yl-6-phenyl-[1,3,5]triazin-2-yl)-amine (16).

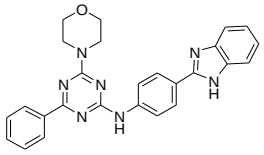

White solid; yield: 72%; mp: 267-269 ^oC; ^1H NMR (400 MHz, $CDCl_3$): δ = 8.06 (d, 1H, *J* = 8.72 Hz, ArH), 8.00 (d, 1H, *J* = 4.68 Hz, ArH), 7.85 (d, 1H, *J* = 8.24 Hz, ArH), 7.77 (d, 1H, *J* = 8.96 Hz, ArH), 7.72 (d, 2H, *J* = 8.72 Hz, ArH), 7.62 (bs, 1H, NH), 7.54-7.52 (m, 3H, ArH), 7.08 (t, 2H, *J* = 8.72 Hz, ArH), 6.77-6.70 (m, 2H, ArH), 3.99-3.95 (m, 8H, mor-CH_2); ^{13}C NMR (100 MHz, $CDCl_3$): δ = 152.0, 137.6, 135.8, 134.0, 132.1, 129.7, 129.2, 128.6, 128.5, 128.0, 125.8, 119.2, 115.7, 101.5 (ArC), 66.8 (O-CH_2), 43.7 (N-CH_2); MS(ESI), m/z: 449.5 (M^++1); Anal. Calcd for $C_{26}H_{23}N_7O$: C, 69.47; H, 5.16; N, 21.81, Found: C, 69.64; H, 5.12; N, 21.98.

[4-(3*H*-Benzimidazol-5-yl)-phenyl]-[6-(4-fluoro-phenyl)-2-morpholin-4-yl-[1,3,5]triazin-2-yl]-amine (17).

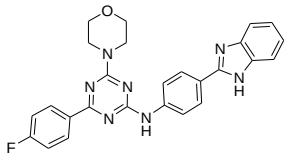

White solid; yield: 71%; mp: 279-281 ^{o}C; ^{1}H NMR (400 MHz, $CDCl_3$): δ = 8.34 (d, 2H, *J* = 7.32 Hz, ArH), 8.03 (bs, 1H, NH), 7.67 (d, 1H, *J* = 8.28 Hz, ArH), 7.48 (d, 1H, *J* = 7.32 Hz, ArH), 7.40-7.37 (m, 2H, ArH), 7.35-7.29 (m, 3H, ArH), 7.16 (d, 1H, *J* = 2.32 Hz, ArH), 7.07 (d, 2H, *J* = 6.40 Hz, ArH), 3.98-3.61 (m, 8H, mor-CH_2); ^{13}C NMR (100 MHz, $CDCl_3$): δ = 151.9, 138.8, 135.8, 134.9, 134.0, 129.1, 128.0, 126.0, 122.1, 119.1, 115.5, 115.3, 101.7 (ArC), 66.7 (O-CH_2), 43.7 (N-CH_2); MS(ESI), m/z: 467.4 (M^++1); Anal. Calcd for $C_{26}H_{22}FN_7O$: C, 66.80; H, 4.74; N, 20.97, Found: C, 66.85; H, 4.71; N, 21.05.

[4-(3*H*-Benzimidazol-5-yl)-phenyl]-(6-furan-2-yl-2-morpholin-4-yl-[1,3,5]triazin-4-yl)-amine (18).

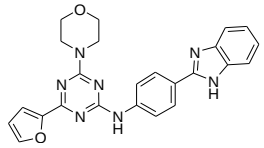

White solid; yield: 66%; mp: 282-284 ^{o}C; ^{1}H NMR (400 MHz, $CDCl_3$): δ = 8.00 (d, 2H, *J* = 4.72 Hz, ArH), 7.83 (bs, 1H, NH), 7.72 (d, 2H, *J* = 8.24 Hz, ArH), 7.52-7.48 (m, 3H, ArH), 7.07 (t, 3H, *J* = 8.68 Hz, ArH), 6.96 (s, 1H, ArH), 6.80 (bs, 1H, NH), 3.77-3.69 (m, 8H, mor-CH_2); ^{13}C NMR (100 MHz, $CDCl_3$): δ = 152.9, 142.8, 135.6, 132.5, 129.1, 128.1, 126.2, 109.4 (ArC), 66.7 (O-CH_2), 44.1 (N-CH_2); MS(ESI), m/z: 439.4 (M^++1); Anal. Calcd for $C_{24}H_{21}N_7O_2$: C, 65.59; H, 4.82; N, 22.31, Found: C, 65.86; H, 4.87; N, 22.39.

4-(3*H*-Benzimidazol-5-yl)-phenyl]-(2-morpholin-4-yl-6-thiophen-2-yl-[1,3,5]triazin-2-yl)-amine (19).

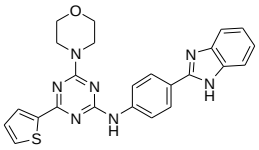

White solid; yield: 67%; mp: 288-290 ^{o}C; ^{1}H NMR (400 MHz, $CDCl_3$): δ = 7.50 (q, 3H, *J* = 5.04 Hz, ArH), 7.37-7.31 (m, 3H, ArH), 7.14 (d, 2H, *J* = 5.96 Hz, ArH), 7.03 (t, 3H, *J* = 8.72 Hz, ArH), 6.86 (bs, 1H, NH), 3.79-3.78 (m, 4H, mor-CH_2), 3.75-3.74 (m, 4H, mor-CH_2); ^{13}C NMR (100 MHz, $CDCl_3$): δ = 152.6, 143.0, 135.8, 135.1, 133.6, 132.0, 129.1, 128.0, 126.2, 121.7, 115.5, 115.3, 109.1 (ArC), 66.9 (O-CH_2), 43.8 (N-CH_2); MS(ESI), m/z: 455.5 (M^++1); Anal. Calcd for $C_{24}H_{21}N_7OS$: C, 63.28; H, 4.65; N, 21.52; S, 7.04, Found: C, 63.15; H, 4.61; N, 21.59; S, 7.08.

***N*-[4-(1*H*-Benzimidazol-2-yl)-phenyl]-*N*'-(4-fluoro-phenyl)-6-(2-methoxy-phenyl)-[1,3,5]triazine-2,4-diamine (20).**

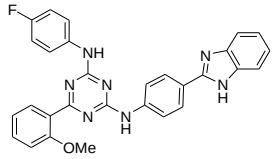

White solid; yield: 65%; mp: 288-290 ^{o}C; ^{1}H NMR (400 MHz, $CDCl_3$): δ 7.98 (d, 3H, *J* = 8.72 Hz, ArH), 7.81 (s, 1H, ArH), 7.67 (d, 3H, *J* = 8.00 Hz, ArH), 7.52-7.50 (m, 5H, ArH, NH), 7.27 (d, 2H, *J* = 2.76 Hz, ArH), 7.06 (t, 3H, *J* = 8.24 Hz, ArH), 3.96 (s, 3H, OCH_3); ^{13}C NMR (100 MHz, $CDCl_3$): δ = 152.7, 144.8, 139.2, 135.5, 132.6, 132.0, 129.2, 129.0, 127.9, 127.4, 126.7, 126.2, 122.5, 121.5, 117.0, 113.9, 111.9, 109.4 (ArC), 55.3 (OCH_3); MS (ESI), m/z: 503.5 (M^++1); Anal. Calcd for $C_{29}H_{22}FN_7O$: C, 69.17; H, 4.40; N, 19.47, Found: C, 69.03; H, 4.33; N, 19.41.

[4-(3*H*-Benzimidazol-5-yl)-phenyl]-[6-(4-chloro-phenyl)-2-morpholin-4-yl-[1,3,5]triazin-2-yl]-amine (20).

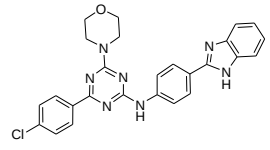

White solid; yield: 68%; mp: 276-278 ^{o}C; ^{1}H NMR (400 MHz, $CDCl_3$): δ = 8.35 (d, 2H, *J* = 5.48 Hz, ArH), 8.01 (bs, 1H, NH), 7.67 (d, 1H, *J* = 8.24 Hz, ArH), 7.33-7.31 (m, 4H, ArH), 7.16 (d, 2H, *J* = 8.68 Hz, ArH), 7.07 (d, 3H, *J* = 5.96 Hz, ArH), 3.99-3.73 (m, 8H, mor-CH_2); ^{13}C NMR (100 MHz, $CDCl_3$): δ = 152.4, 139.4, 135.6, 132.8, 129.2, 128.1, 125.7, 119.2, 116.2, 102.1 (ArC), 66.6 (O-CH_2), 43.9 (N-CH_2); MS(ESI), m/z: 483.5 (M^++1); Anal. Calcd for $C_{26}H_{22}ClN_7O$: C, 64.53; H, 4.58; N, 20.26, Found: C, 64.64; H, 4.41; N, 20.31.

[4-(3*H*-Benzimidazol-5-yl)-phenyl]-[6-(4-trifluoro-phenyl)-2-morpholin-4-yl-[1,3,5]triazin-2-yl]-amine (21).

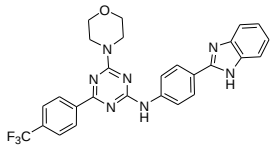

White solid; yield: 65%; mp: 279-281 ^{o}C; ^{1}H NMR (400 MHz, $CDCl_3$): δ = 8.03 (s, 1H, ArH), 7.50-7.46 (m, 2H, ArH), 7.31-7.28 (m, 2H, ArH), 7.24-7.22 (m, 2H, ArH), 7.13 (d, 1H, *J* = 8.72 Hz, ArH), 7.06 (d, 2H, *J* = 6.88 Hz, ArH), 6.99-6.97 (m, 2H, ArH), 6.86 (bs, 1H, NH), 3.81-3.78 (m, 4H, mor-CH_2), 3.74-3.71 (m, 4H, mor-CH_2); ^{13}C NMR (100 MHz, $CDCl_3$): δ = 152.0, 138.7, 136.8, 135.8, 134.1, 131.6, 129.6, 129.2, 128.3, 128.0, 125.9, 119.1, 115.6, 101.4 (ArC), 66.8 (O-CH_2), 43.7 (N-CH_2); MS(ESI), m/z: 517.5 (M^++1); Anal. Calcd for $C_{27}H_{22}F_3N_7O$: C, 62.66; H, 4.28; N, 18.95, Found: C, 67.59; H, 4.18; N, 18.85.

CHAPTER 3

FUSED HETEROCYCLIC MOIETIES LINKED BENZIMIDAZOLES

Nitrogen based heterocycles have received a great deal of attention in the literature due to their role as active pharmacophores. Fused heterocyclic systems are often considered important scaffolds in medicinal and pharmaceutical chemistry. Amongst these heterocyclic systems, pyrrolopyridine, quinazolinone and pyrazolo[3,4-*d*]pyrimidine frameworks hve been exploited to encompass an array of pharmacological activities.

3.1. PYRROLOPYRIDINE

3.1.1. INTRODUCTION

1*H*-Pyrrolo[2,3-*b*]pyridine (7-azaindole), a fused heterocyclic molecular framework, has been drawing much attention in biochemical and physicochemical studies,[119,120] due to its characteristic condensed ring system. It consists of fused pyridine and pyrrole ring system and having opposite л-electron densities. As 1*H*-pyrrolo[2,3-*b*]pyridine differs from indole by the presence of additional ring nitrogen on the six membered ring, it shows an excellent potential as bioisostere of the indole ring. Due to the presence of an additional nitrogen atom, this structural moiety possesses an advantage to act as hydrogen-bond donor and acceptor framework, a property that has been successfully utilized in drug discovery.[121-123] The 1*H*-pyrrolo[2,3-*b*]pyridine ring system is a key structural unit present in a number of therapeutically important pharmaceutical agents, such as anticancer, anti-inflammatory, anti-psychotic, antiallergic, angiotensin II antagonists, melatonin receptor MT1 agonists, COX-2 inhibitors, selective ligand for G2 binding sites,[124,125] and influenza virus inhibitor.[126] Apart from biological activities, this moiety is also used as key intermediate in the synthesis of various active compounds.

OBJECTIVE

There are only *N*-alkylated/acylated pyrrolopyridine have been known in literature but with respect to azoles (benzimidazoles, benzothiazole) and imidazopyridine at position C3 of pyrrole ring of pyrrolopyridine along with acylation and alkylation at N1 position has not been known. Further, Suzuki-Miyaura cross coupling reaction at C6 position of imidazopyridine has not given any report.

3.1.2. CHEMISTRY

The synthesis of N_1-substituted-2-(1*H*-pyrrolo[2,3-*b*]pyridine-3-yl)-azole ring system has been depicted in Tables 1-3 and Scheme 1. Duff reaction was first carried out by heating of 1*H*-pyrrolo[2,3-*b*]pyridine **1** in the presence of hexamethylenetetramine (HMTA) in acetic acid at 110 ^{0}C for 2 h to give 1*H*-pyrrolo[2,3-*b*]pyridine-3-carboxaldehyde **2** in 55% yield. The formyl function at C3-position provided a convenient handle for the generation of the corresponding azoles. Thus, compound **2** was allowed to heat with 2-aminothiophenol at 160 ^{o}C for 15 h to obtain 2-(1*H*-pyrrolo[2,3-*b*]pyridine-3-yl)-benzothiazole (**3**) in 89% yield (Table 1). The influence of the electronic properties of amines on the yield was evaluated by varying the structure of aryl ring viz., benzene-1,2-diamine, 4-nitro-benzene-1,2-diamine and 6-bromopyridine-2,3-diamine. Generally, the substrate with thio groups gave higher yield of products than those with amino groups and electron withdrawing nitro and bromo groups are more predominant than that of unsubstituted benzimidazole.

The potential of the present strategy was further expanded to the acylation and alkylation of 1*H*-pyrrolo[2,3-*b*]pyridine-azoles with different acyl and alkyl halides. 2-(1*H*-Pyrrolo[2,3-*b*]pyridine-3-yl)- benzothiazole (**3**) was first treated with benzoyl chloride in the presence NaH in dry THF under inert atmosphere at 0-10 ^{o}C for 2 h to give compound **7** in 85% yield (Table 2). By comparing the reactivity and reaction yields, it seems that the ability of acylating agent is considerably important for the reaction results. Acyl chlorides regardless of aliphatic or aromatic could be smoothly converted into the corresponding products in excellent yields.

Table 1. Synthesis of azoles substituted 1*H*-pyrrolo[2,3-*b*]pyridine

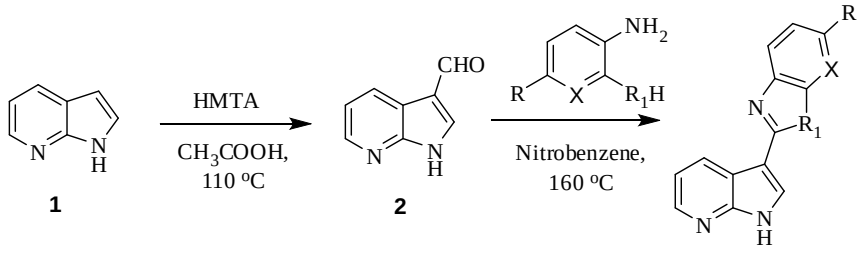

Compounds	Starting material	Yield (%)	mp (^{o}C)
3	2-aminothiophenol	89	219-221
4	benzene-1,2-diamine	75	134-136
5	4-nitro-benzene-1,2-diamine	77	149-151
6	6-bromopyridine-2,3-diamine	78	249-251

At the same time, allyl bromide was also amenable to this reaction system and delivered good yield of product (Table 2, entry 3). Subsequently, all other tested substrates (butyl bromide and oxiranyl chloride) were provided the corresponding products with excellent results (Table 2, entries 4,5), but these reactions could be possible at the temperature of 100 ^{o}C. Similarly, compounds **4** and **5** were also treated with various acyl chlorides viz., benzoyl chloride and chloroacetyl chloride as well as alkyl halides such as allyl bromide, butyl bromide and oxiranyl chloride at the same reaction conditions to give respective compounds **12-16** (Table 2, enteries 6-10) and **17-21** (Table 2, enteries 11-15). The acylation and alkylation were observed selectively only in the NH group of 1*H*-pyrrolo[2,3-*b*]pyridine. This perhaps implies the more reactivity of NH group of 1*H*-pyrrolo[2,3-*b*]pyridine that may be due to the presence of adjacent nitrogen of pyridine ring. It has also been observed that acylation and alkylation of benzothiazole derivatives have been proved to be the suitable reaction component than benzimidazole analogues, due to the requirement of low temperature, and higher yields of products were obtained.

Table 2. Acylation and alkylation 1*H*-pyrrolo[2,3-*b*]pyridine

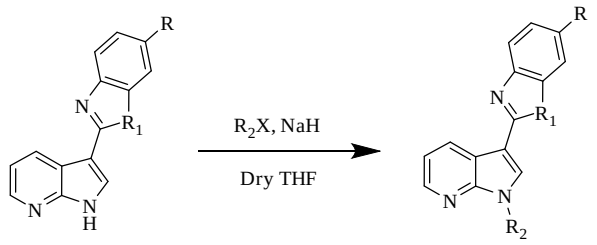

3-6 R = H, Br, NO_2; R_1 = S, NH **7-26**

S.No	Compounds	Reactant	R_2X	Yield (%)	mp (^{0}C)
1	**7**	**3**	benzoyl chloride	85	209-211
2	**8**	**3**	chloroacetyl chloride	79	129-131
3	**9**	**3**	allyl bromide	92	69-71
4	**10**	**3**	butyl bromide	85	99-101
5	**11**	**3**	oxiranyl chloride	82	149-151
6	**12**	**4**	benzoyl chloride	77	209-211
7	**13**	**4**	chloroacetyl chloride	65	159-161
8	**14**	**4**	allyl bromide	82	169-171
9	**15**	**4**	butyl bromide	74	179-181
10	**16**	**4**	oxiranyl chloride	62	169-171
11	**17**	**5**	benzoyl chloride	68	219-221
12	**18**	**5**	chloroacetyl chloride	71	216-218
13	**19**	**5**	allyl bromide	77	171-173
14	**20**	**5**	butyl bromide	72	189-191
15	**21**	**5**	oxiranyl chloride	69	174-176
16	**22**	**6**	benzoyl chloride	81	222-224
17	**23**	**6**	4-nitrobenzoyl chloride	79	249-251
18	**24**	**6**	4-flourobenzoyl chloride	77	209-211
19	**25**	**6**	4-methoxybenzoyl chloride	74	199-201
20	**26**	**6**	chloroacetyl chloride	72	229-231

With excellent results of 1*H*-pyrrolo[2,3-*b*]pyridine in the presence of benzothiazole and benzimidazole, this moiety was further explored with imidazopyridine for acylation and alkylation with different acyl and alkyl halides. Thus, compound **6** was treated with benzoyl chloride in the presence of sodium hydride in THF gave monoacylated product **22** in 81% yield. Substituted acyl chlorides having electron withdrawing groups such as nitro and fluoro as well as an electron releasing group for example, methoxy group at para position were also used to this reaction system and good yield of products were obtained (Table 2, entries 16-20).

Further experiments were conducted to explore the generality and scope of the present protocol by using other alkyl halides. Treatment of compound **3** with benzyl chloride and methyl iodide at the same reaction conditions to give compounds **27a** and **28a** in 88% and 84% yields respectively (Table 3). But, when the alkylation of **4** and **5** were carried out with benzyl chloride and methyl iodide, NH group of benzimidazole was also alkylated. This may be due to the more reactivity of these halides towards both 1*H*-pyrrolo[2,3-*b*]pyridine as well as benzimidazole, and the feasibility for the formation of dialkylation is more than the monoalkylation on comparing with the yields of both the products. On the other hand, treatment of compound **6** with benzyl halides as well as chloro and fluoro substituted benzyl halides at the same reaction conditions, gave monoalkylation and dialkylation products.

Table 3. Monoalkylation and dialkylation 1*H*-pyrrolo[2,3-*b*]pyridine

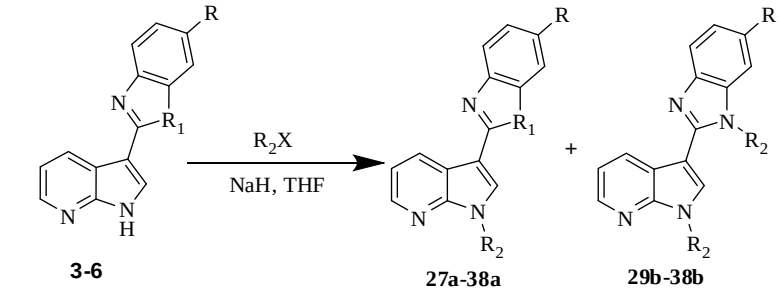

3-6
R = H, Br, NO_2; R_1 = S, NH

27a-38a **29b-38b**

S.No.	Reactant	R_2X	Products (%) Monoalkylation	Dialkylation
1	**3**	benzyl chloride	**27a** (88)	--
2	**3**	methyl iodide	**28a** (84)	--
3	**4**	benzyl chloride	**29a** (< 5)	**29b** (84)
4	**4**	methyl iodide	**30a** (29)	**30b** (68)
5	**5**	benzyl chloride	**31a** (27)	**31b** (73)
6	**5**	methyl iodide	**32a** (<5)	**32b** (81)
7	**6**	benzyl chloride	**33a** (34)	**33b** (69)
8	**6**	4-chlorobenzyl chloride	**34a** (26)	**34b** (69)
9	**6**	3-chlorobenzyl chloride	**35a** (23)	**35b** (62)
10	**6**	2-chloro benzyl chloride	**36a** (19)	**36b** (61)

11	**6**	4-fluorobenzyl chloride	**37a** (33)	**37b** (61)
12	**6**	2-fluorobenzyl chloride	**38a** (32)	**38b** (58)

Suzuki-Miyaura coupling reactions were also performed with compound **6** and aryl boronic acids in the presence of Cs_2CO_3 in 1,4-dioxane using $Pd(PPh_3)_4$ to give arylation at C6 position of imidazopyridine **39-44** in 70-86% yields. A survey of different bases (Cs_2CO_3, Na_2CO_3, K_2CO_3 and DIPEA) and solvents (DMF, THF, toluene, 1,4-dioxane) revealed that Cs_2CO_3 and 1,4-dioxane were found to be the best choice for arylation of imidazopyridine. It has been observed that arylation with unsubstituted phenyl gave higher yield of product than electron donating or electron withdrawing groups, present at phenyl ring (Scheme 1).

Scheme 1[a]. Arylation at C6 position of imidazopyridine functionalized 1*H*-pyrrolo[2,3-*b*]pyridine.

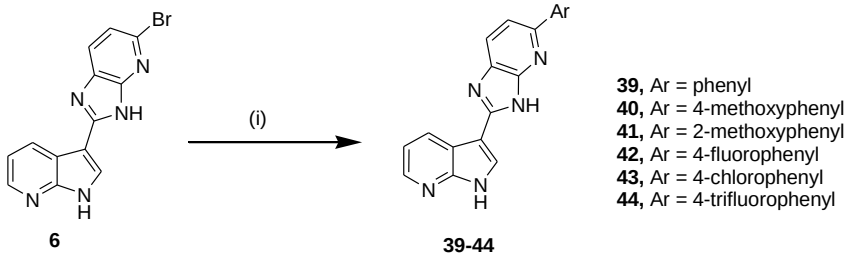

[a]Reagents and conditions: (i) $ArB(OH)_2$, $Pd(PPh_3)_4$, Cs_2CO_3, 1,4-dioxane, reflux.

3.1.3. BIOLOGY

In order to examine the binding modes of compounds **39-44** with ct-DNA, absorption spectral titrations were performed by maintaining constant concentration of compounds at 15 μM and varying the DNA concentration in the range of 0-20 μM. These compounds were selected for DNA binding studies due to presence of aryl group at C6-position of imidazopyridine ring that were contributed for the formation of conjugated backbone, responsible for absorption of photons. In the electronic spectrum of all these tested compounds, an intense band at 322-327 nm was observed, attributed to π-π* transitions. A decrease in absorption intensity i.e. hypochromism was observed in compounds **39-44** with the addition of ct-DNA, that indicates change in the conformation of DNA (compound **39:** 47%, compound **40:** 12%, compound **41:** 16%, compound **42:** 28%, compound **43:** 10% and compound **44:** 31%). No shift in λ_{max} was noticed by incremental addition of DNA for all the tested compounds (Figure 1).

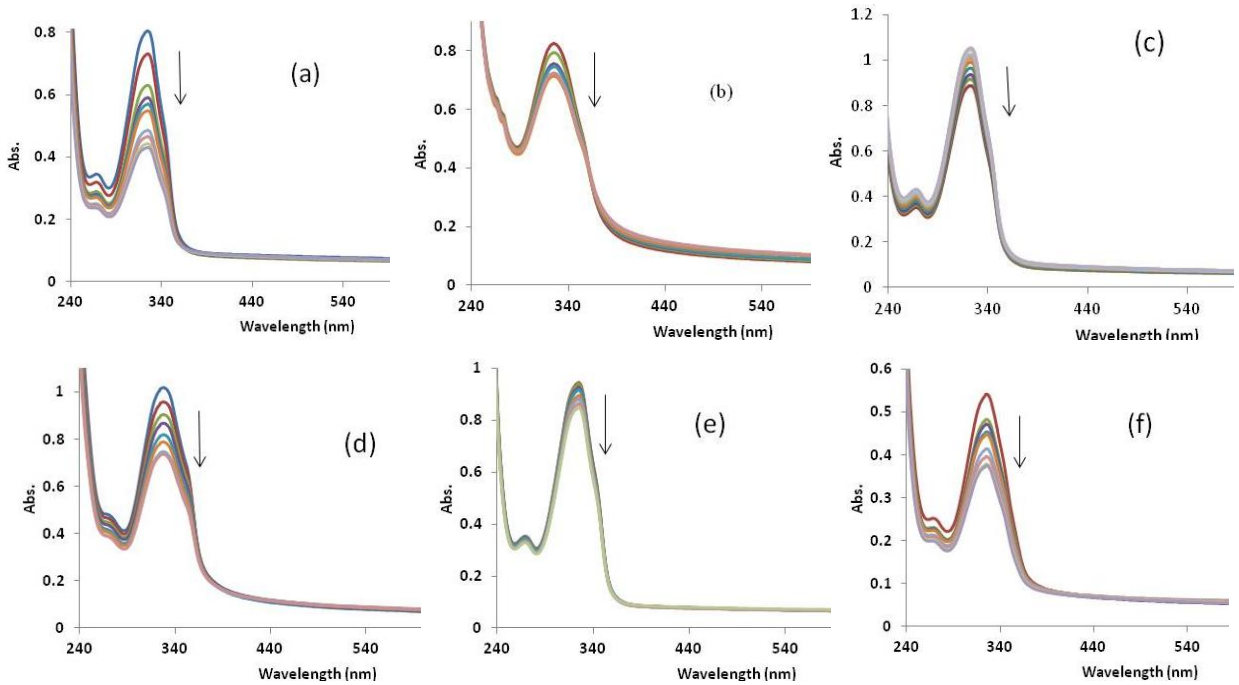

Figure 1. Absorption spectra of compounds (a) **39**; (b) **40**; (c) **41**; (d) **42**; (e) **43**; (f) **44** upon successive addition of ct-DNA.

Fluorescence emission titrations were also carried out with compounds **39-44**; compounds **39** and **44** showed respective 44% and 35% quenching after 8 μM and 10 μM addition of DNA, while compounds **40** and **41** caused enhancement in the fluorescence intensity after gradual addition of DNA (**40** - 30% and **41** - 26%). Compounds **42** and **43** showed no significant changes in their fluorescence emission with addition of DNA (Figure 2). Binding studies of acylated and alkylated 1*H*-pyrrolo[2,3-*b*]pyridine compounds with ct-DNA were also performed but no significant change in absorption and emission spectra were observed. In order to further illustrate the binding strength of the compounds with DNA, the binding constants (K) were determined by monitoring the changes in absorbance and emission intensity at the corresponding λ_{max} with increasing concentration of DNA (Table 4), using Benesi-Hildbrand equation.[85]

Table 4. Binding constants of compounds **39-44** with ct-DNA

Compd	Hypochromism (%)	Quenching/enhancement	K through UV-vis. (M^{-1})	K through fluorescence (M^{-1})
39	47	44 (q)	2.52×10^4	1.91×10^4
40	12	35 (q)	6.50×10^4	1.50×10^4
41	16	30 (e)	2.66×10^5	2.79×10^4
42	28	26 (e)	2.96×10^4	--
43	10	--	3.97×10^4	--
44	31	--	4.72×10^3	9.97×10^3

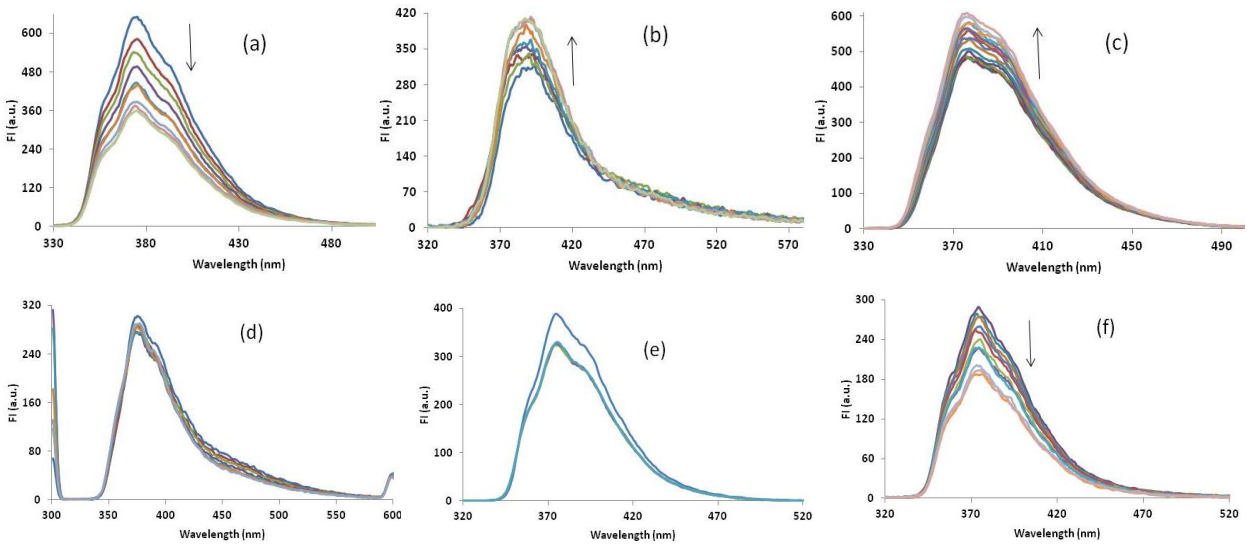

Figure 2. Emission spectra of compounds (a) **39**; (b) **40**; (c) **41**; (d) **42**; (e) **43**; (f) **44** upon successive addition of ct-DNA.

The effect of ionic strength[127] and iodide[128] on the binding of compounds **39-44** with ct-DNA was investigated with UV-Visible and fluorescence spectroscopy. The results indicated that the absorbance and emission intensities of compounds **39**, **42** and **44** were quenched with increasing concentration of Na^+ and I^- (0–10 μM) that signified the electrostatic interaction of compounds with DNA while the absorbance and emission intensities of compounds **40**, **41** and **43** did not give significant change with increasing concentration of Na^+ (Figure **3**) and I^- (Figure **4**) that indicated for their non-electrostatic type of binding to DNA.

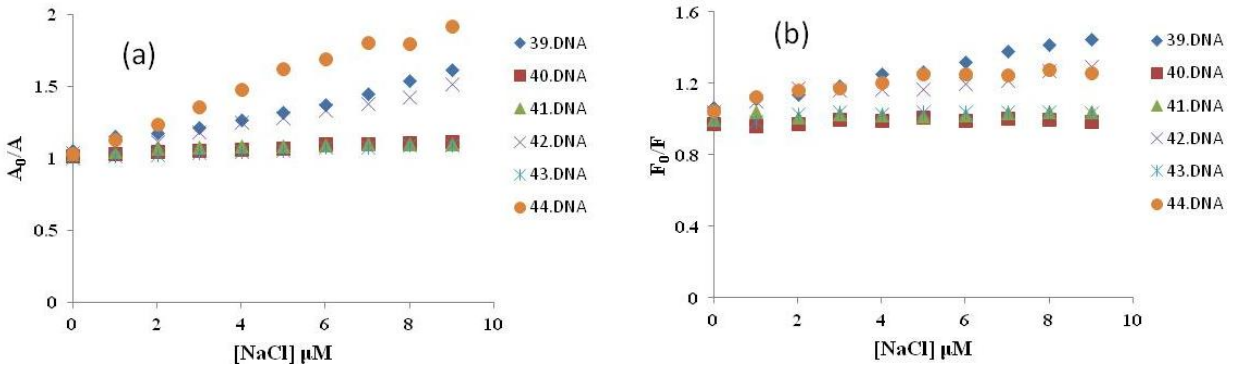

Figure 3. Effects of salt concentration on the (a) absorption and (b) emission spectra of compounds **39-44**.DNA complexes where A_0 or F_0 and A or F are the absorbance or fluorescence intensities of compound in the absence and presence of ct-DNA.

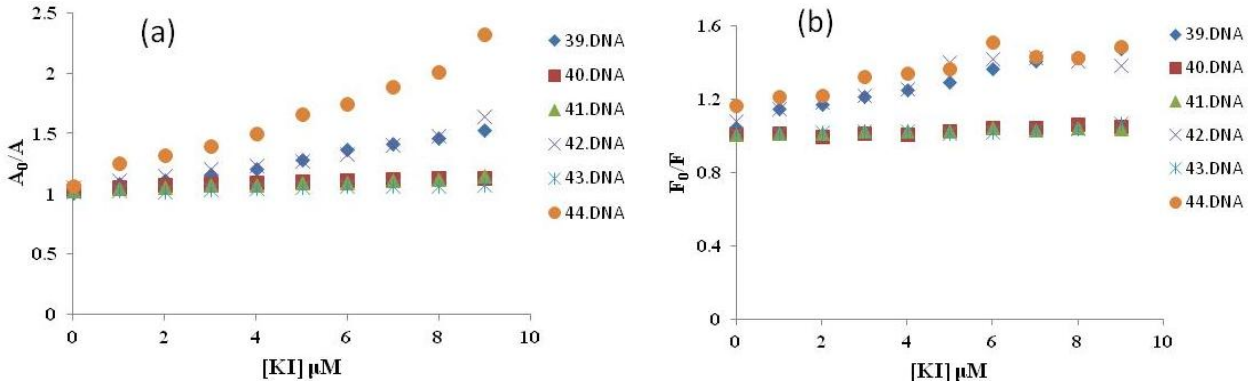

Figure 4. Effects of iodide concentration on the (a) absorption and (b) emission spectra of compounds **39-44**.DNA complex where A_0 or F_0 and A or F are the absorbance or fluorescence intensities of compound in the absence and presence of ct-DNA.

3.1.4. CONCLUSION

We have reported the first benzothiazole, benzimidazole and imidazopyridine mediated 1*H*-pyrrolo[2,3-*b*]pyridine at C3 position. Acylation and alkylation of these 1*H*-pyrrolo[2,3-*b*]pyridine derivatives have been done with varieties of acyl and alkyl halides in moderate to good yields. Palladium catalyzed Suzuki-Miyaura cross-coupling reactions have also been approached for arylation with substituted aryl boronic acids at C6 position of imidazopyridine. Further, UV–visible and fluorescence studies with compounds **39-44**, having aryl groups at C6 position of imidazopyridine, showed significant interactions with ct-DNA. The effect of ionic strength and iodide were also supported for the binding of compounds with ct-DNA. Overall, we believed that these novel series of azole and imidazopyridine functionalizations of 1*H*-pyrrolo[2,3-*b*]pyridine and their binding studies with ct-DNA can be considered as an important advancement in the medicinal and pharmaceutical chemistry.

3.1.5. EXPERIMENTAL SECTION

All chemicals and solvents of commercial grade were used without further purification and were supplied by spectrochemicals and Sigma-Aldrich. Melting points were determined in open capillaries and were uncorrected. ^{1}H and ^{13}C NMR spectra were recorded on Jeol ECS-400 MHz spectrometer at 400 MHz and 100 MHz respectively, using $CDCl_3$, DMSO-d_6 and trifluoroacetic acid (TFA) as solvents. The chemical shifts were expressed in parts per million with TMS as an internal reference and *J* values are given in Hz. Mass spectra of the synthesized compounds were recorded at Waters Micromass Q- Tof Micro. Elemental Analysis has been done with Thermo

Scientific (Flash 2000) analyzer. Reactions were monitored by thin layer chromatography (TLC) with silica plate coated with silica gel HF-254 and column chromatography was performed with silica gel 60-120 mesh. Hexane : ethyl acetate and chloroform : methanol were the adopted solvent systems.

Procedure for the synthesis of 1*H*-Pyrrolo[2,3-*b*]pyridine-3-carboxaldehyde (2).

A solution of 1*H*-pyrrolo[2,3-*b*]pyridine (1 g, 0.008 mol) and hexamethylenetetramine (1.71 g, 0.012 mol) in 3 ml of acetic acid was heated at 110 ^{0}C over a period of 2 h. After the completion of the reaction (monitored by TLC), cold water was added to the reaction mixture. White crystalline solid of 1*H*-pyrrolo[2,3-*b*]pyridine-3-carboxaldehyde **(2)** was separated out (0.680 g, 55%); mp[129] 214-215 ^{0}C.

General procedure for synthesis of compounds (3-6).

1*H*-Pyrrolo[2,3-*b*]pyridine-3-carboxaldehyde (**2**) (1 g, 0.6 mmol) and 2-aminothiophenol /benzene-1,2-diamine/pyridine-2,3-diamine (0.6 mmol) were dissolved in minimum quantity of nitrobenzene and heated to 160 ^{0}C for 15 h. The reaction mixture was cooled to room temperature. The solid was separated out, filtered and washed with diethyl ether. The crude product was further purified by column chromatography on silica gel in hexane : ethylacetate (5:2) as eluents to afford the desired products **3-6**.

2-(1*H*-Pyrrolo[2,3-*b*]pyridine-3-yl)-benzothiazole (**3**).

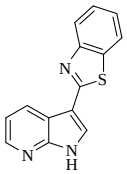

White solid; yield: 89%; mp: 219-221 ^{0}C; ^{1}H NMR (400 MHz, $CDCl_3$): δ = 10.95 (bs, 1H, NH), 8.84 (dd, 1H, ^2J = 9.16 Hz, ^3J = 6.44 Hz, ArH), 8.46 (d, 1H, *J* = 4.56 Hz, ArH), 8.10 (s, 1H, ArH), 8.06 (d, 1H, *J* = 8.28 Hz, ArH), 7.90 (d, 1H, *J* = 7.32 Hz, ArH), 7.49 (t, 1H, *J* = 7.32 Hz, ArH), 7.38-7.32 (m, 2H, ArH); ^{13}C NMR (100 MHz, $CDCl_3$): δ = 162.0, 153.9, 148.8, 144.1, 133.6, 130.4, 126.5, 126.1, 124.5, 121.3, 118.0, 117.8, 111.1 (ArH); MS (ESI), m/z: 252.0 (M^++1); Anal. Calcd for $C_{14}H_9N_3S$: C, 66.91; H, 3.61; N, 16.72; S, 12.76, Found: C, 66.93; H, 3.58; N, 16.73; S, 12.74.

2-(1*H*-Pyrrolo[2,3-*b*]pyridine-3-yl)-1*H*-benzimidazole (4).

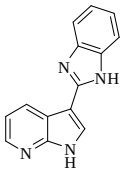

Yellow solid; yield: 75%; mp: 134-136 ^{0}C; ^{1}H NMR (400 MHz, $CDCl_3$): δ = 11.04 (bs, 1H, NH), 8.84 (d, 1H, *J* = 7.76 Hz, ArH), 8.46 (d, 1H, *J* = 4.56 Hz, ArH), 8.10 (s, 1H, ArH), 8.06 (d, 1H, *J* = 7.80 Hz, ArH), 7.90 (d, 1H, *J* = 7.76 Hz, ArH), 7.50 (t, 1H, *J* = 7.32 Hz, ArH), 7.38-7.32 (m, 2H, ArH); ^{13}C NMR (100 MHz, $CDCl_3$): δ = 163.3, 154.3, 150.1, 147.6, 133.6, 130.9, 130.0, 125.7, 123.7, 121.7, 121.2, 120.6, 112.0, 111.8 (ArH);

MS (ESI), m/z: 235.0 (M^++1); Anal. Calcd for $C_{14}H_{10}N_4$: C, 71.78; H, 4.30; N, 23.92, Found: C, 71.48; H, 4.27; N, 23.82.

5-Nitro-2-(1*H*-pyrrolo[2,3-*b*]pyridine-3-yl)-1*H*-benzimidazole (5).

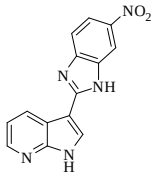

Orange solid; yield: 77%; mp: 149-151 ^{0}C; ^{1}H NMR (400 MHz, $CDCl_3$ + DMSO-d_6): δ = 8.72 (dd, 2H, ^2J = 7.32 Hz, ^3J = 5.96 Hz, ArH), 8.20 (t, 2H, *J* = 5.96 Hz, ArH), 8.18 (bs, 1H, NH), 7.74-7.68 (m, 2H, ArH), 7.04 (d, 1H, *J* = 7.36 Hz, ArH); ^{13}C NMR (100 MHz, $CDCl_3$): δ = 162.0, 153.8, 148.7, 144.1, 133.6, 130.4, 126.5, 126.1, 124.5, 122.4, 122.3, 121.3, 118.0, 117.8, 111.1 (ArH); MS (ESI), m/z: 280.0 (M^++1); Anal. Calcd for $C_{14}H_9N_5O_2$: C, 60.21; H, 3.25; N, 25.08, Found: C, 60.00; H, 3.22; N, 25.01.

5-Bromo-2-(1*H*-pyrrolo[2,3-*b*]pyridine-3-yl)-3*H*-imidazo[4,5-*b*]pyridine (6).

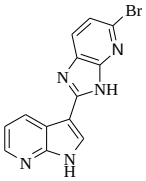

Yellow solid; yield: 78%; mp: 249-251 ^{0}C; ^{1}H NMR (400 MHz, $CDCl_3$): δ = 8.84 (d, 1H, *J* = 7.80 Hz, ArH), 8.46 (bs, 1H, NH), 8.11 (s, 1H, ArH), 8.06 (d, 1H, *J* = 8.28 Hz, ArH), 7.90 (d, 1H, *J* = 7.76 Hz, ArH), 7.50 (t, 1H, *J* = 7.32 Hz, ArH), 7.38-7.32 (m, 1H, ArH); ^{13}C NMR (100 MHz, $CDCl_3$): δ = 162.0, 153.8, 148.7, 144.1, 133.6, 130.4, 126.5, 126.1, 124.5, 122.3, 121.3, 118.0, 117.8, 111.1; MS (ESI), m/z: 314.0 (M^++1); Anal. Calcd for $C_{13}H_8BrN_5$: C, 49.70; H, 2.57; N, 22.29, Found: C, 50.00; H, 2.56; N, 22.43.

General procedure for the synthesis of compounds 7-38.

To the suspension of sodium hydride (60% in mineral oil, 1.19 mmol) in dry THF (20 ml), 2-(1*H*-pyrrolo[2,3-*b*]pyridine-3-yl)-azoles (**3-6**) (0.8 mmol), and acyl/alkyl halides (1.1 mmol) were added under nitrogen atmosphere. The reaction mixture was stirred at 0-100 ^{0}C for 2 h. The reaction was poured into water and extracted with chloroform. The organic layer was washed with brine, dried over anhydrous sodium sulphate and filtered. The filtrate was concentrated to get the crude product. The crude was purified by column chromatography eluting 5% methanol in chloroform to afford the desired products **7-38.**

(3-Benzothiazol-2-yl-pyrrolo[2,3-*b*]pyridine-1-yl)-phenyl-methanone (7).

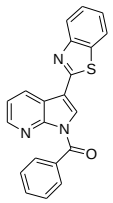

White solid; yield: 85%; mp: 209-211 ^{0}C; ^{1}H NMR (400 MHz, $CDCl_3$): δ = 8.83 (d, 1H, *J* = 7.36 Hz, ArH), 8.39 (s, 1H, ArH), 8.11-8.01 (m, 3H, ArH), 7.88 (d, 2H, *J* = 8.24 Hz, ArH), 7.49-7.30 (m, 6H, ArH); ^{13}C NMR (100 MHz, $CDCl_3$): δ = 162.0, 153.8, 148.3, 142.8, 133.6, 131.2, 129.8, 128.3, 127.0, 126.1, 124.5, 122.3, 121.3, 118.6, 117.5, 110.9 (ArH); MS (ESI), m/z: 356.0 (M^++1); Anal. Calcd for $C_{21}H_{13}N_3OS$: C, 70.97; H, 3.69; N, 11.82; S, 9.02, Found: C, 70.78; H, 3.66; N, 11.83; S, 9.0.

1-(3-Benzothiazol-2-yl-pyrrolo[2,3-*b*]pyridine-1-yl)-2-chloro-ethanone (8).

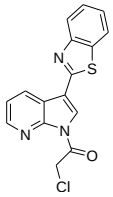

Green solid; yield: 79%; mp: 129-131 ^{0}C; ^{1}H NMR (400 MHz, $CDCl_3$): δ = 9.01 (d, 1H, *J* = 7.76 Hz, ArH), 8.30 (d, 1H, *J* = 1.04 Hz, ArH), 8.06 (d, 2H, *J* = 5.04 Hz, ArH), 7.90 (d, 1H, *J* = 4.24 Hz. ArH), 7.49 (t, 1H, *J* = 7.36 Hz, ArH), 7.40-7.35 (m, 2H, ArH), 4.21 (s, 2H, aliph-CH_2); ^{13}C NMR (100 MHz, $CDCl_3$): δ = 172.7, 161.4, 153.8, 146.6, 140.6, 133.6, 133.0, 127.5, 126.2, 124.7, 122.4, 121.4, 119.7, 117.4, 111.3 (ArH), 42.0 (CH_2); MS (ESI), m/z: 328.0 (M^++1); Anal. Calcd for $C_{16}H_{10}ClN_3OS$: C, 58.63; H, 3.07; N, 12.82; S, 9.78, Found: C, 58.71; H, 3.05; N, 12.84; S, 9.60.

2-(1-Allyl-1*H*-pyrrolo[2,3-*b*]pyridine-3-yl)-benzothiazole (9).

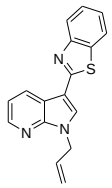

Yellow solid; yield: 92%; mp: 69-71 ^{0}C; ^{1}H NMR (400 MHz, $CDCl_3$): δ = 9.02 (d, 1H, *J* = 7.36 Hz, ArH), 8.44 (s, 1H, ArH), 7.96 (d, 1H, *J* = 7.80 Hz, ArH), 7.82 (d, 1H, *J* = 7.76 Hz, ArH), 7.72 (d, 1H, *J* = 5.96 Hz, ArH), 7.41 (t, 1H, *J* = 6.88 Hz, ArH), 7.28-7.23 (m, 1H, ArH), 7.13 (t, 1H, *J* = 5.96 Hz, ArH), 6.19-6.09 (m, 1H, allyl-CH), 5.39-5.28 (m, 4H, allyl-CH_2); ^{13}C NMR (100 MHz, $CDCl_3$): δ = 163.3, 154.3, 150.1, 147.6, 133.6, 133.4, 130.9, 130.0, 127.3, 125.7, 123.7, 121.7, 121.2, 120.6, 112.0, 111.8 (ArH), 54.8 (N-CH_2); MS (ESI), m/z: 292.0 (M^++1); Anal. Calcd for $C_{17}H_{13}N_3S$: C, 70.08; H, 4.50; N, 14.42; S, 11.00, Found: C, 70.10; H, 4.46; N, 14.43; S, 10.85.

2-(1-Butyl-1*H*-pyrrolo[2,3-*b*]pyridine-3-yl)-benzothiazole (10).

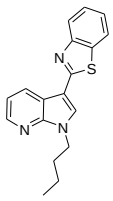

Yellow solid; yield: 85%; mp: 99-101 ^{0}C; ^{1}H NMR (400 MHz, $CDCl_3$): δ = 9.06 (d, 1H, *J* = 7.32 Hz, ArH), 8.47 (s, 1H, ArH), 7.98 (d, 1H, *J* = 7.80 Hz, ArH), 7.85 (d, 1H, *J* = 7.76 Hz, ArH), 7.75 (d, 1H, *J* = 5.96 Hz, ArH), 7.45 (t, 1H, *J* = 7.36 Hz, ArH), 7.31-7.27 (m, 1H, ArH), 7.15 (t, 1H, *J* = 6.84 Hz, ArH), 4.75 (t, 2H, *J* = 7.32 Hz, N-CH_2), 2.10-2.02 (m, 2H, CH_2), 1.46-1.39 (m, 2H, CH_2), 0.99 (t, 3H, *J* = 7.36 Hz, CH_3); ^{13}C NMR (100 MHz, $CDCl_3$): δ = 163.2, 154.2, 153.8, 149.5, 146.7, 133.7, 133.4, 130.8, 125.7, 123.8, 122.3, 121.7, 121.2, 112.2, 111.6 (ArH), 53.9 (N-CH_2), 31.7 (CH_2), 19.9 (CH_2), 13.6 (CH_3); MS (ESI), m/z: 308.1 (M^++1); Anal. Calcd for $C_{18}H_{17}N_3S$: C, 70.33; H, 5.57; N, 13.67; S, 10.43, Found: C, 70.22; H, 5.51; N, 13.63; S, 10.29.

2-(1-Oxiranylmethyl-1*H*-pyrrolo[2,3-*b*]pyridine-3-yl)-benzothiazole (11).

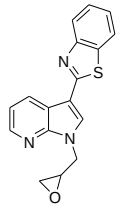

White solid; yield: 82%; mp: 149-151 ^{0}C; ^{1}H NMR (400 MHz, $CDCl_3$ + DMSO-d_6): δ = 8.78 (t, 1H, *J* = 8.28 Hz, ArH), 8.40 (t, 1H, *J* = 4.60 Hz, ArH), 8.03 (d, 2H, *J* = 8.24 Hz, ArH), 7.99 (s, 1H, ArH), 7.87 (d, 1H, *J* = 7.80 Hz, ArH), 7.49 (t, 1H, *J* = 8.20 Hz, ArH), 7.37 (t, 1H, *J* = 8.24 Hz, ArH), 4.65-4.62 (m, 3H, CH, CH_2), 4.65 -4.62 (m, 3H, CH, CH_2), 4.47-4.42 (m, 2H, CH_2); ^{13}C NMR (100 MHz, $CDCl_3$ + TFA): δ =163.9, 140.2, 140.1, 138.1, 137.1, 137.0, 136.6, 131.1, 129.4, 128.7, 123.1, 122.6, 119.5, 117.9, 116.1, 113.2, 105.0 (ArH), 69.4 (N-CH_2), 51.2 (CH_2); MS (ESI), m/z: 308.0 (M^++1); Anal. Calcd for $C_{17}H_{13}N_3OS$: C, 66.43; H, 4.26; N, 13.67; S, 10.43, Found: C, 66.23; H, 4.23; N, 13.63; S, 10.31.

3-(1*H*-Benzimidazol-2-yl)-pyrrolo[2,3-*b*]pyridine-3-yl]-phenyl-methanone (12).

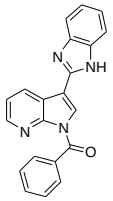

White solid; yield: 77%; mp: 209-211 ^{0}C; ^{1}H NMR (400 MHz, $CDCl_3$ + DMSO-d_6): δ = 10.81 (bs, 1H, NH), 8.86 (d, 2H, *J* = 7.80 Hz, ArH), 8.38 (d, 2H, *J* = 3.68 Hz, ArH), 8.14 (s, 2H, ArH), 7.58-7.50 (m, 3H, ArH), 7.13-6.97 (m, 4H, ArH); ^{13}C NMR (100 MHz, $CDCl_3$): δ = 168.4, 167.4, 154.0, 140.3, 134.8, 129.4, 129.3, 129.1, 128.4, 126.3, 125.0, 122.9, 121.5, 119.6 (ArH); MS (ESI), m/z: 339.1 (M^++1); Anal. Calcd for $C_{21}H_{14}N_4O$: C, 74.54; H, 4.17; N, 16.56, Found: C, 74.33; H, 4.12; N, 16.51.

1-[3-(1*H*-Benzimidazol-2-yl)-pyrrolo[2,3-b]pyridine-3-yl]-2-chloro-ethanone (13).

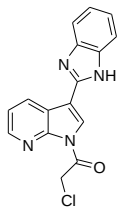

Yellow solid; yield: 65%; mp: 159-161 ^{0}C; ^{1}H NMR (400 MHz, $CDCl_3$): δ = 10.09 (s, 1H, NH), 8.32 (q, 1H, *J* = 4.60 Hz, ArH), 7.93 (s, 1H, ArH), 7.82-7.80 (m, 1H, ArH), 7.72 (q, 1H, *J* = 7.80 Hz, ArH), 7.46-7.44 (m, 1H, ArH), 7.34 (s, 1H, ArH), 7.30-7.27 (m, 1H, ArH), 7.07-7.03 (m, 1H, ArH), 5.51 (s, 2H, CH_2); ^{13}C NMR (100 MHz, $CDCl_3$): δ = 168.7, 152.6, 142.1, 135.6, 133.4, 133.1, 132.7, 132.5, 129.1, 128.2, 128.1, 126.3, 116.9, 110.8, 109.5 (ArH), 47.3 (CH_2); MS (ESI), m/z: 311.0 (M^++1); Anal. Calcd for $C_{16}H_{11}ClN_4O$: C, 61.84; H, 3.57; N, 18.03, Found: C, 61.93; H, 3.54; N, 18.00.

2-(1-Allyl-1*H*-pyrrolo[2,3-*b*]pyridine-3-yl)-1*H*-benzimidazole (14).

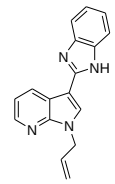

Yellow solid; yield: 82%; mp: 169-171 ^{0}C; ^{1}H NMR (400 MHz, $CDCl_3$): δ = 7.98 (s, 1H, ArH), 7.89 (s, 1H, ArH), 7.80-7.77 (m, 2H, ArH, NH), 7.67 (d, 1H, *J* = 5.96 Hz, ArH), 7.51-7.49 (m, 1H, ArH), 7.29-7.27 (m, 2H, ArH), 6.87 (t, 1H, *J* = 6.40 Hz, ArH), 6.18-6.11 (m, 1H, allyl-CH), 5.56 (d, 2H, *J* = 4.56 Hz, allyl-CH_2), 5.41-5.33 (m, 2H, allyl-CH_2); ^{13}C NMR (100 MHz, $CDCl_3$): δ = 152.6, 142.1, 135.6, 133.4, 133.1,

132.7, 132.5, 129.1, 128.2, 128.1, 126.3, 116.9, 110.8, 109.5 (ArH), 47.3 (N-CH_2); MS (ESI), m/z: 275.1 (M^++1); Anal. Calcd for $C_{17}H_{14}N_4$: C, 74.43; H, 5.14; N, 20.42, Found: C, 74.25; H, 5.10; N, 20.36.

2-(1-Butyl-1*H*-pyrrolo[2,3-*b*]pyridine-3-yl)-1*H*-benzimidazole (15).

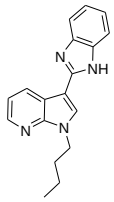

Brown solid; yield: 74%; mp: 179-181 ^{0}C; ^{1}H NMR (400 MHz, $CDCl_3$): δ = 7.97 (s, 1H, ArH), 7.89 (s, 1H, ArH), 7.81-7.76 (m, 2H, ArH, NH), 7.63 (d, 1H, *J* = 5.96 Hz, ArH), 7.52-7.50 (m, 1H, ArH), 7.29-7.27 (m, 3H, ArH), 4.68 (t, 2H, *J* = 7.32 Hz, N-CH_2), 2.07-2.01 (m, 2H, CH_2), 1.46-1.40 (m, 2H, CH_2), 0.99 (t, 3H, *J* =7.32 Hz, CH_3); ^{13}C NMR (100 MHz, $CDCl_3$): δ = 148.7, 144.8, 143.8, 143.5, 142.7, 133.9, 129.8, 129.3, 128.5, 126.8, 122.7, 122.0, 120.1, 110.0, 109.5, 108.4 (ArH), 53.4 (N-CH_2), 41.0 (CH_2), 19.9 (CH_2), 13.5 (CH_3); MS (ESI), m/z: 291.1 (M^++1); Anal. Calcd for $C_{18}H_{18}N_4$: C, 74.46; H, 6.25; N, 19.30, Found: C, 74.38; H, 6.20; N, 19.24.

2-(1-Oxiranylmethyl-1*H*-pyrrolo[2,3-*b*]pyridine-3-yl)-1*H*-benzimidazole (16).

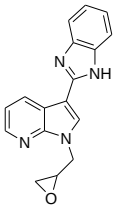

Yellow solid; yield: 62%; mp: 169-171 ^{0}C; ^{1}H NMR (400 MHz, $CDCl_3$): δ = 9.17 (bs, 1H, NH), 9.09 (d, 1H, *J* = 8.24 Hz, ArH), 8.93 (s, 1H, ArH), 8.67 (d, 1H, *J* = 5.96 Hz, ArH), 8.17 (d, 1H, *J* = 8.24 Hz, ArH), 8.12 (d, 1H, *J* = 8.24 Hz, ArH), 7.96-7.89 (m, 2H, ArH), 7.84 (t, 1H, *J* = 7.80 Hz, ArH), 5.38-5.36 (m, 1H, CH), 5.10 (d, 2H, *J* = 12.84 Hz, CH_2), 4.88-4.78 (m, 2H, CH_2); ^{13}C NMR (100 MHz, $CDCl_3$): δ = 148.5, 144.5, 143.8, 142.7, 133.9, 130.8, 129.6, 129.5, 128.4, 122.7, 122.0, 120.6, 120.1, 110.0, 109.9, 108.8 (ArH), 54.6 (CH_2), 41.0 (CH_2); MS (ESI), m/z: 291.1 (M^++1); Anal. Calcd for $C_{17}H_{14}N_4O$: C, 70.33; H, 4.86; N, 19.30, Found: C, 70.10; H, 4.82; N, 19.35.

3-(5-Nitro-1*H*-benzimidazol-2-yl)-pyrrolo[2,3-*b*]pyridine-3-yl]-phenyl-methanone (17).

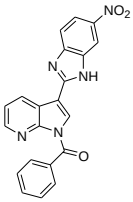

Yellow solid; yield: 68%; mp: 219-221 ^{0}C; ^{1}H NMR (400 MHz, $CDCl_3$): δ = 8.34-8.31 (m, 1H, ArH), 8.25 (d, 1H, *J* = 7.80 Hz, ArH), 8.15-8.11 (m, 3H, ArH), 7.85 (t, 1H, *J* = 6.88 Hz, ArH), 7.69 (d, 1H, *J* = 7.80 Hz, ArH), 7.54 (t, 1H, *J* = 7.80 Hz, ArH), 7.22-7.13 (m, 4H, ArH); ^{13}C NMR (100 MHz, $CDCl_3$): δ = 163.0, 162.9, 154.2, 149.8, 146.4, 146.3, 146.1, 134.2, 133.5, 131.8, 127.0, 125.8, 123.9, 121.8, 117.7, 112.4, 111.9 (ArH); MS (ESI), m/z: 384.1 (M^++1); Anal. Calcd for $C_{21}H_{13}N_5O_3$: C, 65.79; H, 3.42; N, 18.27, Found: C, 65.62; H, 3.39; N, 18.22.

2-Chloro-1-[3-(5-nitro-1*H*-benzimidazol-2-yl)-pyrrolo[2,3-*b*]pyridine-3-yl]-ethanone (18).

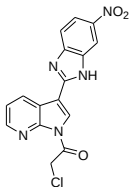

Yellow solid; yield: 71%; mp: 216-218 ^{0}C; ^{1}H NMR (400 MHz, DMSO-d_6): δ = 8.52 (d, 2H, *J* = 8.28 Hz, ArH), 8.01 (d, 1H, *J* = 1.84 Hz, ArH), 7.98 (d, 1H, *J* = 1.36 Hz, ArH), 7.63 (t, 2H, *J* = 8.18 Hz, ArH), 7.21 (t, 1H, *J* = 7.80 Hz, ArH), 4.43 (s, 2H, CH_2); ^{13}C NMR (100 MHz, $CDCl_3$): δ = 148.5, 144.5, 143.8, 142.7, 130.8, 129.6, 129.5, 128.4, 122.7, 122.0, 120.6, 120.1, 110.0, 109.9, 108.8 (ArH), 41.0 (CH_2); MS (ESI), m/z: 356.0 (M^++1); Anal. Calcd for $C_{16}H_{10}ClN_5O_3$: C, 54.02; H, 2.83; N, 19.69, Found: C, 54.08; H, 2.81; N, 19.71.

2-(1-Allyl-1*H*-pyrrolo[2,3-*b*]pyridine-3-yl)-5-nitro-1*H*-benzimidazole (19).

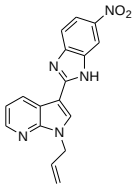

Yellow solid; yield: 77%; mp: 171-173 ^{0}C; ^{1}H NMR (400 MHz, $CDCl_3$): δ = 8.22-8.19 (m, 1H, ArH), 8.08 (d, 1H, *J* = 3.20 Hz, ArH), 8.01 (m, 1H, ArH), 7.85-7.83 (m, 1H, ArH), 7.72-7.69 (m, 1H, ArH), 7.55 (d, 1H, *J* = 9.16 Hz, ArH), 6.93-6.86 (m, 1H, ArH), 6.20-6.10 (m, 1H, allyl-CH), 5.64 (d, 1H, *J* = 7.80 Hz, allyl-CH_2), 5.42-5.32 (m, 3H, allyl-CH_2); ^{13}C NMR (100 MHz, $CDCl_3$): δ = 149.2, 147.1, 146.1, 145.6, 143.6, 143.3, 138.0, 130.8, 129.6, 129.2, 120.7, 120.4, 118.6, 117.9, 117.1, 110.0, 109.9, 107.5, 107.0 (ArH), 54.6 (N-CH_2); MS (ESI), m/z: 320.1 (M^++1); Anal. Calcd for $C_{17}H_{13}N_5O_2$: C, 63.94; H, 4.10; N, 21.93, Found: C, 63.75; H, 4.07; N, 21.87.

2-(1-Butyl-1*H*-pyrrolo[2,3-*b*]pyridine-3-yl)-5-nitro-1*H*-benzimidazole (20).

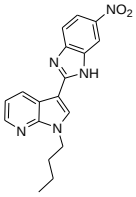

Brown solid; yield: 72%; mp: 189-191 ^{0}C; ^{1}H NMR (400 MHz, $CDCl_3$): δ = 8.47 (s, 1H, NH), 7.98 (d, 1H, *J* = 7.80 Hz, ArH), 7.85 (d, 1H, *J* = 7.76 Hz, ArH), 7.75 (d, 1H, *J* = 5.96 Hz, ArH), 7.47-7.41 (m, 1H, ArH), 7.39-7.27 (m, 2H, ArH), 7.16 (t, 1H , *J* = 6.84 Hz, ArH), 4.75 (t, 2H, *J* = 7.32 Hz, N-CH_2), 2.10-2.02 (m, 2H, CH_2), 1.46-1.39 (m, 2H, CH_2), 0.99 (t, 3H, *J* = 7.36 Hz, CH_3); ^{13}C NMR (100 MHz, $CDCl_3$): δ = 163.4, 163.2, 163.0, 154.2, 153.8, 149.5, 146.7, 133.7, 133.4, 130.8, 125.7, 123.8, 121.7, 121.2, 112.2, 111.6 (ArH), 53.9 (N-CH_2), 31.7 (CH_2), 19.9 (CH_2), 13.6 (CH_3); MS (ESI), m/z: 336.1 (M^++1); Anal. Calcd for $C_{18}H_{17}N_5O_2$: C, 64.47; H, 5.11; N, 20.88, Found: C, 64.28; H, 5.07; N, 20.83.

5-Nitro-2-(1-oxiranylmethyl-1*H*-pyrrolo[2,3-*b*]pyridine-3-yl)-1*H*-benzimidazole (21).

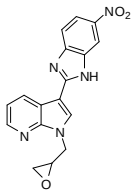

Yellow solid; yield: 69%; mp: 174-176 ^{0}C; ^{1}H NMR (400 MHz, $CDCl_3$ + DMSO-d_6): δ = 8.67-8.64 (m, 1H, ArH), 8.31 (d, 1H, *J* = 7.80 Hz, ArH), 7.81 (t, 1H, *J* = 7.80 Hz, ArH), 7.40 (d, 1H, *J* = 8.24 Hz, ArH), 7.07 (d, 1H, *J* = 8.24 Hz, ArH), 6.81 (d, 2H, *J* = 8.24 Hz, ArH), 4.42-4.38 (m, 2H, CH_2), 4.09-4.07 (m, 2H, CH_2), 3.61-

3.60 (m, 1H, CH); ^{13}C NMR (100 MHz, TFA+DMSO-d_6+$CDCl_3$): δ = 165.3, 150.2, 140.8, 139.6, 137.1, 136.5, 133.3, 130.7, 122.0, 119.0, 113.8 (ArH), 62.0 (CH_2), 40.0 (CH_2); MS (ESI), m/z: 336.1 (M^++1); Anal. Calcd for $C_{17}H_{13}N_5O_3$: C, 60.89; H, 3.91; N, 20.89, Found: C, 60.71; H, 3.86; N, 20.83.

2-(1-Benzyl-1*H*-pyrrolo[2,3-*b*]pyridine-3-yl)-benzothiazole (22a).

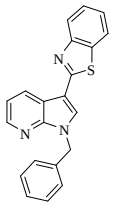

Yellow solid; yield: 88%; mp: 149-151 ^{0}C; ^{1}H NMR (400 MHz, $CDCl_3$): δ = 9.06 (d, 1H, *J* = 6.44 Hz, ArH), 8.83 (d, 1H, *J* = 7.80 Hz, ArH), 8.52 (s, 1H, ArH), 8.08-8.04 (m, 1H, ArH), 7.99 (d, 1H, *J* = 8.24 Hz, ArH), 7.90 (d, 1H, *J* = 7.80 Hz, ArH), 7.86 (d, 1H, *J* = 7.76 Hz, ArH), 7.71 (d, 1H, *J* = 6.44 Hz, ArH), 7.50-7.41 (m, 1H, ArH), 7.38-7.29 (m, 3H, ArH), 7.13 (t, 1H, *J* = 5.96 Hz, ArH), 5.96 (s, 2H, N-CH_2); ^{13}C NMR (100 MHz, $CDCl_3$): δ = 163.3, 154.3, 153.9, 150.6, 147.8, 134.4, 133.5, 130.2, 129.1, 128.8, 128.5, 127.4, 125.7, 123.7, 121.7, 121.2, 112.1, 111.9 (ArH), 55.8 (N-CH_2); MS (ESI), m/z: 342.0 (M^++1); Anal. Calcd for $C_{21}H_{15}N_3S$: C, 73.87; H, 4.43; N, 12.31; S, 9.39, Found: C, 73.68; H, 4.39; N, 12.28; S, 9.30.

2-(1-Methyl-1*H*-pyrrolo[2,3-*b*]pyridine-3-yl)-benzothiazole (23a).

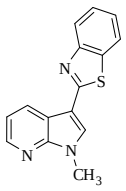

Yellow solid; yield: 84%; mp: 219-221 ^{0}C; ^{1}H NMR (400 MHz, $CDCl_3$): δ = 9.09 (d, 1H, *J* = 7.32 Hz, ArH), 8.47 (s, 1H, ArH), 7.99 (d, 1H, *J* = 8.28 Hz, ArH), 7.86 (d, 1H, *J* = 8.24 Hz, ArH), 7.76 (d, 1H, *J* = 5.96 Hz, ArH), 7.46 (t, 1H, *J* = 1.40 Hz, ArH), 7.32 (t, 1H, *J* = 7.32 Hz, ArH), 7.18-7.14 (m, 1H, ArH), 4.39 (s, 3H, CH_3); ^{13}C NMR (100 MHz, $CDCl_3$): δ = 163.0, 154.2, 149.8, 146.4, 134.2, 133.5, 131.8, 127.0, 125.8, 123.9, 121.8, 121.2, 112.4, 111.9 (ArH), 40.9 (N-CH_3); EIMS, m/z: 266.0 (M^++1); Anal. Calcd for $C_{15}H_{11}N_3S$: C, 67.90; H, 4.18; N, 15.84; S, 12.08, Found: C, 67.66; H, 4.15; N, 15.74; S, 12.01.

1-Benzyl-2-(1-benzyl-1*H*-pyrrolo[2,3-*b*]pyridine-3-yl)-1H-benzimidazole (24b).

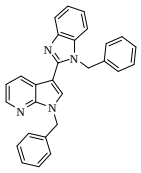

Yellow solid; yield: 84%; mp: 199-201 ^{0}C; ^{1}H NMR (400 MHz, $CDCl_3$): δ = 8.00 (s, 1H, ArH), 7.94 (s, 1H, ArH), 7.80 (d, 3H, *J* = 7.76 Hz, ArH), 7.63 (d, 1H, *J* = 5.96 Hz, ArH), 7.51-7.48 (m, 1H, ArH), 7.35-7.32 (m, 7H, ArH), 7.30-7.24 (m, 3H, ArH), 6.85 (t, *J* = 6.40 Hz, 1H, ArH), 5.91 (s, 2H, N-CH_2), 5.56 (s, 2H, N-CH_2); ^{13}C NMR (100 MHz, $CDCl_3$): δ = 147.9, 143.1, 142.7, 133.9, 130.1, 129.2, 128.9, 128.7, 128.2, 122.9, 122.2, 120.2, 110.7, 110.0, 109.1 (ArH), 56.0 (N-CH_2), 41.0 (N-CH_2); MS (ESI), m/z: 415.1 (M^++1); Anal. Calcd for $C_{28}H_{22}N_4$: C, 81.13; H, 5.35; N, 13.52, Found: C, 81.15; H, 5.31;

N, 13.48.

2-(1-Methyl-1*H*-pyrrolo[2,3-*b*]pyridine-3-yl)-1*H*-benzimidazole (25a).

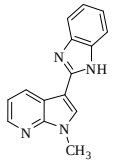

Yellow solid; yield: 29%; mp: 190-192 ^{0}C; ^{1}H NMR (400 MHz, $CDCl_3$): δ = 9.09 (d, 1H, *J* = 7.32 Hz, ArH), 8.47 (s, 1H, ArH), 7.99 (d, 1H, *J* = 8.28 Hz, ArH), 7.86 (d, 1H, *J* = 8.24 Hz, ArH), 7.76 (d, 1H, *J* = 5.96 Hz, ArH), 7.46 (t, 1H, *J* = 1.40 Hz, ArH), 7.32 (t, 1H, *J* = 7.32 Hz, ArH), 7.18-7.14 (m, 1H, ArH), 4.39 (s, 3H, N-CH_3); ^{13}C NMR (100 MHz, $CDCl_3$): δ = 150.3, 149.7, 144.8, 143.5, 136.0, 134.4, 131.5, 128.9, 122.3, 122.1, 118.7, 112.1, 110.7, 106.2 (ArH), 41.4 (N-CH_3); MS (ESI), m/z: 249.1 (M^++1); Anal. Calcd for $C_{15}H_{12}N_4$: C, 72.56; H, 4.87; N, 22.57, Found: C, 72.38; H, 4.83; N, 22.48.

1-Methyl-2-(1-methyl-1*H*-pyrrolo[2,3-*b*]pyridine-3-yl)-1*H*-benzimidazole (25b).

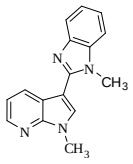

Yellow solid; yield: 68%; mp: 215-217 ^{0}C; ^{1}H NMR (400 MHz, $CDCl_3$): δ = 9.01 (d, 1H, *J* = 7.80 Hz, ArH), 8.30 (s, 1H, ArH), 8.09 (s, 1H, ArH), 7.81-7.71 (m, 2H, ArH), 7.39-7.34 (m, 1H, ArH), 7.28-7.23 (m, 1H, ArH), 7.12-7.08 (m, 1H, ArH), 4.38 (s, 3H, N-CH_3), 4.01 (s, 3H, N-CH_3); ^{13}C NMR (100 MHz, $CDCl_3$): δ = 150.3, 149.7, 145.0, 143.5, 134.4, 131.5, 128.9, 122.3, 122.1, 121.2, 118.7, 112.1, 110.7, 106.2 (ArH), 41.4 (N-CH_3), 40.6 (N-CH_3); MS (ESI), m/z: 263.1 (M^++1); Anal. Calcd for $C_{16}H_{14}N_4$: C, 73.26; H, 5.38; N, 21.36, Found: C, 73.00; H, 5.34; N, 21.27.

2-(1-Benzyl-1*H*-pyrrolo[2,3-*b*]pyridine-3-yl)-5-nitro-1*H*-benzimidazole (26a).

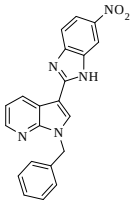

Yellow solid; yield: 27%; mp: 134-136 ^{0}C; ^{1}H NMR (400 MHz, $CDCl_3$): δ = 8.59 (d, 2H, *J* = 2.28 Hz, ArH), 8.16 (s, 1H, ArH), 7.72 (d, 1H, *J* = 2.28 Hz, ArH), 7.41-7.34 (m, 6H, ArH, NH), 7.19-7.17 (m, 3H, ArH), 5.34 (s, 2H, N-CH_2); ^{13}C NMR (100 MHz, $CDCl_3$): δ = 154.8, 146.1, 146.0, 134.3, 133.9, 133.8, 129.8, 129.4, 129.2, 128.9, 128.8, 127.0, 120.8, 114.2 (ArH), 49.5 (CH_2); MS (ESI), m/z: 370.1 (M^++1); Anal. Calcd for $C_{21}H_{15}N_5O_2$: C, 68.28; H, 4.09; N, 18.96, Found: C, 68.40; H, 4.06; N, 18.91.

1-Benzyl-2-(1-benzyl-1*H*-pyrrolo[2,3-*b*]pyridine-3-yl)-5-nitro-1*H*-benzimidazole (26b).

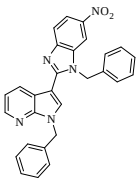

Yellow solid; yield: 73%; mp: 172-174 ^{0}C; ^{1}H NMR (400 MHz, $CDCl_3$): δ = 9.18 (d, 1H, *J* = 7.32 Hz, ArH), 8.94 (s, 1H, ArH), 8.06 (s, 1H, ArH), 7.70 (d, 1H, *J* = 6.44 Hz, ArH), 7.57 (d, 1H, *J* = 0.92 Hz, ArH), 7.49 (d, 1H, *J* = 4.12 Hz, ArH), 7.47 (d, 1H, *J* = 2.28 Hz, ArH), 7.40-7.34 (m, 9H, ArH), 7.13 (t, 1H, *J* = 7.76 Hz, ArH), 5.96 (s, 2H, N-CH_2), 5.83 (s, 2H, N-CH_2); ^{13}C NMR (100 MHz, $CDCl_3$): δ = 148.5, 144.5, 143.8,

142.7, 133.2, 130.8, 129.6, 129.5, 128.4, 126.5, 126.4, 122.7, 122.0, 120.6, 120.1, 110.0, 109.9, 108.8 (ArH), 54.6 (N-CH_2), 41.0 (N-CH_2); MS (ESI), m/z: 460.1 (M^++1); Anal. Calcd for $C_{28}H_{21}N_5O_2$: C, 73.19; H, 4.61; N, 15.24, Found: C, 73.04; H, 4.57; N, 15.21.

1-Methyl-2-(1-methyl-1*H*-pyrrolo[2,3-*b*]pyridine-3-yl)-5-nitro-1*H*-benzimidazole (27b).

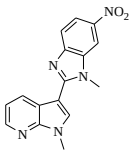

Orange solid; yield: 81%; mp: 189-191 ^{0}C; ^{1}H NMR (400 MHz, $CDCl_3$): δ = 9.16 (t, 1H, *J* = 8.24 Hz, ArH), 8.41-8.37 (m, 1H, ArH), 8.22 (d, 1H, *J* = 2.28 Hz, ArH), 7.83 (d, 1H, *J* = 5.96 Hz, ArH), 7.77 (d, 1H, *J* = 8.72 Hz, ArH), 7.39 (d, 1H, *J* = 9.16 Hz, ArH), 7.21 (t, 1H, *J* = 6.40 Hz, ArH), 4.42 (s, 3H, N-CH_3), 4.11 (s, 3H, N-CH_3); ^{13}C NMR (100 MHz, $CDCl_3$): δ = 155.2, 153.9, 146.1, 143.3, 143.0, 142.3, 140.4, 135.9, 134.9, 134.8, 132.0, 128.9, 118.2, 117.6, 115.0, 112.2, 112.1, 108.3, 105.6 (ArH), 40.6 (2xN-CH_3); MS (ESI), m/z: 308.1 (M^++1); Anal. Calcd for $C_{16}H_{13}N_5O_2$: C, 62.53; H, 4.26; N, 22.79, Found: C, 62.54; H, 4.23; N, 22.72.

3-(5-Bromo-3*H*-imidazo[4,5-*b*]pyridine-2-yl)-pyrrolo[2,3-*b*]pyridine-1-yl]-phenyl-methanone (28).

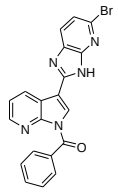

Yellow solid; yield: 81%; mp: 222-224 ^{0}C; ^{1}H NMR (400 MHz, $CDCl_3$): δ = 8.33 (d, 1H, *J* = 8.24 Hz, ArH), 8.13 (d, 3H, *J* = 8.24 Hz, ArH), 7.71 (d, 1H, *J* = 7.32 Hz, ArH), 7.64-7.56 (m, 2H, ArH), 7.54-7.48 (m, 3H, ArH), 7.46 (s, 1H, ArH); ^{13}C NMR (100 MHz, $CDCl_3$): δ = 172.8, 171.9, 169.5, 165.9, 142.2, 141.7, 135.6, 134.7, 133.8, 132.0, 131.9, 130.1, 129.1, 128.8, 128.4, 127.3, 122.8, 120.5, 114.5; MS (ESI), m/z: 418.0 (M^++1); Anal. Calcd for $C_{20}H_{12}BrN_5O$: C, 57.43; H, 2.89; N, 16.74, Found: C, 57.55; H, 2.87; N, 16.78.

[3-(5-Bromo-3*H*-imidazo[4,5-*b*]pyridine-2-yl)-pyrrolo[2,3-*b*]pyridine-1-yl]-(4-nitro-phenyl)-methanone (29).

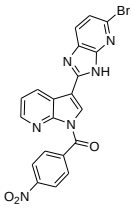

Yellow solid; yield: 79%; mp: 249-251 ^{0}C; ^{1}H NMR (400 MHz, $CDCl_3$): δ = 8.52 (d, 2H, *J* = 7.82 Hz, ArH), 8.38 (d, 2H, *J* = 8.72 Hz, ArH), 8.29-8.22 (m, 3H, ArH), 7.93 (t, 1H, *J* = 8.24 Hz, ArH), 7.77 (d, 1H, *J* = 7.80 Hz, ArH), 7.64 (t, 1H, *J* = 7.80 Hz, ArH); ^{13}C NMR (100 MHz, $CDCl_3$): δ = 162.0, 153.8, 148.3, 142.8, 133.6, 131.2, 129.8, 128.3, 127.0, 126.1, 124.5, 122.3, 121.3, 118.6, 117.5, 110.9 (ArH); MS (ESI), m/z: 463.0 (M^++1); Anal. Calcd for $C_{20}H_{11}BrN_6O_3$: C, 51.85; H, 2.39; N, 18.14, Found: C, 51.94; H, 2.38; N, 18.18.

[3-(5-Bromo-3*H*-imidazo[4,5-*b*]pyridine-2-yl)-pyrrolo[2,3-*b*]pyridine-1-yl]-(4-fluoro-phenyl)-methanone (30).

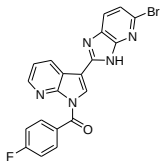

Yellow solid; yield: 77%; mp: 209-211 ^{0}C; ^{1}H NMR (400 MHz, $CDCl_3$): δ = 8.34 (t, 1H, *J* = 5.52 Hz, ArH), 8.25 (d, 1H, *J* = 7.80 Hz, ArH), 8.15 (d, 2H, *J* = 5.52 Hz, ArH), 7.85 (t, 1H, *J* = 6.88 Hz, ArH), 7.69 (d, 1H, *J* = 7.80 Hz, ArH), 7.54 (t, 1H, *J* = 7.80 Hz, ArH), 7.22-7.13 (m, 3H, ArH); ^{13}C NMR (100 MHz, $CDCl_3$): δ = 166.8, 164.2, 159.3, 156.1, 146.8, 136.6, 130.7, 130.6, 128.6, 128.2, 127.1, 126.3, 116.7, 116.0, 115.8 (ArH); MS (ESI), m/z: 436.0 (M^++1); Anal. Calcd for $C_{20}H_{11}BrFN_5O$: C, 55.07; H, 2.54; N, 16.05, Found: C, 55.17; H, 2.52; N, 16.09.

[3-(5-Bromo-3*H*-imidazo[4,5-*b*]pyridine-2-yl)-pyrrolo[2,3-*b*]pyridine-1-yl]-(4-methoxy-phenyl)-methanone (31).

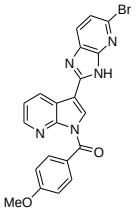

Yellow solid; yield: 74%; mp: 199-201 ^{0}C; ^{1}H NMR (400 MHz, $CDCl_3$): δ = 8.27 (d, 2H, *J* = 8.68 Hz, ArH), 8.07 (d, 2H, *J* = 6.88 Hz, ArH), 7.82 (t, 1H, *J* = 6.40 Hz, ArH), 7.66 (d, 1H, *J* = 8.24 Hz, ArH), 7.49 (t, 1H, *J* = 6.64 Hz, ArH), 7.01 (d, 1H, *J* = 9.16 Hz, ArH), 6.95 (d, 2H, *J* = 7.36 Hz, ArH), 3.87 (s, 3H, OCH_3); ^{13}C NMR (100 MHz, $CDCl_3$): δ = 171.1, 163.9, 163.2, 159.7, 157.0, 147.2, 136.4, 132.2, 130.2, 128.5, 127.6, 126.8, 122.4, 121.6, 116.6, 114.0, 113.6 (ArH), 55.4 (OCH_3); MS (ESI), m/z: 448.0 (M^++1); Anal. Calcd for $C_{21}H_{14}BrN_5O_2$: C, 56.27; H, 3.15; N, 15.62, Found: C, 56.37; H, 3.13; N, 15.65.

1-[3-(5-Bromo-3*H*-imidazo[4,5-*b*]pyridine-2-yl)-pyrrolo[2,3-*b*]pyridine-1-yl]-2-chloro-ethanone (32).

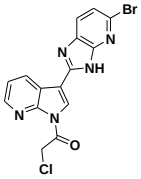

White solid; yield: 72%; mp: 229-231 ^{0}C; ^{1}H NMR (400 MHz, $CDCl_3$): δ = 12.20 (bs, NH, ArH), 8.69 (d, 2H, *J* = 8.28 Hz, ArH), 8.12 (d, 1H, *J* = 1.80 Hz, ArH), 8.10 (d, 1H, *J* = 1.36 Hz, ArH), 7.58 (t, 1H, *J* = 7.32 Hz. ArH), 7.17 (t, 1H, *J* = 7.32 Hz, ArH), 4.21 (s, 2H, CH_2); ^{13}C NMR (100 MHz, $CDCl_3$): δ = 172.7, 161.4, 153.9, 146.6, 140.6, 133.7, 133.0, 127.5, 126.2, 124.7, 122.4, 121.4, 119.7, 117.4, 111.3 (ArH), 42.0 (CH_2); MS (ESI), m/z: 390.0 (M^++1); Anal. Calcd for $C_{15}H_9BrClN_5O$: C, 46.12; H, 2.32; N, 17.93, Found: C, 46.39; H, 2.31; N, 18.04.

2-(1-Benzyl-1*H*-pyrrolo[2,3-*b*]pyridine-3-yl)-5-bromo-3*H*-imidazo[4,5-*b*]pyridine (33a).

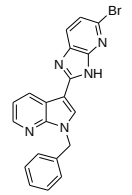

Yellow solid; yield: 34%; mp: 169-171 ^{0}C; ^{1}H NMR (400 MHz, $CDCl_3$): δ = 8.00 (d, 1H, *J* = 1.84 Hz, ArH), 7.63 (d, 1H, *J* = 8.68 Hz, ArH), 7.51 (s, 1H, ArH), 7.31-7.28 (m, 4H, ArH), 7.06 (d, 3H, *J* = 8.24 Hz, ArH), 6.95 (d, 1H, *J* = 8.68 Hz, ArH), 5.29 (s, 2H, N-CH_2); ^{13}C NMR (100 MHz, $CDCl_3$): δ = 159.8, 157.0, 147.2, 136.4, 132.2, 130.2, 128.5, 127.6, 126.8, 122.4, 116.6, 114.0, 113.6 (ArH), 55.4 (N-CH_2); MS (ESI), m/z: 404.0 (M^++1); Anal. Calcd for $C_{20}H_{14}BrN_5$: C, 59.42; H, 3.49; N, 17.32, Found: C, 59.55; H, 3.47; N, 17.36.

3-Benzyl-2-(1-benzyl-1*H*-pyrrolo[2,3-*b*]pyridine-3-yl)-5-bromo-3*H*-imidazo[4,5-*b*]pyridine (33b).

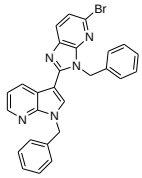

Yellow solid; yield: 69%; mp: 182-184 ^{0}C; ^{1}H NMR (400 MHz, $CDCl_3$): δ = 8.36 (d, 1H, *J* = 7.80 Hz, ArH), 7.81 (d, 1H, *J* = 3.68 Hz, ArH), 7.65-7.60 (m, 1H, ArH), 7.55-7.51 (m, 1H, ArH), 7.30-7.28 (m, 4H, ArH), 7.21-7.14 (m, 2H, ArH), 7.09-7.04 (m, 3H, ArH), 6.99 (d, 1H, *J* = 1.80 Hz, ArH), 6.94 (d, 1H, *J* = 8.72 Hz, ArH), 6.87-6.84 (m, 1H, ArH), 5.31 (s, 2H, N-CH_2), 5.19 (s, 2H, N-CH_2); ^{13}C NMR (100 MHz, $CDCl_3$): δ = 149.1, 147.1, 146.1, 145.8, 145.6, 143.6, 143.3, 138.0, 129.6, 129.2, 120.7, 120.4, 118.6, 117.9, 117.1, 110.0, 109.9, 107.0 (ArH), 54.6 (N-CH_2), 41.8 (N-CH_2); MS (ESI), m/z: 494.0 (M^++1); Anal. Calcd for $C_{27}H_{20}BrN_5$: C, 65.59; H, 4.08; N, 14.17, Found: C, 65.72; H, 4.05; N, 14.19.

5-Bromo-2-[1-(4-chloro-benzyl)-1*H*-pyrrolo[2,3-*b*]pyridine-3-yl]-3*H*-imidazo[4,5-*b*]pyridine (34a).

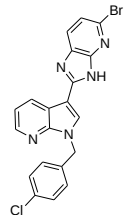

Yellow solid; yield: 26%; mp: 157-159 ^{0}C; ^{1}H NMR (400 MHz, $CDCl_3$): δ = 8.85 (d, 1H, *J* = 7.36 Hz, ArH), 8.39 (s, 1H, ArH), 8.11 (bs, 1H, NH), 8.05 (d, 1H, *J* = 8.28 Hz, ArH), 8.01 (s, 1H, ArH), 7.88 (d, 1H, *J* = 8.24 Hz, ArH), 7.49-7.44 (m, 3H, ArH), 7.37-7.30 (m, 2H, ArH) 5.17 (s, 2H, N-CH_2); ^{13}C NMR (100 MHz, $CDCl_3$): δ = 163.3, 154.3, 150.1, 147.6, 133.6, 133.4, 130.9, 130.0, 125.7, 123.7, 121.7, 121.2, 120.6, 112.0 (ArH), 54.8 (N-CH_2); MS (ESI), m/z: 438.0 (M^++1); Anal. Calcd for $C_{20}H_{13}BrClN_5$: C, 54.75; H, 2.99; N, 15.96, Found: C, 54.91; H, 2.97; N, 16.01.

5-Bromo-3-(4-chloro-benzyl)-2-[1-(4-chloro-benzyl)-1*H*-pyrrolo[2,3-*b*]pyridine-3-yl]-3*H*-imidazo[4,5-*b*]pyridine (34b).

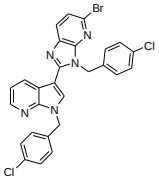

Yellow solid; yield: 69%; mp: 179-181 ^{0}C; ^{1}H NMR (400 MHz, $CDCl_3$ + DMSO-d_6): δ = 9.20 (d, 1H, *J* = 6.88 Hz, ArH), 8.94 (s, 1H, ArH), 7.68 (d, 1H, *J* = 5.48 Hz, ArH), 7.54 (d, 1H, *J* = 1.36 Hz, ArH), 7.50-7.47 (m, 2H, ArH), 7.41-7.35 (m, 7H, ArH), 7.12 (t, 1H, *J* = 6.44 Hz, ArH), 5.98 (s, 2H, N-CH_2), 5.84 (s, 2H, N-CH_2); ^{13}C NMR (100 MHz, $CDCl_3$): δ = 159.9, 155.2, 153.5, 147.4, 141.0, 134.9, 134.7, 132.7, 131.6, 130.4, 129.3, 128.9, 128.1, 127.6, 127.5, 127.0, 126.2, 123.6, 120.6, 118.9, 113.8, 113.2, 110.9 (ArH), 55.1 (N-CH_2), 47.2 (N-CH_2); MS (ESI), m/z: 563.2 (M^++1); Anal. Calcd for $C_{27}H_{18}BrCl_2N_5$: C, 57.57; H, 3.22; N, 12.43, Found: C, 57.75; H, 3.20; N, 12.47.

5-Bromo-2-[1-(3-chloro-benzyl)-1*H*-pyrrolo[2,3-*b*]pyridine-3-yl]-3*H*-imidazo[4,5-*b*]pyridine (35a).

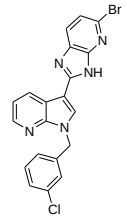

Yellow solid; yield: 23%; mp: 209-211 ^{0}C; ^{1}H NMR (400 MHz, $CDCl_3$): δ = 8.32 (d, 1H, *J* = 4.52 Hz, ArH), 7.93 (s, 1H, ArH), 7.82-7.80 (m, 1H, ArH), 7.72 (q, 1H, *J* = 7.80 Hz, ArH), 7.46-7.44 (m, 1H, ArH), 7.34 (s, 1H, ArH), 7.30-7.27 (m, 3H, ArH), 7.07-7.03 (m, 1H, ArH), 6.50 (bs, 1H, NH), 5.51 (s, 2H, N-CH_2); ^{13}C NMR (100 MHz, $CDCl_3$): δ = 149.2, 148.9, 147.1, 146.1, 145.6, 138.5, 133.4, 130.8, 129.6, 129.2, 120.7, 118.6, 117.3, 117.1, 110.0, 109.9, 107.5 (ArH), 54.6 (N-CH_2); MS (ESI), m/z: 438.0 (M^++1); Anal. Calcd for $C_{20}H_{13}BrClN_5$: C, 54.75; H, 2.99; N, 15.96, Found: C, 54.81; H, 2.91; N, 15.85.

5-Bromo-3-(3-chloro-benzyl)-2-[1-(3-chloro-benzyl)-1*H*-pyrrolo[2,3-*b*]pyridine-3-yl]-3*H*-imidazo[4,5-*b*]pyridine (35b).

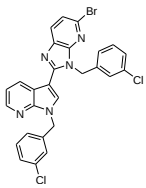

Yellow solid; yield: 62%; mp: 259-261 ^{0}C; ^{1}H NMR (400 MHz, $CDCl_3$): δ = 7.61 (d, 2H, *J* = 8.68 Hz, ArH), 7.43-7.40 (m, 2H, ArH), 7.33-7.27 (m, 3H, ArH), 7.24-7.12 (m, 3H, ArH), 7.02-7.00 (m, 2H, ArH), 6.95 (d, 2H, *J* = 8.24 Hz, ArH), 5.18 (s, 2H, N-CH_2), 5.06 (s, 2H, N-CH_2); ^{13}C NMR (100 MHz, $CDCl_3$): δ = 162.4, 152.7, 142.4, 139.2, 135.5, 132.8, 132.6, 132.0, 129.2, 129.0, 127.9, 127.4, 126.7, 126.2, 122.5, 121.5, 117.0, 113.9, 111.9, 109.4, 55.3 (N-CH_2), 47.1 (N-CH_2); MS (ESI), m/z: 563.2 (M^++1); Anal. Calcd for $C_{27}H_{18}BrCl_2N_5$: C, 57.57; H, 3.22; N, 12.43, Found: C, 57.72; H, 3.15; N, 12.39.

5-Bromo-2-[1-(2-chloro-benzyl)-1*H*-pyrrolo[2,3-*b*]pyridine-3-yl]-3*H*-imidazo[4,5-*b*]pyridine (36a).

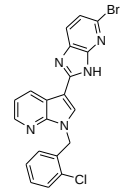

Yellow solid; yield: 19%; mp: 169-171 ^{0}C; ^{1}H NMR (400 MHz, $CDCl_3$): δ = 9.10 (d, 1H, *J* = 8.24 Hz, ArH), 9.01-8.97 (m, 2H, ArH), 8.95 (d, 1H, *J* = 7.32 Hz, ArH), 8.56 (t, 2H, *J* = 7.32 Hz, ArH), 8.43 (t, 2H, *J* = 8.24 Hz, ArH), 7.84-7.80 (m, 2H, ArH), 5.27 (s, 2H, N-CH_2); ^{13}C NMR (100 MHz, $CDCl_3$ + TFA): δ = 140.2, 140.1, 138.1, 137.1, 137.0, 136.6, 131.1, 129.4, 128.7, 123.1, 122.6, 119.5, 118.5, 117.9, 116.1, 115.6, 113.2, 112.8, 110.0, 105.0 (ArH), 51.2 (N-CH_2); EIMS, m/z: 438.0 (M^++1); Anal. Calcd for $C_{20}H_{13}BrClN_5$: C, 54.75; H, 2.99; N, 15.96, Found: C, 54.78; H, 2.93; N, 16.20.

5-Bromo-3-(2-chloro-benzyl)-2-[1-(2-chloro-benzyl)-1*H*-pyrrolo[2,3-*b*]pyridine-3-yl]-3*H*-imidazo[4,5-*b*]pyridine (36b).

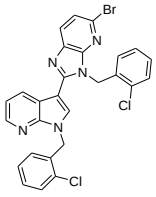

Yellow solid; yield: 61%; mp: 194-196 ^{0}C; ^{1}H NMR (400 MHz, $CDCl_3$+ DMSO-d_6): δ = 7.64 (d, 2H, *J* = 8.68 Hz, ArH), 7.59 (s, 2H, ArH), 7.52-7.43 (m, 4H, ArH), 7.31-7.25 (m, 1H, ArH), 7.15 (d, 2H, *J* = 5.96 Hz, ArH), 7.03 (d, 1H, *J* = 4.56 Hz, ArH), 6.91-6.90 (m, 2H, ArH), 5.28 (s, 2H, N-CH_2), 5.08 (s, 2H, N-CH_2); ^{13}C NMR (100 MHz, $CDCl_3$): δ = 149.2, 148.9, 147.1, 146.1, 145.6, 130.8, 129.6, 129.2, 120.7, 118.6, 117.1, 110.0, 109.9, 107.5 (ArH), 54.6 (N-CH_2), 41.8 (N-CH_2); MS (ESI), m/z: 563.2 (M^++1); Anal. Calcd for $C_{27}H_{18}BrCl_2N_5$: C, 57.57; H, 3.22; N, 12.43, Found: C, 57.81; H, 3.21; N, 12.53.

5-Bromo-2-[1-(4-fluoro-benzyl)-1*H*-pyrrolo[2,3-*b*]pyridine-3-yl]-3*H*-imidazo[4,5-*b*]pyridine (37a).

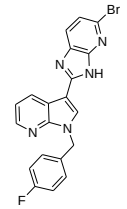

Yellow solid; yield: 33%; mp: 189-191 ^{0}C; ^{1}H NMR (400 MHz, $CDCl_3$): δ = 7.98 (s, 1H, ArH), 7.61 (d, 1H, *J* = 8.24 Hz, ArH), 7.46 (s, 1H, ArH), 7.32-7.28 (m, 3H, ArH), 7.05 (d, 3H, *J* = 6.84 Hz, ArH), 6.95 (d, 1H, *J* = 8.72 Hz, ArH), 5.29 (s, 2H, N-CH_2); ^{13}C NMR (100 MHz, $CDCl_3$): δ = 152.6, 142.1, 135.6, 133.4, 133.1, 132.7, 132.5, 129.1, 128.2, 128.1, 126.3, 116.9, 110.8, 109.5 (ArH), 47.3 (N-CH_2); MS (ESI), m/z: 422.2 (M^++1); Anal. Calcd for $C_{20}H_{13}BrFN_5$: C, 56.89; H, 3.10; N, 16.59, Found: C, 56.71; H, 3.19; N, 16.51.

5-Bromo-3-(4-fluoro-benzyl)-2-[1-(4-fluoro-benzyl)-1*H*-pyrrolo[2,3-*b*]pyridine-3-yl]-3*H*-imidazo[4,5-*b*]pyridine (37b).

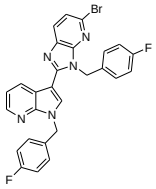

Yellow solid; yield: 61%; mp: 219-221 ^{0}C; ^{1}H NMR (400 MHz, $CDCl_3$ + DMSO-d_6): δ = 7.79-7.70 (m, 1H, ArH), 7.59-7.57 (m, 2H, ArH), 7.48 (d, 2H, *J* = 8.72 Hz, ArH), 7.35 (d, 1H, *J* = 7.32 Hz, ArH), 7.27-7.20 (m, 4H, ArH), 6.98-6.88 (m, 4H, ArH), 5.32 (s, 2H, N-CH_2), 5.16 (s, 2H, N-CH_2); ^{13}C NMR (100 MHz, $CDCl_3$): δ = 164.9, 164.3, 151.8, 138.6, 135.9, 135.7, 135.0, 134.2, 129.1, 127.9, 126.0, 122.1, 119.0, 115.4, 115.2 (ArH), 54.7 (N-CH_2), 46.8 (N-CH_2); MS (ESI), m/z: 530.3 (M^++1); Anal. Calcd for $C_{27}H_{18}BrF_2N_5$: C, 61.14; H, 3.42; N, 13.20, Found: C, 61.19; H, 3.48; N, 13.11.

5-Bromo-2-[1-(2-fluoro-benzyl)-1*H*-pyrrolo[2,3-*b*]pyridine-3-yl]-3*H*-imidazo[4,5-*b*]pyridine (38a).

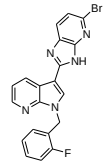

Yellow solid; yield: 32%; mp: 219-221 ^{0}C; ^{1}H NMR (400 MHz, $CDCl_3$): δ = 8.13 (s, 1H, ArH), 7.72 (s, 1H, ArH), 7.51 (d, 1H, *J* = 8.24 Hz, ArH), 7.28-7.26 (m, 3H, ArH), 7.12 (d, 1H, *J* = 8.28 Hz, ArH), 7.02 (d, 3H, *J* = 7.36 Hz, ArH), 5.26 (s, 2H, CH_2); ^{13}C NMR (100 MHz, $CDCl_3$): δ = 153.2, 142.9, 135.6, 133.9, 132.8, 129.8, 129.7, 129.5, 129.2, 128.2, 128.2, 126.3, 122.4, 120.8, 115.7, 109.4, 47.4 (CH_2); EIMS, m/z: 422.2 (M^++1); Anal. Calcd for $C_{20}H_{13}BrFN_5$: C, 56.89; H, 3.10; N, 16.59, Found: C, 57.00; H, 3.08; N, 16.62.

5-Bromo-3-(2-fluoro-benzyl)-2-[1-(2-fluoro-benzyl)-1*H*-pyrrolo[2,3-*b*]pyridine-3-yl]-3*H*-imidazo[4,5-*b*]pyridine (38b).

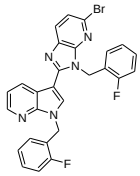

Yellow solid; yield: 58%; mp: 229-231 ^{0}C; ^{1}H NMR (400 MHz, $CDCl_3$): δ = 7.60 (d, 2H, *J* = 8.72 Hz, ArH), 7.46-7.42 (m, 3H, ArH), 7.34 (d, 1H, *J* = 3.20 Hz, ArH), 7.29-7.28 (m, 2H, ArH), 7.21 (s, 1H, ArH), 7.16-7.13 (m, 1H, ArH), 7.01-7.00 (m, 2H, ArH), 6.97-6.91 (m, 2H, ArH), 5.60 (s, 2H, N-CH_2), 5.20 (s, 2H, N-CH_2); ^{13}C NMR (100 MHz, $CDCl_3$): δ = 162.8, 159.9, 153.5, 147.4, 134.9, 132.7, 130.4, 128.9, 128.1, 127.5, 127.0, 126.2, 123.6, 118.9, 113.2, 110.9 (ArH), 55.1 (N-CH_2), 47.2 (N-CH_2); MS (ESI), m/z: 530.3 (M^++1); Anal. Calcd for $C_{27}H_{18}BrF_2N_5$: C, 61.14; H, 3.42; N, 13.20, Found: C, 61.16; H, 3.33; N, 13.13.

General procedure for synthesis of compounds (39-44).

To a stirred solution of 5-bromo-2-(1*H*-pyrrolo[2,3-*b*]pyridine-3-yl)-3*H*-imidazo[4,5-*b*]pyridine (**6**) (0.200 g, 0.6 mmol) in 1,4-dioxane (20 mL), arylboronic acid (0.7 mmol), $Pd(PPh_3)_4$ (10 mol%) and cesium carbonate (0.076g, 0.9 mmol) were added and refluxed for 8 h in an inert

atmosphere. After completion of reaction, extracted the reaction mixture with chloroform, dried over Na_2SO_4, filtered and concentrated to get crude product which was purified through column chromatography using chloroform:methanol (50:1) as eluents afforded compounds **39-44**.

5-Phenyl-2-(1*H*-pyrrolo[2,3-*b*]pyridine-3-yl)-3*H*-imidazo[4,5-*b*]pyridine (39).

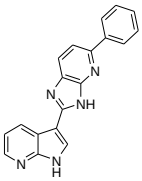

White solid; yield: 86%; mp: 122-124 ^{0}C; ^{1}H NMR (400 MHz, $CDCl_3$): δ = 8.14 (d, 3H, *J* = 8.00 Hz, ArH), 7.79 (d, 3H, *J* = 8.68 Hz, ArH), 7.59-7.57 (m, 3H, ArH, NH), 7.23-7.20 (m, 3H, ArH); ^{13}C NMR (100 MHz, $CDCl_3$): δ = 168.4, 167.4, 154.0, 140.3, 134.8, 129.4, 129.3, 128.4, 126.3, 125.0, 122.9, 121.5, 119.6; MS (ESI), m/z: 311.1 (M^++1); Anal. Calcd for $C_{19}H_{13}N_5$: C, 73.30; H, 4.21; N, 22.49, Found: C, 73.31; H, 4.18; N, 22.50.

5-(4-Methoxy-phenyl)-2-(1*H*-pyrrolo[2,3-*b*]pyridine-3-yl)-3*H*-imidazo[4,5-*b*]pyridine (40).

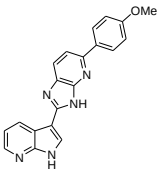

White solid; yield: 82%; mp: 149-151 ^{0}C; ^{1}H NMR (400 MHz, $CDCl_3$): δ = 7.98 (d, 1H, *J* = 8.72 Hz, ArH), 7.73 (d, 2H, *J* = 8.68 Hz, ArH), 7.68 (d, 2H, *J* = 8.24 Hz, ArH), 7.53-7.50 (m, 2H, ArH), 7.30 (bs, 1H, NH), 7.25 (s, 1H, ArH), 7.06 (t, 2H, *J* = 9.16 Hz, ArH), 3.97 (s, 3H, OCH_3); ^{13}C NMR (100 MHz, $CDCl_3$ + DMSO- d_6): δ = 168.9, 168.6, 165.3, 164.9, 150.2, 140.8, 139.6, 136.5, 133.3, 130.7, 126.9, 122.3, 122.0, 121.0, 119.0, 118.8, 113.8 (ArH), 62.0 (OCH_3); MS (ESI), m/z: 341.1 (M^++1); Anal. Calcd for $C_{20}H_{15}N_5O$: C, 70.37; H, 4.43; N, 20.52, Found: C, 70.38; H, 4.39; N, 20.52.

5-(2-Methoxy-phenyl)-2-(1*H*-pyrrolo[2,3-*b*]pyridine-3-yl)-3*H*-imidazo[4,5-*b*]pyridine (41).

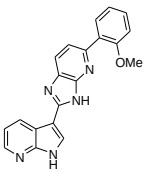

White solid; yield: 79%; mp: 129-131 ^{0}C; ^{1}H NMR (400 MHz, $CDCl_3$): δ = 7.92 (d, 2H, *J* = 6.84 Hz, ArH), 7.69-7.64 (m, 2H, ArH), 7.52 (d, 2H, *J* = 5.96 Hz, ArH), 7.45-7.43 (m, 3H, ArH, NH), 7.21 (s, 1H, ArH), 6.96 (t, 1H, *J* = 8.24 Hz, ArH), 3.85 (s, 3H, OCH_3); ^{13}C NMR (100 MHz, $CDCl_3$): δ = 163.2, 159.7, 157.0, 147.2, 136.4, 132.2, 130.2, 128.5, 127.6, 126.8, 122.4, 116.6, 114.0, 113.6 (ArH), 55.4 (OCH_3); MS (ESI), m/z: 341.1 (M^++1); Anal. Calcd for $C_{20}H_{15}N_5O$: C, 70.37; H, 4.43; N, 20.52, Found: C, 70.49; H, 4.35; N, 20.50.

5-(4-Fluoro-phenyl)-2-(1*H*-pyrrolo[2,3-*b*]pyridine-3-yl)-3*H*-imidazo[4,5-*b*]pyridine (42).

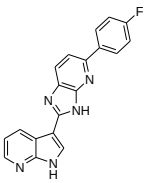

White solid; yield: 78%; mp: 111-113 ^{0}C; ^{1}H NMR (400 MHz, $CDCl_3$): δ = 8.96 (d, 1H, *J* = 8.24 Hz, ArH), 8.17-8.15 (m, 2H, ArH, NH), 8.03 (d, 2H, *J* = 7.32 Hz, ArH), 7.66 (t, 1H, *J* = 7.80 Hz, ArH), 7.56-7.48 (m, 3H, ArH), 7.17 (d, 2H, *J* = 7.36 Hz, ArH); ^{13}C NMR (100 MHz, $CDCl_3$): δ = 153.8, 148.3, 142.8, 133.6, 131.2,

129.8, 128.3, 127.0, 126.1, 124.5, 122.3, 121.3, 118.6, 117.5, 110.9 (ArH); MS (ESI), m/z: 329.1 (M^++1); Anal. Calcd for $C_{19}H_{12}FN_5$: C, 69.29; H, 3.67; N, 21.27, Found: C, 69.30; H, 3.64; N, 21.27.

5-(4-Chloro-phenyl)-2-(1*H*-pyrrolo[2,3-*b*]pyridine-3-yl)-3*H*-imidazo[4,5-*b*]pyridine (43).

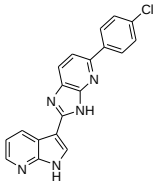

White solid; yield: 77%; mp: 159-161 ^{0}C; ^{1}H NMR (400 MHz, $CDCl_3$ + DMSO-d_6): δ = 8.10 (d, 3H, *J* = 8.24 Hz, ArH), 8.05 (s, 1H, ArH), 7.75 (d, 2H, *J* = 8.72 Hz, ArH), 7.56-7.54 (m, 3H, ArH, NH), 7.18 (d, 1H, *J* = 5.96 Hz, ArH), 7.16 (d, 1H, *J* = 5.96 Hz, ArH); ^{13}C NMR (100 MHz, $CDCl_3$ + DMSO-d_6): δ = 149.9, 146.6, 142.2, 141.7, 136.5, 136.4, 127.8, 127.6, 125.3, 124.6, 120.3, 119.5, 119.3, 115.6, 114.3, 113.0, 102.9; MS (ESI), m/z: 345.7 (M^++1); Anal. Calcd for $C_{19}H_{12}ClN_5$: C, 66.00; H, 3.50; N, 20.25, Found: C, 65.89; H, 3.47; N, 20.20.

2-(1*H*-Pyrrolo[2,3-*b*]pyridine-3-yl)-5-(4-trifluoromethyl-phenyl)-3*H*-imidazo[4,5-*b*]pyridine (44).

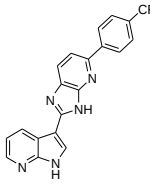

White solid; yield: 70%; mp: 149-151 ^{0}C; ^{1}H NMR (400 MHz, $CDCl_3$): δ = 8.85 (d, 1H, *J* = 7.80 Hz, ArH), 8.45 (d, 1H, *J* = 3.68 Hz, ArH), 8.11 (s, 1H, ArH), 8.06 (d, 2H, *J* = 8.24 Hz, ArH), 7.90 (d, 1H, *J* = 7.80 Hz, ArH), 7.50 (t, 2H, *J* = 7.32 Hz, ArH), 7.37-7.32 (m, 3H, ArH, NH); ^{13}C NMR (100 MHz, $CDCl_3$): δ = 161.4, 153.9, 146.6, 140.6, 133.7, 133.6, 133.4, 133.0, 127.5, 126.2, 124.9, 124.7, 124.5, 122.4, 121.4, 119.7, 117.4, 111.3, 111.1 (ArH); MS (ESI), m/z: 379.3 (M^++1); Anal. Calcd for $C_{20}H_{12}F_3N_5$: C, 63.32; H, 3.19; N, 18.46, Found: C, 63.30; H, 3.16; N, 18.25.

3.2. QUINAZOLINONE

3.2.1. INTRODUCTION

Quinazolin-4-one exists as a privileged structure in many pharmaceutical molecules and biologically active compounds,[130] such as antifungal,[131] antibacterial,[132] antimalarial,[133] antiviral,[134] antimycobacterial,[135] antiinflammatory,[136] antioxidant,[137] and anticancer.[138] The substitution pattern and spatial considerations of the π-systems with quinazolin-4-one nucleus proved to be critical for DHFR inhibition. Free radicals and oxygen derivatives can easily react with most biological molecules, including proteins, lipids, lipoproteins, and DNA; they can be responsible for wide range of human conditions, such as arthritis, hemorrhagic shock, coronary

artery diseases, cancer, AIDS, and age-related degenerative brain diseases.[139] Hence, there is a constant need for searching new and effective therapeutic agents. DNA and proteins are the most abundant macromolecules in cells and are crucial in maintaining normal cell functions.

OBJECTIVE

A novel series of quinazolin-4-one analogs was designed bearing benzimidazol-yl-amine at 3-position as hydrophobic π-system regions and substituting phenyl or phenyl functions with electron withdrawing and electron donating groups at 2-position of quinazolin-4-one as isosteres of the prototypes to explore the scope of this class as DHFR inhibitors as well as for ct-DNA and BSA interactions.

3.2.2. CHEMISTRY

The synthetic strategy to prepare the quinazolin-4-one benzimidazole conjugates (**14-25**) is depicted in Scheme 2. Anthranilic acid was reacted with aromatic and aliphatic acyl chlorides in the presence of triethylamine in chloroform at room temperature for 2 h to get compounds **1-6** followed by cyclization through dehydrative cyclization mechanism, in the presence of pyridine in ethanol at 70-80 ^{0}C for 8 h to obtain 2-aryl/methyl-4*H*-benzo[*d*][1,3]oxazin-4-one (**7-12**). 1-Benzyl-2-methyl-1*H*-benzimidazol-5-ylamine (**13a**) and 3-benzyl-2-methyl-3*H*-benzimidazol-5-ylamine (**13b**) were synthesized by refluxing of 2-methyl-5-nitro-1*H*-benzimidazole with benzyl chloride in the presence of K_2CO_3 in ethanol for 8 h followed by reduction with $SnCl_2.2H_2O$ in 2N HCl. Finally, 1/3-benzyl-2-methyl-1*H*/3*H*-benzimidazol-5-ylamine **(13a** and **13b)** and 2-aryl/methyl-4*H*-benzo[*d*][1,3]oxazin-4-one (**7-12**) were refluxed in ethanol in the presence of pyridine for 4 h to afford corresponding 3-(1/3-benzyl-2-methyl-1*H*/3*H*-benzimidazol-5-yl)-2-aryl/methyl-3*H*-quinazolin-4-one (**14-25**) in 68-80% yield (Table 5). ^{1}H NMR spectrum of compound **14** showed 3H singlet at δ 2.57 of CH_3, 2H singlet at δ 5.32 of benzyl-CH_2, 2H doublet at δ 7.05, 3H, 3H and 5H multiplets at δ 8.02, 7.34 and δ 7.53, three 1H doublets at δ 8.73, 7.23 and 7.07, and 1H singlet at δ 8.65 of aromatic-H. ^{13}C NMR spectrum also showed the peaks at δ 13.4 of CH_3, δ 47.2 of benzyl-CH_2 and δ 162.1 of carbonyl of quinazolin-4-one. The probable mechanism of the reaction involves the ring opening of 2-aryl/methyl-4*H*-benzo[*d*][1,3]oxazin-4-one (**7-12**) by the attack of substituted 1/3-benzyl-2-methyl-1*H/3H*-benzimidazol-5-ylamine, followed by removal of water molecule to close the ring. The above

reaction was also attempted in the presence of glacial acetic acid but desired product was not formed, instead, *N*-(1/3-benzyl-2-methyl-1*H*/3*H*-benzimidazol-5-yl)-acetamide was obtained. These synthesized compounds were further evaluated for their DHFR immunoassay as well as DNA intercalations and BSA bindings.

Scheme 2[a]. Synthesis of quinazolinone-benzimidazole conjugates.

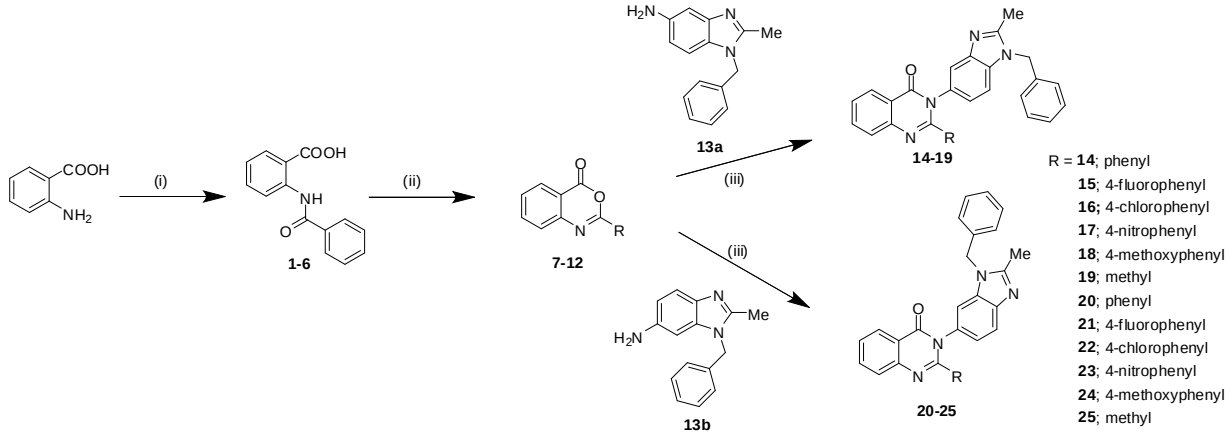

[a]Reagents and conditions: (i) RCOCl, triethylamine, $CHCl_3$, room temperature, 78-89%; (ii) pyridine, ethanol, 70-80 °C, 90%; (iii) **13a**/**13b**, pyridine, ethanol, reflux, 68-80%.

Table 5. Physicochemical properties and DHFR activities of synthesized compounds **14-25**.

Compd	Benzimidazole	R	mp (°C)	% Yields	Molecular formulae	IC_{50} (μM)
14	13a	phenyl	182-184	76	$C_{29}H_{22}N_4O$	0.011
15	13a	4-fluorophenyl	164-166	74	$C_{29}H_{21}FN_4O$	0.034
16	13a	4-chlorophenyl	161-163	71	$C_{29}H_{21}ClN_4O$	-
17	13a	4-nitrophenyl	214-216	69	$C_{29}H_{21}N_5O_3$	0.532
18	13a	4-methoxyphenyl	149-151	69	$C_{30}H_{24}N_4O_2$	-
19	13a	methyl	112-114	80	$C_{24}H_{20}N_4O$	27.62
20	13b	phenyl	175-177	75	$C_{29}H_{22}N_4O$	1.075
21	13b	4-fluorophenyl	158-160	72	$C_{29}H_{21}FN_4O$	0.095
22	13b	4-chlorophenyl	167-169	72	$C_{29}H_{21}ClN_4O$	-
23	13b	4-nitrophenyl	234-236	71	$C_{29}H_{21}N_5O_3$	-
24	13b	4-methoxyphenyl	163-165	68	$C_{30}H_{24}N_4O_2$	-
25	13b	methyl	121-123	79	$C_{24}H_{20}N_4O$	13.84

3.2.3. BIOLOGY

3.2.3.1. Dihydrofolate Reductase Inhibition and Structure-Activity Relationship

In the present investigation, two groups of quinazolin-4-one analogous were synthesized; differ in the types of benzimidazole, attached at C2-position. These compounds were evaluated as DHFR inhibitors using DHFR inhibitory assay kit using methotrexate (MTX), as a positive

control. The obtained results are shown in table 5 that revealed effective inhibition of the dihydrofolate reductase enzyme, with IC_{50} values ranging from 0.011 µM to 27.62 µM. Structure-activity relationship (SAR) studies indicated that different substitution on the aromatic ring, exerted varied DHFR activity. 1-Benzyl-2-methyl-1*H*-benzimidazol-5-ylamine (**14-19**) and 3-benzyl-2-methyl-3*H*-benzimidazol-5-ylamine (**20-25**) functions affected the magnitude of DHFR inhibition. By introducing different substituents at C2-position of quinazoline ring, the order of activity proved to be; phenyl (**14**, IC_{50} = 0.011 µM) > 4-fluorophenyl (**15**, IC_{50} = 0.034 µM) > 4-nitrophenyl (**17**, IC_{50} = 0.532 µM) > methyl (**19**, IC_{50} = 27.62 µM). The 4-chlorophenyl (**16**) and 4-methoxyphenyl (**18**) at C-2 position of quinazolin-4-one did not exert any DHFR inhibitory activity. In the 3-benzyl-2-methyl-3*H*-benzimidazol-5-ylamine series, the presence of phenyl ring, as in case of **20** with IC_{50} = 1.075 µM, showed tenfold decrease in activity compared to its analogue **14**. Replacing the phenyl group **20** with 4-fluorophenyl group, produced **21** with IC_{50} = 0.095 µM with slightly increase in activity. While replacing the phenyl group with methyl group, as in case of **25** with IC_{50} = 13.84 µM, decreased thirteen fold DHFR activity. Thus, it has been observed that quinazolin-4-one and benzimidazole conjugates **14** gave comparable or even superior dihydrofolate reductase enzyme inhibitory activity (IC_{50} = 0.011 µM) to methotrexate with IC_{50} value of 0.020 µM. These results demonstrated the great effects of functional groups on phenyl ring at C2 position of quinazolin-4-one on biological activities, indicated that electron withdrawing chloro or nitro groups and electron donating methoxy group have detrimental effect on the activity of compounds.

3.2.3.2. Interactions of Compound 14 with Calf Thymus DNA

The binding studies of small molecules with DNA are important and helpful for developing novel and more efficient drugs, which are attracting considerable attention in biomedical science. Thus, the binding behavior of active compound **14** with calf thymus (ct)-DNA was studied on the molecular level by UV-visible and fluorescence spectroscopic methods.

In absorption spectroscopy, hypochromism and hyperchromism are very important spectral features to know the changes in DNA double-helical structure.[140] Due to the strong interactions between the electronic states of the intercalating chromophore and DNA bases; the change in absorption strongly suggests a close proximity of the aromatic chromophore to the DNA bases. We, therefore, investigated the binding of the most active compound **14** at fixed concentration

(25 μM and pH = 7.0) towards ct-DNA with stepwise addition of DNA into it. As shown in figure 5a, compound **14** (25 μM) showed absorption maxima at 258 nm. With incremental addition of ct-DNA to the solution of compound **14**, decrease in the absorption intensity at 258 nm was observed with concomitant formation of new band at λ_{max} 307 nm. This was attributed to the formation of compound **14**.DNA complex. An isobestic point at about 273 nm, revealed that different species are in equilibrium and there is no stepwise formation of the complexed species. Upon incremental addition of ct-DNA, tailing in absorption intensity between 350nm and 800 nm was observed which indicated the possibility of aggregation in the presence of DNA.

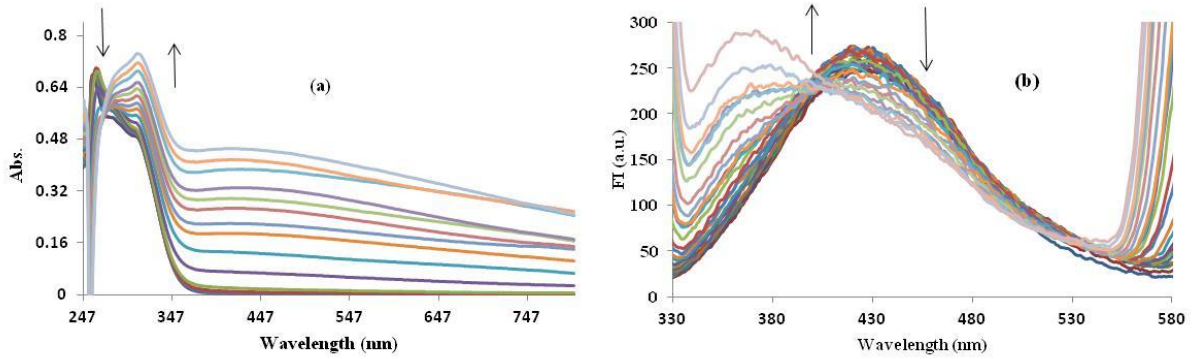

Figure 5. Effect of addition of ct-DNA on (a) absorption and (b) emission spectra of compound **14** (25 μM, pH 7.0) in phosphate buffer.

Compound **14** on excitation at 330 nm showed an emission band at 411 nm. Upon incremental addition of ct-DNA (0-5.5 μM) to compound **14**, emission at 411 nm quenched and led to formation of new emission band at 365 nm (Figure 5b). The binding constant K_a for ligand–DNA binding was determined from the Benesi-Hildebrand equation-2[85] for UV-visible and fluorescence titrations that suggested strong interactions with ct-DNA.

$$1/(A_f - A_{obs}) = 1/(A_f - A_{fc}) + \{1/[K(A_f - A_{fc})]\}[DNA] \quad \text{------ 2}$$

where K is the binding constant, A_f is the absorbance of the free host, A_{obs} is the absorbance observed, and A_{fc} is the absorbance at saturation. The plot of $1/(A_f - A_{obs})$ versus 1/[DNA] was constructed using the titration data and linear fitting, yielding the binding constant, 3.91×10^4 M^{-1} through absorption titration and 9.08×10^4 M^{-1} through emission titration.

The binding of ligand to nucleic acids of DNA may possibly induced conformational changes depending upon the strength and mode of its interaction with nucleic acids. In order to evaluate strength of interaction of compound with DNA, the thermal behavior of ct-DNA in the presence

of compound **14** was also determined. An increase of 15.0 ^{o}C in thermal melting temperature of ct-DNA (67.7 ^{o}C) in the presence of compound **14** (82.7 ^{o}C) also indicated strong intercalation properties of this compound with DNA.

In order to study the interaction properties of compound **14** with DNA, ethidium bromide (EB) was employed. The incremental addition of compound **14** to EB.DNA complex, decrease in absorption band at 285 nm and 480 nm was observed due to formation of its complex (Figure 6a) whereas, addition of EB to **14**.DNA complex caused increase in absorption intensity at 298 nm with slight increase at 525 nm (Figure 6b). These results clearly indicated that compound **14** intercalated into double helix of DNA by replacing EB.DNA complex. The EB.DNA complex showed emission band at 606 nm. Upon incremental addition of compound **14** into it, decrease in emission intensity at 606 nm was observed (Figure 7a). Compound **14**.DNA complex showed the emission band at 370 nm which on addition of EB, was decreased (Figure 7b).

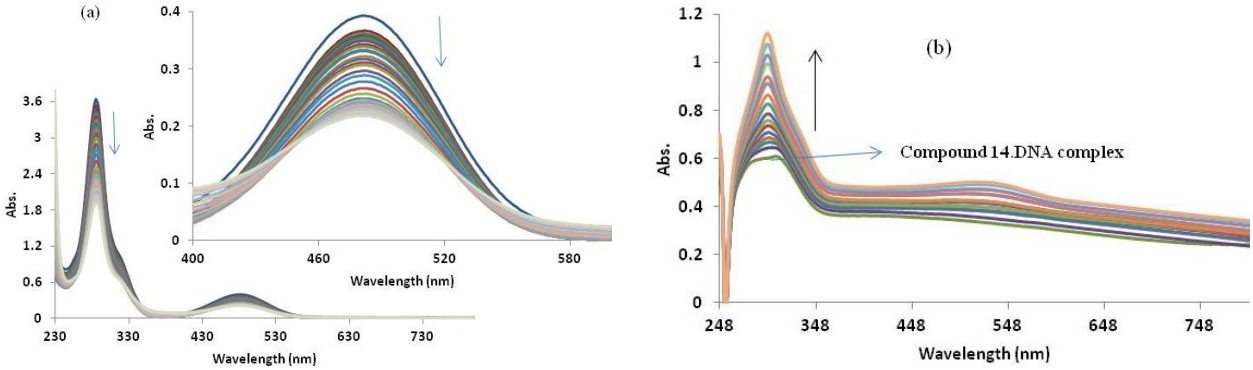

Figure 6. (a) Effect of increasing concentrations of compound **14** on UV absorption spectra of EB.DNA complex, and (b) effect of increasing concentrations of ethidium bromide on UV absorption spectra of compound **14**.DNA complex.

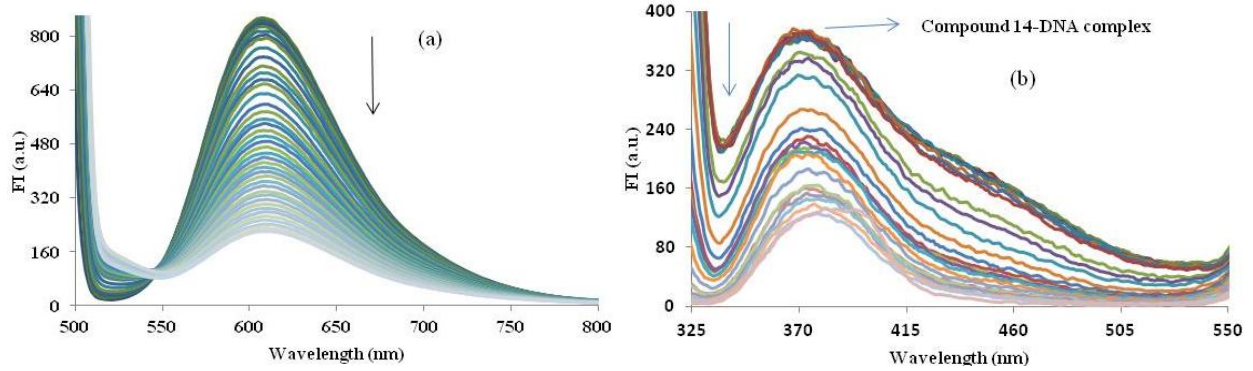

Figure 7. (a) Effect of increasing concentrations of compound **14** on the emission spectra of EB.DNA complex and (b) effect of increasing concentrations of ethidium bromide on the emission spectra of com
pound **14**.DNA complex.

3.2.3.3. Interactions of Compound 14 with BSA

Bovine serum albumin (BSA) was chosen as a target protein molecule for studying the interaction because of its medically important, unusual ligand-binding properties, availability, and structural homology with Human serum albumin (I).[141] In order to explore the structural changes of protein and its complex formation with drug molecule, UV-visible and fluorescence studies were performed on compound **14** and BSA. As shown in figure 8a, absorption peak observed at 278 nm was attributed to the aromatic rings of tryptophan (Trp-214), tyrosine (Tyr-411) and phenylalanine (Phe) residues in BSA. Upon incremental addition of compound **14** to the solution of BSA, a new absorption band appeared at 329 nm, indicating that compound **14** interacted with BSA by changing the environment around the mentioned amino acids by extending the peptide strands of BSA. However, the absorption maximum remains unchanged, implying that the interactions of compound **14** and BSA were non-covalent interactions. These occurred via π–π stacking between the aromatic rings of compound **14** and amino acid residues.

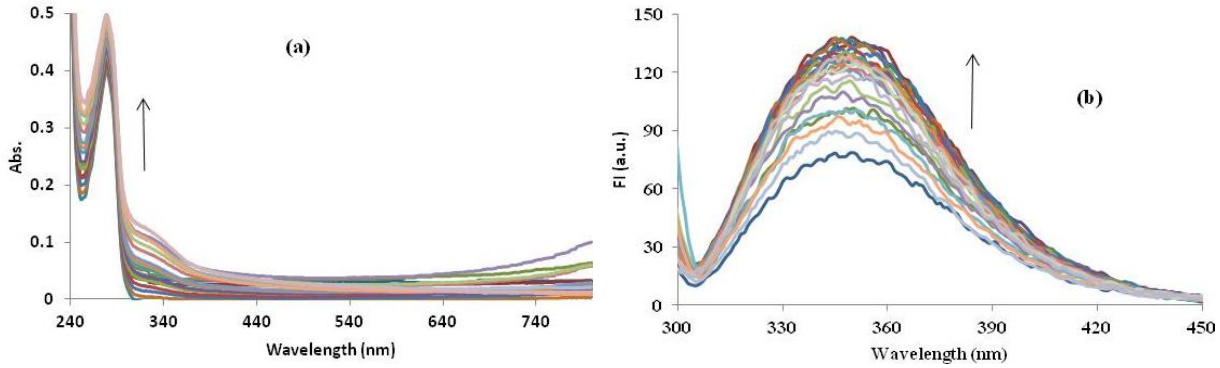

Figure 8. Effect of compound **14** on (a) absorption and (b) emission of BSA.

Upon excitation of BSA solution at Trp-214 absorption (290 nm), showed the emission band at 345 nm, owing to the tryptophan (Trp), tyrosine (Tyr), and phenylalanine (Phe) residues as shown in figure 8b.[142,143] Incubation of BSA solution with different concentration of compound caused a gradual enhancement in fluorescence intensity of the mixture; however, the maximum emission wavelength of BSA remains unchanged.

On the basis of the variations in the absorption spectra of BSA upon binding to **14**, the binding constant K_a for ligand-BSA binding was determined from the Benesi-Hildebrand equation for UV-visible and fluorescence titrations that again suggested strong interaction of compound **14** with BSA. A plot of $1/(A_f - A_{obs})$ versus 1/[BSA] was constructed using the

titration data and linear fitting, yielding the binding constant, 2.29 x 10^4 M^{-1} at 340 nm through absorption titration and 4.20 x 10^4 M^{-1} through emission titration.

3.2.3.4. Molecular Modeling Studies

Based on *in vitro* DHFR enzyme inhibition studies, the most active compound **14** was selected to evaluate the putative binding mode with amino acids in the active site of the enzyme using molecular docking technique. We have carried out the docking studies by placing compound **14** into the binding site of target-specific region of the DHFR (PDB ID 1BOZ).[144] The docked model of compound **14** and DHFR enzyme was described in figure 9, in which compound **14** is surrounded by side chains of various amino acids such as L131, A124, H127 and F148 indicating that molecule is well fitted in the active pocket. The docking results revealed that the interaction of compound **14** with DHFR for the binding site is dominated by hydrogen bonding interactions with C6, Y156 and M125 amino acid residues.

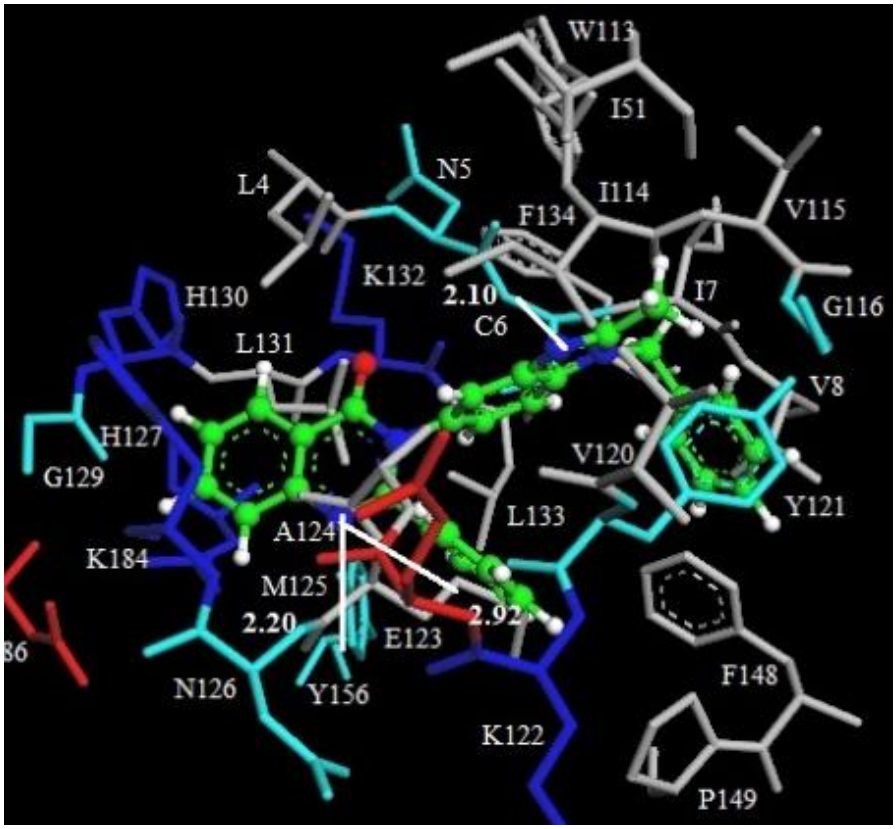

Figure 9. Compound **14** docked in the active site of DHFR (1BOZ).

As shown in figure 9, N1 of quinazolin-4-one of compound **14** showed hydrogen bonding interactions with OH and NH of Y156 and M125 amino acid residues respectively of 1BOZ (bond distance: N…HO = 2.20 Å in case of tyrosine and N…HN = 2.92 Å in case of methionine). Nitrogen atom of benzimidazole of compound **14** also showed hydrogen bonding interactions with SH of C6 amino acid residue (bond distance: N…HS = 2.10 Å in case of cysteine). Therefore, docking of compound **14** in the active site of enzyme indicated the probable mode of action for DHFR activity.

3.2.4. CONCLUSION

The present work led to the development of novel quinazolin-4-one - benzimidazole conjugates and some of which shown promising dihydrofolate reductase inhibitory activity. As per the results of dihydrofolate reductase enzyme immunoassay, compound **14** exhibited significant activity for inhibition of dihydrofolate reductase with IC_{50} value of 0.011 μM. The preliminary interactive investigations of compound **14** with calf thymus DNA by UV-visible and fluorescence spectroscopy revealed that compound **14** was effectively intercalated with ct-DNA to form **14**.DNA complex. The binding studies of compound **14** with bovine serum albumin demonstrated that BSA could effectively store and carry compound by electrostatic interaction. Molecular modeling studies indicating considerable interactions of compound in the active site of amino acids of dihydrofolate reductase enzyme that also favor the enzyme immunoassay results. All these results should be a promising starting point to optimize the structure of quinazoline-benzimidazoles to access potent antitumor agents.

3.2.5. EXPERIMENTAL SECTION

All materials were obtained from commercial suppliers and used without further purification unless otherwise noted. Melting points were determined in open capillaries and were uncorrected. Reactions were monitored by thin-layer chromatography (TLC), carried out on silica gel plates (GF 254) using UV light as visualizing agents. Column chromatography was performed with silica gel 60-120 mesh. ^{1}H NMR and ^{13}C NMR spectra were recorded on Jeol ECS 400 (^{1}H, 400 MHz; ^{13}C, 100 MHz) NMR spectrometer at ambient temperature, using $CDCl_3$ as solvent. Chemical shifts are reported in parts per million (ppm) with TMS as an internal reference and *J* values are given in Hz. Mass spectrometric data were recorded at Waters

Micromass Q-Tof Micro. Elemental analysis has been done with Thermo Scientific (Flash 2000) analyzer. Hexane: ethyl acetate and chloroform: methanol was the adopted solvent systems. UV-visible studies were carried out on Specord PC machines using slit width of 1.0 nm and matched quartz cells. The fluorescence spectra were determined on Varian Cary Eclipse fluorescence spectrometer.

General procedure for the synthesis of compounds 1-6.[145]

To a stirred solution of anthranilic acid (0.1 mol) in chloroform (20 ml), acyl chloride (0.2 mol) and triethylamine (0.12 mol) were added dropwise with constant stirring by maintaining the temperature near 0-5 °C for 1 h. The reaction mixture was then stirred for another 2 h at room temperature. After the completion of reaction, the reaction mixture was neutralized with saturated sodium bicarbonate solution. The solid was separated out, filtered, washed with water and dried. The crude product obtained was purified through column chromatography using ethyl acetate:hexane as eluents to get solid compounds **1-6**.

General procedure for the preparation of compounds 7-12.

Compounds **1-6** (0.05 mol) was dissolved in anhydrous ethanol (10 ml) and pyridine (0.05 mol) and heated at 70-80 ^{0}C for 8 h with vigorous stirring until a solid product was formed. The solvent was evaporated by vacuum under reduced pressure and further purified through column chromatography using ethylacetate:hexane (9:1) as eluents to get solid of 2-substituted-4*H*-benzo[*d*][1,3]oxazin-4-one **7-12.**

General procedure for the preparation of 1-benzyl-2-methyl-1*H*-benzimidazol-5-ylamine and 3-benzyl-2-methyl-1*H*-benzimidazol-5-ylamine (**13a**, **13b**).

To a solution of 2-methyl-5-nitro-1*H*-benzimidazole (9.0 g, 0.05 mol) in ethanol (50 mL), K_2CO_3 (6.98 g, 0.075 mol) and benzyl chloride (9.63 g, 0.075 mol) were added and refluxed for 8 h. After the completion of the reaction (monitored by TLC), the reaction mixture was filtered and concentrated to give yellow solid. The residual mass was crystallized from ethanol to give mixture of 1-benzyl-2-methyl-5-nitro-1*H*-benzimidazole and 3-benzyl-2-methyl-5-nitro-3*H*-benzimidazole in 75% yield. To a suspension of $SnCl_2.2H_2O$ (15.45 g, 0.067 mol) in 2N HCl (47.6 mL), 1/3-benzyl-2-methyl-5-nitro-1*H*/3*H*-benzimidazole (4.25 g, 0.019 mol) was added and heated at 110 ^{o}C for 7 h. After completion of the reaction, the suspension was neutralized with 2N NaOH and diluted with ethanol. Filtered the solid product and extracted the filtrate with chloroform, dried over Na_2SO_4, filtered and concentrated to get mixture of products which were

separated through column chromatography using ethyl acetate: methanol (20:1) as eluent to get pure solid compounds **13a** and **13b**.

General procedure for the synthesis of compounds 14-25.

To a solution of 2-substituted-4*H*-benzo[*d*][1,3]oxazin-4-one **7-12** (0.01 mol) in ethanol, 1/3-benzyl-2-methyl-1*H*-benzimidazol-5-ylamine **13a**/**13b** (0.012 mol) and catalytic amount of pyridine were added, and refluxed for 4 h. On cooling, solid product was separated out. Filtered the solid and purified through column chromatography using chloroform:methanol (2:1) as eluents to get solid compounds **14-25**.

3-(1-Benzyl-2-methyl-1*H*-benzimidazol-5-yl)-2-phenyl-3*H*-quinazolin-4-one (**14**).

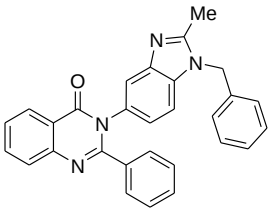

White solid; yield: 76%; mp: 182-184 ^{o}C; ^{1}H NMR (400 MHz, $CDCl_3$): δ = 8.73 (d, 1H, *J* = 8.24 Hz, ArH), 8.65 (s, 1H, ArH), 8.02-8.00 (m, 3H, ArH), 7.53-7.45 (m, 5H, ArH), 7.34-7.29 (m, 3H, ArH), 7.23 (d, 1H, *J* = 8.72 Hz, ArH), 7.07 (d, 1H, *J* = 1.84 Hz, ArH), 7.05 (d, 2H, *J* = 1.36 Hz, ArH), 5.32 (s, 2H, N-CH_2), 2.57 (s, 3H, CH_3); ^{13}C NMR (100 MHz, $CDCl_3$): δ = 162.1, 154.0, 153.1, 150.2, 147.4, 146.8, 141.1, 140.9, 135.0, 134.5, 131.7, 129.6, 129.0, 128.4, 127.7, 126.0, 123.9, 123.5, 123.4, 123.0, 120.8, 119.2, 111.1 (ArC), 47.2 (N-CH_2), 13.4 (CH_3); MS (ESI), m/z: 442.5 (M^++1); Anal. Calcd for $C_{29}H_{22}N_4O$: C, 78.71; H, 5.01; N, 12.66, Found: C, 78.73; H, 4.97; N, 12.68.

3-(1-Benzyl-2-methyl-1*H*-benzimidazol-5-yl)-2-(4-fluoro-phenyl)-3*H*-quinazolin-4-one (**15**).

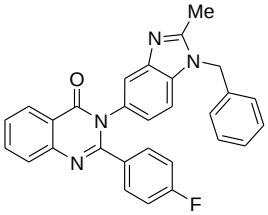

White solid; yield: 74%; mp: 164-166 ^{o}C; ^{1}H NMR (400 MHz, $CDCl_3$): δ = 9.21 (s, 1H, ArH), 8.48 (d, 1H, *J* = 8.24 Hz, ArH), 7.99 (d, 3H, *J* = 7.32 Hz, ArH), 7.94 (s, 1H, ArH), 7.71 (d, 1H, *J* = 8.24 Hz, ArH), 7.57 (t, 2H, *J* = 7.32 Hz, ArH), 7.50-7.43 (m, 3H, ArH), 7.10 (d, 2H, *J* = 7.32 Hz, ArH), 6.84 (t, 2H, *J* = 7.32 Hz, ArH), 5.31 (s, 2H, N-CH_2), 2.57 (s, 3H, CH_3); ^{13}C NMR (100 MHz, $CDCl_3$): δ = 167.4, 165.8, 152.4, 139.4, 138.9, 135.5, 134.4, 132.9, 132.1, 131.9, 128.9, 128.7, 128.5, 127.9, 127.3, 126.4, 126.1, 122.9, 121.7, 119.1, 116.1, 102.3 (ArC), 47.1 (N-CH_2), 13.9 (CH_3); MS (ESI), m/z: 460.5 (M^++1); Anal. Calcd for $C_{29}H_{21}FN_4O$: C, 75.64; H, 4.60; N, 12.17, Found: C, 75.75; H, 4.56; N, 12.34.

3-(1-Benzyl-2-methyl-1*H*-benzimidazol-5-yl)-2-(4-chloro-phenyl)-3*H*-quinazolin-4-one (**16**).

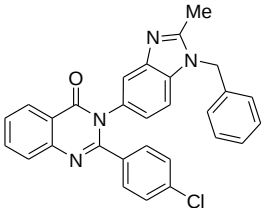

White solid; yield: 71%; mp: 161-163 ^{o}C; ^{1}H NMR (400 MHz, $CDCl_3$): δ = 8.33 (d, 1H, *J* = 7.36 Hz, ArH), 7.70-7.64 (m, 2H, ArH), 7.56-7.53 (m, 3H, ArH), 7.48-7.46 (m, 3H, ArH), 7.39 (d, 1H, *J* = 5.96 Hz, ArH), 7.31-7.28 (m, 3H, ArH), 7.22 (d, 1H, *J* = 8.72 Hz, ArH), 7.06-7.01 (m, 2H, 2H, ArH), 5.28 (s, 2H, N-CH_2), 2.55 (s, 3H, CH_3); ^{13}C NMR (100 MHz, $CDCl_3$): δ = 162.2, 153.9, 153.2, 147.5, 146.9, 141.3, 140.8, 135.1, 134.6, 134.4, 131.7, 130.0, 129.1, 128.4, 128.0, 127.8, 127.3, 126.1, 123.8, 123.6, 123.1, 121.0, 119.5, 110.2 (ArC), 47.4 (N-CH_2), 13.4 (CH_3); MS (ESI), m/z: 476.9 (M^++1); Anal. Calcd for $C_{29}H_{21}ClN_4O$: C, 73.03; H, 4.44; N, 11.75, Found: C, 73.10; H, 4.56; N, 11.88.

3-(1-Benzyl-2-methyl-1*H*-benzimidazol-5-yl)-2-(4-nitro-phenyl)-3*H*-quinazolin-4-one (**17**).

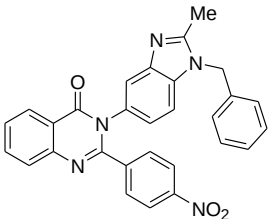

White solid; yield: 69%; mp: 214-216 ^{o}C; ^{1}H NMR (400 MHz, $CDCl_3$): δ = 8.87 (s, 1H, ArH), 8.55 (d, 1H, *J* = 8.24 Hz, ArH), 8.01-7.97 (m, 2H, ArH), 7.91 (s, 1H, ArH), 7.72 (d, 1H, *J* = 8.72 Hz, ArH), 7.58 (d, 1H, *J* = 7.80 Hz, ArH), 7.37-7.28 (m, 4H, ArH), 7.17 (t, 2H, *J* = 8.72 Hz, ArH), 7.10 (d, 2H, *J* = 6.08 Hz, ArH), 6.92 (t, 1H, *J* = 7.32 Hz, ArH), 5.34 (s, 2H, N-CH_2), 2.58 (s, 3H, CH_3); ^{13}C NMR (100 MHz, $CDCl_3$): δ = 167.4, 166.2, 164.6, 163.7, 139.1, 135.5, 132.4, 130.7, 129.8, 129.7, 129.0, 128.0, 127.1, 126.3, 125.9, 123.0, 121.7, 121.4, 119.2, 116.1, 115.9, 115.7, 102.4 (ArC), 47.2 (N-CH_2), 14.0 (CH_3); MS (ESI), m/z: 487.5 (M^++1); Anal. Calcd for $C_{29}H_{21}N_5O_3$: C, 71.45; H, 4.34; N, 14.37, Found: C, 71.59; H, 4.31; N, 14.43.

3-(1-Benzyl-2-methyl-1*H*-benzimidazol-5-yl)-2-(4-methoxy-phenyl)-3*H*-quinazolin-4-one (**18**).

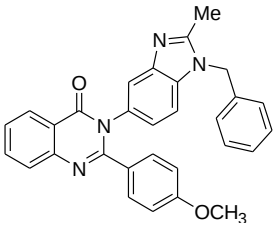

White solid; yield: 69%; mp: 149-151 ^{o}C; ^{1}H NMR (400 MHz, $CDCl_3$): δ = 8.32 (d, 1H, *J* = 7.80 Hz, ArH), 8.20 (d, 1H, *J* = 10.08 Hz, ArH), 8.02 (d, 2H, *J* = 4.48 Hz, ArH), 7.76-7.72 (m, 2H, ArH), 7.58-7.49 (m, 1H, ArH), 7.28-7.26 (m, 2H, ArH), 7.15 (t, 3H, *J* = 8.68 Hz, ArH), 7.01 (s, 1H, ArH), 6.93 (d, 1H, *J* = 8.24 Hz, ArH), 6.84 (d, 1H, *J* = 5.04 Hz, ArH), 6.59 (d, 1H, *J* = 8.24 Hz, ArH), 5.10 (s, 2H, N-CH_2), 3.71 (s, 3H, OCH_3), 2.55 (s, 3H, CH_3); ^{13}C NMR (100 MHz, $CDCl_3$): δ = 162.8, 159.9, 155.2, 153.5, 147.4, 141.0, 134.9, 134.7, 132.7, 130.4, 129.3, 128.9, 128.1, 127.5, 127.0, 126.2, 123.6, 122.1, 120.6, 118.9, 113.8, 113.2, 110.9 (ArC), 55.1 (O-CH_3), 47.2 (N-CH_2), 13.6 (CH_3); MS (ESI), m/z: 472.5 (M^++1); Anal.

Calcd for $C_{30}H_{24}N_4O_2$: C, 76.25; H, 5.12; N, 11.86, Found: C, 76.15; H, 5.08; N, 11.84.

3-(1-Benzyl-2-methyl-1*H*-benzimidazol-5-yl)-2-methyl-3*H*-quinazolin-4-one (19).

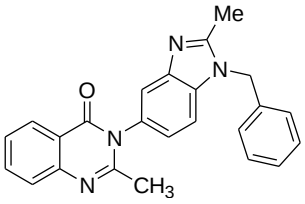

White solid; yield: 80%; mp: 112-114 ^{o}C; ^{1}H NMR (400 MHz, $CDCl_3$): δ = 7.98 (s, 2H, ArH), 7.61 (d, 2H, *J* = 8.24 Hz, ArH), 7.46 (s, 1H, ArH), 7.32-7.28 (m, 2H, ArH), 7.05 (d, 3H, *J* = 6.84 Hz, ArH), 6.95 (d, 2H, *J* = 8.72 Hz, ArH), 5.29 (s, 2H, N-CH_2), 2.54 (s, 3H, CH_3), 2.16 (s, 3H, CH_3); ^{13}C NMR (100 MHz, $CDCl_3$): δ = 168.7, 152.6, 142.1, 135.6, 133.1, 132.5, 129.1, 128.2, 128.1, 126.3, 116.9, 110.8, 109.5 (ArC), 47.3 (N-CH_2), 24.9 (CH_3), 14.0 (CH_3); MS (ESI), m/z: 380.1 (M^++1); Anal. Calcd for $C_{24}H_{20}N_4O$: C, 75.77; H, 5.30; N, 14.73, Found: C, 75.80; H, 5.26; N, 14.76.

3-(3-Benzyl-2-methyl-3*H*-benzimidazol-5-yl)-2-phenyl-3*H*-quinazolin-4-one (**20**).

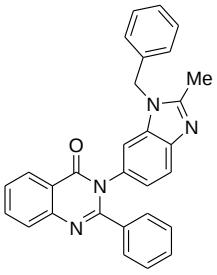

White solid; yield: 75%; mp: 175-177 ^{o}C; ^{1}H NMR (400 MHz, $CDCl_3$): δ = 8.39 (d, 1H, *J* = 7.76 Hz, ArH), 8.26-8.14 (m, 3H, ArH), 8.00 (d, 1H, *J* = 4.24 Hz, ArH), 7.86 (t, 2H, *J* = 7.32 Hz, ArH), 7.61-7.52 (m, 4H, ArH), 7.32 (d, 3H, *J* = 5.04 Hz, ArH), 7.12 (d, 1H, *J* = 8.72 Hz, ArH), 7.02 (t, 2H, *J* = 9.16 Hz, ArH), 5.29 (s, 2H, N-CH_2), 2.58 (s, 3H, CH_3); ^{13}C NMR (100 MHz, $CDCl_3$): δ = 167.5, 165.7, 152.7, 141.4, 139.5, 135.2, 132.6, 132.4, 131.8, 129.0, 128.7, 128.2, 128.0, 127.3, 127.2, 126.2, 122.9, 121.6, 121.2, 117.5, 111.8, 109.6 (ArC), 47.2 (N-CH_2), 13.6 (CH_3); MS (ESI), m/z: 442.5 (M^++1); Anal. Calcd for $C_{29}H_{22}N_4O$: C, 78.71; H, 5.01; N, 12.66, Found: C, 78.75; H, 4.95; N, 12.70.

3-(3-Benzyl-2-methyl-1*H*-benzimidazol-5-yl)-2-(4-fluoro-phenyl)-3*H*-quinazolin-4-one *(*21).

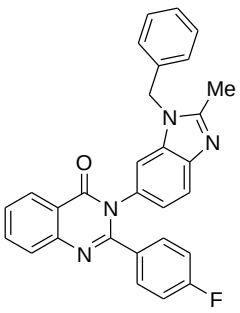

White solid; yield: 72%; mp: 158-160 ^{o}C; ^{1}H NMR (400 MHz, $CDCl_3$): δ = 8.98 (s, 1H, ArH), 8.63 (d, 1H, *J* = 8.24 Hz, ArH), 8.00 (d, 1H, *J* = 1.36 Hz, ArH), 8.02-7.98 (m, 2H, ArH), 7.64 (d, 1H, *J* = 8.24 Hz, ArH), 7.53 (d, 1H, *J* = 8.72 Hz, ArH), 7.41 (t, 2H, *J* = 7.68 Hz, ArH), 7.32-7.30 (m, 2H, ArH), 7.22 (d, 1H, *J* = 8.72 Hz, ArH), 7.15 (t, 2H, *J* = 8.72 Hz, ArH), 7.07 (d, 1H, *J* = 7.80 Hz, ArH), 6.96 (t, 1H, *J* = 6.88 Hz, ArH), 5.31 (s, 2H, N-CH_2), 2.56 (s, 3H, CH_3); ^{13}C NMR (100 MHz, $CDCl_3$): δ = 167.6, 166.2, 164.6, 163.7, 152.8, 141.9, 139.3, 135.3, 132.7, 132.4, 130.6, 129.8, 129.0, 128.0, 127.2, 126.2, 122.9, 121.6, 121.2, 117.3, 115.9, 111.9, 109.6 (ArC), 47.2 (N-CH_2), 13.8 (CH_3); MS (ESI), m/z: 460.5 (M^++1); Anal. Calcd for $C_{29}H_{21}FN_4O$: C, 75.64; H, 4.60; N, 12.17, Found: C, 75.74; H, 4.59; N, 12.16.

3-(3-Benzyl-2-methyl-1*H*-benzimidazol-5-yl)-2-(4-chloro-phenyl)-3*H*-quinazolin-4-one (22).

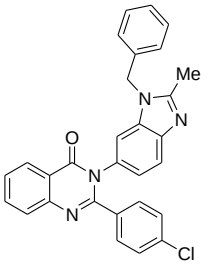

White solid; yield: 72%; mp: 167-169 ^{o}C; ^{1}H NMR (400 MHz, $CDCl_3$): δ = 7.61 (d, 1H, *J* = 8.24 Hz, ArH), 7.49 (d, 2H, *J* = 8.24 Hz, ArH), 7.42-7.39 (m, 2H, ArH), 7.26-7.24 (m, 5H, ArH), 7.16 (d, 1H, *J* = 8.68 Hz, ArH), 7.05 (t, 1H, *J* = 7.32 Hz, ArH), 6.97-6.90 (m, 4H, ArH), 5.12 (s, 2H, N-CH_2), 2.49 (s, 3H, CH_3); ^{13}C NMR (100 MHz, $CDCl_3$): δ = 164.5, 160.3, 157.9, 152.1, 140.0, 135.9, 135.7, 134.4, 129.0, 127.9, 126.3, 122.8, 119.1, 116.7, 115.6, 115.3 (ArC), 47.0 (N-CH_2), 14.1 (CH_3); MS (ESI), m/z: 476.9 (M^++1); Anal. Calcd for $C_{29}H_{21}ClN_4O$: C, 73.03; H, 4.44; N, 11.75, Found: C, 73.12; H, 4.40; N, 11.72.

3-(3-Benzyl-2-methyl-1*H*-benzimidazol-5-yl)-2-(4-nitro-phenyl)-3*H*-quinazolin-4-one (**23**).

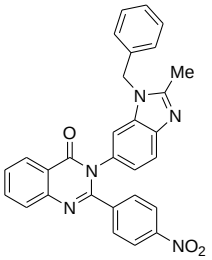

White solid; yield: 71%; mp: 234-236 ^{o}C; ^{1}H NMR (400 MHz, $CDCl_3$): δ = 8.39 (d, 1H, *J* = 7.76 Hz, ArH), 8.25 (d, 2H, *J* = 7.36 Hz, ArH), 8.16 (d, 1H, *J* = 8.28 Hz, ArH), 8.00 (d, 1H, *J* = 4.24 Hz, ArH), 7.86 (t, 2H, *J* = 8.24 Hz, ArH), 7.61-7.53 (m, 3H, ArH), 7.32 (d, 2H, *J* = 5.48 Hz, ArH), 7.19 (d, 2H, *J* = 8.24 Hz, ArH), 7.00 (t, 2H, *J* = 3.84 Hz, ArH), 5.30 (s, 2H, N-CH_2), 2.59 (s, 3H, CH_3); ^{13}C NMR (100 MHz, $CDCl_3$): δ = 163.3, 162.2, 153.9, 153.3, 149.5, 147.5, 146.9, 141.3, 140.9, 135.1, 134.6, 130.8, 130.0, 129.1, 128.5, 128.0, 127.7, 126.1, 123.8, 123.3, 121.0, 120.0, 119.6, 115.3, 110.2 (ArC), 47.4 (N-CH_2), 13.5 (CH_3); MS (ESI), m/z: 487.5 (M^++1); Anal. Calcd for $C_{29}H_{21}N_5O_3$: C, 71.45; H, 4.34; N, 14.37, Found: C, 71.49; H, 4.36; N, 14.32.

3-(3-Benzyl-2-methyl-1*H*-benzimidazol-5-yl)-2-(4-methoxy-phenyl)-3*H*-quinazolin-4-one (24).

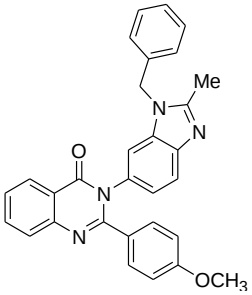

White solid; yield: 68%; mp: 163-165 ^{o}C; ^{1}H NMR (400 MHz, $CDCl_3$): δ = 9.27 (s, 1H, ArH), 8.55 (d, 1H, *J* = 8.24 Hz, ArH), 8.15 (d, 1H, *J* = 1.84 Hz, ArH), 7.96 (d, 1H, *J* = 6.84 Hz, ArH), 7.95 (d, 1H, *J* = 7.36 Hz, ArH), 7.58 (t, 2H, *J* = 8.24 Hz, ArH), 7.30-7.26 (m, 3H, ArH), 7.21 (d, 1H, *J* = 8.68 Hz, ArH), 7.06 (d, 1H, *J* = 7.80 Hz, ArH), 6.97-6.95 (m, 2H, ArH), 6.84 (t, 1H, *J* = 8.24 Hz, ArH), 5.28 (s, 2H, N-CH_2), 3.85 (s, 3H, OCH_3), 2.53 (s, 3H, CH_3); ^{13}C NMR (100 MHz, $CDCl_3$): δ = 167.6, 165.4, 162.4, 152.7, 142.4, 139.2, 135.5, 132.8, 132.6, 132.0, 129.2, 129.0, 127.9, 127.4, 126.7, 126.2, 122.5, 121.5, 117.0, 113.9, 111.9, 109.4 (ArC), 55.3 (O-CH_3), 47.1 (N-CH_2), 13.9 (CH_3); MS (ESI), m/z: 472.5 (M^++1); Anal. Calcd for $C_{30}H_{24}N_4O_2$: C, 76.25; H, 5.12; N, 11.86, Found: C, 76.30; H, 5.19; N, 11.82.

3-(3-Benzyl-2-methyl-1*H*-benzimidazol-5-yl)-2-methyl-3*H*-quinazolin-4-one (25).

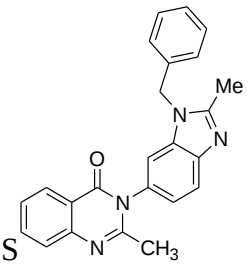

White solid; yield: 79%; mp: 121-123 ^{o}C; ^{1}H NMR (400 MHz, $CDCl_3$): δ = 8.13 (s, 1H, ArH), 7.72 (s, 1H, ArH), 7.51 (d, 1H, *J* = 8.24 Hz, ArH), 7.31-7.26 (m, 4H, ArH), 7.12 (d, 2H, *J* = 8.28 Hz, ArH), 7.02 (t, 3H, *J* = 5.28 Hz, ArH), 5.26 (s, 2H, N-CH_2), 2.53 (s, 3H, CH_3), 2.15 (s, 3H, CH_3); ^{13}C NMR (100 MHz, $CDCl_3$): δ = 169.4, 151.4, 141.2, 136.8, 134.9, 133.9, 133.6, 131.4, 130.3, 128.4, 126.3, 122.3, 119.8, 118.0, 117.1, 110.3, 108.3 (ArC), 47.5 (N-CH_2), 24.1 (CH_3), 12.6 (CH_3); MS (ESI), m/z: 380.1 (M^++1); Anal. Calcd for $C_{24}H_{20}N_4O$: C, 75.77; H, 5.30; N, 14.73, Found: C, 75.73; H, 5.22; N, 14.71.

3.3. PYRAZOLOPYRIMIDINE

3.3.1. INTRODUCTION

The pyrazolo[3,4-*d*]pyrimidine nucleus represents an interesting scaffold for the development of drug-candidates aiming at a wide range of biological targets[146,147] and has been exploited to encompass an array of pharmacological activities such as antiviral,[148] CNS depressant,[149] tuberculostatic[150] antimicrobial,[151] antitumor,[152] antileishmanial,[153] antiinflammatory,[154] and in the development of kinase inhibitors.[155,156] Due to its structure, isosteric to that of purine, this nitrogen-containing heterocycle behaves as a 'privileged scaffold',[157] acting in antagonism with natural purines and showing different specificity for the biological targets depending on its chemical functionalization. Pharmacological actions of this moiety have mediated by means of interaction with biological molecules, including DNA and bovine serum albumin. The mode and affinity of DNA binding was interfered with its replication that leads to inhibit the growth of tumor cells and study of protein binding explored the structural changes of protein and its complex formation with drug molecule.

OBJECTIVE

A novel series of pyrazolo[3,4-*d*]pyrimidine analogs was designed bearing aminobenzimidazole at C4-position as hydrophobic π-system regions and substituting primary and secondary amine functions at C6-position of pyrazolopyrimidine as isosteres of the prototypes to explore the scope of this class for ct-DNA and BSA interactions.

3.3.2. CHEMISTRY

Our first key intermediate was the 5-aminopyrazole-4-carbonitrile **1,** which was easily prepared from condensation of ethoxymethylenemalonitrile with hydrazine. On further hydrolysis with sulphuric acid and then fused with molten urea at 190 ^{0}C gave the intermediate product **3**, followed by $POCl_3$-mediated chlorination provided 4,6-dichloropyrazolopyrimidine (**4**). The aromatic nucleophilic substitution of chloro-containing heterocycles (**4**) at C4 position with 4-(1*H*-benzimidazol-2-yl)-phenylamine (**5**) in the presence of potassium carbonate in isopropyl alcohol at room temperature yielded the desired product [4-(1*H*-benzimidazol-2-yl)-phenyl]-(6-chloro-1*H*-pyrazolo[3,4-*d*]pyrimidin-4-yl)-amine **6** in 79% yield, followed by different amines substitution at C6 position in the presence of potassium carbonate in *n*-butanol at reflux condition gave target compounds **7-18** in 66-78% yields that have been outlined in Scheme 3.

Scheme 3[a]. Synthetic route for the preparation of target compounds **7-18**.

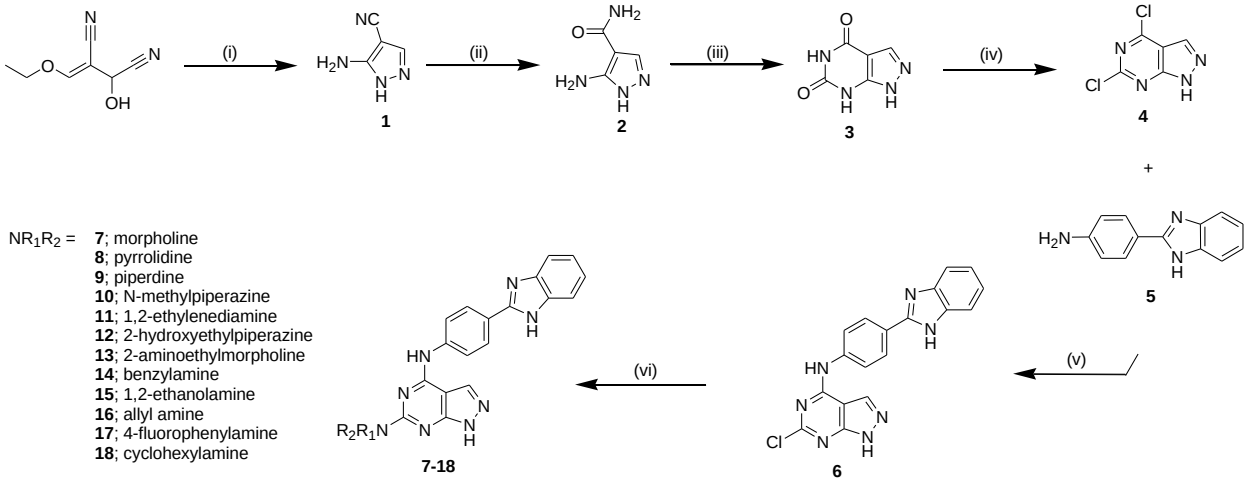

[a]Reagents and conditions: (i) hydrazine, 100 °C; (ii) H_2SO_4, 0-5 °C; (iii) urea, 190 °C; (iv) $POCl_3$, triethylamine, 100 °C; (iv) 5, K_2CO_3, IPA, rt; (v) HNR_1R_2, K_2CO_3, n-butanol, reflux.

3.3.3. BIOLOGY

All the synthesized compounds were submitted to National Cancer Institute (NCI) disease-oriented human cell lines for their evaluation of *in-vitro* antitumor activities. Six compounds (**7, 8**, **11, 12, 14** and **17**) were selected and evaluated against 60 human cell lines at one dose concentration level i.e. 10^{-5} M which included nine tumor subpanels namely; leukemia, non-small lung, colon, central nervous system, melanoma, ovarian, renal, prostate and breast cancer

cells. Further, we used these compounds for DNA binding interaction studies and fluorescence quenching studies for bovine serum albumin interaction.

3.3.3.1. DNA Binding Interaction

In order to seek for the potential anti-tumor target of pyrazolopyrimidine derivatives, both UV-Visible and fluorescence spectroscopy were used to ascertain the binding properties of compounds **7**, **8**, **11**, **12**, **14** and **17** with calf thymus (ct) DNA in phosphate buffer (10 mM, pH 7.4). As shown in Figure 10, upon incremental addition of ct-DNA to compounds **7**, **8**, **11**, **12**, **14** and **17** (10 µM) showed decrease in the absorption maxima intensity (λ_{max}) at 324-335 nm along with concomitant increase in absorption intensity within range of 257-265 nm λ_{max} with an isobestic point within range of 277-292 nm (Table 6). These results revealed that different species are in equilibrium and there is no stepwise formation of the complexed species.

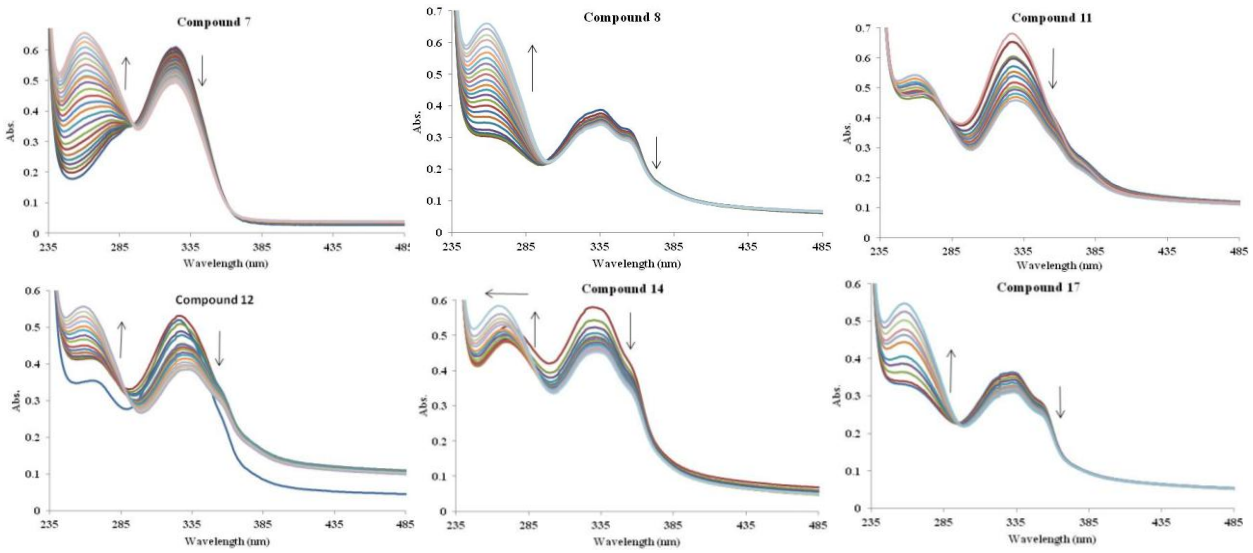

Figure 10. UV-Vis spectral changes of compounds **7**, **8**, **11**, **12**, **14** and **17** at the concentration of 10 µM upon addition of ct-DNA (0 µM- 20 µM) in phosphate buffer (10 mM, pH 7.4).

On excitation at 300 nm, compounds **7**, **8**, **11**, **12**, **14** and **17** showed an intense emission band between 382 nm and 466 nm. On incremental addition of ct-DNA to compounds **7, 8**, **11**, **12**, **14** and **17** caused, 68%, 28%, 57%, 67%, 33% and 65% emission quenching as shown in figure 11. On the basis of these variations in absorption and emission spectra of compounds **7, 8**, **11**, **12**, **14** and **17** upon binding with DNA, the binding constant K_a for compound.DNA

complexes were determined from the Benesi–Hildebrand equation[85] for UV-visible and fluorescence titrations that suggested strong interactions with ct-DNA (Table 6).

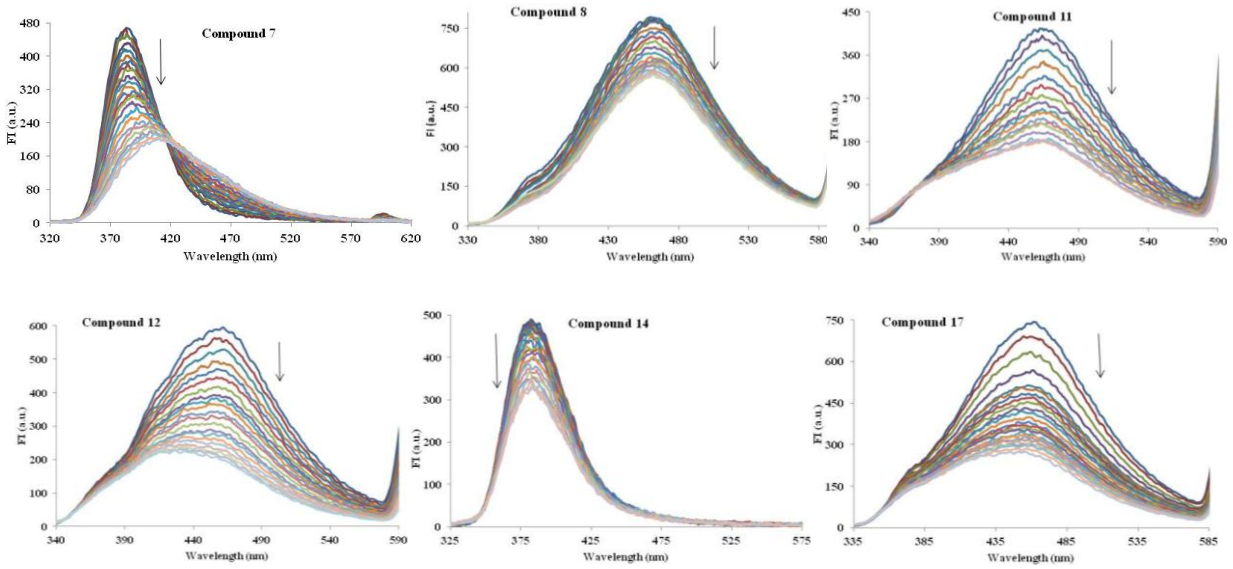

Figure 11. Fluorescence spectral changes of compounds **7**, **8**, **11**, **12**, **14** and **17** (λ_{ex} = 300 nm) at the concentration of 10 μM upon addition of ct-DNA (0 μM- 20 μM) in phosphate buffer (10 mM, pH 7.4).

Table 6. Photophysical properties of compounds **7**, **8**, **11**, **12**, **14** and **17** with ct-DNA.

Compds.	Hypochromism (%) at λ_{max} (nm)	Hyperchromism (%) at λ (nm)	Isobestic point (nm)	K_a through UV-visible (M^{-1})	Quenching (%) at λ_{em} (nm)	K_a through fluorescence (M^{-1})
7	19 (324)	70 (260)	292	1.92×10^4	68 (383)	8.39×10^2
8	12 (335)	52 (259)	298	7.70×10^3	28 (460)	2.74×10^2
11	33 (327)	12 (259)	277	1.47×10^4	57 (466)	1.68×10^4
12	27 (326)	37 (259)	292	7.20×10^3	67 (461)	5.64×10^4
14	22 (330)	13 (264)	280	2.63×10^3	33 (382)	8.42×10^3
17	14 (332)	40 (257)	294	8.37×10^3	65 (461)	2.61×10^3

3.3.3.2. Fluorescence Quenching for Bovine Serum Albumin Interaction

To explore the complex formation of protein with drug molecule, fluorescence quenching studies were performed. Upon excitation of BSA solution at Trp-214 absorption (280 nm), showed the emission band at 352 nm, owing to the tryptophan (Trp), tyrosine (Tyr), and phenylalanine (Phe) residues as shown in figure 12. Incubation of BSA solution with different concentrations of compounds **7**, **8**, **11**, **12**, **14** and **17** caused a gradual quenching i.e. 44%, 21%, 35%, 31%, 54% and 33% in the fluorescence intensity of the mixture indicating the interaction

of compounds **7**, **8**, **11**, **12**, **14** and **17** with BSA by changing in the environment around the mentioned amino acids by extending the peptide strands of BSA. However, the emission maximum remains unchanged, implying that the interactions of compounds and BSA were non-covalent interactions via π–π stacking between the aromatic rings of compounds **7**, **8**, **11**, **12**, **14** and **17** and amino acid residues located in the binding cavity of BSA.

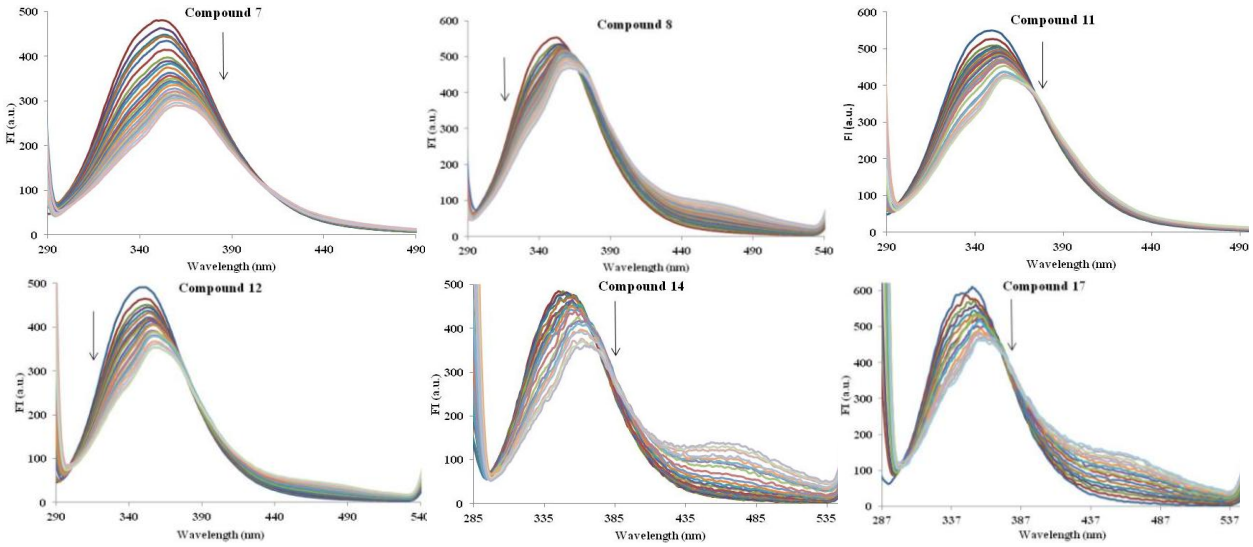

Figure 12. An emission spectral change of BSA at the concentration of 10 μM upon addition of compounds **7**, **8**, **11**, **12**, **14** and **17** (0 μM- 30 μM) in phosphate buffer (10 mM, pH 7.4).

3.3.4. CONCLUSION

The present work has led to the development of novel pyrazolo[3,4-*d*]pyrimidine benzimidazole analogues and some of which shown promising interacting property with DNA and BSA. The preliminary interactive investigations of compounds **7, 8, 11, 12, 14** and **17** with calf thymus DNA by UV-visible and fluorescence spectroscopy revealed that compounds **7, 8, 11, 12, 14** and **17** were effectively intercalated with ct-DNA to form compound.DNA complexes. The binding studies of compounds **7, 8, 11, 12, 14** and **17** with bovine serum albumin demonstrated that BSA were effectively store and carry compound to the active target site. These compounds could be considered as useful tempelates for future development and further derivatization or modification to obtain more potent compounds.

3.3.5. EXPERIMENTAL SECTION

All materials were obtained from commercial suppliers and used without further purification unless otherwise noted. Melting points were determined in open capillaries and were

uncorrected. Reactions were monitored by thin-layer chromatography (TLC), carried out on silica gel plates (GF 254) using UV light as visualizing agents. Column chromatography was performed with silica gel 60-120 mesh. ^{1}H NMR and ^{13}C NMR spectra were recorded on Jeol ECS 400 (^{1}H, 400 MHz; ^{13}C, 100 MHz) NMR spectrometer at ambient temperature, using $CDCl_3$ as solvent. Chemical shifts are reported in parts per million (ppm) with TMS as an internal reference and *J* values are given in Hz. Mass spectrometric data were recorded at Waters Micromass Q-Tof Micro. Elemental analysis has been done with Thermo Scientific (Flash 2000) analyzer. Hexane: ethyl acetate and chloroform: methanol was the adopted solvent systems. UV-visible studies were carried out on Specord PC machines using slit width of 1.0 nm and matched quartz cells. The fluorescence spectra were determined on Varian Cary Eclipse fluorescence spectrometer.

Procedure for the synthesis of 5-amino-1*H*-pyrazole-4-carbonitrile (1).

Hydrazine (5 g, 0.156 mol) was carefully added into ethoxymethylenemalononitrile (8.64 g, 0.070 mol) in ethanol and heated on the steam-bath for 30 minutes. After completion of the reaction, white precipitate gradually appeared and placed in a refrigerator overnight. The product was then filtered and washed with a small amount of cold absolute ethanol to afford the desired product 5-amino-1*H*-pyrazole-4-carbonitrile (**1**) as white solid; (3.05 g, 86%); mp 170-172 ^{0}C.[158]

Procedure for the synthesis of 5-amino-1*H*-pyrazole-4-carboxylic acid amide (2).

5-Amino-1*H*-pyrazole-4-carbonitrile (**1**, 5g) was added to cooled concentrated sulfuric acid (10 ml) with stirring so that the temperature did not rise above 20 ^{0}C. The addition took about one-half hour and solution was stirred at room temperature for 4 h. The acid solution was then poured with stirring into ice and the solution set aside overnight in the refrigerator. The solution was then filtered and the product washed free of excess sulfuric acid to afford the desired product 5-amino-1*H*-pyrazole-4-carboxylic acid amide (**2**) as white solid; (5.19 g, 89%); mp 215-217 ^{0}C.[158]

Procedure for the synthesis of 1,7-dihydro-pyrazolo[3,4-*d*]pyrimidine-4,6-dione (3).

5-Amino-1*H*-pyrazole-4-carboxylic acid amide (**2,** 5g, 0.0396 mol) and urea (10 g, 0.1666 mol) were heated together at 190 ^{0}C for 20 minutes. The clear solution went mushy and heating was continued for another 20 minutes at 190 ^{0}C until the mushy melt became too solid to stir. The resulting solid was dissolved in hot dilute sodium hydroxide and the boiling basic solution was then carefully acidified with hydrochloric acid. The solution was allowed to stand approximately ten minutes and was then filtered to afford the desired product 1,7-dihydro-pyrazolo[3,4-

d]pyrimidine-4,6-dione **(3)** as white solid; (3.73 g, 62%).

Procedure for the synthesis of 4,6-dichloro-1*H*-pyrazolo[3,4-*d*]pyrimidine (4).

To 1,7-dihydro-pyrazolo[3,4-*d*]pyrimidine-4,6-dione **(3)** (1.233 mol), phosphorus oxychloride (2.84 mol) was added with stirring at 20 °C. After stirring for 15 min, the mixture was heated at 55 °C, and triethylamine (2.53 mol) was added over a period of 1 h at a rate that maintains the internal temperature below 65 °C then mixture was slowly heated to an internal temperature of 85 °C for 10 min and then heated at 108-110 °C for 4 h to obtain a clear brown-yellow solution. The reaction mixture was cooled to an internal temperature of 40 °C and added to warm water over a period of 30-40 min. and solid was collected by filtration to afford pure 4,6-dichloro-1*H*-pyrazolo[3,4-*d*]pyrimidine (**4**) as light yellow solid; (5.35 g, 87 %); mp: 173-175 ^{o}C.

General procedure for the synthesis of 4-(1*H*-benzimidazol-2-yl)-phenylamine (5).

A mixture of 4-aminobenzoic acid (5 g, 5.78 mmol) and *o*-phenylenediamine (3.9 g, 3.68 mmol) were stirred in a syrupy polyphosphoric acid (12.5 gm) at 200 ^{0}C for 5 h. The reaction was monitored with TLC. The reaction mixture was cooled and poured into crushed ice. The precipitate was then stirred in cold water. Ammonium hydroxide solution was added until the *p*H 7 was achieved. The resulting solid was filtered and washed several times with methanol and column chromatographed on silica gel in ethylacetate: hexane (4:1) to afford the desired product 4-(1*H*-benzimidazol-2-yl)-phenylamine (**5**).

Synthesis of [4-(1*H*-benzimidazol-2-yl)-phenyl]-(6-chloro-1*H*-pyrazolo[3,4-*d*]pyrimidin-4-yl)-amine (6).

To a solution of 4-(1*H*-benzimidazol-2-yl)-phenylamine (**5**, 1 g, 0.005 mol) in isopropyl alcohol (25 ml), 4,6-dichloro-1*H*-pyrazolo[3,4-*d*]pyrimidine (**4**) (0.99 g, 0.005 mol) was added and stirred at room temperature for 24 h. After washing the crude solid with isopropyl alcohol, dried to obtain pure [4-(1*H*-benzimidazol-2-yl)-phenyl]-(6-chloro-1*H*-pyrazolo[3,4-*d*]pyrimidin-4-yl)-amine (**6**).

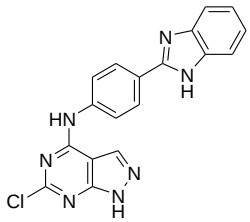

White solid; yield: 79%; mp: > 300 ^{o}C; ^{1}H NMR (400 MHz, $CDCl_3$ + DMSO-d_6): δ = 9.75 (s, 1H, ArH), 8.13-8.08 (m, 2H, ArH), 7.92 (d, 1H, *J* = 8.60 Hz, ArH), 7.72 (d, 1H, *J* = 8.28 Hz, ArH), 7.62 (bs, 1H, NH), 7.15-7.13 (m, 2H, ArH), 6. 66 (d, 2H, *J* = 8.72 Hz, ArH), 5.02 (bs, 1H, NH); ^{13}C NMR (100 MHz, $CDCl_3$): δ = 147.6, 142.5, 132.2, 130.2, 129.3, 124.0, 120.8 (ArC); MS (ESI), m/z: 361.7 (M^++1); Anal. Calcd for $C_{18}H_{12}ClN_7$: C, 59.76; H, 3.34; N, 27.10, Found:

C, 59.83; H, 3.32; N, 27.14.

General procedure for the synthesis of compounds 7-18.

[4-(1*H*-Benzimidazol-2-yl)-phenyl]-(6-chloro-1*H*-pyrazolo[3,4-*d*]pyrimidin-4-yl)-amine **(6)** (0.100 g, 2 mmol) was refluxed with various amines (7 mmol) and potassium carbonate (0.057 g, 4 mmol) in *n*-butanol (20 ml) for 24 h and reaction was monitored by TLC. Crude solid was obtained with evaporation of the solvent under vacuum that was purified by column chromatography using chloroform:methanol as eluents to give pure compounds **7-18**.

[4-(1*H*-Benzimidazol-2-yl)-phenyl]-(6-morpholin-4-yl-1*H*-pyrazolo[3,4-*d*]pyrimidin-4-yl)-amine (7).

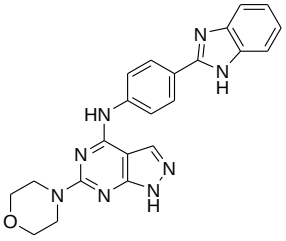

White powder; yield: 77%; mp: > 300 ^{o}C; ^{1}H NMR (400 MHz, $CDCl_3$ + DMSO-d_6): δ = 8.08 (d, 2H, *J* = 8.72 Hz, ArH), 7.85 (s, 1H, ArH), 7.82 (d, 2H, *J* = 8.72 Hz, ArH), 7.76 (d, 2H, *J* = 8.68 Hz, ArH), 7.50 (bs, 1H, NH), 6.75 (d, 2H, *J* = 8.72 Hz, ArH), 3.86 (t, 6H, *J* = 5.04 Hz, mor-CH_2), 3.73-3.71 (m, 2H, mor-CH_2); ^{13}C NMR (100 MHz, $CDCl_3$ + DMSO-d_6): δ = 164.6, 163.8, 150.8, 142.6, 137.3, 127.1, 122.3, 120.8, 119.1, 114.1 (ArC), 66.0 (O-CH_2), 63.0 (N-CH_2); MS (ESI), m/z: 495.5 (M^++1); Anal. Calcd for $C_{27}H_{26}FN_9$: C, 65.44; H, 5.29; N, 25.44, Found: C, 65.55; H, 5.25; N, 25.49.

[4-(1*H*-Benzimidazol-2-yl)-phenyl]-(6-pyrrolidin-1-yl-1*H*-pyrazolo[3,4-*d*]pyrimidin-4-yl)-amine (8).

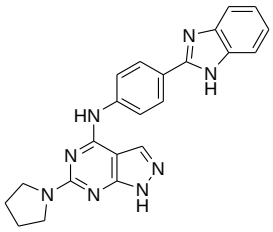

White powder; yield: 69%; mp: > 300 ^{o}C; ^{1}H NMR (400 MHz, $CDCl_3$ + DMSO-d_6): δ = 8.01 (d, 1H, *J* = 9.16 Hz, ArH), 7.98 (s, 1H, ArH), 7.88 (bs, 1H, ArH), 7.86 (d, 1H, *J* = 8.68 Hz, ArH), 7.69 (d, 1H, *J* = 5.04 Hz, ArH), 7.67 (d, 1H, *J* = 5.04 Hz, ArH), 7.18 (d, 1H, *J* = 3.20 Hz, ArH), 7.17 (d, 1H, *J* = 3.20 Hz, ArH), 7.00 (t, 2H, *J* = 8.72 Hz, ArH), 3.61-3.59 (m, 4H, pyrr-CH_2), 1.99-1.94 (m, 4H, pyrr-CH_2); ^{13}C NMR (100 MHz, $CDCl_3$ + DMSO-d_6): δ = 163.9, 151.6, 138.7, 135.6, 135.2, 134.3, 133.2, 128.6, 127.5, 125.9, 122.7, 118.1, 116.4, 114.9, 114.7, 101.8 (ArC), 46.4 (N-CH_2), 29.2 (CH_2); MS (ESI), m/z: 410.4 (M^++1); Anal. Calcd for $C_{23}H_{22}N_8$: C, 67.30; H, 5.40; N, 27.30, Found: C, 67.49; H, 5.32; N, 27.39.

[4-(1*H*-Benzimidazol-2-yl)-phenyl]-(6-piperidin-1-yl-1*H*-pyrazolo[3,4-*d*]pyrimidin-4-yl)-amine (9).

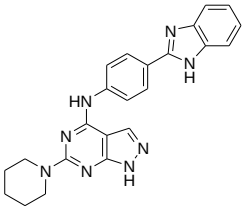

White powder; yield: 72%; mp: > 300 ^{o}C; ^{1}H NMR (400 MHz, $CDCl_3$ + DMSO-d_6): δ = 8.46 (s, 1H, ArH), 8.31 (s, 1H, ArH), 8.12 (d, 1H, *J* = 8.72 Hz, ArH), 7.89 (d, 1H, *J* = 8.24 Hz, ArH), 7.70-7.66 (m, 1H, ArH), 7.61-7.59 (m, 2H, ArH), 7.22-7.19 (m, 1H, ArH), 7.03 (t, 2H, *J* = 8.24 Hz, ArH), 3.83-3.80 (m, 4H, pip-CH_2), 1.71-1.62 (m, 6H, pip-CH_2); ^{13}C NMR (100 MHz, $CDCl_3$ + DMSO-d_6): δ = 151.6, 142.2, 135.7, 135.5, 128.4, 127.3, 125.8, 120.8, 114.4, 114.2, 108.5 (ArC), 46.5 (N-CH_2), 26.2 (CH_2), 25.2 (CH_2); MS (ESI), m/z: 412.4 (M^++1); Anal. Calcd for $C_{22}H_{20}N_8O$: C, 64.07; H, 4.89; N, 27.17, Found: C, 64.34; H, 4.76; N, 27.27.

[4-(1*H*-Benzimidazol-2-yl)-phenyl]-[6-(4-methyl-piperazin-1-yl)-1*H*-pyrazolo[3,4-*d*]pyrimidin-4-yl]-amine (10).

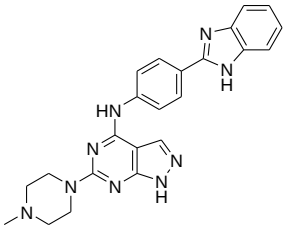

White powder; yield: 74%; mp: > 300 ^{o}C; ^{1}H NMR (400 MHz, $CDCl_3$ + DMSO-d_6): δ = 8.14 (d, 1H, *J* = 8.68 Hz, ArH), 8.04 (s, 1H, ArH), 7.95 (bs, 1H, ArH), 7.81 (d, 1H, *J* = 8.68 Hz, ArH), 7.64-7.60 (m, 2H, ArH), 7.22 (d, 1H, *J* = 3.20 Hz, ArH), 7.20 (d, 1H, *J* = 3.20 Hz, ArH), 7.04 (t, 2H, *J* = 8.68 Hz, ArH), 3.88 (t, 4H, *J* = 5.04 Hz, pip-CH_2), 2.53 (t, 2H, *J* = 4.56 Hz, pip-CH_2), 2.48 (t, 2H, *J* = 5.04 Hz, pip-CH_2), 2.30 (s, 3H, N-CH_3); ^{13}C NMR (100 MHz, $CDCl_3$ + DMSO-d_6): δ = 165.8, 158.5, 156.1, 151.6, 142.1, 135.6, 128.4, 127.3, 125.8, 114.4, 114.2, 108.5 (ArC), 46.5 (N-CH_2), 40.9 (N-CH_2), 13.4 (N-CH_3); MS (ESI), m/z: 425.4 (M^++1); Anal. Calcd for $C_{23}H_{23}N_9$: C, 64.92; H, 5.45; N, 29.63, Found: C, 64.99; H, 5.32; N, 29.68.

***N*^{6}-(2-Amino-ethyl)-*N*^{4}-[4-(1*H*-benzimidazol-2-yl)-phenyl]-1*H*-pyrazolo[3,4-*d*]pyrimidine-4,6-diamine (11).**

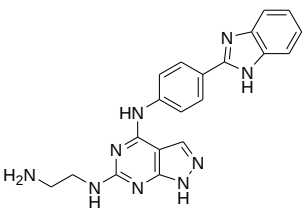

White powder; yield: 73%; mp: > 300 ^{o}C; ^{1}H NMR (400 MHz, $CDCl_3$ + DMSO-d_6): δ = 8.12 (d, 1H, *J* = 8.68 Hz, ArH), 7.82-7.79 (m, 2H, ArH), 7.62-7.60 (m, 2H, ArH), 7.22-7.20 (m, 2H, ArH), 7.03 (t, 2H, *J* = 8.72 Hz, ArH), 3.64 (bs, 1H, NH), 3.53 (t, 2H, *J* = 4.12 Hz, N-CH_2), 2.99 (t, 2H, *J* = 5.52 Hz, N-CH_2); ^{13}C NMR (100 MHz, $CDCl_3$ +

DMSO-d_6): δ = 148.7, 144.7, 135.1, 131.5, 128.3, 125.2, 119.5, 114.7, 114.5, 113.3 (ArC), 52.3 (N-CH_2), 42.6 (N-CH_2); MS (ESI), m/z: 385.4 (M^++1); Anal. Calcd for $C_{20}H_{19}N_9$: C, 62.32; H, 4.97; N, 32.71, Found: C, 62.45; H, 4.93; N, 32.65.

2-(4-{4-[4-(1*H*-Benzimidazol-2-yl)-phenylamino]-1*H*-pyrazolo[3,4-*d*]pyrimidin-6-yl}-piperazin-1-yl)-ethanol (12).

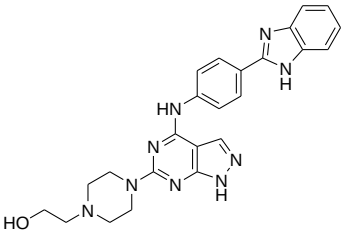

White powder; yield: 72%; mp: > 300 ^oC; ^1H NMR (400 MHz, $CDCl_3$ + DMSO-d_6): δ = 8.14 (d, 1H, *J* = 9.16 Hz, ArH), 7.95 (s, 1H, ArH), 7.85 (bs, 1H, NH), 7.80 (d, 1H, *J* = 8.68 Hz, ArH), 7.63-7.59 (m, 3H, ArH), 7.23-7.19 (m, 2H, ArH), 7.04 (t, 1H, *J* = 8.92 Hz, ArH), 3.88 (t, 4H, *J* = 4.56 Hz, N-CH_2), 3.72 (t, 2H, *J* = 5.48 Hz, N-CH_2), 3.67 (t, 2H, *J* = 5.48 Hz, N-CH_2), 2.62-2.57 (m, 4H, N-CH_2); ^{13}C NMR (100 MHz, $CDCl_3$ + DMSO-d_6): δ = 164.4, 163.5, 163.1, 151.4, 142.2, 135.7, 134.8, 130.3, 128.3, 127.2, 125.8, 115.2, 109.2, 108.5 (ArC), 66.1 (O-CH_2), 46.4 (N-CH_2), 45.4 (N-CH_2), 43.0 (N-CH_2); MS (ESI), m/z: 455.5 (M^++1); Anal. Calcd for $C_{24}H_{25}N_9O$: C, 63.28; H, 5.53; N, 27.67, Found: C, 63.49; H, 5.49; N, 27.75.

***N*^{4}-[4-(1*H*-Benzimidazol-2-yl)-phenyl]-*N*^{6}-(2-morpholin-4-yl-ethyl)-1*H*-pyrazolo[3,4-*d*]pyrimidine-4,6-diamine (13).**

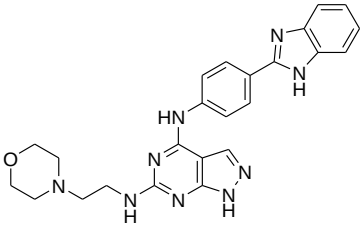

White powder; yield: 70%; mp: > 300 ^oC; ^1H NMR (400 MHz, $CDCl_3$ + DMSO-d_6): δ = 8.43-8.23 (m, 1H, ArH), 8.10 (d, 2H, *J* = 8.68 Hz, ArH), 7.86 (s, 1H, ArH), 7.66-7.58 (m, 3H, ArH), 7.20 (d, 1H, *J* = 3.20 Hz, ArH), 7.19 (d, 1H, *J* = 3.20 Hz, ArH), 7.04 (t, 1H, *J* = 8.24 Hz, ArH), 5.93 (bs, 1H, NH), 3.71-3.55 (m, 8H, mor-CH_2), 2.62 (t, 2H, *J* = 5.96 Hz, N-CH_2), 2.57-2.52 (m, 2H, N-CH_2); ^{13}C NMR (100 MHz, $CDCl_3$ + DMSO-d_6): δ = 165.3, 164.5, 163.7, 150.6, 137.2, 135.7, 135.1, 135.0, 128.4, 127.2, 125.3, 117.7, 114.8, 100.5 (ArC), 66.1 (O-CH_2), 52.9 (N-CH_2), 42.9 (N-CH_2), 36.5 (N-CH_2); MS (ESI), m/z: 455.5 (M^++1); Anal. Calcd for $C_{24}H_{25}N_9O$: C, 63.28; H, 5.53; N, 27.67, Found: C, 63.12; H, 5.47; N, 27.76.

N^4-[4-(1*H*-Benzimidazol-2-yl)-phenyl]-N^6-benzyl-1*H*-pyrazolo[3,4-*d*]pyrimidine-4,6-diamine (14).

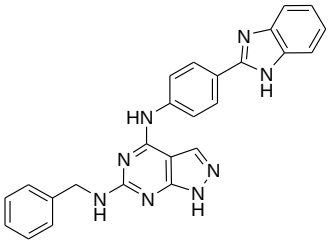

White powder; yield: 66%; mp: > 300 ^oC; ^1H NMR (400 MHz, $CDCl_3$ + DMSO-d_6): δ = 8.57 (s, 1H, ArH), 8.03 (d, 1H, *J* = 1.84 Hz, ArH), 7.32 (d, 1H, *J* = 8.72 Hz, ArH), 7.26 (d, 3H, *J* = 7.32 Hz, ArH), 7.21-7.16 (m, 3H, ArH), 7.13 (d, 3H, *J* = 8.72 Hz, ArH), 7.01 (d, 3H, *J* = 5.92 Hz, ArH), 5.27 (s, 2H, N-CH_2); ^{13}C NMR (100 MHz, $CDCl_3$ + DMSO-d_6): δ = 164.0, 163.8, 158.8, 156.4, 151.0, 137.9, 135.7, 135.3, 135.1, 134.2, 128.3, 127.2, 125.9, 121.8, 117.7, 116.1, 114.4, 114.2, 101.6 (ArC), 46.2 (N-CH_2); MS (ESI), m/z: 432.4 (M^++1); Anal. Calcd for $C_{25}H_{20}N_8$: C, 69.43; H, 4.66; N, 25.91, Found: C, 69.54; H, 4.60; N, 25.98.

2-{4-[4-(1*H*-Benzimidazol-2-yl)-phenylamino]-1*H*-pyrazolo[3,4-*d*]pyrimidin-6-ylamino}-ethanol (15).

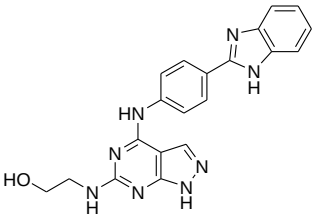

White powder; yield: 78%; mp: > 300 ^oC; ^1H NMR (400 MHz, $CDCl_3$ + DMSO-d_6): δ = 8.12 (t, 2H, *J* = Hz, ArH), 8.02 (bs, 1H, NH), 7.80 (s, 1H, ArH), 7.63-7.61 (m, 2H, ArH), 7.50-7.45 (m, 1H, ArH), 7.19-7.16 (m, 1H, ArH), 7.00 (d, 1H, *J* = 7.32 Hz, ArH), 6.31 (s, 1H, ArH), 3.75 (t, 2H, *J* = 4.56 Hz, O-CH_2), 3.57 (t, 2H, *J* = 3.20 Hz, N-CH_2); ^{13}C NMR (100 MHz, $CDCl_3$ + DMSO-d_6): δ = 165.4, 163.6, 163.3, 151.3, 141.6, 135.1, 128.1, 127.0, 125.5, 121.0, 120.7, 114.1, 113.9, 108.2 (ArC), 60.5 (O-CH_2), 46.2 (N-CH_2); MS (ESI), m/z: 386.4 (M^++1); Anal. Calcd for $C_{20}H_{18}N_8O$: C, 62.17; H, 4.70; N, 29.00, Found: C, 62.10; H, 4.66; N, 29.20.

N^6-Allyl-N^4-[4-(1*H*-benzimidazol-2-yl)-phenyl]-1*H*-pyrazolo[3,4-*d*]pyrimidine-4,6-diamine (16).

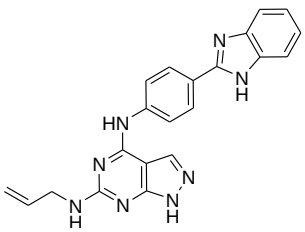

White powder; yield: 69%; mp: > 300 ^oC; ^1H NMR (400 MHz, $CDCl_3$ + DMSO-d_6): δ = 8.13 (d, 1H, *J* = 8.68 Hz, ArH), 8.01 (d, 1H, *J* = 8.72 Hz, ArH), 7.76 (t, 1H, *J* = 8.72 Hz, ArH), 7.64-7.61 (m, 2H, ArH), 7.29-7.23 (m, 2H, ArH), 7.02 (d, 2H, *J* = 8.92 Hz, ArH), 6.62 (bs, 1H, NH), 6.02-5.93 (m, 1H, allyl-CH), 5.29 (d, 2H, *J* = 18.32 Hz, allyl-CH_2), 5.15

(d, 2H, *J* = 10.08 Hz, N-CH_2); ^{13}C NMR (100 MHz, $CDCl_3$ + DMSO-d_6): δ = 164.4, 150.5, 126.5, 121.8, 121.7, 119.2, 114.2, 114.0 (ArC), 53.9 (N-CH_2); MS (ESI), m/z: 382.4 (M^++1); Anal. Calcd for $C_{21}H_{18}N_8$: C, 65.95; H, 4.74; N, 29.30, Found: C, 65.76; H, 4.71; N, 29.39.

N^4-[4-(1*H*-Benzimidazol-2-yl)-phenyl]-N^6-(4-fluoro-phenyl)-1*H*-pyrazolo[3,4-*d*]pyrimidine-4,6-diamine (17).

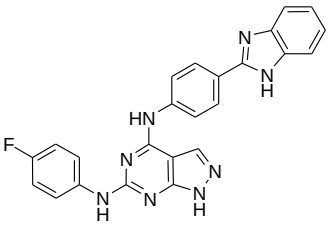

White powder; yield: 67%; mp: > 300 ^{o}C; ^{1}H NMR (400 MHz, $CDCl_3$ + DMSO-d_6): δ = 8.47 (bs, 1H, NH), 8.27 (s, 1H, ArH), 8.22 (d, 1H, *J* = 8.72 Hz, ArH), 7.92 (d, 1H, *J* = 8.68 Hz, ArH), 7.87 (d, 1H, *J* = 7.80 Hz, ArH), 7.69-7.66 (m, 4H, ArH), 7.29-7.27 (m, 1H, ArH), 7.09 (s, 1H, ArH), 7.05 (d, 2H, *J* = 8.68 Hz, ArH); ^{13}C NMR (100 MHz, DMSO-d_6): δ = 150.6, 139.8, 138.3, 138.1, 127.3, 124.4, 122.7, 122.5, 120.6, 120.5, 114.6, 114.8 (ArC); MS (ESI), m/z: 436.4 (M^++1); Anal. Calcd for $C_{24}H_{17}FN_8$: C, 66.05; H, 3.93; N, 25.67, Found: C, 66.05; H, 3.79; N, 25.61.

N^4-[4-(1*H*-Benzimidazol-2-yl)-phenyl]-N^6-cyclohexyl-1*H*-pyrazolo[3,4-*d*]pyrimidine-4,6-diamine (18).

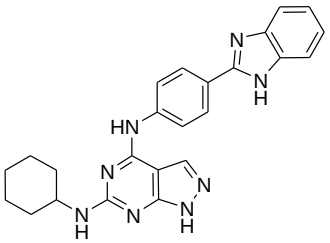

White powder; yield: 68%; mp: > 300 ^{o}C; ^{1}H NMR (400 MHz, $CDCl_3$ + DMSO-d_6): δ = 8.27 (bs, 1H, NH), 8.16 (s, 1H, ArH), 8.11 (d, 1H, *J* = 8.72 Hz, ArH), 7.90 (d, 1H, *J* = 6.88 Hz, ArH), 7.84 (s, 1H, ArH), 7.68-7.65 (m, 3H, ArH), 7.20-7.17 (m, 1H, ArH), 7.01 (t, 1H, *J* = 8.68 Hz, ArH), 5.54 (bs, 1H, NH), 3.87-3.84 (m, 1H, CH), 2.06-2.04 (m, 2H, CH_2), 1.86-1.60 (m, 4H, CH_2), 1.39-1.08 (m, 4H, CH_2); ^{13}C NMR (100 MHz, $CDCl_3$ + DMSO-d_6): δ = 151.6, 142.2, 135.3, 133.8, 130.8, 128.3, 127.2, 125.6, 115.7, 110.2, 108.5 (ArC), 52.8 (N-CH_2), 46.5 (CH_2), 43.0 (CH_2), 36.4 (CH_2); MS (ESI), m/z: 424.5 (M^++1); Anal. Calcd for $C_{24}H_{14}N_8$: C, 67.90; H, 5.70; N, 26.40, Found: C, 67.72; H, 5.40; N, 26.21.

In Vitro Anticancer Screening Protocol[159-161]

The human tumor cell lines of the cancer screening panel were grown in RPMI 1640 medium containing 5% fetal bovine serum and 2 μM L-glutamine. For a typical screening experiment, cells were inoculated into 96 well microtiter plates in 100 μL at plating densities ranging from 5000 to 40,000 cells/well depending on the doubling time of individual cell lines. After cell inoculation, the microtiter plates were incubated at 37^{o} C, 5% CO_2, 95% air and 100% relative humidity for 24 h prior to addition of experimental drugs. After 24 h, two plates of each cell line were fixed *in situ* with TCA, to represent a measurement of the cell population for each cell line at the time of drug addition (Tz). Experimental drugs were solubilized in dimethyl sulfoxide at 400 fold the desired final maximum test concentration and stored frozen prior to use. At the time of drug addition, an aliquot of frozen concentrate was thawed and diluted to twice the desired final maximum test concentration with complete medium containing 50 μg/mL gentamicin. Additional four, 10-fold or ½ log serial dilutions were made to provide a total of five drug concentrations plus control. Aliquots of 100 μL of these different drug dilutions were added to the appropriate microtiter wells already containing 100 μL of medium, resulting in the required final drug concentrations. Following drug addition, the plates were incubated for an additional 48 h at 37^{o} C, 5% CO_2, 95% air, and 100% relative humidity. For adherent cells, the assay was terminated by the addition of cold TCA. Cells were fixed *in situ* by the gentle addition of 50 μL of cold 50% (w/v) TCA (final concentration, 10% TCA) and incubated for 60 mins at 4 ^{o}C. The supernatant was discarded, and the plates were washed five times with tap water and air dried. Sulforhodamine B (SRB) solution (100 μL) at 0.4% (w/v) in 1% acetic acid was added to each well, and plates were incubated for 10 mins at room temperature. After staining, unbound dye was removed by washing five times with 1% acetic acid and the plates were air dried. Bound stain was subsequently solubilized with 10 mM trizma base, and the absorbance was read on an automated plate reader at a wavelength of 515 nm. For suspension cells, the methodology was the same except that the assay was terminated by fixing settled cells at the bottom of the wells by gently adding 50 μL of 80% TCA (final concentration, 16% TCA). Using the seven absorbance measurements [time zero, (Tz), control growth, I, and test growth in the presence of drug at the five concentration levels (Ti)], the percentage growth was calculated at each of the drug concentrations levels. Percentage growth inhibition was calculated as:

$[(Ti – Tz)/(C-Tz)] \times 100$

for concentrations for which Ti>/= Tz

[(Ti – Tz)/Tz] × 100

for concentrations for which Ti < Tz.

Three dose response parameters were calculated for each experimental agent. Growth inhibition of 50% (GI_{50}) was calculated from [(Ti-Tz)/(C-Tz)] ×100 = 50, which was the drug concentration resulting in a 50% reduction in the net protein increase (as measured by SRB staining) in control cells during the drug incubation. The drug concentration resulting in total growth inhibition (TGI) was calculated from Ti =Tz. The LC_{50} (concentration of drug resulting in a 50% reduction in the measured protein at the end of the drug treatment as compared to that at the beginning) indicating a net loss of cells following treatment was calculated from [(Ti-Tz) / Tz] ×100 = -50. Values were calculated for each of these three parameters if the level of activity was reached; however, if the effect was not reached or was exceeded, the value for that parameter was expressed as greater or less than the maximum or minimum concentration tested.

Dihydrofolate Reductase Inhibition Assay

The dihydrofolate reductase inhibition assay was performed as per the manual of the DHFR assay kit (Sigma product code CS0340). All the dilutions were made in assay buffer, pH 7.5. 10 mM stock solutions of dihydrofolic acid and NADPH in assay buffer were prepared. Stock solutions of the test compounds with different concentrations were prepared in DMSO, and an amount of 20 μL of each was taken to attain final concentration of 10^{-8}, 10^{-7}, 10^{-6} and 10^{-5} M in the respective wells of 96-well plate containing assay buffer. An amount of 0.1 unit of DHFR as supplied in the kit was diluted, and an amount of 20 μL of its 3×10^{-3} unit was used in each reaction. Each well of the 96-well plate was charged with 157.8 μL of assay buffer. Then 1.2 μL of NADPH solution was added to each well except 1A and 1B, and 20 μL of test compound (including methotrexate as positive control) was added to each well except 1A−H. The reaction was started by the addition of 1μL of dihydrofolic acid to each well except 1C and 1D. 1G and 1H contained 20 μL of DMSO to check any inhibition of enzyme activity due to DMSO. The change in absorbance at 340 nm was monitored as a function of time. Percentage inhibition of enzymatic activity was calculated after nullifying the effects of NADPH, folate, and solvent. IC_{50} was calculated by plotting a graph between percentage inhibition and the corresponding concentration of the compound using Graphpad Prism version 6.01.

DNA Binding Study Protocol

Preparation of stock and ct-DNA solution: Stock solution of compounds (10 mM) was prepared in AR grade DMSO. The DNA binding experiments were carried out by making dilution of the stock solution with phosphate buffer. Stock solution of ct-DNA (Sigma product code D4522) was prepared by dissolving powdered lyophilized DNA in phosphate buffer (10 mM, pH 7.0). The purity of ct-DNA was verified by monitoring the ratio of the absorbance at 260 nm and 280 nm, and the ratio of A260/A280 was 1.82, indicating that the ct-DNA was sufficiently free of protein contamination. The concentration of ct-DNA in terms of the nucleotide phosphate (i.e. nucleotide) was determined to be 2.56×10^{-3} mol L^{-1} by UV-vis absorption at 260 nm using a molar absorption coefficient of ε_{260} = 6600 L $mol^{-1}cm^{-1}$ (expressed as the molarity of phosphate groups). All stock solutions were stored at 0–4 ^{0}C.

UV-vis absorption spectra: All the spectra were recorded at ambient temperature (300 K). UV-Vis spectra were recorded on a Shimadzu-2400 PC spectrometer with a 1 cm cuvette. Any background buffer signal was electronically subtracted. Absorption titrations were performed with constant ligand concentration of 20 μM and increasing ct-DNA concentration (up to 20 μM). The control experiment was done by adding equal volumes of buffer solution instead of DNA solution to the same concentration of compound. The control experiment showed no significant change in the absorption spectra of the compound.

Fluorescence spectra: Emission spectra were recorded with a Cary Eclipse Fluorescence Spectrophotometer at ambient temperature. A slit width of 10 nm was used with suitable λ_{ex}. The titration experiment was accomplished with a constant ligand concentration (20 μM) and by varying the concentration of DNA in cuvette (0.5-150 μM).

Binding Constants: Binding constant K_a for the ligand.DNA complex was estimated from absorbance and fluorescence titration data using the Benesi–Hildebrand equation that is represented as follow:

$$1/(A_f - A_{obs}) = 1/(A_f - A_{fc}) + \{1/[K_a(A_f - A_{fc})]\}[\text{ligand}]$$

where K_a is the binding constant, A_f is the absorbance of the free host, A_{obs} is the absorbance observed, and A_{fc} is the absorbance at saturation. K_a was determined from the ratio of intercept to slope obtained from the linear fit of the plot of $1/(A_f - A_{obs})$ vs.1/[ligand].

DNA thermal denaturation: Thermal melting curves were measured with Shimadzu-2400 PC spectrometer equipped with a Peltier temperature controller system (±0.1 °C). ct-DNA was treated with compounds (ratio of DNA to compound = 1:1) and kept at 25 °C for 5 minutes. All the solutions were degassed before the experiment. The absorbance of ct-DNA (50 μM) in buffer (pH 7.4) was measured at 260 nm. DNA melting experiment was carried out by monitoring the absorbance of ct-DNA at 260 nm at various temperatures in the presence and absence of drug with a ramp rate of 0.5 ^{o}C/min in a phosphate buffer (pH 7.0). T_m was determined from the 1st derivative of the absorbance vs. temperature curve.

Competitive binding study with Ethidium bromide and Hoechst 33258: Competitive binding of ligands with DNA in the presence of intercalator, ethidium bromide and classical minor groove binder, Hoechst 33258 were also studied. Ethidium bromide and Hoechst 33258 (Sigma) were dissolved in Milli-Q water to prepare a stock solution with 1 mM strength and diluted immediately before use. Fluorescence spectra were taken in the presence of ethidium bromide and Hoechst 33258 (10 μM) while increasing the amount of ct-DNA (0 to 20 μM) and using an excitation wavelength of 480 nm and 353 nm. Compounds were added with an increasing concentration of 2 μM (up to 30 μM), mixed thoroughly after each addition and the emission spectrum was recorded with λ_{ex} = 480 nm and λ_{ex} = 353 nm.

Viscosity measurements: Viscosity measurements were conducted on a viscometer, immersed in a thermostated water-bath maintained at a constant temperature at 25 ± 0.1 ^{0}C. The experiments were carried out by adding different amounts of ligand into the viscometer while keeping the ct-DNA concentration constant. The flow time (t) of the solution through the capillary was measured with a digital stopwatch, and the average flow time of five parallel measurements was used to evaluate the relative viscosity of the samples. The data were presented as the relative viscosity of ct-DNA $(\eta/\eta_0)^{1/3}$ versus LDR (ligand-DNA ratio), where η and η_0 represent the viscosity of ct-DNA in the presence and absence of ligand, respectively. Viscosity values were calculated from the observed flow time DNA-containing solutions corrected for the flow time of buffer alone (t_0), $\eta = (t-t_0)/t_0$.

Ionic strength and iodide quenching effect: The concentration of sodium chloride/potassium iodide was increasing gradually when the concentration of the complex and DNA was fixed. The fluorescence spectrum was recorded after the system reaching equilibrium in 10 minutes.

BSA Binding Study Protocol

Materials and methods: The stock solution of BSA (Sigma Chemical Co., USA) was prepared by dissolving an appropriate amount of solid BSA in 0.1 M phosphate buffer at pH 7.4 and stored at 0−4 °C in the dark. Stock solutions of compounds (10^{-3} mol L^{-1}) were prepared in DMSO because of their lower solubility in water. All stock solutions were diluted to the required concentrations with phosphate buffer (pH 7.4). All other reagents were of analytical reagent grade.

UV-Visible absorption and fluorescence spectra: The UV-visible absorption and fluorescence emission spectra were measured with a 1 cm quartz cell. All the spectra were recorded at ambient temperature (300 K). UV-Vis spectra were recorded on Shimadzu-2400 PC spectrometer. The wavelength of the spectra was between 200 and 800 nm. All the UV-visible spectra were recorded after equilibration of solution for 5 min. Emission spectra were recorded with Varian Cary Eclipse fluorescence spectrometer. The excitation and emission wavelengths for BSA were 280 nm and 351 nm with a slit width of 10 nm. Very dilute solutions of BSA and compounds **5-21** were used to avoid inner filter effect. The titration experiments were performed by varying the concentration of compounds **5-21** and keeping the BSA concentration (10 µM).

Binding constant K was estimated from absorption and fluorescence titration data using the Benesi–Hildebrand equation. K was determined from the ratio of intercept to slope obtained from the linear fit of the plot of $1/(A_0 - A)$ vs. 1/[ligand] and $1/(F_0 - F)$ vs. 1/[ligand], where A_0 and A are the absorption intensities and F_0 and F are the emission intensities of the BSA in the absence and presence of compounds, respectively.

$$1/(A_0 - A) = 1/(A_0 - A_{fc}) + \{1/[K(A_0 - A_{fc})]\}[\text{ligand}]$$

To determine the binding number of triazine-benzimidazole analogues with BSA, the double-logarithmic equation was used:

$$\log[(F_0\text{-}F)/F] = \log K + n \log [Q]$$

where, F_0 and F are the emission intensities of BSA in the absence and presence of triazine-benzimidazole analogues, respectively. A plot of $\log[(F_0\text{-}F)/F]$ vs. log[Q] will produce a straight line; whose slope is equal to n. The number of binding sites n as calculated from the plot is approximately equal to 1 for BSA and it is in good agreement with the literature reports.

Docking Study Protocol

Compounds were built using the builder tool kit of the software package Argus Lab 4.0.1.23 and energy minimized with semi-empirical quantum mechanical method PM3. Crystal coordinates was downloaded from protein data bank and in the molecule tree view of the software, the monomeric structures of the crystal co-ordinate was selected and the active site was defined as 15 Å around the ligand. Validation of the docking programme was checked by docking the known inhibitors of the respective enzymes in their binding sites. The molecule to be docked in the active site of the enzyme was pasted in the work space carrying the structure of the enzyme. The docking programme implements an efficient grid based docking algorithm which approximates an exhaustive search within the free volume of the S19 binding site cavity. The conformational space was explored by the geometry optimization of the flexible ligand (rings were treated as rigid) in combination with the incremental construction of the ligand torsions. Thus, docking occurs between the flexible ligand parts of the compound and enzyme. The docking was repeated several times (approx. 10000 iterations) until no change in the position of the ligand and a constant value of the binding energy was observed. The ligand orientation was determined by a shape scoring function based on Ascore and the final positions were ranked by lowest interaction energy values. H-bond between the respective compound and enzyme were explored. During computational docking, a pose is typically generated, scored and compared to the previous pose(s). The current pose is then accepted or rejected on the basis of the score for that pose.

REFERENCES

1. http://www.cancer.org/research/cancerfactsstatistics/cancerfactsfigures2015.
2. R. Ali, Z. Mirza, G. M. D. Ashraf, M. A. Kamal, S. A. Ansari, G. A. Damanhouri, A. M. Abuzenadah, A. G. Chaudhary and I. A. Sheikh, *Anticancer Res*., 2012, **32**, 2999.
3. A. Y. Louie and T. J. Meade, *Chem. Rev*., 1999, **99**, 2711.
4. P. Singla, V. Luxami and K. Paul, *Eur. J. Med. Chem*., 2015, **102**, 39.
5. K. Arya and A. Dandia, *Bioorg. Med. Chem. Lett.,* 2007, **17**, 3298.
6. S. Melato, D. Prosperi, P. Coghi, N. Basilico and D. Monti, *ChemMedChem.,* 2008, **3**, 873.
7. A. Baliani, G. J. Bueno, M. L. Stewart, V. Yardley, R. Brun, M. P. Barrett and I. H. Gilbert, *J. Med. Chem.*, 2005, **48**, 5570.
8. Y. Z. Xiong, F. E. Chen, J. Balzarini, E. De clercq and C. Pannecouque, *Eur. J. Med. Chem.,* 2008, **43**, 1230.
9. K. Srinivas, U. Srinivas, K. Bhanuprakash, K. Harakishore, U. S. N. Murthy and V. J. Rao, Eur. *J. Med. Chem.* 2006, **41**, 1240.
10. J. C. Verheijen, D. J. Richard, K. Curran, J. Kaplan, M. Lefever, P. Nowak, D. J. Malwitz, N. Brooijmans, L. Toral-Barza, W.-G. Zhang, J. Lucas, I. Hollander, S. Ayral-Kaloustian, T. S. Mansour, K. Yu and A. Zask, *J. Med. Chem.* 2009, **52**, 8010.
11. P. S. Shirude, R. Shandil, C. Sadler, M. Naik, V. Hosagrahara, S. Hameed, V. Shinde, C. Bathula, V. Humnabadkar, N. Kumar, J. Reddy, V. Panduga, S. Sharma, A. Ambady, N. Hegde, J. Whiteaker, R. E. McLaughlin, H. Gardner, P. Madhavapeddi, V. Ramachandran, P. Kaur, A. Narayan, S. Guptha, D. Awasthy, C. Narayan, J. Mahadevaswamy, K. G. Vishwas, V. Ahuja, A. Srivastava, K. R. Prabhakar, S. Bharath, R. Kale, M. Ramaiah, N. R. Choudhury, V. K. Sambandamurthy, S. Solapure, P. S. Iyer, S. Narayanan and M. Chatterji, *J. Med. Chem.* 2013, **56**, 9701.
12. X. Wang, C.-X. Zhou, J.-W. Yan, J.-Q. Hou, S.-B. Chen, T.-M. Ou, L.-Q. Gu, Z.-S. Huang and J. H. Tan, *ACS. Med. Chem. Lett.*, 2013, **4**, 909.
13. A. Sharma, V. Luxami and K. Paul, *Eur. J. Med. Chem.* 2015, **93**, 414.
14. I. Giorgi, M. Leonardi, D. Pietra, G. Biagi, A. Borghini, I. Massarelli, O. Ciampi and A. M. Bianucci, *Bioorg. Med. Chem.,* 2009, **17**, 1817.

15. R. Duval, S. Kolb, E. Braud, D. Genest and C. Garbay, *J. Comb. Chem.*, 2009, **11**, 947.
16. J. R. Kumar, J. L. Jawahar and D. P. Pathak, *Eur. J. Chem*., 2006, **3**, 278.
17. A. T. Mavrova, K. K. Anichina, D. I. Vuchev, J. A. Tsenov, M. S. Kondeva and M. K. Micheva, *Bioorg. Med. Chem*., 2005, **13,** 5550.
18. A. Kamal, P. P. Kumar, K. Sreekanth, B. N. Seshadri and P. Ramulu, *Bioorg. Med. Chem. Lett*., 2008, **18**, 2594.
19. E. A. Rashedy and H. Y. Aboul-Enein, *Mini–Rev. Med. Chem*., 2013, **13**, 399.
20. A. Todorovic, C. G. Joseph, N. B. Sorensen, M. S. Wood and C. Haskell-Luevano, *Chem. Biol. Drug Des*., 2007, **69**, 338.
21. A. W. White, N. J. Curtin, B. W. Eastman, B. T. Golding, Z. Hostomsky, S. Kyle, J. Li, K. A. Maegely, D. J. Skalitzy, S. E. Webber, X. H. Yu and R. J. Griffin, *Bioorg. Med. Chem. Lett*., 2004, **14,** 2433.
22. A. R. Mackenzie, A. P. Marchington, D. S. Middleton, S. D. Newman, C. N. Selway and N. T. Terrett, *Bioorg. Med. Chem. Lett*., 2003, **13**, 2211.
23. A. A. Selcen, Z. Sevil, Z. Istvan, C. Gunes, R. Borbala, G. H. Semih and T. Zeki, *J. Enzyme Inhib. Med. Chem*. 2009, **24,** 844.
24. S. Hirashima, T. Suzuki, T. Ishida, S. Noji, S. Yata, I. Ando, M. Komatsu, S. Ikeda and H. Hashimoto, *J. Med. Chem*., 2006, **49,** 4721.
25. A. W. Denny, G. W. Rewcastle and B. C. Baguley, *J. Med. Chem*., 1990, **33,** 814.
26. A. L. Smith, N. D. D'Angelo, Y. Y. Bo, S. K. Booker, V. J. Cee, B. Herberich, F. T. Hong, C. L. M. Jackson, B. A. Lanman, L. Liu, N. Nishimura, L. H. Pettus, A. B. Reed, S. Tadesse, N. A. Tamayo, R. P. Wurz, K. Yang, K. L. Andrews, D. A. Whittington, J. D. McCarter, T. S. Miguel, L. Zalameda, J. Jiang, R. Subramanian, E. L. Mullady, S. Caenepeel, D. J. Freeman, L. Wang, N. Zhang, T. Wu, P. E. Hughes and M. H. Norman, *J. Med. Chem.*, 2012, **55**, 5188.
27. M. H. Norman, K. L. Andrews, Y. Y. Bo, S. K. Booker, S. Caenepeel, V. J. Cee, N. D. D'Angelo, D. J. Freeman, B. J. Herberich, F. T. Hong, C. L. M. Jackson, J. Jiang, B. A. Lanman, L. Liu, J. D. McCarter, E. L. Mullady, N. Nishimura, L. H. Pettus, A. B. Reed, T. S. Miguel, A. L. Smith, M. M. Stec, S. Tadesse, A. Tasker, D. Aidasani, X. Zhu, R. Subramanian, N. A. Tamayo, L. Wang, D. A. Whittington, B. Wu, T. Wu, R. P. Wurz, K. Yang, L. Zalameda, N. Zhang and P. E. Hughes, *J. Med. Chem.*, 2012, **55**,

7796.

28. N. D. D'Angelo, T. S. Kim, K. Andrews, S. K. Booker, S. Caenepeel, K. Chen, D. D'Amico, D. Freeman, J. Jiang, L. Liu, J. D. McCarter, T. S. Miguel, E. L. Mullady, M. Schrag, R. Subramanian, J. Tang, R. C. Wahl, L. Wang, D. A. Whittington, T. Wu, N. Xi, Y. Xu, P. Yakowec, K. Yang, L. P. Zalameda, N. Zhang, P. Hughes and M. H. Norman, *J. Med. Chem.*, 2011, **54**, 1789.
29. R. P. Wurz, L. Liu, K. Yang, N. Nishimura, Y. Bo, L. H. Pettus, S. Caenepeel, D. J. Freeman, J. D. McCarter, E. L. Mullady, T. S. Miguel, L. Wang, N. Zhang, K. L. Andrews, D. A. Whittington, J. Jiang, R. Subramanian, P. E. Hughes and M. H. Norman, *Bioorg. Med. Chem. Lett.*, 2012, **22**, 5714.
30. G. W. Rewcastle, S. A. Gamage, J. U. Flanagan, R. Frederick, W. A. Denny, B. C. Baguley, P. Kestell, R. Singh, J. D. Kendall, E. S. Marshall, C. L. Lill, W. J. Lee, S. Kolekar, C. M. Buchanan, S. M. F. Jamieson and P. R. Shepherd, *J. Med. Chem*., 2011, **54**, 7105.
31. G. W. Rewcastle, S. A. Gamage, J. U. Flanagan, J. D. Kendall, W. A. Denny, B. C. Baguley, C. M. Buchanan, M. Chao, P. Kestell, S. Kolekar, W. J. Lee, C. L. Lill, A. Malik, R. Singh, S. M. F. Jamieson and P. R. Shepherd, *Eur. J. Med. Chem.*, 2013, **64**, 137.
32. E. A. Peterson, A. A. Boezio, P. S. Andrews, C. M. Boezio, T. L. Bush, A. C. Cheng, D. Choquette, J. R. Coats, A. E. Colletti, K. W. Copeland, M. DuPont, R. Graceffa, B. Grubinska, J. L. Kim, R. T. Lewis, J. Liu, E. L. Mullady, M. H. Potashman, K. Romero, P. L. Shaffer, M. K. Stanton, J. C. Stellwagen, Y. Teffera, S. Yi, T. Cai and D. S. La, *Bioorg. Med. Chem. Lett.*, 2012, **22**, 4967.
33. R. Kumar, L. Gupta, P. Pal, S. Khan, N. Singh, S. B. Katiyar, S. Meena, J. Sarkar, S. Sinha, J. K. Kanaujiya, S. Lochab, A. K. Trivedi and P. M. S. Chauhan, *Eur. J. Med. Chem.*, 2010, **45**, 2265.
34. A. M. Venkatesan, Z. Chen, O. D. Santos, C. Dehnhardt, E. D. Santos, S. A. Kaloustian, R. Mallon, I. Hollander, L. Feldberg, J. Lucas, K. Yu, I. Chaudhary and T. S. Mansour, *Bioorg. Med. Chem. Lett.*, 2010, **20**, 5869.
35. A. M. Venkatesan, C. M. Dehnhardt, E. D. Santos, Z. Chen, O. D. Santos, S. A. Kaloustian, G. Khafizova, N. Brooijmans, R. Mallon, I. Hollander, L. Feldberg, J.

Lucas, K. Yu, J. Gibbons, R. T. Abraham, I. Chaudhary and T. S. Mansour, *J. Med. Chem*., 2010, **53**, 2636.

36. Z. Brzozowski and F. Sączewski, *Eur. J. Med. Chem*., 2002, **37**, 709.
37. I. Paquin, S. Raeppel, S. Leit, F. Gaudette, N. Zhou, O. Moradei, O. Saavedra, N. Bernstein, F. Raeppel, G. Bouchain, S. Fre´chette, S. H. Woo, A. Vaisburg, M. Fournel, A. Kalita, M. F. Robert, A. Lu, M. C. T. Bourget, P. T. Yan, J. Liu, J. Rahil, A. R. MacLeod, J. M. Besterman, Z. Li and D. Delorme, *Bioorg. Med. Chem. Lett.*, 2008, **18**, 1067.
38. F. Sączewski, A. Bułakowska, P. Bednarski and R. Grunert, *Eur. J. Med. Chem*., 2006, **41**, 219.
39. S. S. Machakanur, B. R. Patil, D. S. Badiger, R. P. Bakale, K. B. Gudasi and S. W. A. Bligh, *J. Mol. Struct.*, 2012, **1011,** 121.
40. V. Garaj, L. Puccetti, G. Fasolis, J. Y. Winum, J. L. Montero, A. Scozzafava, D. Vullo, A. Innocentia and C. T. Supuran, *Bioorg. Med. Chem. Lett*., 2005, **15**, 3102.
41. T. Lee and Y. H. Seo, *Bioorg. Med. Chem. Lett*., 2013, **23**, 6427.
42. A. Suda, K. Kawasaki, S. Komiyama, Y. Isshiki, D. O. Yoon, S. J. Kim, Y. J. Na, K. Hasegawa, T. A. Fukami, S. Sato, T. Miura, N. Ono, T. Yamazaki, R. Saitoh, N. Shimma, Y. Shiratori and T. Tsukuda, *Bioorg. Med. Chem.*, 2014, **22**, 892.
43. D. Łażewska, M. Więcek, J. Ner, K. Kamińska, T. Kottke, J. S. Schwed, M. Zygmunt, T. Karcz, A. Olejarz, K. Kuder, G. Latacz, M. Grosicki, J. Sapa, J. K. Wojciechowska, H. Stark and K. K. Kononowicz, *Eur. J. Med. Chem*., 2014, **83**, 534.
44. H. Kothayer, A. A. Elshanawani, M. E. A. Kull, O. I. E. Sabbagh, M. P. V. Shekhar, A. Brancale, A. T. Jones and A. D. Westwell, *Bioorg. Med. Chem. Lett*., 2013, **23**, 6886.
45. P. A. Harris, D. Bandyopadhyay, S. B. Berger, N. Campobasso, C. A. Capriotti, J. A. Cox, L. Dare, J. N. Finger, S. J. Hoffman, K. M. Kahler, R. Lehr, J. D. Lich, R. Nagilla, R. T. Nolte, M. T. Ouellette, C. S. Pao, M. C. Schaeffer, A. Smallwood, H. H. Sun, B. A. Swift, R. D. Totoritis, P. Ward, R. W. Marquis, J. Bertin and P. J. Gough, *ACS Med. Chem. Lett.*, 2013, **4**, 1238.
46. R. Cincinelli, L. Musso, L. Merlini, G. Giannini, L. Vesci, F. M. Milazzo, N. Carenini, P. Perego, S. Penco, R. Artali, F. Zunino, C. Pisano and S. Dallavalle, *Bioorg. Med. Chem.*, 2014, **22**, 1089.

47. K. S. Kim, L. Zhang, R. Schmidt, Z.-W. Cai, D. Wei, D. K. Williams, L. J. Lombardo, G. L. Trainor, D. Xie, Y. Zhang, Y. An, J. S. Sack, J. S. Tokarski, C. Darienzo, A. Kamath, P. Marathe, Y. Zhang, J. Lippy, R. Jeyaseelan Sr., B. Wautlet, B. Henley, J. G. Brown, V. Manne, J. T. Hunt, J. Fargnoli and R. M. Borzilleri, *J. Med. Chem.*, 2008, **51**, 5330.

48. Y. Nakajima, T. Inoue, K. Nakai, K. Mukoyoshi, H. Hamaguchi, K. Hatanaka, H. Sasaki, A. Tanaka, F. Takahashi, S. Kunikawa, H. Usuda, A. Moritomo, Y. Higashi, M. Inami and S. Shirakami, *Bioorg. Med. Chem.*, 2015, **23**, 4871.

49. J. A. Alonso, M. Andrés, M. Bravo, M. Calbet, P. R. Eastwood, P. Eichhorn, C. Esteve, M. Ferrer, E. Gómez, J. González, M. Mir, I. Moreno, S. Petit, R. S. Roberts, S. Sevilla, B. Vidal, L. Vidal, P. Vilaseca and M. Zanuy, *Bioorg. Med. Chem. Lett.*, 2014, **24**, 5123.

50. M. J. Boyd, U. K. Bandarage, H. Bennett, R. R. Byrn, I. Davies, W. Gu, M. Jacobs, M. W. Ledeboer, B. Ledford, J. R. Leeman, E. Perola, T. Wang, Y. Bennani, M. P. Clark and P. S. Charifson, *Bioorg. Med. Chem. Lett.*, 2015, **25**, 1990.

51. C. Esteve, J. González, S. Gual, L. Vidal, S. Alzina, S. Sentellas, I. Jover, R. Horrillo, J. De Alba, M. Miralpeix, G. Tarrasón and B. Vidal, *Bioorg. Med. Chem. Lett.*, 2015, **25**, 1217.

52. A. Carbone, M. Pennati, B. Parrino, A. Lopergolo, P. Barraja, A. Montalbano, V. Spanò, S. Sbarra, V. Doldi, M. De Cesare, G. Cirrincione, P. Diana and N. Zaffaroni, *J. Med. Chem.*, 2013, **56**, 7060.

53. S. Gourdain, J. Dairou, C. Denhez, L. C. Bui, F. Rodrigues-Lima, N. Janel, J. M. Delabar, K. Cariou and R. H. Dodd, *J. Med. Chem.*, 2013**, 56**, 9569.

54. A. Kamal, E. V. Bharathi, J. S. Reddy, M. J. Ramaiah, D. Dastagiri, M. K. Reddy, A. Viswanath, T. L. Reddy, T. B. Shaik, S. N. C. V. L. Pushpavalli and M. P. Bhadra, *Eur. J. Med. Chem.*, 2011, **46**, 691.

55. S. Dadiboyena, A. Arfaoui, H. Amri, F. J. Piedrafita and A. Nefzi, *Bioorg. Med. Chem. Lett.*, 2015, **25**, 685.

56. Y. Nkizinkiko, B. V. S. S. Kumar, V. U. Jeankumar, T. Haikarainen, J. Koivunen, C. Madhuri, P. Yogeeswari, H. Venkannagari, E. Obaji, T. Pihlajaniemi, D. Sriram and L. Lehtiö, *Bioorg. Med. Chem.*, 2015, **23**, 4139.

57. A. Nencini, C. Pratelli, J. M. Quinn, M. Salerno, P. Tunici, A. De Robertis, S. Valensin, F. Mennillo, M. Rossi, A. Bakker, T. Benicchi, F. Cappelli, E. Turlizzi, M. Nibbio, N. P. Caradonna, U. Zanelli, M. Andreini, M. Magnani and M. Varrone, *Eur. J. Med. Chem.*, 2015, **95**, 526.
58. A. M. Alafeefy, M. Ceruso, A.-M. S. Al-Tamimi, S. D. Prete, C. Capasso and C. T. Supuran, *Bioorg. Med. Chem.*, 2014, **22**, 5133.
59. D. S. Matharu, D. P. Flaherty, D. S. Simpson, C. E. Schroeder, D. Chung, D. Yan, J. W. Noah, C. B. Jonsson, E. L. White, J. Aubé, R. K. Plemper, W. E. Severson and J. E. Golden, *J. Med. Chem.*, 2014, **57**, 10314.
60. M. N. Modica, S. Intagliata, V. Pittala, L. Salerno, M. A. Siracusa, A. Cagnotto, M. Salmona and G. Romeo, *Bioorg. Med. Chem. Lett.*, 2015, **25**, 1427.
61. F. A. M. Al-Omary, G. S. Hassan, S. M. El-Messery, M. N. Nagi, El-S. E. Habib and H. I. El-Subbagh, *Eur. J. Med. Chem.*, 2013, **63**, 33.
62. L. Yuan, C. W. Song, C. H. Li, Y. Li, L. Dong and S. F. Yin, *Eur. J. Med. Chem.*, 2013, **67**, 152.
63. J. Liu, W. Zhang, M. A. Stashko, D. DeRyckere, C. T. Cummings, D. Hunter, C. Yang, C. N. Jayakody, N. Cheng, C. Simpson, J. Norris-Drouin, S. Sather, D. Kireev, W. P. Janzen, H. S. Earp, D. K. Graham, S. V. Frye and X. Wang, *Eur. J. Med. Chem.*, 2013, **65**, 83.
64. G. L. Reddy, S. K. Guru, M. Srinivas, A. S. Pathania, P. Mahajan, A. Nargotra, S. Bhushan, R. A. Vishwakarma and S. D. Sawant, *Eur. J. Med. Chem.*, 2014, **80**, 201.
65. S. D. Sawant, G. L. Reddy, M. I. Dar, M. Srinivas, G. Gupta, P. K. Sahu, P. Mahajan, A. Nargotra, S. Singh, S. C. Sharma, M. Tikoo, G. Singh, R. A. Vishwakarma and S. H. Syed, *Bioorg. Med. Chem.*, 2015, **23**, 2121.
66. C.-H. Zhang, M.-W. Zheng, Y.-P. Li, X.-D. Lin, M. Huang, L. Zhong, G.-B. Li, R.-J. Zhang, W.-T. Lin, Y. Jiao, X.-A. Wu, J. Yang, R. Xiang, L.-J. Chen, Y.-L. Zhao, W. Cheng, Y.-Q. Wei and S.-Y. Yang, *J. Med. Chem.*, 2015, **58**, 3957.
67. J.-Y. Le Brazidec, A. Pasis, B. Tam, C. Boykin, C. Black, D. Wang, G. Claassen, J.-H. Chong, J. Chao, J. Fan, K. Nguyen, L. Silvian, L. Ling, L. Zhang, M. Choi, M. Teng, N. Pathan, S. Zhao, T. Li and A. Taveras, *Bioorg. Med. Chem. Lett.*, 2012, **22**, 2070.
68. J. Liu, C. Yang, C. Simpson, D. DeRyckere, A. V. Deusen, M. J. Miley, D. Kireev, J.

N. Drouin, S. Sather, D. Hunter, V. K. Korboukh, H. S. Patel, W. P. Janzen, M. Machius, G. L. Johnson, H. S. Earp, D. K. Graham, S. V. Frye and X. Wang, *ACS Med. Chem. Lett.*, 2012, **3**, 129.

69. D. J. Richard, J. C. Verheijen, K. Curran, J. Kaplan, L. T.-Barza, I. Hollander, J. Lucas, K. Yu and A. Zask, *Bioorg. Med. Chem. Lett.*, 2009, **19**, 6830.

70. S. M. Sondhi, N. Singh, A. Kumar, O. Lozachc and L. Meijerc, *Bioorg. Med. Chem.*, 2006, **14**, 3758.

71. S. Verma, D. Nagarathnam, J. Shao, L. Zhang, J. Zhao, L. Wang, T. Li, E. Mull, I. Enyedy, C. Wang, Q. Zhu, M. Altieri, J. Jordan, T. A. T. Dang and S. Reddy, *Bioorg. Med. Chem. Lett.*, 2005, **15**, 1973.

72. M. J. Bamford, M. J. Alberti, N. Bailey, S. Davies, D. K. Dean, A. Gaiba, S. Garland, J. D. Harling, D. K. Jung, T. A. Panchal, C. A. Patt, J. G. Steadman, A. K. Takle, J. T. Townsend, D. M. Wilson and J. Witherington, *Bioorg. Med. Chem. Lett.*, 2005, **15**, 3402.

73. M. J. Bamford, N. Bailey, S. Davies, D. K. Dean, L. Francis, T. A. Panchal, C. A. Parr, S. Sehmi, J. G. Steadman, A. K. Takle, J. K. Townsend and D. M. Wilson, *Bioorg. Med. Chem. Lett.*, 2005, **15**, 3407.

74. K. A. Emmitte, G. M. Adjebang, C. W. Andrews, G. A. Badiang Alberti, R. Bambal, S. D. Chamberlain, R. G. Davis-Ward, H. D. Dickson, D. F. Hassler, K. R. Hornberger, J. R. Jackson, K. W. Kuntz, K. W. Lansing, R. A. Mook Jr., K. E. Nailor, M. A. Pobanz, S. C. Smith, C. M. Sung and M. Cheung, *Bioorg. Med. Chem. Lett.*, 2009, **19**, 1694.

75. (a) K. Zimmermann, M. D. Wittman, M. G. Saulnier, U. Velaparthi, D. R. Langley, X. Sang, D. B. Frennesson, J. Carboni, A. Li, A. Greer, M. Gottardis, R. Attar, Z. Yang, P. Balimane, L. N. Discenza and D. Vyas, *Bioorg. Med. Chem. Lett*., 2008, **18**, 4075; (b) K. Zimmermann, M. D. Wittman, M. G. Saulnier, U. Velaparthi, D. R. Langley, X. Sang, D. B. Frennesson, J. Carboni, A. Li, A. Greer, M. Gottardis, R. Attar, Z. Yang, P. Balimane, L. N. Discenza and D. Vyas, *Bioorg. Med. Chem. Lett*., 2010, **20**, 1744.

76. M. P. Winters, D. J. Robinson, H. H. Khine, S. S. Pullen, J. R. Woska, E. L. Raymond, R. Sellati, C. L. Cywin, R. J. Snow, M. A. Kashem, J. A. Wolak, J. King, P. V. Kaplita, L. H. Liu, T. M. Farrell, R. DesJarlais, G. P. Roth, H. Takahashi and K. J. Moriarty, *Bioorg. Med. Chem. Lett.*, 2008, **18**, 5541.

77. N. Baindur, N. Chadha, B. M. Brandt, D. Asgari, R. J. Patch, C. Schalk-HiHi, T. E. Carver, I. P. Petrounia, C. A. Baumann, H. Ott, C. Manthey, B. A. Springer and M. R. Player, *J. Med. Chem.*, 2005, **48**, 1717.

78. R. Menicagli, S. Samaritani, G. Signore, S. Vaglini and L. D. Via, *J. Med. Chem.*, 2004, **47**, 4649.

79. D. Bartholomew, in: A. J. Boulton (Ed.), Comprehensive Heterocyclic Chemistry II, vol. 6, Pergamon, Oxford, 1996, pp. 575.

80. D. L. Comins, S. Óconnor, in: A. R. Katritzky (Ed.), Advances in Heterocyclic Chemistry, vol. 44, Academic Press, New York, 1988, pp. 243.

81. Crystallographic data for the structural analysis have been deposited at the Cambridge Crystallographic Data Centre. (E-mail: deposit@ccdc.cam.ac.uk).

82. Z. Brzozowski, F. Saczewski and M. Gdaniec, *Eur. J. Med. Chem.*, 2000, **35**, 1053.

83. H. S. A. Elzahabi, *Eur. J. Med. Chem*., 2011, **46**, 4025.

84. C. Y. Chi and W. H. Prusoff, *Biochem. Pharmcol.*, 1973, **22**, 3099.

85. H. A. Benesi and J. H. Hildebrand, *J. Am. Chem. Soc.*, 1949, **71**, 2703.

86. Compounds were constructed and docked with builder tool kit of software package ArgusLab 4.0.1 (www.arguslab.com).

87. A. Gangjee, W. Li, R. L. Kisliuk, V. Cody, J. Pace, J. Piraino and J. Makin, *J. Med. Chem*., 2009, **52**, 4892.

88. W. I. P. Mainwaring, J. H. Parish, J. D. Pickering and N. H. Mann, *Nucleic Acid Biochemistry and Molecular Biology*, Blackwell Scientific Publications, Oxford, 1982.

89. E. F. Gale, E. Cundliffe, P. E. Reynolds, M. H. Richmond and M. J. Waring, *The Molecular Basis of Antibiotic Action*, John Wiley & Sons Ltd., Chichester, 2nd edn, 1981.

90. F. Anam, A. Abbas, K. Mun Lo, Z. Ur Rehman, S. Hameed and M. M. Naseer, *New J. Chem.*, 2014, **38**, 5617.

91. (a) M. F. Brana, M. Cacho, A. Gradillas, B. de Pascual-Teresa and A. Ramos, *Curr. Pharm. Des*., 2001, **7**, 1745; (b) N. Shahabadi and M. Maghsudi, *Mol. BioSyst.*, 2014, **10**, 338.

92. (a) E. B. Veale and T. Gunnlaugsson, *J. Org. Chem.*, 2010, **75**, 5513; (b) E. B. Veale, D. O. Frimannsson, M. Lawler and T. Gunnlaugsson, *Org. Lett.*, 2009, **11**, 4040.

93. (a) J. R. Carreon, M. A. Roberts, L. M. Wittenhagen and S. O. Kelley, *Org. Lett.*, 2005, **7**, 99; (b) M. Krishnamurthy, B. D. Gooch and P. A. Beal, *Org. Lett.*, 2004, **6**, 63; (c) C. Bailly and J-P. Hénichart, *Bioconjugate Chem.*, 1991, **2**, 37914.
94. S. Kashanian, S. H. Zeidali, K. Omidfar and N. Shahabadi, *Mol. Biol. Reprod. Med*., 2012, **39**, 10045.
95. D. Sahoo, P. Bhattacharya and S. Chakrovarti, *J. Phys. Chem. B*, 2010, **114**, 2044.
96. Y. Zhang, G. Zhang, Y. Li and Y. Hu, *J. Agric. Food Chem.*, 2013, **61**, 2638.
97. P. E. Pjura, K. Grzeskowiak and R. E. Dickerson, *J. Mol. Biol.* 1987, **197**, 257.
98. (a) P. D. Ross and S. Subramanian, *Biochemistry*, 1981, **20**, 3096; (b) H. Wu, F. Jia, F. Kou, B. Liu, J. Yuan and Y. Bai, *Transition Met. Chem*., 2011, **36**, 847.
99. S. U. Rehman, Z. Yaseen, M. A. Husain, T. Sarwar, H. M. Ishqi and M. Tabish, *PloS One*, 2014, **9**, 93913.
100. G. Zhang, L. Wang, X. Zhou, Y. Li and D. Gong, *J. Agric. Food Chem.*, 2014, **62**, 991.
101. M. Banik, R. Mukherjee, M. Patra, A. K. Chatterjee, R. Chakraborty, A. P. Chattopadhyay and T. Basu, *J. Nanopar. Res.*, 2014, **16**, 2196.
102. T. Sarwar, M. A. Husain, S. Ur Rehman, H. M. Ishqi and M. Tabish, *Mol. BioSyst.*, 2015, **11**, 522.
103. A. Solankee and Y. Prajapati, *Rasayan J. Chem.* 2009, **2**, 9.
104. P. T. Selvam, P. P. Radhika, S. Janagaraj and A. S. Kumar, *Research in Biotechnology*, 2011, **2**, 50.
105. C. V. Kumar and A. S. Buranaprapuk, *Angew. Chem. Int. Ed. Engl.*, 1997, **36**, 2085.
106. T. Jr. Peters, *Adv. Protein Chem.*, 1985, **37**, 161.
107. N. Tayeh, T. Rungassamy and J. R. Albani, *J. Pharm. Biomed. Anal.*, 2009, **50**, 107.
108. B. Elsadek and F. Kratz, *J. Controlled Release*, 2012, **157**, 4.
109. F. Kratz and B. Elsadek, *J. Controlled Release*, 2012, **161**, 429.
110. F. Kratz, *J. Controlled Release*, 2008, **132**, 171.
111. Y. J. Hu, Y. Liu and X. H. Xiao, *Biomacromolecules*, 2009, **10**, 517.
112. F. F. Tian, F. L. Jiang, X. L. Han, C. Xiang, Y. S. Ge, J. H. Li, Y. Zhang, R. Li, X. L. Ding and Y. Liu, *J. Phys. Chem. B*, 2010, **114**, 14842.
113. T. Forster, *Ann. Phys.*, 1948, **437**, 55.
114. T. Forster, *Discuss. Faraday Soc*., 1959, **27**, 7.

115. J. R. Lakowicz, Principles of Fluorescence Spectroscopy, Kluwer Academic/Plenum Publishers, Dordrecht, The Netherlands, 2004.
116. X. Pan, P. Qin, R. Liu and J. Wang, *J. Agric. Food Chem.*, 2011, **59**, 6650.
117. A. S. Sharma, S. Anandakumar and M. Ilanchelian, *J. Luminescence*, 2014, **151**, 206.
118. B. Yang, F. Hao, J. Li, K. Wei, W. Wang and R. Liu, *Food and Chem. Toxico.*, 2014, **65**, 227.
119. V. Levacher, R. Benoit, J. Duflos, G. Dupas and J. Bourguignon, *Tetrahedron*, 1991, **47**, 429.
120. L. N. Yakhontov and A. A. Prokopov, *Russ. Chem. Rev.*, 1980, **49**, 428.
121. K. S. Kim, L. Zhang, R. Schmidt, Z. W. Cai, D. Wei, D. K. Williams, L. J. Lombardo, G. L. Trainor, D. Xie, Y. Zhang, Y. An, J. S. Sack, J. S. Tokarski, C. Darienzo, A. Kamath, P. Marathe, Y. Zhang, J. Lippy, Sr. R. Jeyaseelam, B. Wautlet, B. Henley, J. Gullo-Brown, V. Manne, J. T. Hunt, J. Fargnoli and R. M. Borzilleri, *J. Med. Chem.*, 2008, **51**, 5330.
122. J. I. Manchester, D. D. Dussault, J. A. Rose, P. A. Boriack-Sjodin, M. Uria-Nickelsen, G. Loannidis, S. Bist, P. Fleming and K. G. Hull, *Bioorg. Med. Chem. Lett.*, 2012, **22**, 5150.
123. F. Zuccotto, E. Ardini, E. Casale and M. Angiolini, *J. Med. Chem*., 2010, **53**, 2681.
124. (a) J. R. Henry, K. C. Rupert, J. H. Dodd, I. J. Turchi, S. A. Wadsworth, D. E. Cavender, B. Fahmy, G. C. Olini, J. E. Davis, J. L. Pellegrino-Gensey, P. H. Schafer and J. J. Siekierka, *J. Med. Chem*., 1998, **41**, 4196; (b) J. R. Henry and J. H. Dodd, *Tetrahedron Lett.*, 1998, **39**, 8763.
125. J. J. Kulagowski, H. B. Broughton, N. R. Curtis, I. M. Mawer, M. P. Ridgill, R. Baker, F. Emms, S. Freedman, B. R. Marwood, S. Patel, S. Patel, C. I. Ragan and P. D. Leeson, *J. Med. Chem.*, 1996, **39**,1941.
126. M. P. Clark, M. W. Ledeboer, I. Davies, R. A. Byrn, S. M. Jones, E. Perola, A. Tsai, M. Jacobs, K. Nti-Addae, U. K. Bandarage, M. J. Boyd, R. S. Bethiel, J. J. Court, H. Deng, J. P. Duffy, W. A. Dorsch, L. J. Farmer, H. Gao, W. Gu, K. Jackson, D. H. Jacobs, J. M. Kennedy, B. Ledford, J. Liang, F. Maltais, M. Murcko, T. Wang, M. W. Wannamaker, H. B. Bennett, J. R. Leeman, C. McNeil, W. P. Taylor, C. Memmott, M. Jiang, R. Rijnbrand, C. Bral, U. Germann, A. Nezami, Y. Zhang, F. G. Salituro, Y. L.

Bennani and P. S. Charifson, *J. Med. Chem.*, 2014, **57**, 6668.

127. M. T. Jr.Record, T. M. Lohman and P. D. Haseth, *J. Mol. Biol.*, 1976, **107**, 145.

128. Y. Zhang, G. W. Zhang, Y. Li and Y. T. Hu, *J. Agric. Food Chem.*, 2013, **61**, 2638.

129. M. M. Robison and B. L. Robison, *J. Am. Chem. Soc.*, 1955, **77**, 457.

130. (a) P. C. Sharma, G. Kaur, R. Pahwa, A. Sharma and H. Rajak, *Curr. Med. Chem.*, 2011, **18**, 4786; (b) I. Khan, A. Ibrar, N. Abbas and A. Saeed, *Eur. J. Med. Chem*., 2014, **76**, 193; (c) R. Rajput and A. P. Mishra, *Int. J. Pharm. Pharm. Sci*., 2012, **4**, 66.

131. X. Wang, P. Li, Z. Li, J. Yin, M. He, W. Xue, Z. Chen and B. Song, *J. Agric. Food Chem*., 2013, **61**, 9575.

132. X. Wang, J. Yin, L. Shi, G. Zhang and B. Song, *Eur. J. Med. Chem*., 2014, **77**, 65.

133. Y. Takeuchi, M. Koike, K. Azuma, H. Nishioka, H. Abe, H.-S. Kim, Y. Wataya and T. Harayama, *Chem. Pharm. Bull*., 2001, **49**, 721.

134. (a) Z. Wang, M. Wang, X. Yao, Y. Li, J. Tan, L. Wang, W. Qiao, Y. Geng, Y. Liu and Q. Wang, *Eur. J. Med. Chem*., 2012, **53**, 275; (b) A. L. Leivers, M. Tallant, J. B. Shotwell, S. Dickerson, M. R. Leivers, O. B. McDonald, J. Gobel, K. L. Creech, S. L. Strum, A. Mathis, S. Rogers, C. B. Moore and J. Botyanszki, *J. Med. Chem*., 2014, **57**, 2091.

135. M. B. Patel, U. Harikrishnan, N. N. Valand, N. R. Modi and S. K. Menon, *Arch. Pharm*., 2013, **346**, 210.

136. A. M. Alafeefy, A. A. Kadi, A. S. El-Azab, S. G. Abdel-Hamide and M. H. Daba, *Arch. Pharm*., 2008, **341**, 377.

137. A. A. Al-Amiery, A. A. H. Kadhum, M. Shamel, M. Satar, Y. Khalid and A. B. Mohamad, *Med. Chem. Res.*, 2014, **23**, 236.

138. H.-Ze Li, H.-Y. He, Y.-Y. Han, X. Gu, L. He, Q.-R. Qi, Y.-L. Zhao and L. Yang, *Molecules*, 2010, **15**, 9473.

139. M. K. Prashanth, H. D. Revanasiddappa, K. M. L. Rai and B. Veeresh, *Bioorg. Med. Chem. Lett.*, 2012, **22**, 7065.

140. C. D. Kanakis, S. Nafisi, M. Rajabi, A. Shadaloi, P. A. Tarantilis, M. G. Polissiou, J. Bariyanga and H. A. Tajmir-Riahi, *Spectroscopy*, 2009, **23**, 29.

141. X. L. Han, P. Mei, Y. Liu, Q. Xiao, F. L. Jiang and R. Li, *Spectrochim. Acta Part A*, 2009, **74**, 781.

142. P. Qin, R. Liu, X. Pan, X. Fang and Y. Mou, *J. Agric. Food Chem*., 2010, **58**, 5561.

143. A. Papadopoulou, R. J. Green and R. A. Frazier, *J. Agric. Food Chem*., 2005, **53**, 158.

144. A. Gangjee, A. P. Vidwans, A. Vasudevan, S. F. Queener, R. L. Kisliuk, V. Cody, R. Li, N. Galitsky, J. R. Luft and W. Pangborn, *J. Med. Chem*., 1998, **41**, 3426.

145. (a) A. R. R. Rao and R. H. Bahekar, *Indian J. Chem*., 1999, **38B**, 434; (b) P. M. Chandrika, A. R. R. Rao, B. Narsaiah and M. B. Raju, *Int. J. Chem. Sci*., 2008, **6**, 1119; (c) S. S. Laddha, S. G. Wadodkar and S. K. Meghal, *ARKIVOC*, 2006, **xi**, 1; (d) M. Shariat, M. W. Samsudin and Z. Zakaria, *Chem. Cent. J*., 2013, **7**, 58; (e) S. M. E. Rayes, I. A. I. Ali and W. Fathalla, *ARKIVOC*, 2008, **xi**, 86.

146. M. Chauhan and R. Kumar, *Bioorg. Med. Chem.,* 2013, **21**, 5657.

147. S. Schenone, O. Bruno, M. Radi and M. Botta, *Med. Res. Rev.,* 2011, **31**, 1.

148. (a) J. Chern, K. Shia, T. Hsu, C. Tai, C. Lee, Y. Lee, C. Chang, S. Tseng and S. Shih, *Bioorg. Med. Chem. Lett.,* 2004, **14**, 2519; (b) T. A. Bektemirov, E. V. Chekunova, I. A. Korbukh, Y. N. Bulychev, N. G. Yakunina and M. N. Preobrazhenskaya, *Acta Virol.,* 1981, **25**, 326.

149. Y. L. Chen, United States Patent: 2000; Vol. 6051578.

150. (a) A. Trivedi, D. Dodiya, J. Surani, S. Jarsania, H. Mathukiya, N. Ravat and V. Shah, *Arch. Pharm*., 2008, **341**, 435; (b) A. Trivedi, S. Vaghasiya, B. Dholariya, D. Dodiya and V. Shah, *J. Enzyme Inhib. Med. Chem.,* 2010, **25**, 893; (c) A. R. Trivedi, B. H. Dholariya, C. P. Vakhariya, D. K. Dodiya, H. K. Ram, V. B. Kataria, A. B. Siddiqui and V. H. Shah, *Med. Chem. Res*., 2012, **21**, 1887.

151. A. Ali, G. E. Taylor, K. Ellsworth, G. Harris, R. Painter, L. Lynn and K. Young, *J. Med. Chem.,* 2003, **46**, 1824.

152. A. Angelucci, S. Schenone, G. L. Gravina, P. Muzi, C. Festuccia, C. Vicentini, M. Botta and M. Bologna, *Eur. J. Cancer,* 2006, **42**, 2838.

153. J. J. Marr and R. L. Berens, *Mol. Biochem. Parasitol.,* 1983, **7**, 339.

154. R. A. Nugent, C. J. Dunn, N. D. Staite, M. J. Murphy, S. T. Schlachter, D. G. Aspar, S. K. Shields and L. A. Galinet, *Phosphorus, Sulfur Silicon Relat. Elem*., 1996, **109**, 229.

155. (a) P. Dinér, J. P. Alao, J. Söderlund, P. Sunnerhagen and M. Grøtli, *J. Med. Chem.,* 2012, **55**, 4872; (b) L. L. Yang, G. B. Li, H. X. Yan, Q. Z. Sun, S. Ma, P. Ji, Z. R. Wang, S. Feng, J. Zou and S. Y. Yang, *Eur. J. Med. Chem.,* 2012, **56**, 30.

156. (a) A. Kumar, I. Ahmad, B. S. Chhikara, R. Tiwari, D. Mandal and K. Parang, *Bioorg. Med. Chem. Lett*., 2011, **21**, 1342; (b) X. Deng, B. Okram, Q. Ding, J. Zhang, Y. Choi, F. J. Adrián, A. Wojciechowski, G. Zhang, J. Che, B. Bursulaya, S. W. Cowan-Jacob, G. Rummel, T. Sim and N. S. Gray, *J. Med. Chem.*, 2010, **53**, 6934.

157. M. E. Welsch, A. S. Snyder and B. R. Stockwell, *Curr. Opin. Chem. Biol.*, 2010, **14**, 347.

158. R. K. Robins, *J. Am. Chem. Soc*., 1956, **78**, 784.

159. M. R. Grever, S. A. Sehepartz and B. A. Chabners, *Semin. Oncol*. 1992, **19**, 622.

160. A. Monks, D. Schudiero, P. Skehan, R. Shoemaker, K. Paull, D. Vistica, C. Hose, J. Langley, P. Cronise, A. Vaigro-Wolff, M. Gray-Goodrich, H. Campbell, J. Mayo and M. Boyd, *J. Natl. Cancer Inst*., 1991, **83**, 757.

161. M. R. Boyd and K. D. Paull, *Drug Dev. Res*., 1995, **34**, 91.

SUMMARY

Despite many therapeutic successes, cancer is a major worldwide public health problem and the leading cause of human mortality exceeded only by cardiovascular diseases. In 2015, there are estimated 16,58,370 new cancer cases diagnosed worldwide. More than 5,89,430 cancer deaths are reported only in US. More recently, components of the mitotic machinery have been targeted in an attempt to develop novel anticancer agents[1] that are used to control the growth of cancerous cells. Development of new anticancer drugs and more effective treatment strategies for cancers are of utmost importance as traditionally prescribed chemotherapeutic agents have problems with toxicity and drug resistance. In recent years, great advances in elucidating molecular structures have allowed precise determination of the interaction between proteins and DNA with various therapeutic agents. Identifying the exact nature of interaction for a drug is the key to control its specificity and reducing unwanted side effects.[2] Detailed structural information can be employed to design molecules that bind to specific targets, and many of these efforts are aimed at enzymes. Enzyme inhibitors have been used as therapeutic agents with organic molecules by interacting with targets through the weak linkage of hydrogen bonding and van der Waals contact that result in undesirable side effects due to the shorter residency time of the drug at the target, allowing more nonspecific interactions with non-target molecules. Nitrogen-containing heterocycles are present in a wide variety of bioactive natural products and biological molecules that may be good drug candidates. Specifically, triazine, pyrrolopyridine, quinazolinone, pyrazolopyrimidine, benzimidazole and their derivatives, which belong to the N-containing heterocyclic compounds, have caused universal concerns due to their widely and distinct pharmaceutical activities.

Keeping in view the above points, the following objectives have been designed.

(1) To synthesize triazine derivatives linked to azoles (benzimidazole/benzotriazole/benzothiazole) and primary/secondary amines.

(2) To synthesize substituted azoles linked with fused heterocyclic moieties followed by substitution with primary/secondary amines.

(3) To characterize synthesised compounds through spectroscopy techniques.

(4) To evaluate these compounds with different *in vitro* biological studies and predict the structure activity relationship (SAR).

In the present investigation, we have combined the structural artifacts of benzimidazole with triazine, pyrrolopyridines, quinazolinones and pyrazolopyrimidines moieties to make a hybrid

and substituted them with different secondary and primary amines in order to observe the effect of electron-donor and acceptor nitrogen groups within the moieties. Introduction of benzyl group at 1- or 3-position of benzimidazole are also known to increase lipid solubility of polar compounds, a character very much needed for the activity. The strategy of using substituted azoles linked to triazine derivatives or other fused heterocycles are particularly attractive as it is expected to provide a scope of preparing more interactions with the target site and thus, further affect the activity. Characterizations of these molecules were done with different spectroscopic techniques such as NMR and mass spectrometry. In the quest for biologically potent agents, these synthesized molecules were evaluated *in vitro* over 60 human cancer cell lines and dihydrofolate reductase inhibition. These compounds were further evaluated for their interactions with DNA and bovine albumin. SAR study was used to identify the structural features required for the antitumor properties of these new hybrid series and also the role of different structural fragments in affecting the properties of the drug. In order to have an insight into the molecular interaction of compounds, their docking were also planned to scrutinize the mode of interactions of compound with amino acids in the active site of the enzyme.

Chapter 2: Covers synthesis, characterization, evaluation and molecular modelling of triazine-benzimidazole analogous

2.1.1. Synthesis of regioisomeric triazine-benzimidazole hybrids (7-49):

Treatment of *o*-phenylenediamine with acetic acid at 100 $^{\circ}$C for 24 h to give brown solid of 2-methylbenzimidazole (**1)**. Nitration has been done with equal amounts of nitric acid and concentrated sulphuric acid at 0 $^{\circ}$C for 5 h to give 2-methyl-5-nitro-1*H*-benzimidazole **(2).** Treatment of **2** with benzyl chloride in the presence of K_2CO_3 and ethanol at reflux temperature for 8 h to give mixture of 1-benzyl-2-methyl-5-nitro-1*H*-benzimidazole **(3a)** and 3-benzyl-2-methyl-5-nitro-3*H*-benzimidazole **(3b)**. Reduction of **3a** and **3b** with stannous chloride and 2 N HCl at 110 $^{\circ}$C for 7 h gave mixture of products which were separated through column chromatography to pure regioisomeric 1-benzyl-2-methyl-1*H*-benzimidazol-5-ylamine **(4a)** and 3-benzyl-2-methyl-3*H*-benzimidazol-5-ylamine **(4b)** (Scheme 1).

Scheme 1[a]. Synthesis of substituted amino benzimidazole

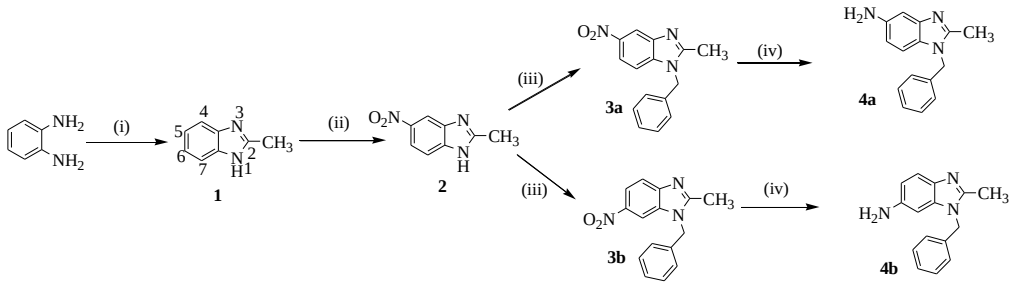

[a]Reagents and Conditions : (i) CH_3COOH, 100 ^oC, 98%; (ii) H_2SO_4, HNO_3, 0 ^oC, 75%; (iii) Benzyl chloride, K_2CO_3, C_2H_5OH, reflux, 75%; (iv) $SnCl_4.2H_2O$, 2N HCl, 110 ^oC, 25-65%.

Compounds **7-49** were synthesized by nucleophilic substitution reactions of **4a** and **4b** with cyanuric chloride followed by displacement with different primary and secondary amines as well as substituted boronic acids. Thus, compound **4a** was treated with cyanuric chloride in the presence of 10% sodium bicarbonate at 0-5 ^oC for 6 h gave (1-benzyl-2-methyl-1*H*-benzimidazol-5-yl)-(4,6-dichloro-[1,3,5]triazin-2-yl)-amine (**5a)** in 96% yield followed by stirring with 4-fluoroaniline and morpholine at room temperature in the presence of 10% sodium bicarbonate for 4 h gave compounds **6a** and **6b** respectively (Scheme **2**).

Scheme 2[a]. Synthesis of monosubstituted and disubstituted triazine

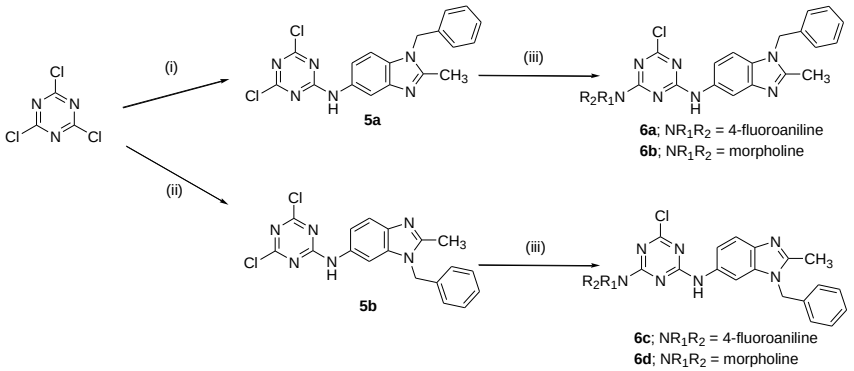

[a]Reagents and conditions: (i) **4a**, $NaHCO_3$, THF, 0−5 °C, 96%; (ii) **4b**, $NaHCO_3$, THF, 0−5 °C, 90%; (iii) 4-fluoroaniline/morpholine, $NaHCO_3$, THF, rt, 70-80%.

Similarly, compound **4b** was also treated with cynauric chloride in the same reaction conditions to obtain (3-benzyl-2-methyl-3*H*-benzimidazol-5-yl)-(4,6-dichloro-[1,3,5]triazin-2-yl)-amine (**5b**) in 90% yield followed nucleophilic substitution with 4-fluoroaniline and morpholine to obtain compounds **6c** and **6d** respectively. Finally, treatment of compound **6a-d** with different primary and secondary amines in the presence of K_2CO_3 in 1,4-dioxane at 110 ^oC for 8 h gave compounds **7-40** in moderate to good yields (Scheme **3**, **4**)**.**

Scheme 3[a]. Synthesis of 2,4,6-trisubstituted triazines with respect to 5-aminobenzimidazole

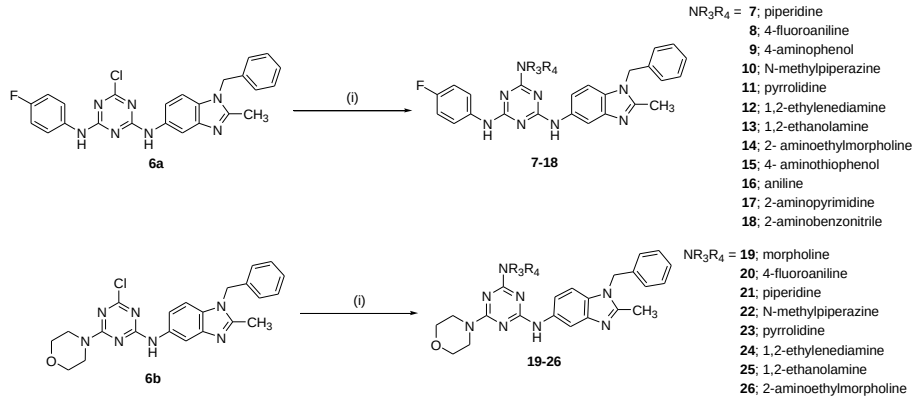

[a]Reagents and conditions: (i) HNR_3R_4, K_2CO_3, 1,4-dioxane, 110 ^{0}C, 55-88%.

Scheme 4[a]. Synthesis of 2,4,6-trisubstituted triazines with respect to 6-aminobenzimidazole

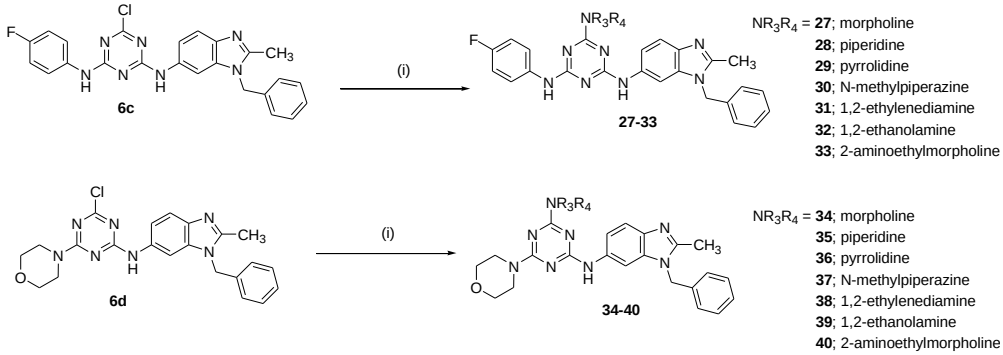

[a]Reagents and conditions: (i) HNR_3R_4, K_2CO_3, 1,4-dioxane, 110 ^{0}C, 68-88%.

Compounds **6a**and **6b** were also underwent Suzuki-Miyaura cross coupling reactions with varieties of aryl boronic acids in the presence of $Pd(PPh_3)_4$ and K_2CO_3 in 1,4-dioxane to give compounds **41-49** in 60-78% yields (Scheme **5**).

Scheme 5[a]. Synthesis of trisubstituted triazine with Suzuki-Miyaura reaction

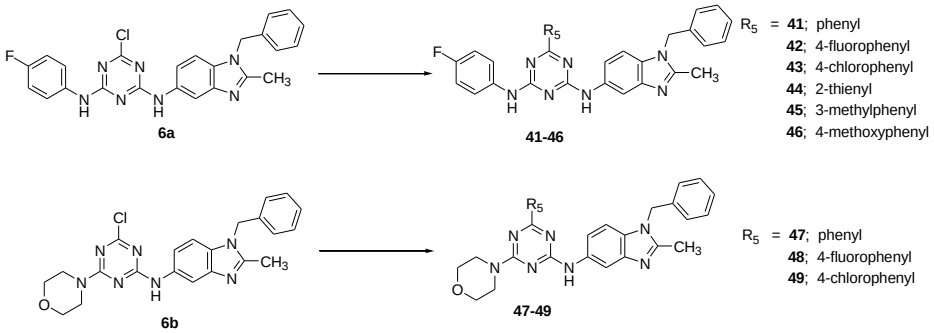

[a]Reagents and conditions: $R_5B(OH)_2$, $Pd(PPh_3)_4$, K_2CO_3, 1,4-dioxane, reflux, 59-78%.

2.1.2. Characterization:

(a) All the synthesized compounds were characterized by ^{1}H and ^{13}C NMR spectra (Bruker FT-NMR 400 MHz and JEOL ECS-400 MHz spectrometers) as well as Mass Spectra (Waters Micromass Q-Tof Micro, Milford, MA).

(b) Single crystal X-ray crystallography of compound **29** was grown in ethanol to develop single crystal with Crystalispro diffractometer with graphite monochromated Mo Kα radiation (λ = 0.71073 Å) using SHELX-97, full-matrix least-square refinement method.

2.1.3. Biological Evaluation:

(a) All the synthesized compounds were submitted to National Cancer Institute (NCI) disease-oriented human cell lines for their evaluation of *in-vitro* antitumor activities.[3-6] Thirty compounds (**6a, 6c-6d**, **8-13, 17, 19-22, 25, 28, 31-34, 36-41, 43, 44, 46** and **49**) were selected and evaluated against 60 cell lines at 10^{-5} M which included nine tumor subpanels and their outputs were reported as a mean graph of the percent growth of treated cells, and presented as percentage growth inhibition (GI %). Compounds **6c**, **6d**, **10**, **11**, **20**, **21**, **33, 43, 44** and **46** were further screened against a panel of 60 different tumor cell lines at 5 dose concentration levels against variety of cell lines. MG MID GI_{50} value (over all the 60 cancer cell lines) of compound **6c** was found to be 6.09 μM and also showed specificity towards leukemia, colon and breast cancer cell lines with GI_{50} values in the range of 3.34-4.91 μM. Nucleophilic displacement with primary and secondary amines enhanced the antitumor activity by 2 to 4 folds. MG MID GI_{50}, TGI and LC_{50} values of compound **6d** has been shown to be 9.79, 28.3 and 35.2 µM respectively. Compounds **10**, **11** and **33** showed broad spectrum antitumor activities with GI_{50}, TGI and LC_{50} values of 1.77, 1.94 and 2.87 μM; 3.96, 5.59 and 16.6 μM and 10.3, 8.59 and 35.2 μM respectively. Compound **33** showed specificity towards leukemia, colon, CNS, melanoma and breast cancer cell lines with GI_{50} in the range of 1.91-2.72 μM. Compound **20** exhibited remarkable anticancer activity against CNS cancer and renal cancer cell lines with GI_{50} values of 1.86 and 1.89 μM respectively. Similarly, compound **21** showed potency against leukemia, colon and renal cancer cell lines with GI_{50} values ranging from 2.50-2.96 μM. Compounds **43**, **44** and **46** also showed excellent antitumor activities with MG MID GI_{50} values over all 60 human tumor cell lines of 7.67, 5.18 and 4.28 μM respectively.

(b) Interaction of these compounds with dihydrofolate reductase has also been studied using dihydrofolate reductase inhibition assay kit. It was observed that these compounds showed excellent inhibitory activities with IC_{50} values ranging from 0.002 μM to 42.4 μM. Compound **33** exhibited more inhibition of DHFR activity as evident from its IC_{50} value of 2.0 ± 0.01 nM and exhibited almost tenfold higher DHFR inhibitory activity than methotrexate (MTX). To find out the site of interaction of these compounds with DHFR, UV−Visible spectral studies and ^{1}H NMR spectral studies have been performed.

(c) We therefore investigated the binding of the most active series, 5 dose compounds viz., **6c-d, 10, 11, 20, 21, 33, 43, 44** and **46** towards ct-DNA, through stepwise addition of DNA at constant concentration and physiological *p*H. The binding constant K_a was determined from the Benesi–Hildebrand[7] equation for UV-Vis and fluorescence titrations, suggested strong interaction of ct-DNA with compounds. In order to evaluate strength of intercalative nature of compounds with DNA, thermal behaviour of ct-DNA in the presence of hybrids was also determined. The thermal denaturation temperature of ct- DNA (60 ^oC), increased significantly in the presence of compound **33** (80.1 ^oC) and **21** (85.0 ^oC) which showed strong intercalation properties of these compounds with DNA.

(d) The compliance of compounds were evaluated with different physicochemical descriptors, favouring their drug like properties. It has been observed that descriptors like total polar surface area (TPSA), molar refractivity, polarizability and solvent accessibility surface area showed great influence on the DHFR activity. Lipophilicity does not exert any effect on activity in all compounds but hydrophilicity produces an important parameter for the activity. Compound **33**, most active in DHFR interaction, showed higher values in all these parameters that also supported the inhibitory activity. In order to have an insight into the molecular interaction of most active compound **33** with DHFR, docking was planned to scrutinize the mode of interaction of compound with amino acids of the DHFR enzyme that indicated the probable mode of action of this compound for anticancer activities.

2.2.1. Synthesis of 4-fluoroaniline linked triazine-benzimidazole analogues (4-21):

2,4,6-Trisubstituted triazines (**4-21**) were prepared in moderate to good yields using nucleophilic substitution and Suzuki-Miyaura cross coupling reactions (Scheme **6**). Cyanuric chloride was reacted with 4-fluoroaniline in the presence of 10% $NaHCO_3$ in THF at 0-5 ^0C for 6 h to obtain (4,6-dichloro-[1,3,5]triazin-2-yl)-(4-fluoro-phenyl)-amine (**1**) in 85% yield.

Compound **1** was treated with 4-(1*H*-benzimidazol-2-yl)-phenylamine (**2**) in the presence of potassium carbonate and THF at room temperature for 24 h to provide *N*-[4-(1*H*-benzimidazol-2-yl)-phenyl]-6-chloro-*N*'-(4-fluoro-phenyl)-[1,3,5]triazine-2,4-diamine **(3)**. Further, treatment of **3** with different primary and secondary amines in the presence of 10% potassium carbonate in 1,4-dioxane at 110 ^{o}C for 6-8 h gave compounds **4-15** in 66-78% yields. Compound **3** was also treated with different aryl boronic acids through Suzuki coupling, in the presence of $Pd(PPh_3)_4$ and K_2CO_3 in 1,4-dioxane afforded compounds **16-21**.

Scheme 6[a]. Synthesis of triazine-benzimidazole analogues.

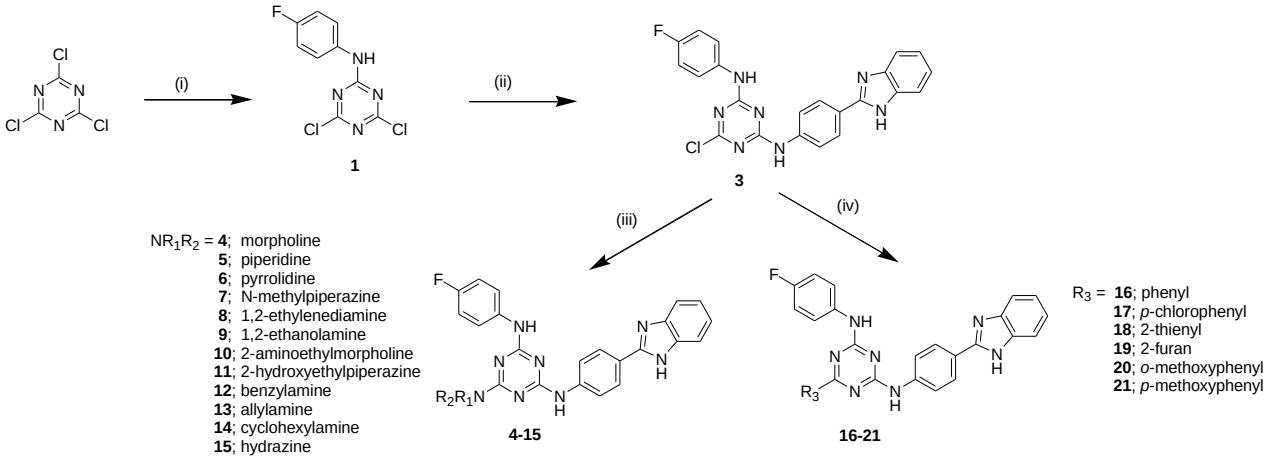

[a]Reagents and conditions: (i) fluoroaniline, $NaHCO_3$, THF, 0−5 °C; (ii) **2**, K_2CO_3, THF, rt; (iii) NHR_1R_2, K_2CO_3, 1,4-dioxane, reflux; (iv) $R_3B(OH)_2$, $Pd(PPh_3)_4$, K_2CO_3, 1,4-dioxane, reflux.

2.2.2. Characterization:

All the synthesized compounds were characterized by ^{1}H and ^{13}C NMR spectra (JEOL ECS-400 MHz spectrometers), Mass Spectra (Waters Micromass Q-Tof Micro, Milford, MA).

2.2.3. Biological Evaluation:

These synthesized compounds were further screened for their interaction with DNA using UV-Visible and fluorescence spectroscopic techniques. The electronic spectra of all the tested compounds showed intense band at the range of 300-335 nm due to the transitions between π-π* energy levels. Addition of ct-DNA to the solution of compounds **4-21** in phosphate buffer resulted in gradual decrease in the absorption intensity. Compounds **7**, **9-11**, **16** and **21** showed comparatively more hypochromicity as compared to other compounds. As there is no change in position of the absorption band (bathochromic or hypsochromic shift) of conjugates, it can be inferred that these compounds exhibit groove binding interactions to ct-DNA.[8] On exciting the

compounds **4-21** at 305 nm, the emission spectra showed intense band between 375-473 nm. The fluorescence intensity of compounds regularly decreased while the maximum emission wavelength did not apparently shift with the increase of ct-DNA concentration. For the quantitative investigation of the binding strength, the binding constants of these compounds with ct-DNA were determined from UV-Visible and fluorescence titration data using Benesi–Hildebrand equation,[7] that indicated strong binding interaction between triazine-benzimidazole analogues and ct-DNA. Thermal melting (T_m) value for the free ct-DNA has been found to be 65.6 ^oC whereas complexes of compounds **7**, **9-11**, **16** and **21** with DNA, the T_m was measured in the range of 57.0-64.4 ^oC. It has been found that triazine-benzimidazole analogues destabilize DNA double helix by 1.2-8.6 degrees which indicated the mode of groove binding of compounds to DNA. In order to rationalize the binding mode, a competitive binding experiment was performed with compounds and DNA in the presence of minor groove binder (Hoechst 33258) and an intercalator (ethidium bromide).[9,10] With increasing concentration of compounds **7, 9-11** and **16**, the emission intensity of Hoechst.DNA complex was enhanced to a significant level while in case of compound **21** the emission intensity of Hoechst.DNA complex was quenched. This indicated that the Hoechst dye was replaced with compounds **7**, **9-11**, **16** and **21** from the minor groove of DNA. A similar experiment was performed with addition of DNA to a solution of ethidium bromide (EB) that provided no significant change in emission intensity of ethidium bromide.DNA complex. Further, viscosity titration method was performed to confirm the binding mode between triazine-benzimidazoles and ct-DNA.

The effect of ionic strength and iodine quenching were determined to evaluate whether there is electrostatic binding between triazine-benzimidazoles and ct-DNA. The ratio of fluorescent intensity of compounds **7, 9-11, 16** and **21** and DNA complexes did not show any significant changes upon successive addition of salt and iodide that further eliminated the possibility of intercalation. These results signified the interaction of compounds **7, 9-11, 16** and **21** with DNA through groove binding mode or/and electrostatic binding. The docking studies of the synthesized ligands clearly showed the importance of the mode of action through the interaction between the triazine derivatives and DNA.

2.3.1. Synthesis of morpholine linked triazine-benzimidazole analogues:

The triazine-benzimidazole analogues were synthesized by their substitution with primary and secondary amines as well as Suzuki-Miyaura cross coupling reactions (**5-21)** that has been

reported in Scheme **7**. Cyanuric chloride was reacted with morpholine in the presence of sodium bicarbonate in THF at 0-5 ^{o}C for 6 h to give 4,6-dichloro-2-morpholin-4-yl-[1,3,5]triazine (**2**) in 89% yield followed by nucleophilic substitution with 4-(1*H*-benzimidazol-2-yl)-phenylamine (**3**) in the presence of potassium carbonate and THF at room temperature for 24 h provided the [4-(3*H*-benzimidazol-5-yl)-phenyl]-(6-chloro-2-morpholin-4-yl-[1,3,5]triazin-2-yl)-amine (**4**) in 84% yield. Further, treatment of compound **4** with different primary and secondary amines in the presence of potassium carbonate and 1,4-dioxane at 110 ^{o}C for 8 h gave compounds **5-15** in moderate to 66-75% yields. Compound **4** was also treated with five and six membered aryl boronic acids in the presence of $Pd(PPh_3)_4$ and K_2CO_3 in 1,4-dioxane afforded compounds **16-21** in 64-75% yields.

Scheme 7[a]. Synthesis of triazine-benzimidazole analogues.

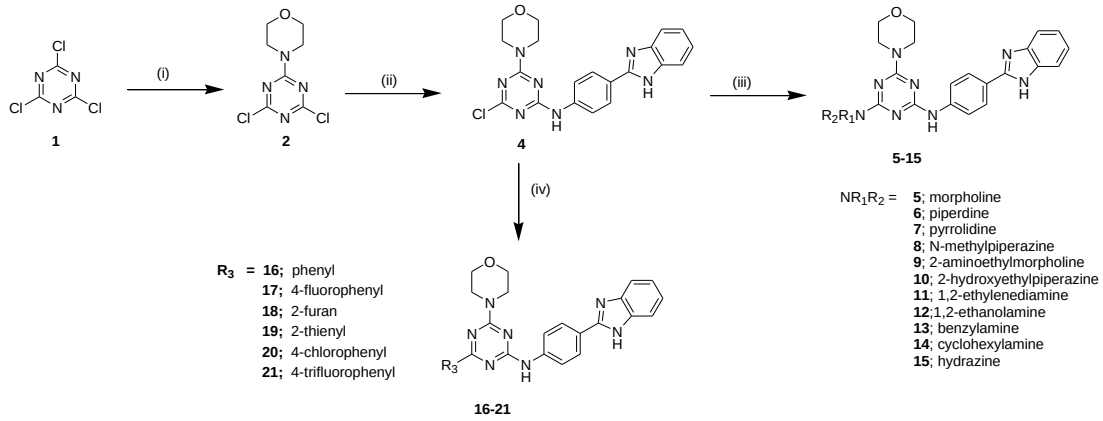

[a]Reagents and conditions: (i) morpholine, $NaHCO_3$, THF, 0−5 °C; (ii) **3**, K_2CO_3, THF, rt; (iii) NHR_1R_2, K_2CO_3, 1,4-dioxane, reflux; (iv) $R_3B(OH)_2$, $Pd(PPh_3)_4$, K_2CO_3, 1,4-dioxane, reflux.

2.3.2. Biological Evaluation:

(a) Regarding the activity toward individual cell lines; all compounds showed selective potency towards leukemia and melanoma cancer cell lines. In leukemia cancer cell lines CCRF-CEM, MOLT-4, RPMI-8226 and SR, compound **6** showed activity with GI values of 91%, 86%, 99%, 90% respectively. Compound **6** showed selectivity towards non small cell lung cancer cell lines like NCI-H460, NCI-H522, A549/ATCC and NCI-H23 with GI values of 99%, 91%, 86% and 80%; compound **17** with GI values of 88%, 92%, 93%, 99%, 82%, 88% and 88% towards A549/ATCC, EKVX, HOP-92, NCI-H460, NCI-H226, NCI-H23 and NCI-H522. Compound **6** and **17** showed selectivity toward colon cancer cells HCT-116, SW-620 and KM12 with GI values of 91% and 95%, 94% and 96%, 85% and 87% respectively; CNS cancer cells SF-539,

SNB-19 and U251 with GI values of 92% and 99%, 89% and 82%, 91% and 93%; ovarian cancer cell OVCAR-3 with GI value of 89% and 94%; prostate cancer cell PC-3 with GI values of 87% and 97% respectively. Compound **17** showed selectivity towards renal cancer cell ACHN with GI values of 91% and breast cancer cell MDA-MB-231/ATCC, MCF7 and BT-549 with GI value in range of 94-96%. Compounds **6, 16, 17** and **20** were further screened against a panel of 60 different tumor cell lines at five dose concentration range as these have shown prominent cell growth inhibition at one dose concentration level against variety of cell lines. Compounds **6**, **16, 17** and **20** showed broad spectrum antitumor activities with GI_{50}, TGI and LC_{50} values of 2.68, 11.0 and 32.3 μM; 1.38, 3.15 and 8.63 μM; 2.37, 7.16 and 7.88 μM and 0.72, 1.80 and 4.88 μM respectively.

(b) To examine the structural changes of BSA with these synthesized compounds **5-21**, absorbance and fluorescence spectral measurements were carried out. The electronic spectrum of BSA showed an intense band at 279 nm that arises due to phenyl rings in Trp (tryptophan), Tyr (tyrosine), and Phe (phenylalanine) residues. However, subsequent addition of compounds **5-21** to BSA solution resulted in a gradual increase in the intensity of peak at 279 nm to some extent, but with the formation of a new band at 324 nm indicating the interaction of compounds with protein by extending the peptide strands of BSA and leading to an increase of hydrophobicity in the vicinity of this residue. On gradual addition of compounds **5-21**, decrease in the fluorescence intensity of BSA at 350 nm accompanies the appearance of one peak within range of 370-373 nm, which can be attributed to the complexation between compounds and protein. On gradual addition of compounds **5-21**, fluorescence intensity of the tryptophan residue present in BSA decreased with a concomitant increase in the fluorescence intensity through an isoemissive point that indicates an efficient energy transfer from the tryptophan residue present in BSA to compounds.

Chapter 3: Covers synthesis, characterization, *in-vitro* evaluation and molecular modelling of fused heterocyclic moieties linked benzimidazoles.

3.1. PYRROLOPYRIDINE

3.1.1. Synthesis of azoles and imidazopyridine substituted pyrrolopyridine (3-44):

The synthesis of N_1-substituted-2-(1*H*-pyrrolo[2,3-*b*]pyridine-3-yl)-azole ring system (**3-44**) has been depicted in scheme **8**. Duff reaction was first carried out by heating of 1*H*-pyrrolo[2,3-*b*]pyridine **1** in the presence of hexamethylenetetramine (HMTA) in acetic acid at 110 ^{0}C for 2 h

to give 1*H*-pyrrolo[2,3-*b*]pyridine-3-carboxaldehyde **2** in 55% yield. The formyl function at C3-position provided a convenient handle for the generation of the corresponding azoles. Thus, compound **2** was allowed to heat with 2-aminothiophenol/benzene-1,2-diamine/4-nitro-benzene-1,2-diamine/6-bromopyridine-2,3-diamine at 160 ^{o}C for 15 h to obtain desired products **3-6** followed by selective mono-acylation and alkylation at N_1 position of 1*H*- pyrrolo[2,3-*b*]pyridine with respective acyl and alkyl halides, and in case of benzyl and methyl halides, dialkylations are predominant.

Scheme 8[a]: Synthesis of azoles substituted 1*H*-pyrrolo[2,3-*b*]pyridine

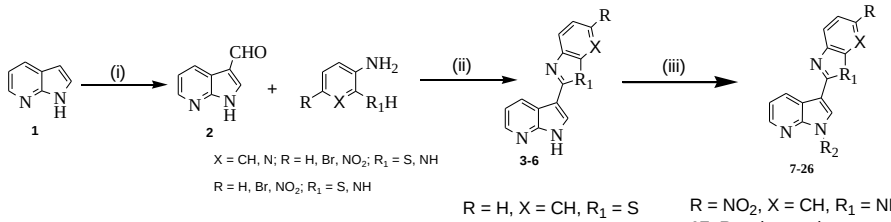

R = H, X = CH, R_1 = S
7; R_2 = benzoyl
8; R_2 = Chloroacetyl
9; R_2 = allyl
10; R_2 = butyl
11; R_2 = oxiranyl

R = H, X = CH, R_1 = NH
12; R_2 = benzoyl
13; R_2 = Chloroacetyl
14; R_2 = allyl
15; R_2 = butyl
16; R_2 = oxiranyl

R = NO_2, X = CH, R_1 = NH
17; R_2 = benzoyl
18; R_2 =Chloroacetyl
19; R_2 =allyl
20; R_2 =butyl
21; R_2 =oxiranyl

R = Br, X = N, R_1 = NH
22; R_2 = benzoyl
23; R_2 = 4-nitrobenzoyl
24; R_2 = 4-flourobenzoyl
25; R_2 = 4-methoxybenzoyl
26; R_2 = chloroacetyl

[a]Reagents and conditions: (i) HMTA, CH_3COOH, 110 °C; (ii) Nitrobenzene, 160 °C; (iii) R_2X, NaH, dry THF.

Treatment of compound **3** with benzyl chloride and methyl iodide at the same reaction conditions to give compounds **27a** and **28a** in 88% and 84% yields respectively (Scheme **9**). But, when the alkylation of **4** and **5** were carried out with benzyl chloride and methyl iodide, NH group of benzimidazole was also alkylated. On the other hand, treatment of compound **6** with benzyl halides at the same reaction conditions, gave monoalkylation and dialkylation products.

Scheme 9[a]: Monoalkylation and dialkylation 1*H*-pyrrolo[2,3-*b*]pyridine

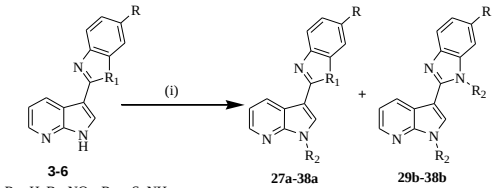

R = H, X = CH, R_1 = S
27a; R_2 = benzyl
28a; R_2 = methyl

R = H, X = CH
29a; R_1 = NH, R_2 = benzyl
29b; R_1 = R_2 = benzyl
30a; R_1 = NH, R_2 = methyl
30b; R_1 = R_2 = methyl

R = NO_2, X = CH
31a; R_1 = NH, R_2 = benzyl
31b; R_1 = R_2 = benzyl
32a; R_1 = NH, R_2 = methyl
32b; R_1 = R_2 = methyl

R = Br, X = N
33a; R_1 = NH, R_2 = benzyl
33b; R_1 = R_2 = benzyl
34a; R_1 = NH, R_2 = 4-chlorobenzyl
34b; R_1 = R_2 = 4-chlorobenzyl
35a; R_1 = NH, R_2 = 3-chlorobenzyl
35b; R_1 = R_2 = 3-chlorobenzyl
36a; R_1 = NH, R_2 = 2-chlorobenzyl
36b; R_1 = R_2 = 2-chlorobenzyl
37a; R_1 = NH, R_2 = 4-fluorobenzyl
37b; R_1 = R_2 = 4-fluorobenzyl
38a; R_1 = NH, R_2 = 2-fluorobenzyl
38b; R_1 = R_2 = 2-fluorobenzyl

[a]Reagents and conditions: (i) R_2X, NaH, dry THF.

Suzuki-Miyaura coupling reactions were also performed with **6** and aryl boronic acids in the presence of Cs_2CO_3 in 1,4-dioxane using $Pd(PPh_3)_4$ to give arylation at C6 position of imidazopyridine **39-44** in 70-86% yields. It has been observed that arylation with unsubstituted phenyl gave higher yield of product than electron donating or electron withdrawing groups, present at phenyl ring (Scheme **10**).

Scheme 10[a]. Arylation at C6 position of imidazopyridine functionalized 1*H*-pyrrolo[2,3-*b*]pyridine.

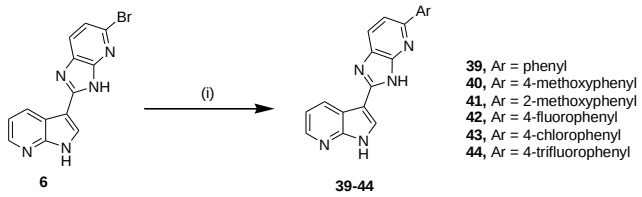

[a]Reagents and conditions: (i) $ArB(OH)_2$, Cs_2CO_3, $Pd(PPh_3)_4$, 1,4-dioxane, reflux.

3.1.2. Characterization:

(a) All the synthesized compounds were characterized by ^1H and ^{13}C NMR spectra (JEOL ECS-400 at 400 and 100 MHz NMR spectrometers) and Mass Spectra (Waters Micromass Q-Tof Micro, Milford, MA).

3.1.3. Biological Evaluation:

(a) In order to examine the binding modes of compounds **39-44** with ct-DNA, absorption and emission spectral titrations were performed. A decrease in absorption intensity i.e. hypochromism was observed in compounds **39-44** with the addition of ct-DNA, that indicates change in the conformation of DNA (compound **39:** 47%, compound **40:** 12%, compound **41:** 16%, compound **42:** 28%, compound **43:** 10% and compound **44:** 31%) while in fluorescence emission titrations; compounds **39** and **44** showed 44% and 35% quenching after 8 μM and 10 μM addition of DNA, and compounds **40** and **41** caused enhancement in the fluorescence intensity after gradual addition of DNA (**40** - 30% and **41** - 26%).

3.2. QUINAZOLINONE

3.2.1. Synthesis of quinazolinone-benzimidazole hybrids (14-25):

The synthetic strategy to prepare the quinazolin-4-one benzimidazole conjugates (**14-25**) is depicted in Scheme **11**. Initially, anthranilic acid was reacted with aromatic and aliphatic acyl chlorides in the presence of triethylamine in chloroform at room temperature for 2 h to give compounds **1-6** followed by cyclization, in the presence of pyridine in ethanol at 70-80 ^{0}C for 8 h

to obtain 2-aryl/methyl-4*H*-benzo[*d*][1,3]oxazin-4-one (**7-12**). 1-Benzyl-2-methyl-1*H*-benzimidazol-5-ylamine (**13a**) and 3-benzyl-2-methyl-3*H*-benzimidazol-5-ylamine (**13b**) were synthesized by refluxing of 2-methyl-5-nitro-1*H*-benzimidazole with benzyl chloride in the presence of K_2CO_3 in ethanol for 8 h followed by reduction with $SnCl_2.2H_2O$ in 2N HCl. Finally, 1/3-benzyl-2-methyl-1*H*/3*H*-benzimidazol-5-ylamine **(13a** and **13b)** and 2-aryl/methyl-4*H*-benzo[*d*][1,3]oxazin-4-one (**7-12**) were refluxed in ethanol in the presence of pyridine for 4 h to afford corresponding 3-(1/3-benzyl-2-methyl-1*H*/3*H*-benzimidazol-5-yl)-2-aryl/methyl-3*H*-quinazolin-4-one (**14-25**).

Scheme 11[a]. Synthesis of quinazolinone-benzimidazole conjugates.

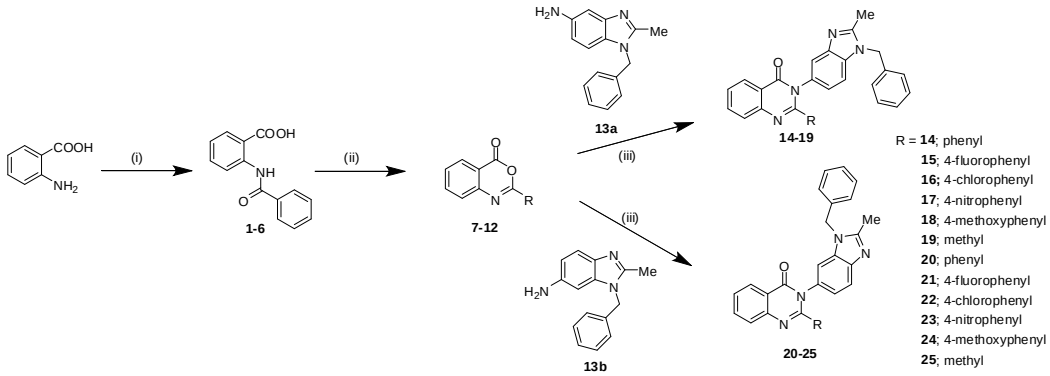

[a]Reagents and conditions: (i) RCOCl, triethylamine, $CHCl_3$, room temperature, 78-89%; (ii) pyridine, ethanol, 70-80 °C, 90%; (iii) **13a**/**13b**, pyridine, ethanol, reflux, 68-80%.

3.2.2. Characterization:

All the synthesized compounds were characterized by ^1H and ^{13}C NMR spectra (JEOL ECS -400 at 400 and 100 MHz NMR spectrometers) and Mass Spectra (Waters Micromass Q-Tof Micro, Milford, MA).

3.2.3. Biological Evaluation:

(a) These compounds were evaluated as DHFR inhibitors using DHFR assay kit. The obtained results revealed effective inhibition of the dihydrofolate reductase enzyme, with IC_{50} values ranging from 0.011 μM to 27.62 μM.

(b) The binding behaviour of active compound **14** with ct-DNA was studied on the molecular level by UV-visible, fluorescence spectroscopic methods and thermal denaturation study as well as ethidium bromide displacement study.

(c) In order to explore the structural changes of protein and its complex formation with drug molecule, UV-visible and fluorescence studies were performed on compound **14** and BSA.

(d) Based on the *in vitro* DHFR enzyme inhibition studies, the most active compound **14** was selected to evaluate the putative binding mode with amino acids in the active site of the enzyme using molecular docking technique.

3.3. PYRAZOLOPYRIMIDINE

3.3.1. Synthesis of Pyrazolopyrimidine-benzimidazole analogues (7-18):

Our first key intermediate was the 5-aminopyrazole-4-carbonitrile **1,** which was easily prepared from condensation of ethoxymethylenemalonitrile with hydrazine. Hydrolysis with sulphuric acid and then fusion with molten urea at 190 ^{0}C gave the intermediate product **3**, followed by $POCl_3$-mediated chlorination provided 4,6-dichloropyrazolopyrimidine. The aromatic nucleophilic substitution at C4 position of 4,6-dichloropyrazolopyrimidine with 4-(1*H*-benzimidazol-2-yl)-phenylamine (**5**) under mild reaction condition yielded [4-(1*H*-benzimidazol-2-yl)-phenyl]-(6-chloro-1*H*-pyrazolo[3,4-*d*]pyrimidin-4-yl)-amine (**7**) followed by substitution with different amines at C6 position in *n*-butanol gave target compounds **7**-**18** (Scheme **12**).

Scheme 12[a]. Synthetic route for the preparation of target compounds **7**-**18**.

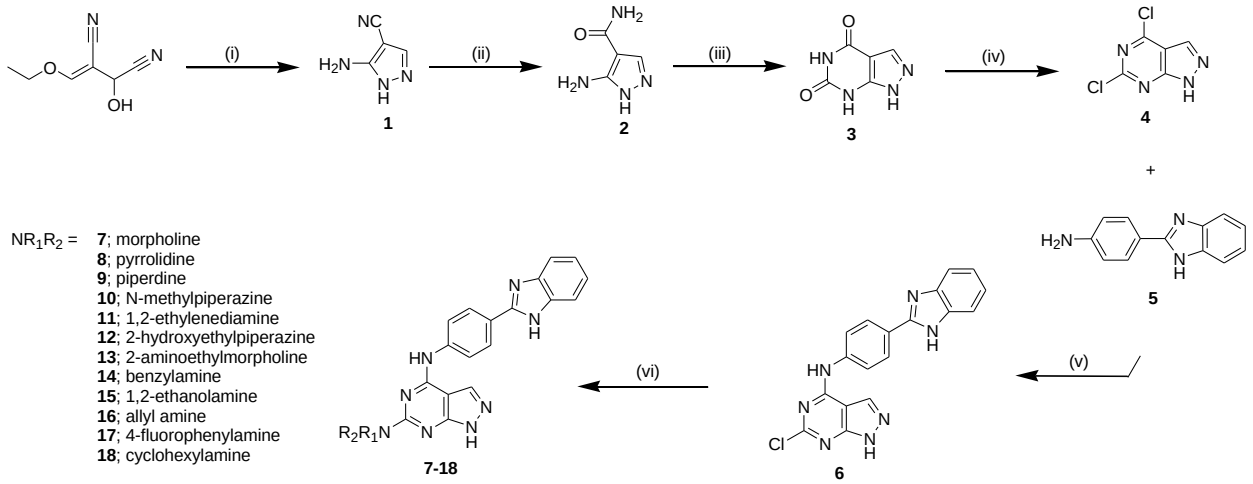

[a]Reagents and conditions: (i) hydrazine, 100 °C; (ii) H_2SO_4, 0-5 °C; (iii) urea, 190 °C; (iv) $POCl_3$, triethylamine, 100 °C; (iv) 5, K_2CO_3, IPA, rt; (v) HNR_1R_2, K_2CO_3, n-butanol, reflux.

3.3.2. Characterization :

(a) All the synthesized compounds were characterized by ^{1}H and ^{13}C NMR spectra (JEOL ECS - 400 at 400 and 100 MHz NMR spectrometers) and Mass Spectra (Waters Micromass Q-Tof Micro, Milford, MA).

3.3.3. Biological Evaluation:

(a) In order to seek for the potential anti-tumor target of pyrazolopyrimidine derivatives, both UV-visible and fluorescence spectroscopy were used to ascertain the binding properties of compounds **6**, **8**, **11**, **12**, **14** and **17** with ct-DNA. Upon incremental addition of ct-DNA to compounds (10 μM), decrease in the absorption maxima intensity (λ_{max}) along with concomitant increase in absorption intensity at another λ_{max} along with an isobestic point were shown. In emission spectral studies, compounds **6**, **8**, **11**, **12**, **14** and **17** caused 68%, 28%, 57%, 67%, 33% and 65% emission quenching.

(b) To explore the complex formation of protein with drug molecule, fluorescence quenching studies were performed. Incubation of BSA solution with different concentrations of compounds **6**, **8**, **11**, **12**, **14** and **17**, caused a gradual quenching i.e. 44%, 21%, 35%, 31%, 54% and 33% in the fluorescence intensity of the mixture indicating the interaction of compounds **6**, **8**, **11**, **12**, **14** and **17** with BSA by changing in the environment around the mentioned amino acids by extending the peptide strands of BSA.

CONCLUSION

We have successfully designed and synthesized the different fragments of amino benzimidazole linked triazine and fused heterocyclic hybrids. These novel molecules have been well characterized by ^{1}H, ^{13}C NMR, mass spectroscopy and in some cases by single X-ray crystallography. These compounds were evaluated *in vitro* towards 60 human cancer cell lines and dihydrofolate reductase inhibition for their anticancer activities. These compounds were then evaluated for their DNA binding study and BSA interactions. Structure activity relationship was studied to find out for the activity of each fragment of compound. Molecular modelling studies indicating considerable interactions of these compounds in the active site of enzyme. The experimental (60 human cancer cell lines and dihyrofolate reductase kinase enzyme) as well as DNA binding and BSA interaction study clearly predicted activity of triazine and fused heterocyclic-benzimidazole hybrids.

REFERENCES

1. R. Ali, Z. Mirza, G. M. D. Ashraf, M. A. Kamal, S. A. Ansari, G. A. Damanhouri, A.

M. Abuzenadah, A. G. Chaudhary and I. A. Sheikh, *Anticancer Res*., 2012, **32**, 2999.

2. A. Y. Louie and T. J. Meade, *Chem. Rev*., 1999, **99**, 2711.
3. Developmental Therapeutics Program, NCI/NIH. www.dtp.nci.nih.gov.
4. M. R. Grever, S. A. Sehepartz and B. A. Chabners, *Semin. Oncol*., 1992, **19**, 622.
5. A. Monks, D. Schudiero, P. Skehan, R. Shoemaker, K. Paull, D. Vistica, C. Hose, J. Langley, P. Cronise, A. Vaigro-Wolff, M. Gray-Goodrich, H. Campbell, J. Mayo and M. J. Boyd, *Natl. Cancer Inst.,* 1991, **83**, 757.
6. M. R. Boyd and K. D. Paull, *Drug Dev. Res.,* 1995, **34**, 91.
7. H. A. Benesi and J. H. Hildebrand, *J. Am. Chem. Soc.,* 1949, **71**, 2703.
8. S. Kashanian, S. H. Zeidali, K. Omidfar and N. Shahabadi, *Mol. Biol. Reprod. Med*., 2012, **39**, 10045.
9. Y. Zhang, G. Zhang, Y. Li and Y. Hu, *J. Agric. Food Chem.*, 2013, **61**, 2638.
10. P. E. Pjura, K. Grzeskowiak and R. E. Dickerson, *J. Mol. Biol.,* 1987, **197**, 257.

LIST OF PUBLICATIONS

1. Prinka Singla, Vijay Luxami and Kamaldeep Paul, "Benzimidazole-biologically attractive scaffold for protein kinase inhibitors", *RSC Advances*, **2014,** *4*, 12422.
2. Prinka Singla, Vijay Luxami and Kamaldeep Paul, "Triazine-benzimidazole hybrids: Anticancer activity, DNA interaction and dihydrofolate reductase inhibitors", *Bioorganic & Medicinal Chemistry***, 2015,** *23*, 1691.
3. Prinka Singla, Vijay Luxami and Kamaldeep Paul, "Triazine as a promising scaffold for its versatile biological behavior", *European Journal of Medicinal Chemistry***, 2015,** *102*, 39.
4. Prinka Singla, Vijay Luxami and Kamaldeep Paul, "Synthesis, *in vitro* antitumor activity, dihydrofolate reductase inhibition, DNA intercalation and Structure activity relationship studies of 1,3,5-triazine analogues", *Bioorganic & Medicinal Chemistry Letters*, **2016,** *26*, 518.
5. Prinka Singla, Vijay Luxami and Kamaldeep Paul, "Triazine-Benzimidazole Conjugates: Synthesis, Spectroscopic and Molecular Modelling Studies for Interaction with calf thymus DNA", *RSC Advances*, **2016,** *6*, 14741.
6. Prinka Singla, Vijay Luxami and Kamaldeep Paul, "Synthesis and *In vitro* evaluation of Triazine analogues as anticancer agents and their interaction studies with Bovine serum albumin", *European Journal of Medicinal Chemistry* (under major revision).
7. Prinka Singla, Vijay Luxami and Kamaldeep Paul, "Synthesis, dihydrofolate reductase inhibition and binding interactions of novel quinazolinone-benzimidazole conjugates to calf thymus DNA and Bovine serum albumin", *New Journal of Chemistry* (under review).
8. Prinka Singla, Vijay Luxami and Kamaldeep Paul, "Synthesis and spectroscopic studies of 1*H*-pyrrolo[2,3-*b*]pyridine derivatives using calf thymus DNA", *RSC Advances* (under review).
9. Prinka Singla, Vijay Luxami and Kamaldeep Paul, "Pyrazolopyrimidine-benzimidazole hybrids: synthesis, *in vitro* evaluation of anticancer activities and DNA and Albumin interaction studies", *RSC Advances* (Communicated).

POSTERS IN CONFERENCES

1. Prinka Singla, Vijay luxami, Kamaldeep Paul "Synthesis of Novel Derivatives of 1, 3, 5-triazines as Anticancer Agents" Chemical Constellation Cheminar-2012 held at Dr. B R Ambedkar National Institute of Technology, Jalandhar on 10-12 Sept, **2012**.
2. Prinka Singla and Kamaldeep Paul "Synthesis and in vitro evaluation of novel s-triazine derivatives as potential anticancer and anti-HIV Agents" 15th CRSI National Symposium in Chemistry held at Banaras Hindu University, Varanasi on 31 Jan-3 Feb, **2013**.
3. Prinka Singla**,** Vijay luxami, Kamaldeep Paul **"**Synthesis and Structural Strategies of Benzimidazole substituted Triazine scaffolds as Biological active entities**"** NCIMSF-2013 held at Thapar University, Patiala on 26-28 Oct, **2013.**